

**Recording and Processing of Tissue-Specific Ocular
Electrical Biosignals for Applications in Biomedical
Devices**

**Thesis submitted as requirement to fulfill the degree
“Doctor of Philosophy” (Ph.D.)**

**at the
Faculty of Medicine
Eberhard Karls University
Tübingen**

by

Margaret Michelle Clouse

from

Butler, Pennsylvania, United States of America

2017

Dean: Professor Dr. I. B. Autenrieth
1. Reviewer: Professor Dr. med. Dr. hc. mult. Eberhart Zrenner
2. Reviewer: Professor Dr. Uwe Ilg

TABLE OF CONTENTS

GLOSSARY	V
LIST OF ABBREVIATIONS.....	VI
1. INTRODUCTION	1
1.1 Project Goals	1
1.2 Thesis Overview	2
1.3 Accommodation.....	3
1.4 Presbyopia.....	12
2. STUDIES TO MEASURE CILIARY MUSCLE ACTIVITY	18
2.1 Introduction.....	18
2.2 Methods.....	18
2.3 Results.....	40
2.4 Discussion	87
2.5 Conclusions.....	113
3. DEVICE DEVELOPMENT	115
3.1 Introduction.....	115
3.2 Device Requirements	115
3.3 Device Specifications.....	120
4. DEVICE CONSTRUCTION	144
4.1 Introduction.....	144
4.2 Design Construction Details	144
4.3 Final Device Construction	155
5. TESTING THE FINISHED DEVICE	157
5.1 Pre-Clinical Tests.....	158
5.2 Clinical Investigations	164
5.3 Proof of Concept.....	166
5.4 Discussion.....	175
5.5 Future Design Suggestions	177

5.6 Conclusions.....	178
SUMMARY	180
ZUSAMMENFASSUNG	182
REFERENCES	184
ERKLÄRUNG ZUM EIGENANTEIL DER DISSERTATIONSSCHRIFT	197
APPENDIX A: CODE.....	198
APPENDIX B: SAMPLE CILIARY MUSCLE STUDY SUBJECT INFORMATION SHEETS.....	221
APPENDIX C: USER’S GUIDE.....	223
AUTHOR’S CONTRIBUTIONS	239
ACKNOWLEDGEMENTS.....	240

GLOSSARY

Presbyope: A person suffering from presbyopia, a condition occurring with advanced age, in which the ability to focus on near targets is lost.

Pseudophake: A person who has had the natural crystalline lens replaced with an intraocular lens.

Ptosis: Drooping of the eyelid.

Emmetrope: A person without refractive errors.

Myope: Near-sighted person.

Hyperope: Far-sighted person.

Cycloplegia: Paralysis of the intraocular muscles of the eye.

LIST OF ABBREVIATIONS

RMS	Root mean square
I ² C	Inter-integrated circuit
ADC	Analog to digital converter
IC	Integrated circuit
IOL	Intraocular lens
D	Diopters
EKG	Electrocardiography
EMG	Electromyography
Sra	Spherical radius
UART	Universal Asynchronous Receiver/Transmitter
DC	Direct current

1. INTRODUCTION

Visual accommodation has been extensively studied throughout the years [(Harper, 2014)]. Despite continuing technological advances in measurement techniques, the exact mechanism of accommodation remains unclear [(Baumeister & Kohnen, 2008), (Heron & Charman, 2004), (Koretz & Handelman, 1986), (Koretz & Handelman, 1983)], as do the means by which the accommodative system loses functionality in the condition of presbyopia [(Baumeister & Kohnen, 2008), (Charman, 2008)]. In order to develop new clinical interventions for presbyopia, the accommodative function must first be elucidated and studied.

Surprisingly few studies have been performed to describe the accommodation process in humans, and even fewer have yielded results that are consistent across laboratory groups. This is in part due to the myriad of measurement techniques [(Bailey, 2011)] used to evaluate a muscle function that has not, as yet, been directly measured noninvasively. If the function of the ciliary muscle could be easily and reliably described across subjects, not only could the accommodative process be better studied, but better, more accurate devices could be developed to aid those suffering from presbyopia.

1.1 Project Goals

The goals of this project are twofold. First, the development of a non-invasive method of measuring the ciliary muscle is desired, which will lead to a useful signal indicative of accommodative activity. Though the force of the ciliary muscle has been approximated *ex vivo* [(Fisher, 1977)], it has never been directly measured in a human subject. The development of a consistent measurement method will allow for more comparable research results than have previously been achieved in the fields of accommodation and presbyopia, and could lead to further discoveries in both fields. For the current study, the measurement method will allow for the elucidation of patterns that

could be used both in the control of a device, and give clues as to the different behaviors of the ciliary muscle between young, presbyopic, and pseudophakic subjects.

Secondly, using the signals recorded from the ciliary muscle, a device will be developed to allow for the control of accommodation in a more natural manner. Though, as discussed above, many devices to aid in the treatment of presbyopia have been developed, none have used a neural signal from the patient's accommodative system as a method of control. It is thought that this method will require less training, and be less cumbersome and costly to the user, thereby increasing quality of life.

By meeting both of these goals, this project will both significantly contribute to the field of visual research, and meet pressing social concerns about presbyopia. It is hoped that, by exploring these two goals, a better understanding of accommodation and presbyopia will be developed, and a better solution for presbyopic patients will be discovered. It is also expected that this work will serve as a foundation for more discoveries in the future.

1.2 Thesis Overview

The introduction will introduce the topic of accommodation. First, the physiological properties and theories will be reviewed for this process, and an overview of the current body of knowledge will be stated. The need for consistent measurement methods and a wider set of experimental data on this topic will be discussed.

Studies to Measure the Ciliary Muscle, the second section, will discuss the development of a method to noninvasively measure accommodation. Subject selection, experimental protocols, and associated pharmacological experiments will be treated here. Results sets forth the experimental findings, which are further clarified in the Discussion. Overall outcomes of the study will be summarized in Conclusions.

Device Development will deal with the design and construction of an accommodative device. Several different options for accommodative restoration will be

discussed, with an exploration of the pros and cons of each solution. Device construction will be described, and preliminary results from a small cohort of presbyopic subjects will be discussed in terms of feasibility and future practicability.

The end of the thesis will offer comments on the experiments and their results, and will discuss the further development and implications of a novel device that will restore accommodation. Future studies will be outlined, and possible improvements to the device will be suggested. Finally, the feasibility of the proposed solution will be discussed.

1.3 Accommodation

1.3.1 Anatomical Elements of Accommodation

Accommodation is the process by which the eye, through the action of the accommodative components, changes focus from a target in the distance to a target in the near field of vision. This process operates independently of refractive errors, such as hyperopia and myopia: refractive errors are inherently linked to the shape of the eye, whereas accommodation is an active reshaping of the lens. The anatomical elements involved in accommodation are found in the anterior portion of the eye.

The most accepted explanation of accommodation is based on the work of Helmholtz [(Atchison, 1995), (Burd et al., 2002)]. This theory states that, in the normally functioning human eye, the contraction of the ciliary muscle leads to a slackening of the zonules, which, in turn, allow the crystalline lens to assume a more spherical shape. When this process is complete, the eye is configured to focus on near targets. During the opposite process, disaccommodation, the ciliary muscle relaxes, pulling the zonules taut. The zonules stretch the crystalline lens into a flatter shape suitable for far vision. As an analogy, one can imagine a gel-filled ball (lens) with rubber bands (zonules) attached to the periphery. In an unaccommodated state, one can imagine that the rubber bands are attached to a fixed point, such that they pull the ball into a flat shape. If the fixation point

is pushed inward, similarly to the motion of the ciliary muscle during accommodation, the tension exerted by the rubber bands decreases, and the ball is able to assume its natural, spherical shape (Figure 1). Though the mechanism of accommodation will be discussed in greater detail later, this basic explanation will serve to provide a basis of understanding for the accommodative components described in the next few pages.

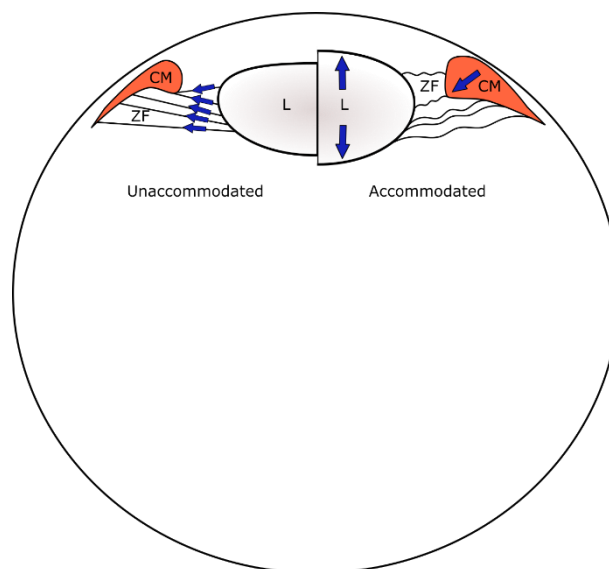


Figure 1: The Helmholtz theory of accommodation. In a relaxed state, the lens is pulled into a flat position by the zonular fibers attached to the ciliary muscle. When the ciliary muscle contracts, the tension on the zonular fibers is loosened, and the lens is able to assume a more spherical shape. L: lens, ZF: zonular fibers, CM: ciliary muscle.

The ciliary muscle is an anatomical enigma. Though it is classified as a multi-unit smooth muscle, it also exhibits several characteristics normally seen in skeletal muscle [(Atchison, 1995), (Flügel et al., 1990), (Rohen et al., 1990), (Samuel et al., 1996), (Tamm & Lütjen-Drecoll, 1996), (Wiederholt et al., 2000)]. It is widely accepted that the ciliary muscle is the active element in the process of accommodation, and, thus, of paramount importance for anyone wishing to study accommodation.

To find the ciliary muscle, one must look in the ciliary body; the ciliary muscle comprises the vast majority of this structure [(Atchison, 1995)]. Traditionally, the muscle fiber groups comprising the ciliary muscle have been divided into three portions, based on the orientations of the fibers: the meridional or longitudinal fibers, the radial fibers,

and the circular fibers [(Atchison, 1995), (Baumeister & Kohnen, 2008), (Charman, 2008), (Tamm & Lütjen-Drecoll, 1996), (Tamm et al., 1992)]. The question as to whether the muscle fibers differ in anything other than orientation has long been debated, though some have found different properties in different groups [(Tamm & Lütjen-Drecoll, 1996)]. Some groups, for example, have found that the longitudinal fibers act more like fast Type II skeletal fibers in terms of response characteristics, whereas the radial fibers respond similarly to slower Type I skeletal fibers [(Flügel et al., 1990), (Wiederholt et al., 2000)]. Regardless of the differences between the muscle fiber groups, a contraction of the ciliary muscle does involve separate changes for the different groups, namely, an increase in the area of the circular fibers [(Armaly, 1968), (Baumeister & Kohnen, 2008), (Tamm & Lütjen-Drecoll, 1996), (Tamm et al., 1991)], either an increase [(Armaly, 1968), (Tamm et al., 1991)] or decrease [(Baumeister & Kohnen, 2008)] in the area of the radial portion, and a decrease in the area of the longitudinal portion [(Baumeister & Kohnen, 2008), (Tamm & Lütjen-Drecoll, 1996), (Tamm et al., 1991)]. The overall effect of this change in area is the forward and inward movement of the ciliary body.

On the level of the entire muscle, the ciliary muscle has its origin at the scleral spur, and its insertion onto the ciliary body at Bruch's membrane [(Atchison, 1995), (Beers & van der Heijde, 1994), (Stark, 1988)]. Though the origin attaches through tendon-like structures [(Tamm & Lütjen-Drecoll, 1996)], the insertion is effected by elastic fibers. These posterior insertions will be discussed later, as they are especially important to current theories of presbyopia.

The cells of the ciliary muscle contain a large amount of mitochondria [(Atchison, 1995), (Lütjen-Drecoll et al., 1988), (Tamm & Lütjen-Drecoll, 1996)], and are innervated much more densely than other smooth muscle tissue (Samuel, Lütjen-Drecoll, & Tamm, 1996; Tamm, Flügel-Koch, Mayer, & Lütjen-Drecoll, 1995), with each cell being individually innervated [(Armaly, 1968)]. Input to the ciliary muscle is mostly parasympathetic [(Izci & Gonul, 2006), (Kaufman et al., 1991), (May & Warren, 1993), (Rohen et al., 1990)], though there is some small amount of inhibitory sympathetic innervation [(Armaly, 1968), (Baumeister & Kohnen, 2008), (Charman, 2008), (Culhane

et al., 1999), (Stark, 1988)]. Studies of the electrical activity of the ciliary muscle show that the muscle is not spontaneously active [(Samuel et al., 1996), (Suzuki, 1983), (Wiederholt et al., 2000)], and that muscle excitation is actuated by the neurotransmitter acetylcholine [(Suzuki, 1983)], though the junction potential change observed is small. A direct application of current to the ciliary muscle does not effect a muscular contraction, and action potentials are not observable [(Suzuki, 1983)]. Overall, the ciliary muscle can be said to rely more heavily on a neural contribution than other tissues.

1.3.1.1 Zonules

Perhaps one of the most difficult topics in accommodation is the action and arrangement of the zonules. The zonules are the elastic fibers that allow the ciliary muscle to mechanically move the lens. These fibers can be thought of as rubber bands: pulling on them increases tension, while pushing them in causes them to slacken.

The zonules have, at different times, been divided into different groups, based on their position and function [(Atchison, 1995), (Baumeister & Kohnen, 2008), (Flügel-Koch et al., 2016), (Stark, 1988), (Rohen, 1979)]. As additional research uncovers new types of zonules, this classification becomes increasingly complex. A recent study [(Goldberg, 2015), (Goldberg, 2011)] proposed that zonules be classified in three different groups: an anterior group, composed of the anterior zonule fibers, which cause the main shape changes in the lens; a crossing group, consisting of the anterior vitreous zonule and the posterior insertion zone-to-lens equator zonule (PIZ-LE), whose main function is to provide support and stabilization to the lens; and, finally, a posterior group, composed of the intermediate vitreous zonule, the posterior vitreous zonule, and the pars plana zonule, which is involved in the transfer of energy necessary for the accommodation process, and the prevention of trauma to underlying tissue.

Much could be said of the variation in origin and insertion of the different zonules, but, mechanistically, it is only important that, by attaching and originating in different locations, the zonules apply varying forces to the lens and other accommodative structures. For a more detailed discussion of the workings of the zonules, and the

nomenclature, the reader is directed to the computer-generated models by Goldberg (2015).

1.3.1.2 Lens and Lens Capsule

The lens is the structure that is deformed to allow light to be clearly focused on the retina [(Klaproth, et al., 2011)]. For the purposes of this discussion, two lenticular structures are important: the lens and the lens capsule. Both will be discussed in detail.

The human crystalline lens is composed of elongated anuclear fibers joined together by ball-and-socket-like connections [(Koretz & Handelman, 1986), (Stark, 1988)]. There are two distinct areas within the crystalline lens, namely, the cortex (outer layer) and the nucleus (inner layer). These areas differ in their behavior during accommodation, as well as in their refractive indices [(Baumeister & Kohnen, 2008)]. As a whole, the lens can be described as a viscoelastic body, with the elastic module of the lens approximately three times smaller than that of the lens capsule [(Koretz & Handelman, 1982)]. The entire structure is necessarily transparent, and, though the shape as a whole can be described as biconvex, the anterior and posterior surfaces differ in curvature [(Atchison, 1995)] and thickness [(Fisher, 1969)].

An acellular elastic covering of the lens, the lens capsule is composed of collagen fibers [(Atchison, 1995), (Baumeister & Kohnen, 2008), (Stark, 1988)]. The capsule acts as a force distributor [(Croft et al., 2008), (Nankivil et al., 2015)], shaping the lens during accommodation based on the balance of the forces applied to it by external elements. Rounding of the lens occurs based on the force acting normal to the lens on the elastic lens capsule, and on the viscoelastic lens.

During accommodation, the lens is pushed inward, which causes thickening in the middle portion, forward anterior movement, and a slight posterior movement at the posterior surface [(Drexler et al., 1997), (Ostrin & Glasser, 2005)]. The radius of the lens changes linearly per diopter of accommodation, though the anterior surface of the lens changes considerably more than the posterior surface [(Du et al., 2012), (Koretz &

Handelman, 1982), (Nankivil et al., 2009)]. Changes in thickness are produced by the axial movement of the lens nucleus, accompanied by a decrease in lenticular diameter [(Ostrin & Glasser, 2005)].

1.3.2 Neural Control of Accommodation

As mentioned previously, the ciliary muscle is innervated by both the parasympathetic and, to a lesser extent, sympathetic pathways [(Baumeister & Kohnen, 2008), (Charman, 2008), (Kaufman et al., 1991), (Tamm et al., 1995)]. Parasympathetic innervation mediates the excitatory response, while sympathetic innervation is inhibitory. The pathways differ in location and the components involved. It is beyond the scope of the current work to examine each aspect of the autonomic nervous system involved in the process of accommodation; rather, the following sections serve as a brief introduction to the neural control of accommodation.

Parasympathetic innervation dominates the ciliary muscle and the characteristics of the accommodation response [(Kaufman et al., 1991)]. This pathway begins at the Edinger-Westphal preganglionic cell group, a term used to describe the cells of the Edinger-Westphal nucleus which eventually travel to the ciliary ganglion via the third cranial nerve [(Izci & Gonul, 2006), (May & Warren, 1993)]. In the ciliary ganglion, the preganglionic neurons synapse onto postganglionic neurons which, in turn, travel into the eye via the short ciliary nerve, where they innervate the ciliary muscle (and several other structures) [(Tamm & Lütjen-Drecoll, 1996)]. Within the ciliary muscle, parasympathetic activity is characterized by a quick response time and a large magnitude. An increase in parasympathetic activity leads to an increase in accommodation.

Though its role has long been controversial in the process of accommodation, the sympathetic nervous system is now generally accepted as a contributing element [(Culhane et al., 1999), (Gilmartin et al., 1992)]. Despite the fact that parasympathetic activity is universally present in humans, several studies have suggested that sympathetic innervation is highly dependent on the individual, with some individuals exhibiting much

lower levels of sympathetic innervation than others [(Gilmartin et al., 1992)]. In any case, the role played by the sympathetic nervous system during accommodation is much smaller than that of the parasympathetic nervous system.

Sympathetic input to the eye originates in the intermediolateral nucleus (located in the spinal cord), and eventually reaches the superior cervical ganglion [(Baumeister & Kohnen, 2008)]. From there, postganglionic neurons can take several pathways to reach the eye, including through both the long and short ciliary nerves and the optic canal. Sympathetic innervation in the ciliary muscle is characterized by a slow response time, a limited magnitude, and a dependence on concurrent parasympathetic activity for operation [(Culhane et al., 1999), (Gilmartin et al., 1992)]. An increase in sympathetic activity leads to a slight decrease in accommodation [(Armaly, 1968)].

Because of the response characteristics of the sympathetic component of accommodation, many have speculated about its role in accommodation [(Atchison, 1995)]. One hypothesis suggests that sympathetic accommodation is used during long periods of sustained accommodation, where a high level of parasympathetic activity is concurrently present [(Gilmartin et al., 1992)]. Others suggest that sympathetic activity can be altered with conscious thought, where mental effort changes the ratio of sympathetic to parasympathetic activity [(Atchison, 1995)].

1.3.3 Theories of Accommodation

To this day, the exact mechanism of accommodation has not been conclusively proven. The most widely accepted theory is that of Helmholtz, which states that the active action of the ciliary muscle molds the passive lens into a shape more suited for near vision [(von Helmholtz, 1867)]. Though the development of new methodologies has aided in the understanding of accommodation, and though many theories have been disproven, much still remains to be determined about the mechanism of accommodation.

Despite the fact that the Helmholtz theory is the most accepted, no discussion of accommodation would be complete without mention of anti-Helmholtzian

accommodation theories. McCollim (1989) proposed that accommodation is effected by the action of extraocular muscles, which push the lens into an accommodated state. Schachar (1992), perhaps the most famous of the anti-Helmholtzians, also proposed a theory, stating that the contraction of the ciliary muscle leads to an increase in zonular tension; this causes the lens to thin at the equator, and bulge out at the center. Neither theory is widely accepted [(Atchison, 1995)].

Most other accommodative theories accept the basic tenets proposed by Helmholtz, but postulate the involvement of different elements, such as the vitreous or choroid, in the molding of the lens [(Atchison, 1995)]. There might indeed be a role for these elements, but it has been proven that neither is the main force behind the change in shape of the lens. An additional point of controversy is the involvement of the iris. Aniridic patients can accommodate, but there is some discussion as to whether the lack of an iris decreases the maximum accommodative amplitude [(Atchison, 1995)].

1.3.4 Current Methods to Measure Accommodation

Part of the difficulty inherent in the study of accommodation is the relative inaccessibility, in terms of measurement, of the physiological components. This has spawned a plethora of measurement techniques, which, in turn, has led to contradictory results, and general confusion. Though this issue has been addressed in at least one article [(Bailey, 2011)], there is, as yet, no single measurement technique that has been accepted as a gold standard.

As discussed previously, accommodative activity originates in the Edinger-Westphal nucleus. The most natural way to induce accommodation would, therefore, be to somehow activate this area, and measure the results downstream in the eye; this process combines both stimulation and measurement to achieve results. Several groups have used this approach in rhesus monkeys [(Crawford et al., 1989), (Ostrin & Glasser, 2007)], which are fairly close to humans in terms of accommodative structure anatomy.

However, the rhesus monkey accommodative mechanism does not correlate exactly with its human counterpart [(Burd et al., 2002), (Lütjen-Drecoll et al., 2010)].

A more direct approach to determining the mechanistic properties of accommodation is achieved through the use of a donor human eye. Though this is a useful tool, if obtained from a living donor, the eye generally exhibits some pathologies that have made its removal obligatory; cadaver eyes, though they can be obtained relatively intact, are deceased tissue. Though useful for anatomical studies, neither type of donor eye can be used alone to verify neuronal pathways of accommodation, or in the stimulation of a natural accommodative response. Several researchers have used this approach concurrently with a mechanistic system designed to imitate the forces seen in the accommodating eye. Most famously, Fisher (1977) determined the force of the ciliary muscle from spinning a lens. Though the experiments are well-planned and meticulously performed, the environment is not identical to that of an intact human eye, and results are open to interpretation.

When measuring the accommodative response in a clinical setting, the advent of new technological advances has improved the imaging of accommodative processes. Accommodation can be measured in a human subject by two methods: objective accommodation, where the accommodation measurement is verified independently from the subject, and subjective accommodation, where the subject reports the clarity of his or her vision. Though subjective measurements can be useful, they are not a good measure of the true accommodative state, as the eye under-accommodates (accommodative lag) at high-demand targets [(Seidemann & Schaeffel, 2003)]. Subjective measurements can be made using negative refractive lenses in combination with a Snellen vision chart, or using a ruler on which a sliding target with thin lines is placed [(Duane, 1922)].

Pharmaceuticals, such as pilocarpine and carbachol [(Ostrin & Glasser, 2007a), (Ostrin & Glasser, 2007b), (Lütjen-Drecoll et al., 1988)], have also been used to activate the accommodative response. Theoretically, this is a viable method: components downstream from the ciliary ganglion are activated, obviating the need for upstream neural stimulation. However, several studies have found that pharmacological

stimulation of the accommodative plant does not produce the same effects as stimulation from the Edinger-Westphal nucleus. Indeed, drug-induced accommodation produces a more powerful accommodative response than that seen from stimulation of the natural neural pathway [(Crawford et al., 1989), (Ostrin & Glasser, 2007), (Ostrin & Glasser, 2005)], as well as affecting the response dynamics [(Ostrin & Glasser, 2007)].

Objective measurement techniques commonly used to evaluate accommodation include optical coherence tomography (OCT), Schleimpflug photography, goniovideography, ultrasonography, partial coherence interferometry (PCI), magnetic resonance imaging (MRI), and refractometry. Though each of these modalities allow a change in thickness, distance, or other metrical property to be measured, none can provide a direct measurement of the forces involved in the process of accommodation, or directly characterize the dynamic properties of the ciliary muscle. In other words, they provide a picture of what is happening during accommodation, but do not explain the “how” or “why.”

Using the information gleaned from these studies, several researchers have attempted to model different elements of the accommodating human eye [(Burd et al., 2002), (Hermans et al., 2006), (Koretz & Handelman, 1986), (Koretz & Handelman, 1983), (Koretz & Handelman, 1982), (Kotulak & Schor, 1986), (Schor & Bharadwaj, 2005)]. Though these models can provide a good estimate of accommodative behavior, they depend heavily upon the starting parameters, which, in turn, depend upon the measurement methods used. It is clear, then, why no one model completely explains all aspects of accommodation in the human eye, though many claim to describe the accommodation of a young eye fairly well.

1.4 Presbyopia

Presbyopia refers to the age-related inability to accommodate. Unlike myopia and hyperopia, which are conditions resulting from an abnormal eye shape, presbyopia is not dependent on the refractive errors of the eye. Necessarily, all individuals will experience

presbyopia when they reach the age of approximately fifty. Though there have been many advances in presbyopia research, the exact cause of the condition remains unknown, and there is no cure [(Atchison, 1995), (Baumeister & Kohnen, 2008), (Charman, 2008), (Kasthurirangan & Glasser, 2006), (Tamm & Lütjen-Drecoll, 1996)]. The effects of presbyopia as an age-related condition are shown in Figure 2.

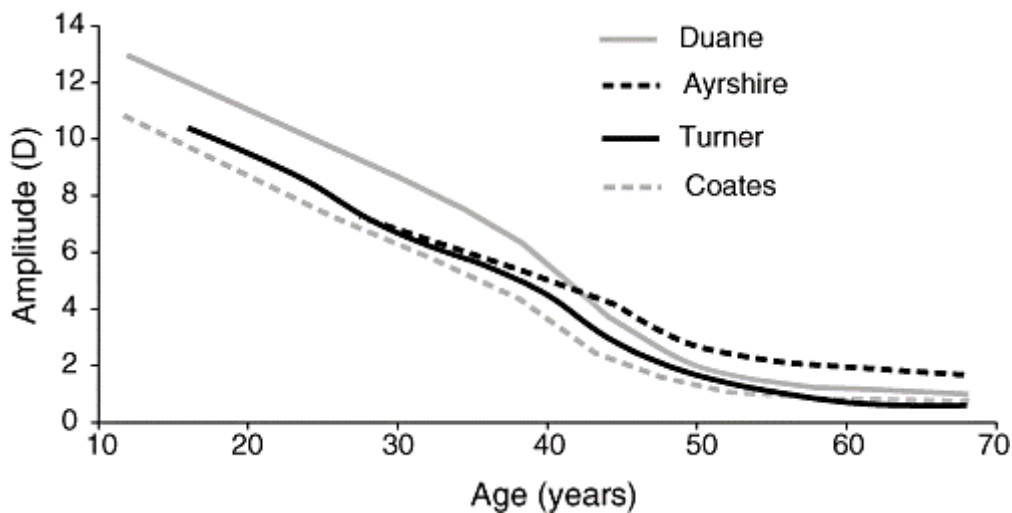


Figure 2: The decline of accommodation amplitude with age, as shown in the four traces above (from studies by Ayrshire, Duane, Turner, and Coates). Before the age of twenty, accommodation is over ten diopters; however, by the age of forty, it has decreased to almost half of that amount. From [(Charman, 2008)]; used with permission.

1.4.1 Age-Related Changes in the Accommodative Plant

With age, different structures in the anterior chamber of the eye experience changes that could potentially cause presbyopia. The most obvious culprit is the lens. Throughout life, the lens continues to grow, and, over time, hardens, and becomes more difficult to deform. It has been shown that the lens itself grows thicker [(Charman, 2008), (Richdale et al., 2016), (Richdale et al., 2013), (Strenk et al., 1999)], steeper [(Adler-Grinberg, 1986), (Richdale et al., 2016), (Richdale et al., 2013), (Strenk et al., 1999)], heavier [(Charman, 2008)], stiffer [(Charman, 2008)], and exhibits changes in its viscoelastic properties [(Beers & van der Heijde, 1996b), (Bharadwaj et al., 2009)] with

age. During accommodation, the aged lens does not deform [(Shao et al., 2015)] or move forward [(Croft et al., 2016), (Croft et al., 2013), (Dubbelman et al., 2005)] as much as a younger lens; indeed, the presbyopic lens shows an overall decrease in movement [(Croft et al., 2016), (Croft et al., 2013), (Croft et al., 2009), (Croft et al., 2006), (Croft et al., 1998)]. Going back to the earlier analogy, the movement of a presbyopic lens is akin to that of a ball filled with putty, rather than gel: it is much harder to actuate movement, though the mechanism to actuate movement has not changed.

The ciliary muscle was, for a time, a subject of debate in terms of its function in the presbyopic eye; it has now been established that the ciliary muscle retains its ability to contract, even in the presbyopic eye [(Croft et al., 2009), (Croft et al., 2008), (Lütjen-Drecoll et al., 2010), (Richdale et al., 2013), (Shao et al., 2015), (Strenk et al., 2010), (Strenk et al., 2006), (Tamm et al., 1992a), (Tamm et al., 1992b)]. Despite the fact that it is still able to contract fully, the ciliary muscle does lose mobility with age [(Croft et al., 2016), (Croft et al., 2009), (Tamm et al., 1992)]. Several changes are observable in the muscle itself, including a decrease in area and length [(Lütjen-Drecoll et al., 1988), (Sheppard & Davies, 2011), (Tamm et al., 1992)], an increase in thickness [(Strenk et al., 2010)], and a stiffening of its posterior attachments [(Croft et al., 2016), (Tamm et al., 1992), (Tamm et al., 1991)].

Though the ciliary muscle and the lens are the most mentioned structures that could contribute to presbyopia, several other changes could affect accommodation in the aging eye. The zonules change in geometry [(Burd et al., 2002), (Charman, 2008)], potentially altering the angle of the forces applied to the lens; the zonules themselves, however, do not show any changes in extension behavior with age [(Charman, 2008)]. Depending on the role that the vitreous plays in accommodation (as yet undetermined), its liquefaction [(Baumeister & Kohnen, 2008), (Koretz & Handelman, 1986)] could play a role in the decreased accommodative amplitude seen in presbyopes. The lens capsule is larger and limper [(Croft et al., 2008)], and, like the lens, exhibits age-related changes in viscoelasticity [(Heron & Charman, 2004)] and thickness [(Burd et al., 2002), (Charman, 2008)]. Other changes that accompany presbyopia include a decrease in the

space between the lens equator and ciliary body [(Charman, 2008)] and a decrease in the depth of the anterior chamber [(Richdale et al., 2016), (Richdale et al., 2013)].

1.4.2 Theories of Presbyopia

As with accommodation, the exact mechanism by which presbyopia affects the accommodative apparatus remains unknown [(Atchison, 1995), (Baumeister & Kohnen, 2008), (Charman, 2008), (Tamm & Lütjen-Drecoll, 1996)]. Most theories can be divided into two broad categories: extralenticular theories, which attribute accommodative decline to structures other than the crystalline lens, and lenticular theories, which place the blame on the crystalline lens. There are also theories which combine both lenticular and extralenticular elements. The more well-known theories will be briefly discussed here.

There are several well-known lenticular theories. The Hess-Gullstrand theory postulates that the ciliary muscle produces the same force over a lifetime, and that, due to the increasing stiffness of the lens, this force becomes unable to actuate a change in accommodation. This implies that, though the ciliary muscle is still able to exert varying levels of force, beyond a certain point, the forces do not do anything to increase the refractive power of the lens. Fincham also proposed a lenticular theory, but argued that the amount of force required to deform the lens increases over time; thus, for a presbyopic subject, the nearest focusing point reflects the maximum amount of ciliary muscle contraction available. There is evidence to both support and refute these theories [(Atchison, 1995)].

Duane (1922) proposed an extralenticular theory in which the contraction of the ciliary muscle decreases with age. This has been conclusively disproven. Other theories implicate different components, such as the choroid, stating that the loss of elasticity in these structures impedes the accommodative process.

A final broad category of theories is the geometrical theory of presbyopia. These theories reflect the lenticular view that the lens is the main cause of presbyopia, but argue that it is not the change in lenticular mechanical properties, but changes rather in size and position, which are the problem. A change in the size and position of the lens would alter the magnitude of the forces acting upon it, leading to decreased accommodative effects from ciliary muscle contraction.

1.4.3 Current Treatments for Presbyopia

Presbyopia is an inevitable consequence of aging that affects every person over the age of fifty; one would think that this would spawn the creation of numerous assistive devices. However, in reality, the options for the treatment of presbyopia are limited. Though there have been several creative attempts to solve the problem, their utility is limited in everyday life.

Probably the most widely adopted solution is the use of reading glasses. These are cheap and available, and do not require any extraordinary effort to use. However, because they are available in only one prescription, it is impossible to instantaneously change focus from a near target to a far target. For reading, they are a good solution; for other tasks, they fall short.

Several devices have attempted to correct this problem through the use of variably-refractive lenses, which are controlled by the user. A mechanical variety, Adlens[®] Adjustables (Adlens Ltd., Oxfordshire, UK), is commercially available: the user can adjust the refraction of the glasses via a knob placed on the frame. Unfortunately, though cheap, these glasses do not have a wide range of refraction, severely limiting their use to those who do not require refractive correction.

Though used primarily for the treatment of cataracts, intraocular lenses (IOLs) have become a method to restore accommodation [(Klaproth et al., 2011), (Richdale et al., 2016)]. Theoretically, if the lens is the main cause of presbyopia, replacing the

hardened lens with a more deformable substance would, indeed, solve the problem. In practice, though the lenses allow for a few diopters of accommodation, no ground-breaking results have been shown. Special accommodating IOLs have also been developed, but these have not performed much better than regular IOLs [(Klaproth et al., 2011)].

Clearly, there is a gap in our body of knowledge regarding the accommodative process and presbyopia, and this has hampered the development of treatments for presbyopia. As yet, only IOLs have attempted to harness the control mechanism of accommodation, and this solution is less than ideal. Several companies, such as Google, have attempted to develop devices to replace accommodation in presbyopes, but these plans remain in the early stages. It is the goal of this study to develop an entirely new class of device, one that will implement artificial accommodation in presbyopes, as well as to elucidate previously-unknown features of accommodation.

2. STUDIES TO MEASURE CILIARY MUSCLE ACTIVITY

2.1 Introduction

As discussed in the previous section, a severe limitation in the study of accommodation and presbyopia is the difficulty of obtaining *in vivo* measurements of the human ciliary muscle. Our goal in performing the following study was to develop a reliable way to measure the ciliary muscle electrical signals in a non-invasive manner, and to determine whether the signals obtained could be used to develop an assistive device for presbyopic subjects.

2.2 Methods

2.2.1 Electrode

Commercially-available Boston XO₂[®] (Bausch + Lomb, Bridgewater, NJ, USA) scleral lenses were pre-fabricated by the manufacturer (MPG&E Handel und Service GmbH, Bordesholm, Germany) with diameters of 20 mm, and two holes at 7 and 9 mm from the center of the lens for lead attachment. These lenses are marketed as rigid lenses that allow for high gas permeability, and are indicated for daily wear for many ocular conditions (Bausch & Lomb, 2015). To fabricate the electrodes, the lenses were first cleaned with ethanol, then heated and dried for several hours, after which gold rods were fixed in the holes using a medical adhesive (EPO-TEK 354-T, Epoxy Technology, Inc., Billerica, MA, USA). After hardening the adhesive by baking for 12 hours at 80° C, a conductive surface coating was deposited on the inner surface of the lens by cathode sputtering, resulting in two concentric 150 nm thick titanium-gold rings. Leads were then connected to the rods using a conductive adhesive (EPO-TEK H20E, Epoxy Technology, Inc.) and baked for 8 hours at 80° C. The contacts were covered with the conductive adhesive and shrink-wrap. Finally, a layer of gold was sputtered on the rings to make

contact between the electrode and the lead connection. The finished electrode is shown in Figure 3.

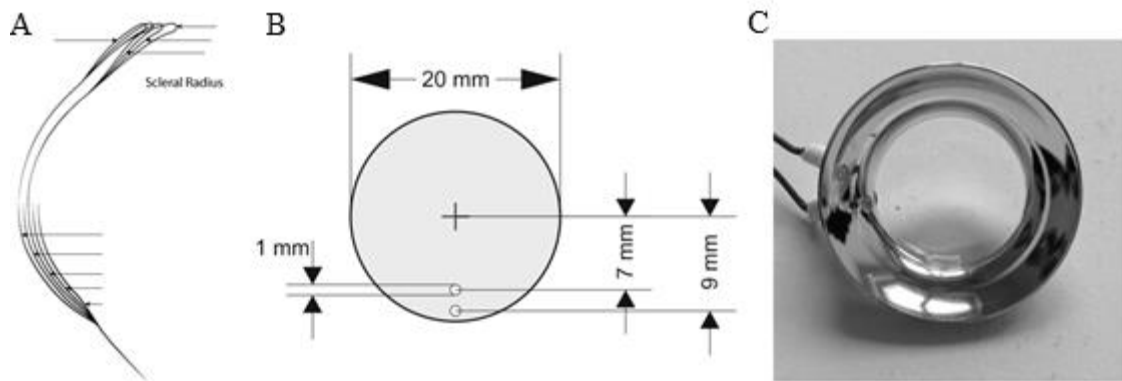


Figure 3: The Boston XO2-Tübingen contact lens electrode. A. When different scleral radii were used, lenses of different steepnesses resulted, as indicated by the arrows. B. Positioning of the holes for the connecting leads at 7 mm and 9 mm. Gold was sputtered in two concentric rings around the electrode, and the holes shown were drilled such that one lead contacted the inner ring, and one contacted the outer ring. C. View of the finished electrode, shown from the inside.

During the course of the experiment, several modifications to the lenses were made to enhance patient comfort and optimize signal quality. Namely, three different electrode sizes were fabricated, with scleral radii (Sra) of 13.25, 12.5, and 11.75 mm. These different radii allowed for a steeper (i.e. 11.75 mm) or a flatter (i.e. 13.25 mm) lens shape, in order to accommodate for a wider range of eye shapes. Lenses were chosen by the study physician to provide the best fit for the subject.

2.2.2 Visual Target Apparatus

Five accommodation targets were fabricated by the University of Tübingen Eye Hospital Workshop, each consisting of a Perspex plate illuminated by embedded white LEDs. The letter “E” was engraved on each, and was scaled in size for each plate according to the target distance. In order to restrict the viewing area of each target and provide better alignment for the participants, the plates were covered by black cardboard

frames, and the orientation of several targets was changed to allow for better target differentiation (see the inset of Figure 4).

The targets were placed on a track at set distances, with the nearest target being placed 20 cm (5 D) from the subject's eye, and the farthest target at 2 m (0.5 D). Correct placement was ensured by markings on the track, a bar between the chin rest and track, and measurement with a ruler prior to experimentation. Subjects were corrected to the farthest target (0.5 D), so that no accommodation would be needed to fixate on said target. Three intermediate targets were placed at 50 cm (2 D), 40 cm (2.5 D), and 28.6 cm (3.5 D) from the fixating eye, as shown in Figure 4. For the pupillary response test, a bright LED light was attached to the main track at a distance of 17 cm away from, and 7 cm below, the subject's eye.

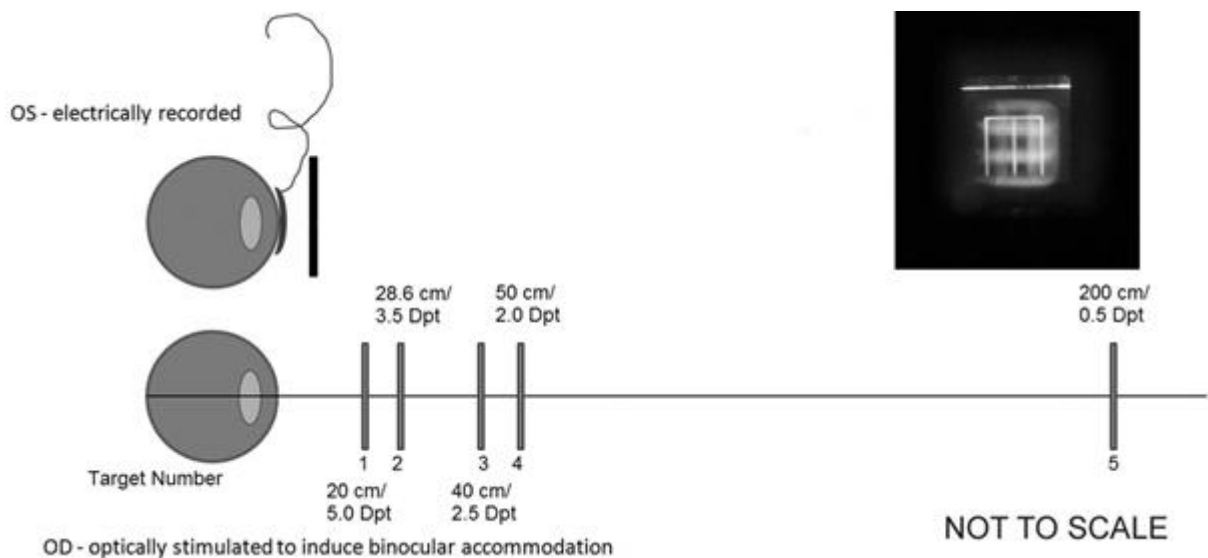


Figure 4: A diagram of the final set-up used. An electrode was placed in the left eye of the subject, which was occluded with an eye patch. The right eye was aligned with illuminated Perspex targets placed at different intervals along the track. Each target was illuminated when the subject was told to focus on it, as shown in the inset. Original figure created by Dr. Ditta Zobor.

An eye patch was used to occlude the recorded eye, while a lens holder in front of the fixating eye allowed for refractive correction. Attached to the target track at a distance of 1 m from the fixating eye was an arm on which a camera was placed, allowing for recording without interfering with the subject's focus. In most cases, the fixating eye was the right eye, and the recorded eye was the left eye, as pictured in Figure 4; however, in cases where the recorded eye was the right eye (i.e. the left eye was not suitable for recordings), the set-up was adjusted for alignment with the fixating (left) eye.

2.2.3 Power Refractor

Pupil size and accommodation of the fixating eye were monitored by an infrared photo refractor positioned in front of the subject, slightly outside the gaze pathway. Recording was performed at a 60 Hz sampling rate via a monochrome infrared sensitive USB camera that captured video images of the eye. The software detected the pupil in the video image, measured its size, the eye's refraction, and the orientation of the pupillary axis; this system also served as a gaze tracker to monitor eye movements [(Schaeffel et al., 1993)] (Figure 5).

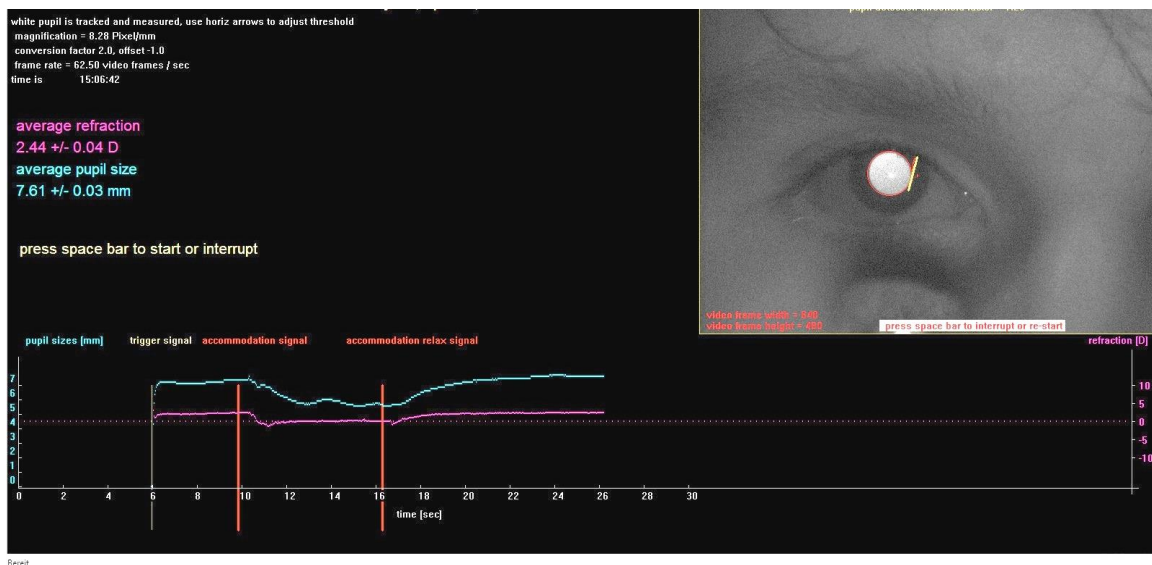


Figure 5: Real time output presentation of the photorefractor for optical measurements of accommodation. Note the 3 vertical lines indicating the time point of the trigger signal, the acoustical (near) accommodation

signal, and the acoustical signal to relax accommodation, respectively. The blue trace represents the size of the pupil, and the purple traces shows the measured refraction in response to the accommodation target.

2.2.4 Electrophysiological Recordings

Electrical signals were recorded with an electrophysiological recording system (espion e², Diagnosys LLC, Lowell, MA, USA), which was connected to the combined infrared pupillometer and photorefractor, and to the each of the five targets and LED described in Section 2.2.2. Settings used for the espion signal acquisition are shown in Table 1.

Table 1: Espion program settings used for the different tested protocols. The flashlight test was much shorter than the accommodation step protocol test, and, therefore, required different settings.

Settings	Accommodation Step	FL (flashlight test)
Sampling frequency	1000 Hz	1000 Hz
Recording time	51000 ms	15000 ms
Sweeps per average	4	15
Linear drift removal	Off	On
Baseline removal	On (baseline: 0 – 1000 ms)	On (baseline 0 – 1400 ms)
Band-pass filter	Off	On (band-pass: 0.1 – 300 Hz)

The targets and LED could be illuminated independently from each other. The different systems were interconnected and controlled using custom software running on a microcontroller (ATMega 8515, Atmel Corporation, San Jose, CA, USA), whereby the autorefractor acted as the leading system. Each time a new recording sequence was started, the autorefractor triggered the microcontroller using a serial connection; the microcontroller was responsible for illuminating the target according to the selected protocol and for triggering the electrophysiological recording system through its trigger-in port.

Since all parts of the system shared a common trigger (controlled by the microcontroller), data of all modalities (pupil diameter, refraction, electrophysiological recordings) used the same timeline and could therefore be merged offline. For each of the protocols, the sampling frequency was 1 kHz, the recording time was 51 s (15 s for the pupillary response test), four sweeps were performed, the sweeps were averaged,

baseline removal (from 0-1 s) was turned on, and both linear drift removal and band-pass filtering were disabled.

2.2.5 Subject Selection

The experimental protocol was approved by the local ethics committee, and conformed to the tenets of the Declaration of Helsinki. Each subject signed a document of informed consent prior to participating in the experiment. Subjects were selected for three different patient groups: control/young subjects, presbyopes, and pseudophakes. These groups are discussed in detail below. Prior to experimentation, all subjects underwent an ophthalmological examination, including visual acuity, funduscopy, intra-ocular pressure, and slit-lamp examinations. Data from these examinations were used to determine the amount of refractive correction required for the experiment.

2.2.5.1 Control Group

Ten subjects (age range: 21-28 years, median age: 26.5) were chosen from the student body of the University of Tübingen. This age range was chosen due to the known absence of presbyopia in subjects between the second and third decade of life. It should be noted that there is no significant difference in accommodative ability between male and female subjects [(Duane, 1922)]; therefore, the gender of the participant was not a factor in subject selection. Two subjects were myopic (NG: -1.0 D, ZL: -0.75 D) in the measured eye; all others were emmetropes. Table 2, below, gives an overview of the subjects.

Table 2: An overview of the ten control subjects who participated in the study, together with the electrode and corrective lens used in the experiment.

Subject	Gender	Age	Electrode Number	Corrective Lens (D)
AR	F	22	2	+0.5
CH	M	23	1	+0.5
CL	M	28	2	+0.5
ER	F	23	1	+0.5
KB	M	27	2	+0.5

NG	M	28	2	-1.0
SD	M	21	2	NA
SK	M	27	1	+0.5
YO	M	26	1	+0.5
ZL	M	27	2	-0.75

2.2.5.2 Presbyopic Group

Presbyopic subjects were recruited from the faculty and patients at the University of Tübingen Eye Hospital. Three volunteers (AK, EH, and NS) declined to participate in repeat measurements. The electrode number noted was the one from which the data used in the final analysis were taken. These ten subjects (age range: 57-69 years, median age: 64) are summarized below (Table 3).

Table 3: An overview of the ten presbyopic subjects who participated in the study, together with the electrode number and corrective lens used for the experiment.

Subject	Gender	Age	Electrode Number	Corrective Lens (D)
AD	F	64	2	-0.75
AK	F	57	2	+4.5
AN	F	65	2	+2.0
EH	F	69	1	+1.75
EK	F	64	1	+0.5
ES	F	64	1	+1.25 -3.5 96°
NN	M	68	1	+0.5
NS	F	58	2	-2.5
RP	M	61	2	-1.5
TZ	M	68	4	+0.25 -1.25 90°

2.2.5.3 Pseudophakic Group

Pseudophakic subjects (age range: 64-74 years, median age: 70) were recruited from the faculty and patients at the University of Tübingen Eye Hospital. Table 4, below, shows an overview of the pseudophakic subjects, and the type of lens implanted in the measured eye.

Table 4: An overview of the pseudophakic subjects who participated in the study, together with the electrode number and corrective lens used in the experiment. The IOL model implanted in the recorded eye is also shown.

Subject	Gender	Age	Electrode Number	Corrective Lens (D)	IOL Model
AD	F	64	4	+4.0	SN60AT Acrysof
DG	F	73	4	+1.25	Tecnis PCB00
DH	F	70	2	+0.5	Tecnis PCB00
EL	F	74	2	+1.5	Tecnis PCB00
FV	M	74	4	+0.5	Tecnis PCB00
HH	M	73	1	+0.5	AMO AR40e
LG	F	69	3	+0.5, -1.25 175°	Tecnis 2CB00
LK	F	68	2	+3.5	Tecnis ZA9003
LW	M	70	2	+0.5	Tecnis ZA9003
SR	F	70	4	+1.25	Tecnis PCB00

2.2.6 Protocol Development

Prior to the development of the final protocol used, the Accommodation Step measurements, two different measurement protocols were used. The first, called the Long Duration protocol, was developed after the observation that presbyopic subjects exhibited a relatively long lag time between the accommodation trigger and their accommodation response. It was thought that, by introducing a test where the subject would have to concentrate for a longer amount of time on the target, a more accurate measurement of the presbyopic muscular responses could be recorded; additionally, the potential duration of accommodation could be established. This protocol is the basis of the Accommodative Step protocol, which was the final experimental protocol. It is interesting to note that a presbyopic subject is capable of sustaining an accommodative response over a long period of time (here, 10 s). The Long Duration protocol is shown in more detail in Figure 6.

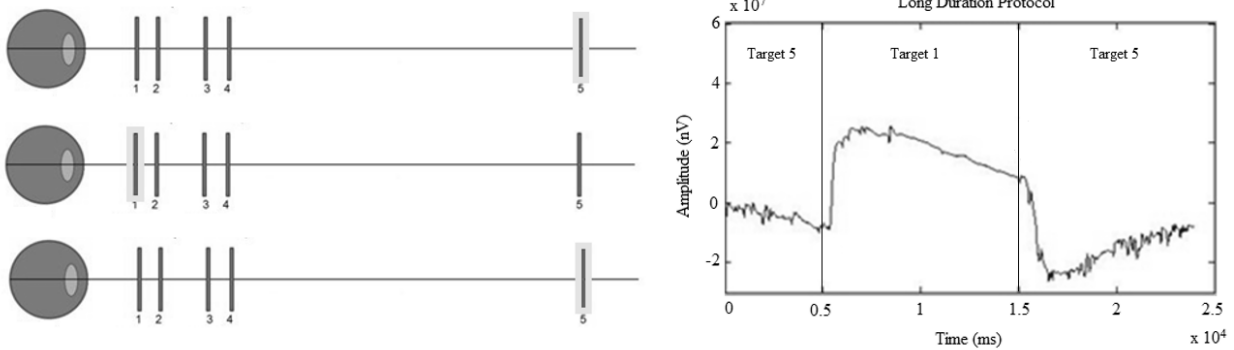


Figure 6: The long duration protocol, with experimental results from presbyopic subject TZ. After starting at Target 5 (0.5 D) for 5 s, the subject was cued to focus on Target 1 (5 D) for 10 s before returning to Target 5. The lines on the response graph show the points at which the subject was cued to change targets.

A second protocol, called the Staircase protocol (Figure 7), was also developed over the course of the measurements. The Staircase protocol alternated 5-second intervals of focusing on the far target (Target 5, 0.5 D) with 5-second intervals of focus on the near targets (1, 2, 3, or 4; 5, 3.5, 2.5, and 2 D, respectively). Two variations of the staircase protocol, one going from the highest to the lowest accommodation (1, 2, 3, 4), and one going from the farthest accommodation (4, 3, 2, 1) were explored. The Staircase protocol was modified to include 7-second intervals, to meet the problem of the lag in presbyopic accommodation. Though this protocol was successful in emmetropic subjects, it was difficult for many presbyopic subjects, due to the long testing time (45 s). For this reason, and because the protocol necessarily led to more blink artifacts in the data from the longer measuring time, it was abandoned in favor of the Accommodation Step measurements.

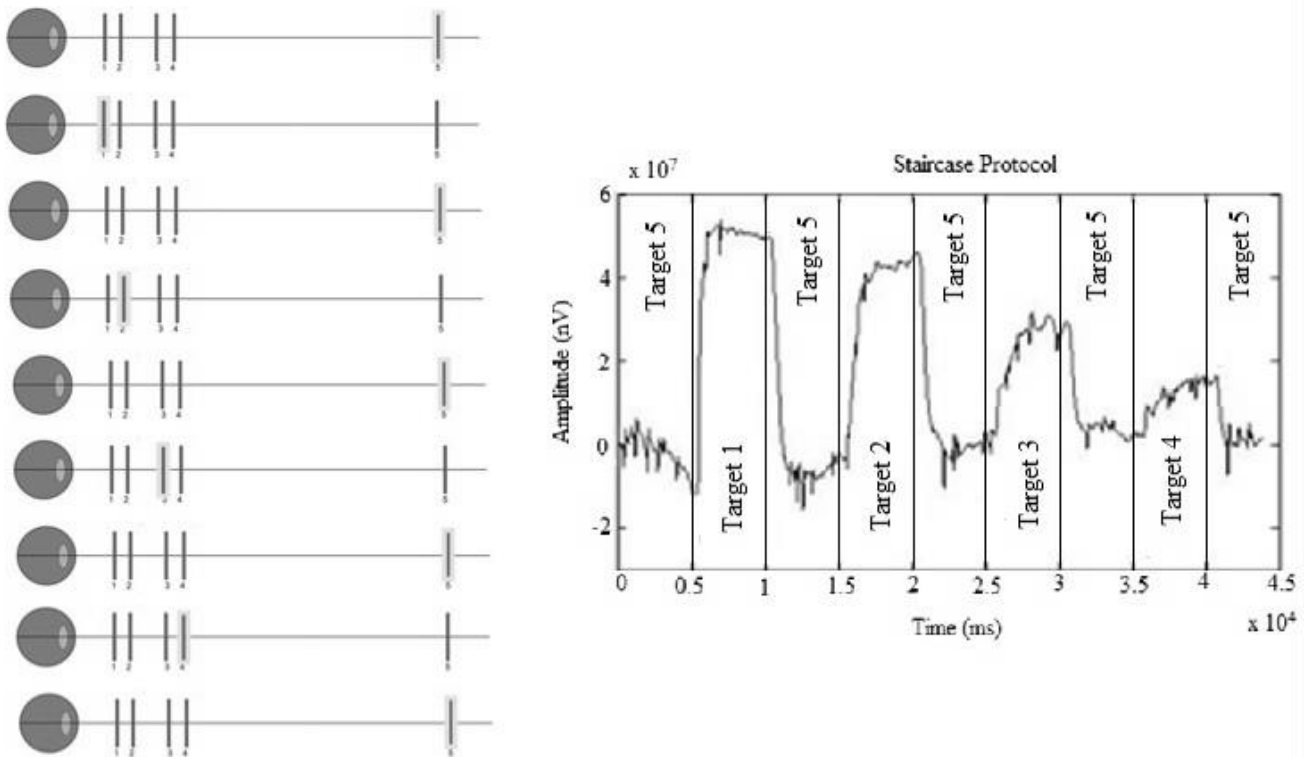


Figure 7: The staircase protocol, with experimental results shown on the left. On the right is the sequence of targets, as seen by the subject. The black lines on the signal graph represent the points at which the subject was signaled to change targets. The data shown were recorded from control subject CH.

2.2.7 Experimental Procedure

2.2.7.1 Initial Set-Up

Prior to the arrival of the subject, the contact lens electrode was first cleaned. Briefly, the electrode was immersed in storage solution (Boston[®] Aufbewahrungslösung, Bausch + Lomb) twenty-four hours before the experiment. Immediately before application, the electrode was cleaned with a lens cleaning solution (Boston[®] Linsenreiniger, Bausch + Lomb) and rinsed with a sterile saline solution.

In order to ascertain the fidelity of the electrode, a custom probe was used that delivered a voltage of either 410 μV or 820 μV DC to the rings of the electrode. The

electrode output was then measured with a multimeter (UNI-T[®] UT803 True RMS Multimeter, Uni-Trend Technology Limited, Dongguan City, China).

The subject was instructed to align his or her fixating (non-recorded) eye with the targets, such that the targets appeared to be superimposed. Alignment was further evaluated with the gaze tracker, and the subject was encouraged to practice gazing at the targets prior to experimentation. A ground electrode was positioned at the center of the subject's forehead. Local anesthetic eye drops (Novesine[®] 0.4%, OmniVision GmbH, Puchheim, Germany) were applied two times at short intervals to the recorded eye to diminish corneal reflexes and corneal irritation. The contact lens electrode was then filled with lubricating gel (Vidisic, Bausch + Lomb), and placed in the recorded eye. The position of the electrode was adjusted until the rings of the electrode were centered on the eye with minimal air bubbles, and the leads were taped onto the subject's temporal orbital rim to prevent misalignment of the electrode. Electrode resistance was measured in espion to evaluate positioning and fit; measurements were taken at a resistance of less than 5 k Ω . All measurements were performed in a quiet room, with light conditions standardized and controlled prior to each measurement.

In some cases, it was difficult to track the pupil consistently, generally due to a large pupil (in control subjects), ptosis, the combination of two lenses for refractive correction, or bright reflections from the skin around the eye. When the pupil was too large to be tracked, light was introduced to the room (i.e. a door was opened). In cases of ptosis, the subject was instructed to keep his or her eye open; when necessary, tape was additionally used to hold back the eye lid. In other cases, the parameters were adjusted until the best consistency for recording could be found.

When the electrode did not fit well, or when the electrode was moved by a blink, occasional dislodgement of the electrode from the recorded eye often resulted. At such times, all recording was stopped, and the electrode was replaced in the subject's eye. When this occurred, it was noted on the subject data sheet, and the trial run was repeated.

2.2.7.2 Pupillary Response Trials

To evaluate the electrical signal produced by pupil contraction, a pupillary response trial was performed prior to the Accommodation Step measurements. The subject was instructed to focus on the target at 0.5 D (2 m), and to maintain focus on that target for the duration of the test. For five seconds, only the 0.5 D target was illuminated; after this, the bright LED was illuminated for five seconds. The test ended with the illumination of the 0.5 D target for an additional five seconds, for a total time of fifteen seconds. This test was performed four times per subject, and the responses were averaged. If the pupillary responses were higher than the subsequent Accommodation Step measurements, the subject was excluded from final data analysis, since the accommodation signal was then too small to be distinguishable from the pupillary response. This happened with only one subject (pseudophakic subject DG). The pupillary response test, with an example recording, is shown in Figure 8.

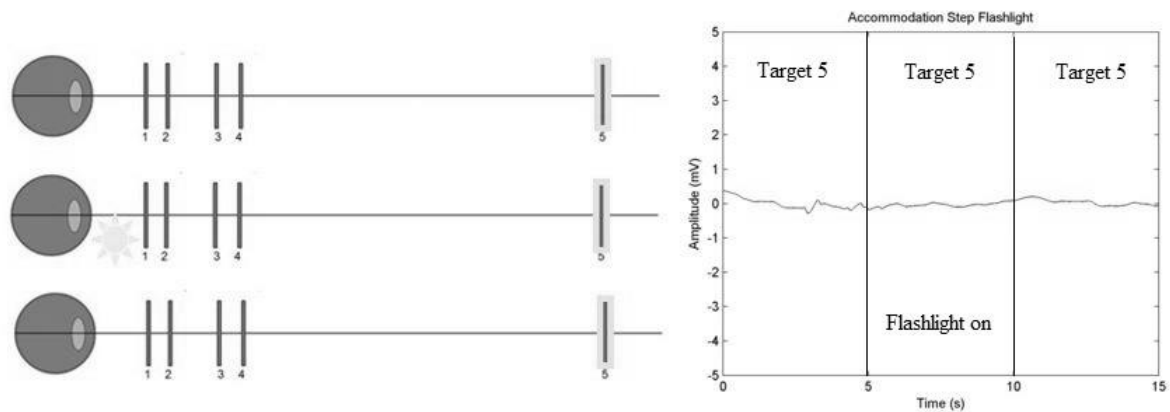


Figure 8: The pupillary response test. This test was used to ascertain the amount of signal caused by the pupillary response, as opposed to the ciliary muscle. The yellow boxes represent the target upon which the subject was instructed to focus. After focusing on the far target for 5 s, a bright LED light was turned on for 5 s; subsequently, the LED was turned off, and an additional 5 s interval was recorded.

2.2.7.3 Accommodation Step Measurements

The Accommodation Step measurements consisted of four accommodation steps, starting and ending each time at the far (0.5 D) target. At the beginning of the test, the

subject was instructed to focus on the 0.5 D target (10 s); at an auditory signal, the subject focused on the next illuminated target (either 5 D, 3.5 D, 2.5 D, or 2 D) for 15 s. Another auditory signal cued the participant to look back at the 0.5 D target, where recording continued for another 20 s. This test was performed four times per accommodation target. Targets were tested from smallest to largest accommodation effort, and repetitions were performed as necessary. For presbyopic and pseudophakic subjects, verbal encouragement was given to ensure that the subjects were continuously attempting to focus on the target, regardless of the subject/s visual feedback (or lack thereof). The tests are shown in Figure 9, Figure 10, Figure 11, and Figure 12.

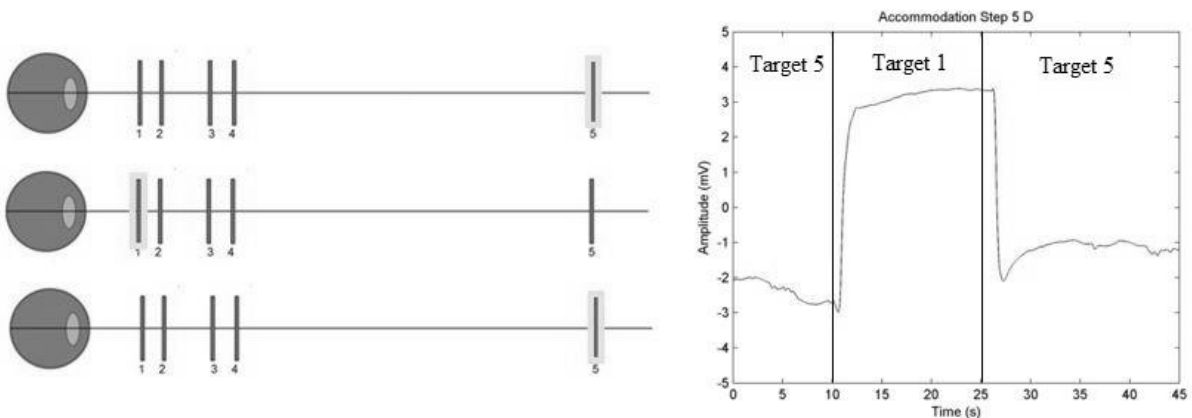


Figure 9: The 5 D Accommodation Step test. An example recording is shown on the right. The black lines in the recording indicate when the subject was cued to focus on a different target. For this particular test, the subject was instructed to focus on the nearest (5 D) target for 15 s, after first focusing on the farthest target (0.5 D) for 10 s. Finally, the subject was cued to focus on the farthest target for an additional 15 s.

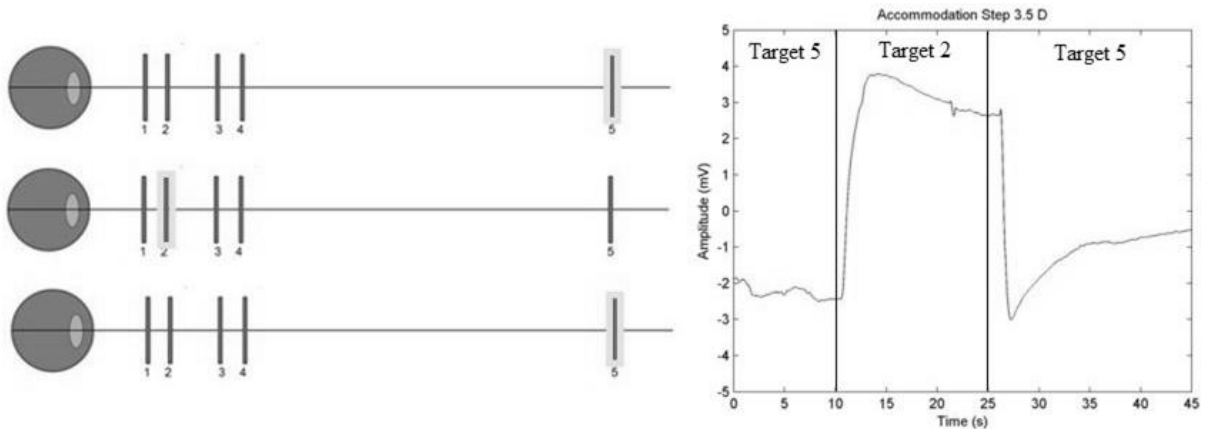


Figure 10: The 3.5 D Accommodation Step test. An example recording is shown on the right. The black lines in the recording indicate when the subject was cued to focus on a different target. For this particular test, the subject was instructed to focus on the 3.5 D target for 15 s, after first focusing on the farthest target (0.5 D) for 10 s. Finally, the subject was cued to focus on the farthest target for an additional 15 s.

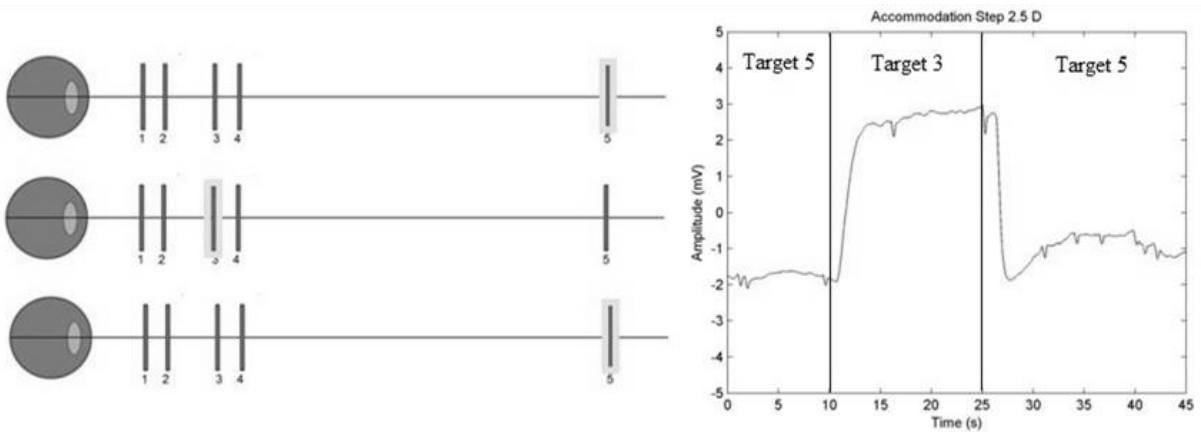


Figure 11: The 2.5 D Accommodation Step test. An example recording is shown on the right. The black lines in the recording indicate when the subject was cued to focus on a different target. For this particular test, the subject was instructed to focus on the 2.5 D target for 15 s, after first focusing on the farthest target (0.5 D) for 10 s. Finally, the subject was cued to focus on the farthest target for an additional 15 s.

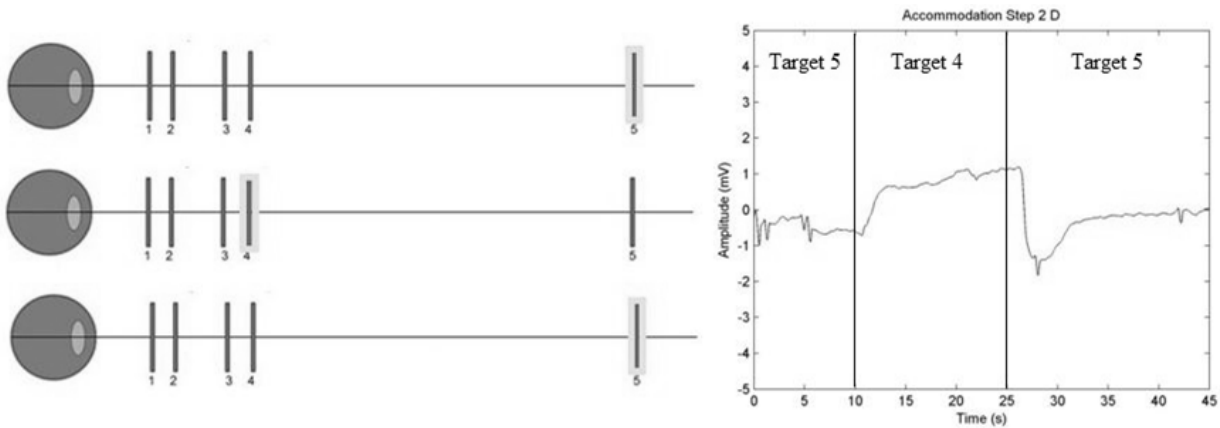


Figure 12: The 2 D Accommodation Step test. An example recording is shown on the right. The black lines in the recording indicate when the subject was cued to focus on a different target. For this particular test, the subject was instructed to focus on the 2 D target for 15 s, after first focusing on the farthest target (0.5 D) for 10 s. Finally, the subject was cued to focus on the farthest target for an additional 15 s.

2.2.8 Testing for Signal Sources Unrelated to Accommodation

Due to the amount of potentials and artifacts recorded by the contact lens electrode, it was necessary to ascertain which among these signals was, in fact, related to accommodation. In order to confirm that the signals recorded were the result of accommodation and not the result of other systems, several tests were performed. These tests are described below.

2.2.8.1 Extraocular Muscle Activity

2.2.8.1.1 The 17 Degree Test

To explore the effects of extraocular muscle activity on the recorded signal, the 17 Degree test was developed. An emmetropic subject was instructed to fixate on the 0.5 D target for 10 s. After this, the subject was instructed to shift his gaze to focus on a black mark located at the same angle and height as the 0.5 D target, but at a 17° viewing angle from the same 0.5 D target. When 15 s had elapsed, the subject was verbally instructed to once again focus on the 0.5 D target. The set-up for this test and the recorded signal from a subject are shown below in Figure 13.

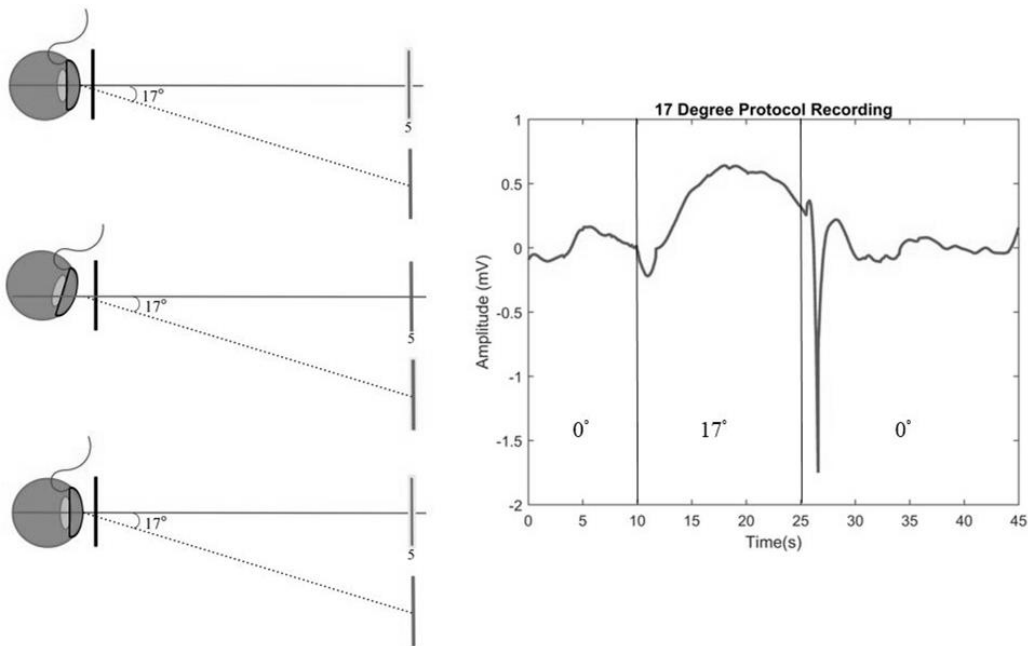


Figure 13: Diagram of the 17 Degree protocol set-up, and an example recording from a subject. Initially, the subject was instructed to look at the far target (number 5) used in the Accommodation Step protocol. After receiving a signal to switch positions, the subject shifted his gaze to a black mark placed at the same height and distance, but at a 17 degree viewing angle. Finally, the subject looked back at the original target.

2.2.8.1.2 Side-by-Side Protocol

Another protocol used to evaluate the effect of extraocular muscle signals on the recorded signal was the Side-by-Side protocol. This test functioned as a negative control, testing the signal measured when the recorded eye remained stationary. The set-up and recorded data are shown in Figure 14.

The recording procedure for the Side-by-Side protocol was the same used in the final trial protocol, the Accommodation Step protocol (see Section 2.2.7.3). However, in the Side-by-Side protocol, the recorded eye, rather than the fixating eye, was aligned with the targets. In addition to the electrophysiological recordings performed, subjects were also monitored with a webcam in real-time, thus allowing for the monitoring of any movement of the eye.

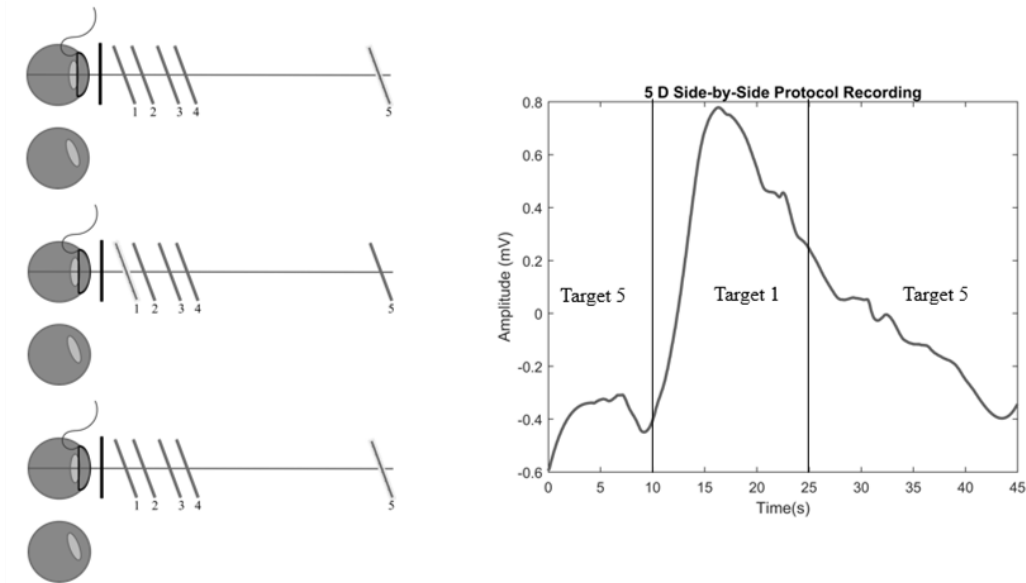


Figure 14: An overview of the Side-by-Side protocol. On the left, a diagram of the 5 D Side-by-Side protocol is shown. On the right, the signal recorded from this protocol is graphed. The vertical lines indicate transition points at which the subject was signaled to focus on a different target. As can be seen from the figure, the recorded eye, rather than the fixating eye, was aligned with the targets to minimize convergence movements.

2.2.8.2 Intraocular Muscle Activity

In addition to ascertaining the extent of extraocular muscle involvement, the activity of intraocular muscles, other than the ciliary muscle, were measured for contribution to the recorded signal. Several tests were performed: the Flashlight or Pupillary Response test (described in Section 2.2.7.2), an electrode placement test, and pharmacological tests.

2.2.8.2.1 Flashlight Test

For more information on this protocol, the reader is directed to Section 2.2.7.2.

2.2.8.2.2 Electrode Placement

As previously mentioned, several different electrodes were fabricated over the course of the study. During the clinical measurements, it became apparent that the fit of the lens was a key contributor to the quality of the resulting measurement. Several subjects seemed to exhibit a reduced accommodation amplitude, or even reversed signal polarity, as the experiment progressed. The cause was generally attributed to be the fit of the electrode, as the subject in question usually complained of poor fit (i.e. the electrode fell out of the eye), or it was noticed during the test period that the electrode was incorrectly centered on the eye. To quantify this effect, one presbyopic subjects was tested by intentional misalignment of the electrode during the 5 D Accommodation Step test. The result (and a comparison to the normal results from the subject) is shown in Figure 15.

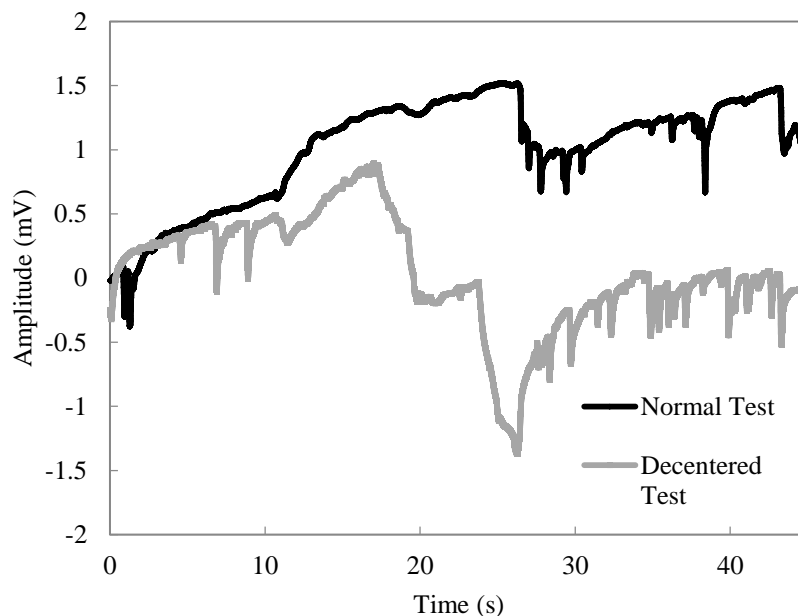


Figure 15: 5 D Accommodation Step test results with a properly fit electrode, and with an intentionally decentered electrode (subject TZ). The blue line represents a properly fit electrode, and the orange shows the same electrode positioned incorrectly on the eye.

Anecdotally, one presbyopic subject (RP) was tested with one lens on his first trial, and a different lens on a repeat visit. The second lens, with a reduced scleral radius, not only fit better, according to the subject, but resulted in recordings of a higher quality

than those of the first visit. Though it was not possible to custom-fit each subject, the electrodes with smaller Sras generally resulted in better signal quality due to tighter fits, and, subsequently, better contact with the underlying surface.

2.2.8.2.3 Pharmacological Measurements

On a subset of pseudophakic and control subjects, phenylephrine (Neosynephrin-POS[®] 1.25%, URSAPHARM Arzneimittel GmbH, Saarbrücken, Germany) was used. By using a concentration below the commercially-available 5%, it was thought that the drug would paralyze the pupillary muscles while still allowing the accommodative apparatus to function normally. Five pseudophakes and five control subjects participated in these experiments.

Cyclopentolate (Cyclopentolate 1% “Thilo”, Alcon Couvreur N.V., Puurs, Belgium) was also used to paralyze the entire intraocular musculature of the eye. Drops were applied a total of three times at ten-minute intervals, with the final recordings being performed twenty minutes after the instillation of the last dose. Pupillary responses were also checked to verify the functionality of the drug. Five control subjects participated in this experiment.

For both of the pharmacological experiments, only the last two steps (3.5 and 5 D) of the Accommodation Step protocol were tested, since these were the steps that should have elicited the greatest accommodation response normally. In cases where one subject participated in both drug trials, the phenylephrine experiments were performed before the cyclopentolate experiments. For each treatment, in cases where normal Accommodation Step tests were performed on the same day as Accommodation Step tests with pharmaceutical interventions, the normal tests were always performed first.

2.2.9 Data Analysis

2.2.9.1 Recording Quality Assessment

“Good” trials were defined as trials in which the Flashlight protocol response amplitude was not the maximum signal amplitude observed for the subject, artifacts were rare, and direct current (DC) drifts were moderate. Though the Flashlight test could be influenced by such factors as blink artifacts, it should still not have produced a stronger signal than the accommodation signal if the responses were indeed separate. Due to the dynamic nature of the ocular environment, which involves fluctuations of different aqueous fluids, there was a persistent DC drift observed in almost all recordings; these were removed where possible.

For each subject, only the best trial results were used for the final amplitude analysis. This was applicable only to subjects that underwent the same test more than once (the presbyopic and pseudophakic groups). Generally, repeat results were not of the same quality as the original results, with original results yielding better responses (there were, however, exceptions to this rule). It was thought that, by averaging the data from both experimental sessions, several dynamic trends would be lost; additionally, because “bad” data usually contained very large outliers, this would have skewed the data.

2.2.9.2 Data Preparation

For each subject, the four test signals recorded for each target were averaged together. Test signals were removed from the final averaged signal if an artifact was present that greatly distorted the response. This situation did not occur frequently, and was generally the result of signal saturation, misplacement of the electrode, or strong, persistent blinking. If artifacts were persistently observed during a single trial, the trial was repeated during the same experimental session when possible.

To further process the data for analysis, the averaged traces were put into a custom MATLAB (The Mathworks, Inc., Natwick, MA, USA) program. A linear detrend was applied to remove drift, and a Savitsky-Golay filter (third order, size 509) was applied to smooth the data. Preliminary calculations were performed, including slope calculations of both accommodation and disaccommodation (two-point calculation), average over the

baseline, and response tonicity. All data were visually inspected, and, when necessary, parameters (i.e. window size) were adjusted to find the best approximation of the desired quantity. Modifications were necessary only when artifacts were present that distorted the signal; in these cases, the window parameters were adjusted to avoid the artifact.

2.2.9.3 Maximum Accommodative Amplitude Calculations

After the raw data was prepared for analysis, another custom MATLAB program was used to estimate the maximum accommodation amplitude. Each of the traces were graphed and visually inspected, and the approximate times of onset and offset were noted. Based on these times, the data sets were split into three different groups. The first group, the time before the onset, was filtered using a polynomial fit (sixth order); this fit was subtracted from the data. A second group, representing the accommodation response, was linearly detrended, in order to preserve the characteristics of the response curve. To this group was added the absolute value of either the beginning or ending point of the segment, whichever was smaller. The final section, post-response, was fitted with a fifth order polynomial; this fit was then subtracted from the data. After the separate analyses, the data were smoothed with the same Savitsky-Golay filter as that described above, concatenated, and graphed.

2.2.9.4 Normalization of Data

Because there was a large variation between individuals of the same group, subject results were normalized to the maximum signal value (on Accommodation Step tests only, or tests without pharmacological intervention) achieved by the individual. In the pharmacological experiments, this maximum value was often exceeded; in these cases, the experiment was almost always performed on a different day from the control measurements. The normalized values were subsequently used in the comparison of different group target/amplitude relationships.

2.2.9.5 Dynamics Calculations

To evaluate the fits to a model commonly used in the literature , the accommodation and disaccommodation curves were imported into MATLAB and fit to either

$$y = A \left(1 - e^{-t/\tau} \right)$$

for accommodation, or

$$y = A \left(e^{-t/\tau} \right)$$

for disaccommodation. The curve fitting toolbox in MATLAB was used to calculate the fit parameters, as well as the errors. A Levenberg-Marquardt algorithm was generally used for fitting the curves, though, in cases where parameters were specified, a Trust-Region algorithm was used instead.

To assess accommodative dynamics, additional tests were performed. Each cleaned and averaged data set was differentiated twice using MATLAB to create both velocity and acceleration profiles for each data point. The maximum accommodation and disaccommodation velocities and accelerations were found by using the MAX and MIN functions over the expected response time (10-15 s for accommodation, 25-30 s for disaccommodation) in Excel 2013 (Microsoft Corp., Redmond, WA, USA).

Statistical analyses for the accommodation and disaccommodation dynamics were performed using IBM SPSS Statistics (IBM Corporation, Armonk, NY, USA). Comparisons between group means were performed using a paired-t test, with a significance level of 0.05.

For all accommodation tests under normal conditions, n=10 for the presbyopic group, n=9 for the pseudophakic group, and n=9 for the control group (unless indicated otherwise). Reasons for exclusion are presented in the previous sections.

All graphs were created using MATLAB; statistical analyses were performed with Minitab (Minitab Inc., State College, PA, USA), IBM SPSS Statistics (IBM Corporation), MATLAB (The Mathworks, Inc.), and Microsoft Excel 2013 (Microsoft Corp.).

2.3 Results

2.3.1 General Group Signal Characteristics

2.3.1.1 Control Group

The control group generally produced the clearest, largest responses out of all the groups. With the power refractor, it was often difficult to consistently record the gaze in a darkened room, due to the large size of the young pupil. Therefore, for many of the subjects, a door was opened to let in natural light and reduce the size of the pupil.

One subject, ER, was excluded based on the prevalence of flat lines and blink artifacts in the data measurement traces, which negated the possibility of intra-subject comparisons. ER also exhibited an atypical response pattern, possibly due to fatigue. Subject ZL reported that he experienced difficulties in accommodation. Another subject, SD, exhibited a high sensitivity to the recording electrode, leading to a noisy response (many blink artifacts). To combat this, anesthetic drops were instilled in both the recorded and the fixating eye. Subject SD was, additionally, not measured with the standard corrective lens of + 0.5 D, as he reported that such a lens blurred his vision. Both ZL and SD exhibited responses that were in accordance with an accommodation response; therefore, their results were included in the final analysis.

An example recording from one control subject, SK, is shown in Figure 16.

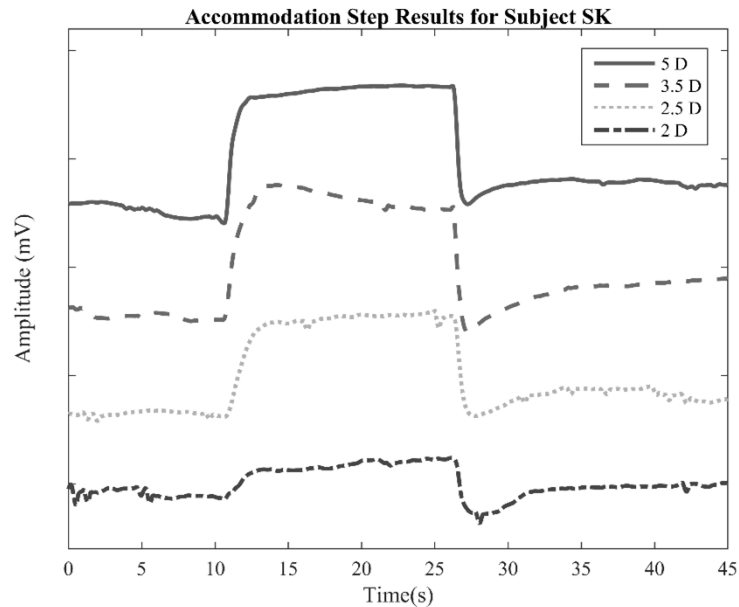


Figure 16: Recordings using the Accommodation Step protocol for control group subject SK. The baselines have been staggered to allow the accommodation response curves to be more easily seen. In this subject, and in the control group in general, signal magnitudes routinely exceeded 1 mV, with some subjects exhibiting a maximum accommodative amplitude of several millivolts for nearer accommodation targets. Each tick represents an amplitude of 5 mV.

2.3.1.2 Presbyopic Group

The trial outcomes from this group depended highly on which electrode was used, due to issues of fit. Common issues encountered during measurement included ptosis, which impeded the pupil tracking, and pupils that were not bright enough to track (usually a result of light-absorbing make-up on the subject's surrounding skin). One subject, AD, was measured as a presbyope (right eye) and as a pseudophake (left eye). No presbyopic subjects were excluded from the final data analysis. An example recording of the accommodation response curves from a presbyope is shown below in Figure 17.

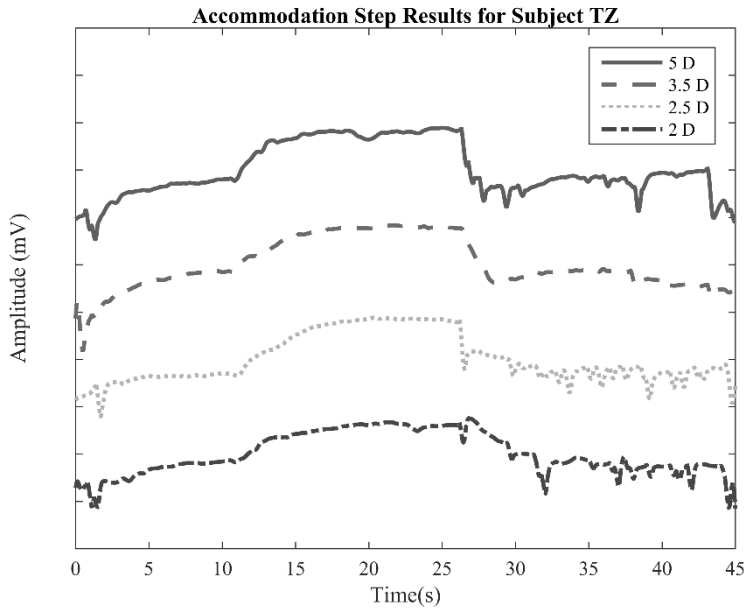


Figure 17: Recordings using the Accommodation Step protocol of presbyopic subject TZ. The baselines have been staggered to allow the shapes to be more easily seen. In this subject, and in the presbyopic group in general, signal magnitudes rarely exceeded 1 mV, with most subjects exhibiting a maximum accommodative amplitude of approximately 0.5 mV for nearer accommodation targets. Each tick represents an amplitude of 0.5 mV.

2.3.1.3 Pseudophakic Group

The pseudophakic group exhibited, as a whole, greater response magnitudes than the presbyopic group. One subject, DG, was excluded from the final analysis, due to the fact that the electrical responses measured were too small to be reliably distinguished from the pupillary response. Subject AD was measured in both the pseudophakic and presbyopic groups (left eye and right eye, respectively), as an inter-subject comparison. DH declined to participate in repeat measurements, and AD was unable to participate in repeat measurements due to logistics during the trial period. An example recording from a pseudophakic subject is shown in Figure 18.

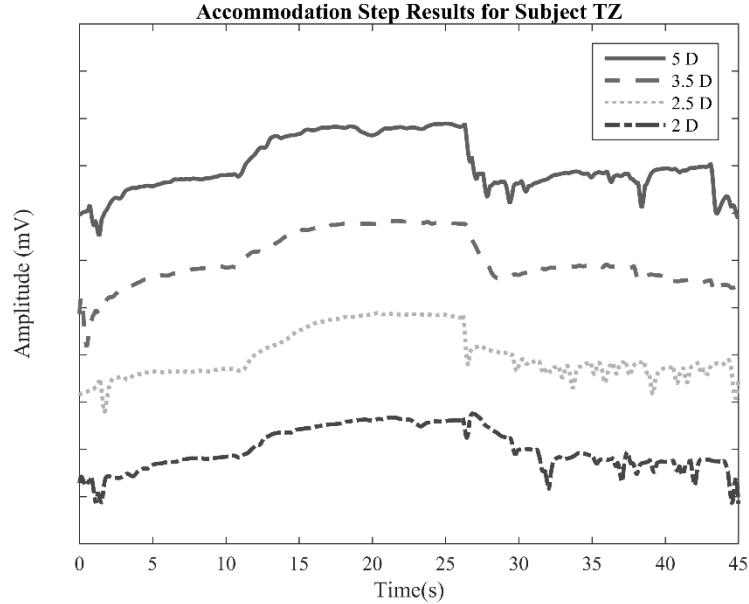


Figure 18: Recordings using the Accommodation Step protocol of pseudophakic subject HH. The baselines have been staggered to allow the shapes to be more easily seen. In this subject, and in the pseudophakic group in general, signal magnitudes could exceed 1 mV, though most subjects exhibited a maximum accommodative amplitude of around 1 mV for nearer accommodation targets. Each tick represents an amplitude of 1 mV.

2.3.2 Maximum Accommodation Amplitudes

The maximum accommodation amplitudes were calculated for each group. Table 5 shows a summary of the maximum accommodation amplitude for each group.

Table 5: Maximum accommodation amplitudes for each of the groups at different accommodation targets. FL: Flashlight protocol (baseline); 2 D, 2.5 D, 3.5 D, 5 D: Accommodation Step protocol targets. (Control, 2.5 D: n=8, n=9 for all other)

Group	Maximum Accommodation Amplitude (mV)				
	FL	2 D	2.5 D	3.5 D	5 D
Control	0.312 ± 0.299	0.802 ± 0.427	1.20 ± 1.46	1.70 ± 1.94	2.13 ± 1.50
Presbyope	0.124 ± 0.055	0.399 ± 0.166	0.513 ± 0.387	0.495 ± 0.327	0.597 ± 0.309
Pseudophake	0.121 ± 0.068	0.427 ± 0.288	0.602 ± 0.591	0.587 ± 0.374	1.00 ± 0.787

As can be seen from the table, a large variation in amplitude existed between members of each group. The control group subjects exhibited the greatest

accommodation amplitudes, though several pseudophakic subject also exhibited amplitudes that were higher than those of the presbyopic subjects. Presbyopic subjects exhibited the lowest signal magnitude, though there was still a clear, measureable signal present during accommodation. Individual maximum accommodation amplitudes are shown, sorted by group, in Table 6.

Table 6: Maximum accommodation amplitudes for experimental subjects at different targets. FL: Flashlight protocol; 2 D, 2.5 D, 3.5 D, 5 D: Accommodation Step protocol targets.

Subject	Group	Maximum Accommodation Amplitude (mV)				
		FL	2 D	2.5 D	3.5 D	5 D
AR	Control	0.220	1.02	¹	2.08	3.00
CH	Control	0.148	0.435	0.555	0.796	1.44
CL	Control	0.191	0.913	0.452	0.422	0.823
KB	Control	0.780	0.560	1.24	2.83	2.81
NG	Control	0.075	0.246	0.234	0.311	0.621
SD	Control	0.113	0.604	0.908	0.738	1.59
SK	Control	0.880	1.51	4.72	6.39	5.53
YO	Control	0.288	1.35	0.427	0.630	1.86
ZL	Control	0.147	0.575	1.06	1.09	1.52
AD	Presbyopic	0.078	0.366	0.927	1.22	1.35
AK	Presbyopic	0.170	0.547	1.43	0.676	0.647
AN	Presbyopic	0.182	1.36	0.390	0.286	0.635
EH	Presbyopic	0.122	0.503	0.522	0.424	0.641
EK	Presbyopic	0.133	0.254	0.200	0.180	0.182
ES	Presbyopic	0.094	0.237	0.341	0.200	0.576
NN	Presbyopic	0.105	0.131	0.423	0.383	0.387
NS	Presbyopic	0.255	0.682	0.323	0.819	0.644
RP	Presbyopic	0.067	0.346	0.345	0.424	0.473
TZ	Presbyopic	0.119	0.417	0.484	0.436	0.699
AD	Pseudophakic	0.071	1.03	1.98	1.45	2.59
DH	Pseudophakic	0.148	0.435	0.555	0.796	1.44
EL	Pseudophakic	0.191	0.913	0.452	0.422	0.823
FV	Pseudophakic	0.169	0.677	0.822	0.401	0.563
HH	Pseudophakic	0.103	0.276	0.361	0.731	1.01
LG	Pseudophakic	0.220	0.456	0.311	0.502	1.90
LK	Pseudophakic	0.153	0.156	0.295	0.406	0.167
LW	Pseudophakic	0.018	0.126	0.092	0.143	0.216
SR	Pseudophakic	0.094	0.294	0.337	0.768	1.12

¹ The signal was too distorted to allow for a calculation of the maximum amplitude

Because such a large variation was seen, even between members of the same group, it was decided to normalize this data to the maximum value recorded during each test session. The normalized data are shown in Table 7, below.

Table 7: Normalized maximum accommodation amplitudes for each of the groups at different accommodation targets. (Control, 2.5 D: n=8; all others n=9). FL: Flashlight protocol; 2 D, 2.5 D, 3.5 D, 5 D: Accommodation Step protocol targets.

Group	Normalized Maximum Accommodation Amplitude				
	FL	2 D	2.5 D	3.5 D	5 D
Control	0.138 ± 0.067	0.440 ± 0.258	0.491 ± 0.171	0.637 ± 0.236	0.973 ± 0.052
Presbyope	0.206 ± 0.132	0.632 ± 0.277	0.699 ± 0.230	0.673 ± 0.264	0.834 ± 0.221
Pseudophake	0.149 ± 0.106	0.548 ± 0.309	0.565 ± 0.271	0.619 ± 0.218	0.844 ± 0.244

These results are shown graphically for each experimental group in Figure 19.

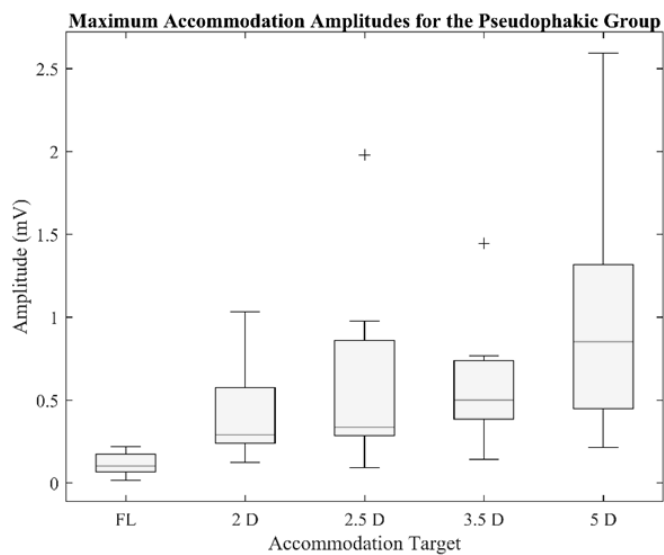
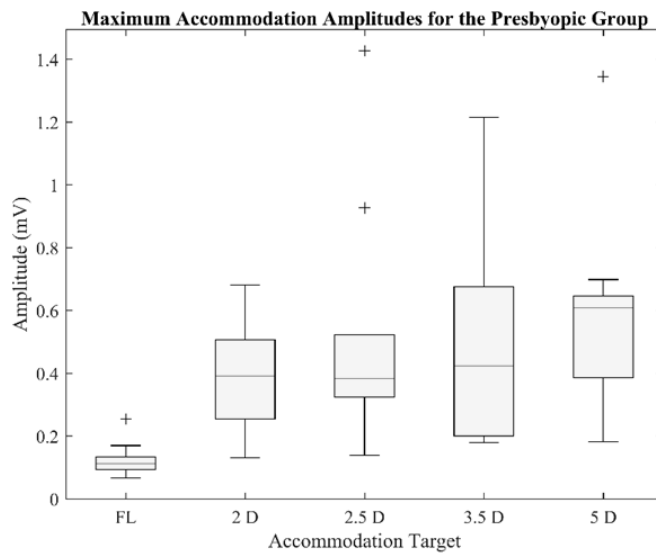
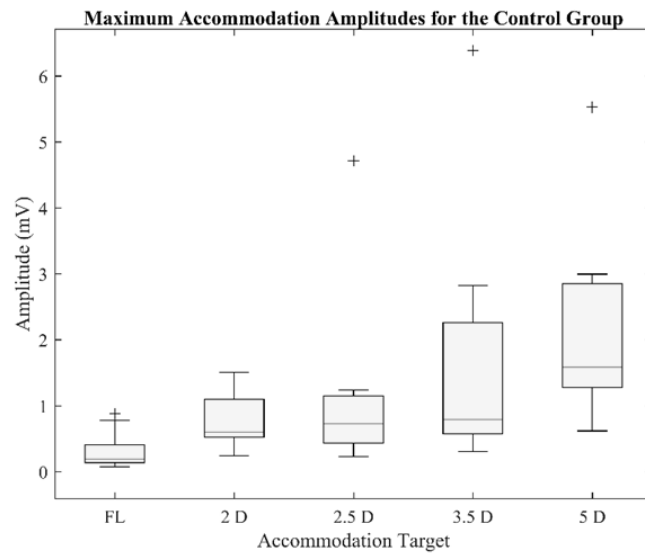


Figure 19: Top: Boxplot showing the normalized accommodation amplitudes for the control group at each of the Accommodation Step targets. With increasing accommodative demand, the control group exhibits a concurrent increase in normalized maximum amplitude. Most subjects from this group exhibited their maximum normalized accommodative amplitude at 5 D. (n=8, 2.5 D) Middle: Boxplot showing the normalized accommodation amplitudes for the presbyopic group at each of the Accommodation Step targets. Though each Accommodation Step target exceeds the amplitudes of the Flashlight test, there is not a clear trend as observed in the control group. (n=10) Bottom: Boxplot showing the normalized accommodation amplitudes for the pseudophakic group at each of the accommodation step targets. Though not as clear as in the control group, an increase in signal amplitude is still observable with an increase in accommodative demand. (n=9) FL: Flashlight protocol; 2 D, 2.5 D, 3.5 D, 5 D: Accommodative Step protocol targets.

As shown in Figure 19 (top), the maximum accommodative amplitude occurred, for most subjects, at 5 D, the nearest target, and that requiring the most amount of accommodative effort. A clear increase can be seen from the Flashlight amplitude, which required no accommodative effort, to the 5 D target. Additionally, with an increase in accommodative demand, a clear increase (though small in some cases) of the measured signal can be seen.

In contrast to the control group, the results from the presbyopic group (Figure 19, middle) exhibit almost no linear increase from farther to nearer targets, though the accommodative signals seen are clearly greater than those of the Flashlight test. Many subjects from the presbyopic group did not produce a maximum signal at 5 D; rather, the maximum signal occurred at intermediate targets (i.e. 2.5 D or 3.5 D).

In Figure 19 (bottom), it can be seen that, though not as clear as in the control group, a trend does exist in the pseudophakic group. The accommodative amplitude observed increases with a concurrent increase in accommodative demand. All Accommodation Step targets also produce a visibly greater response than that of the Flashlight test.

Using a paired-samples t-test, the means of each group were tested for differences. In all three groups, each accommodation step target amplitude differed significantly from that of the flashlight test, except for the pseudophakic group 2 D target. However, the groups differed in the difference between the accommodation step target amplitudes: while, in the control group, the 2 D, 2.5 D, and 3.5 D target amplitudes differed

significantly from the amplitude at 5 D, there were no significant differences between any of the targets in the presbyopic and pseudophakic groups. The values of significance are shown in Table 8.

Table 8: Significance values calculated using paired-samples t-testing for each experimental group at each target. Significance was taken as a score of less than 0.05.

		Target	5 D	3.5 D	2.5 D	2 D
Group	Control	5D	X	0.005	0	0
		3.5D	0.005	X	0.101	0.228
		2.5D	0	0.101	X	0.771
		2D	0	0.228	0.771	X
		FL	0	0	0.002	0.007
Presbyopic	5D	X	0.071	0.181	0.152	
	3.5D	0.071	X	0.794	0.761	
	2.5D	0.181	0.794	X	0.647	
	2D	0.152	0.761	0.647	X	
	FL	0	0	0	0	
Pseudophakic	5D	X	0.143	0.094	0.088	
	3.5D	0.143	X	0.634	0.603	
	2.5D	0.094	0.634	X	0.854	
	2D	0.088	0.603	0.854	X	
	FL	0	0	0.001	0.004	

To describe the behavior of the groups, a regression analysis was performed on the plotted normalized results. These results are summarized in Figure 20 and Table 9.

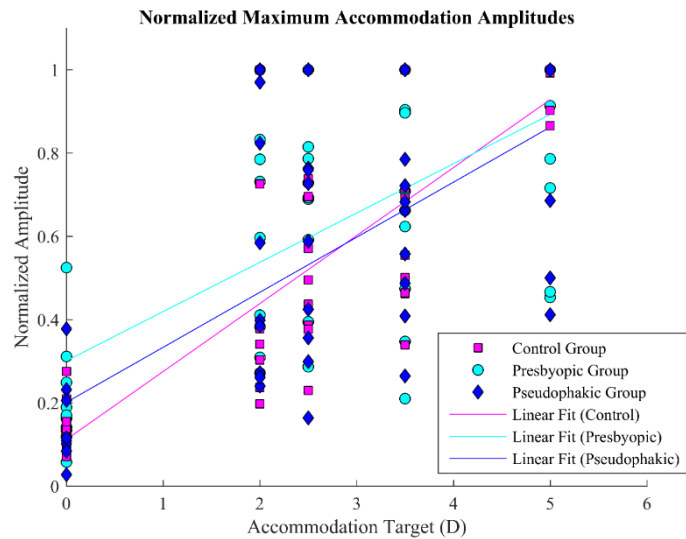


Figure 20: The regression line fit for each experimental group. The Flashlight protocol amplitude was taken as the baseline (0 D accommodation). Each individual produced vastly varying results, which is common in accommodation experiments. Note the steepness of the control group regression, as opposed to the presbyopic regression; the pseudophakic regression is not as steep as that of the control group, but steeper than that of the presbyopic group. Data points are the normalized maximum accommodation amplitude for each subject at each of the four Accommodation Step targets (and Flashlight protocol) tested. (n=8, Control group, 2.5 D)

Table 9: Regression line fit for each experimental group. The R^2 values do not indicate very good fits for the presbyopic and pseudophakic groups, due to the amount of variation seen between subjects. Target represents the target distance (in diopters) of the point at which the subject focuses. Note the difference in slopes between each of the groups, with the control group exhibiting the steepest slope (0.1633), the pseudophakic group exhibiting a slightly flatter slope (0.1322), and the presbyopic group described by the flattest fit. The equation used to fit the data points was a simple $y = mx + b$ model.

Group	Regression Line Equation	R^2 Value
Control	$y = 0.1633(\text{Target}) + 0.1120$	0.7109
Presbyopic	$y = 0.1184(\text{Target}) + 0.3009$	0.4008
Pseudophakic	$y = 0.1322(\text{Target}) + 0.2012$	0.4593

None of the regression fits are excellent, due to the high variation observed between individuals; however, a clear difference can be seen between the different groups. The control group displays the largest slope, indicating that the accommodative amplitude of the control subjects rises at a greater degree per diopter than the other groups. Pseudophakes also outperformed the presbyopes in terms of slope. It is interesting to also

note the y-intercepts; presbyopes exhibited the highest, meaning that the non-accommodating signal amplitude of the presbyopes, relative to their maximum accommodative amplitudes, was higher than for the other groups.

2.3.3 Accommodative Dynamics: Two-Point Analyses

Four parameters of the response curve seen were analyzed for each subject: the initial slope at the start of accommodation (accommodation onset slope), the slope at the end of accommodation (accommodation offset slope), and the difference between the maximum accommodation amplitude and the amplitude observed at accommodation offset (tonicity). Each of these parameters were part of the initial data analysis, and involved simple two-point calculations. These parameters are illustrated in Figure 21.

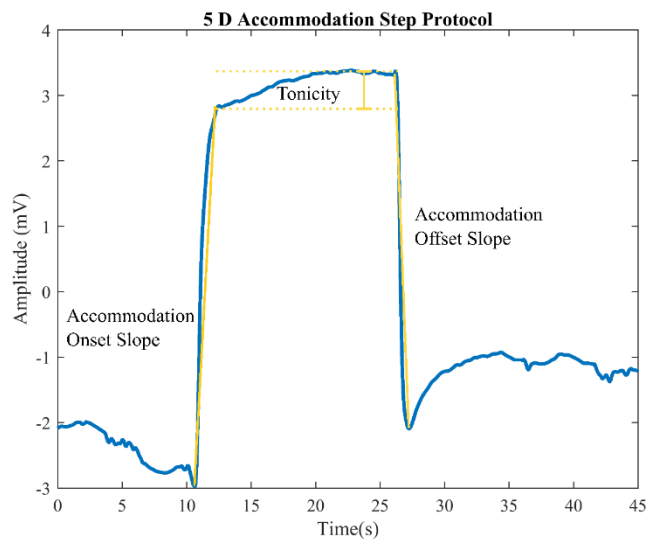


Figure 21: An illustration of the accommodation dynamics parameters evaluated during data analysis. The portions in yellow indicate the parameters analyzed from each signal (shown in blue).

The accommodation onset slopes for each group are shown in Figure 22.

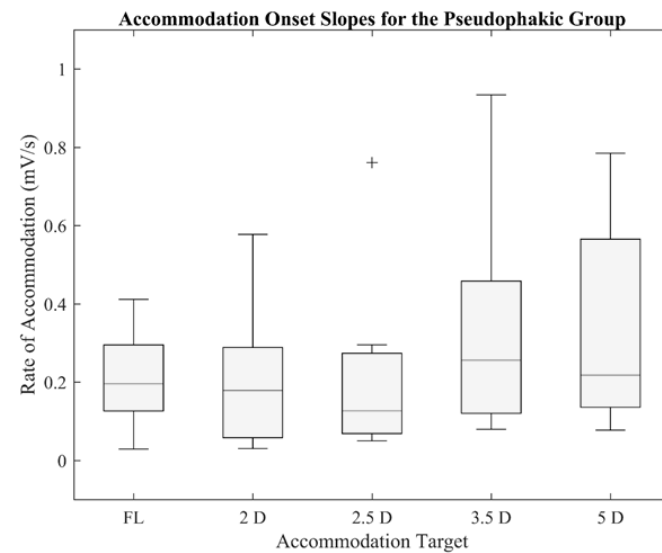
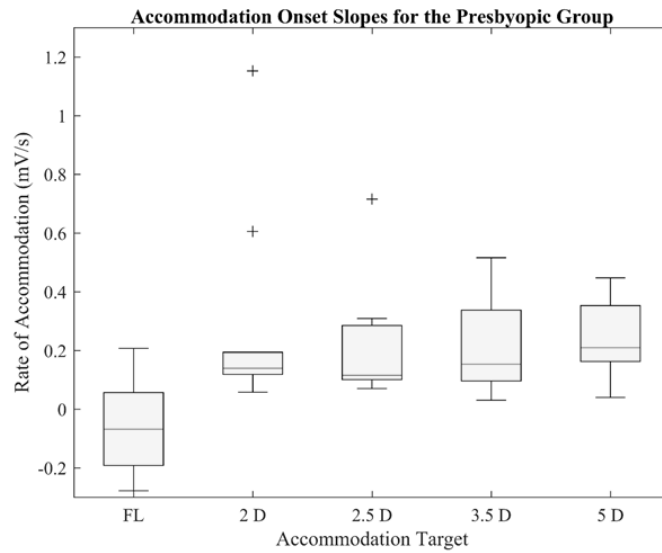
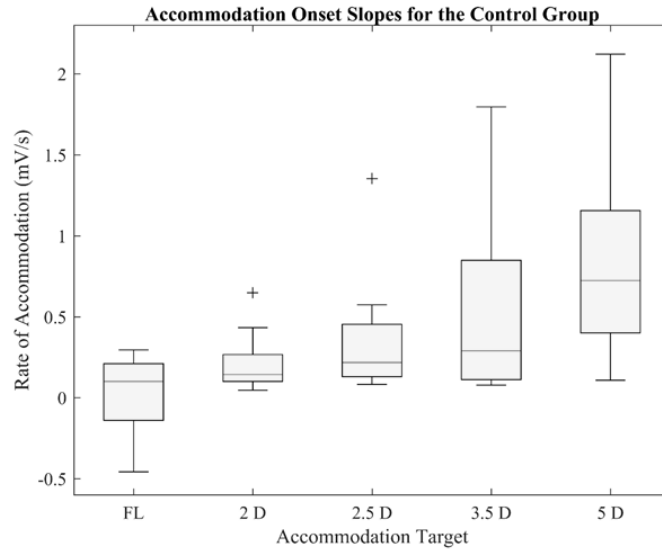


Figure 22: Top: Accommodation onset slopes at each of the accommodation targets for the control group. Though the amplitudes seem to increase with increasing accommodative demand, there is a great variation between subjects, and no conclusive trend can be established. A significant difference existed between both 5 D and 3.5 D targets, and between 5 D and 2 D targets. (n=8 at 2.5 D, otherwise n=9). Middle: Accommodation onset slopes at each of the accommodation targets for the presbyopic group. The rates of accommodation of the accommodative signals appear greater than those observed in the Flashlight test; however, no other clear trend is discernible. (n = 10) Bottom: Accommodation onset slopes at each of the accommodation targets for the pseudophakic group. No significant differences were observed between any of the targets. (n=5 at 2 D, otherwise n=9) FL: Flashlight protocol; 2 D, 2.5 D, 3.5 D, 5 D: Accommodation Step protocol targets.

The accommodation onset slope of the control group (Figure 22, top) showed a slight increase with increasing accommodative demand. A significant difference (paired-samples t-test) was observed between the 5 D and 3.5 D accommodation targets ($p = 0.005$), as well as between the 5 D and 2 D targets ($p = 0.017$). No other significant differences were observed between the targets, or between the targets and the flashlight test.

In the presbyopic group, a strong trend was also not seen (Figure 22, middle). The Accommodation Step values were, however, significantly higher than those observed for the Flashlight protocol (paired-samples t-test; 5 D and FL: $p = 0.001$; 3.5 D and FL: $p = 0.003$; 2.5 D and FL: $p = 0.005$; 2 D and FL: $p = 0.015$).

Figure 22 (bottom graph) shows the accommodative onset slopes observed for the pseudophakic group. No clear pattern of any kind could be discerned from this group; indeed, graphically, all groups appeared approximately the same in terms of rate of change of the signal. No significant differences were observed between any of the targets (paired-samples t-test).

In the pseudophakic group, a paired-samples t-test revealed no significant difference between any of the groups; however, in the presbyopic group, each accommodation target differed significantly from the flashlight test. The normal group differed only between targets, and this only between 5 D and 3.5 D, and 5 D and 2 D targets. Negative rates were observed for the flashlight tests in each of the groups. Significance values obtained using paired-samples t-tests are shown in Table 10.

Table 10: Significance values recorded for accommodation onset slopes calculated using the two-point method. Values were calculated using a paired-samples t-test. Significance was taken as $p < 0.05$.

		Target	5 D	3.5 D	2.5 D	2 D
Group	Control (n = 9)	5D	X	0.005	0.072	0.005
		3.5D	0.005	X	0.303	0.066
		2.5D	0.072	0.303	X	0.323
		2D	0.017	0.066	0.323	X
		FL	0.23	0.269	0.298	0.316
	Presbyopic (n = 10)	5D	X	0.28	0.795	0.681
		3.5D	0.28	X	0.766	0.525
		2.5D	0.795	0.766	X	0.542
		2D	0.681	0.525	0.542	X
		FL	0.001	0.003	0.002	0.02
	Pseudophakic (n = 9)	5D	X	0.687	0.118	0.34
		3.5D	0.687	X	0.196	0.288
		2.5D	0.118	0.196	X	0.329
		2D	0.34	0.288	0.329	X
		FL	0.229	0.395	0.386	0.866

A similar analysis was performed to evaluate the accommodation offset slopes for each group. Within experimental groups, the amplitude observed was relatively constant, though the offset slope of the pseudophakic group differed significantly between the flashlight test and each of the accommodation targets. These results are shown in Figure 23.

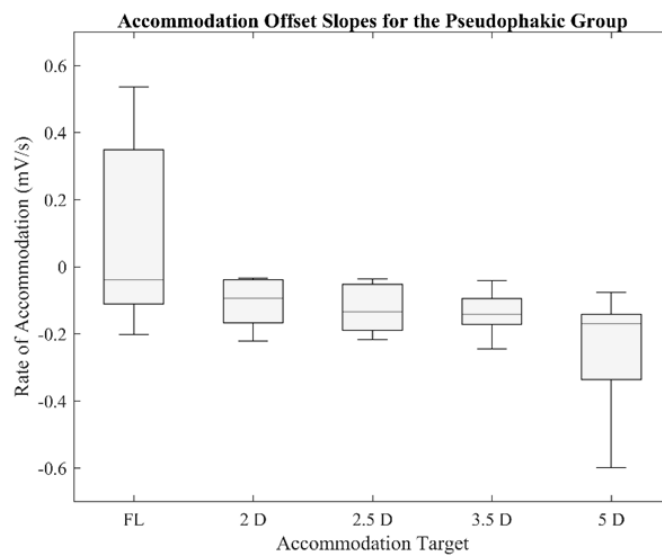
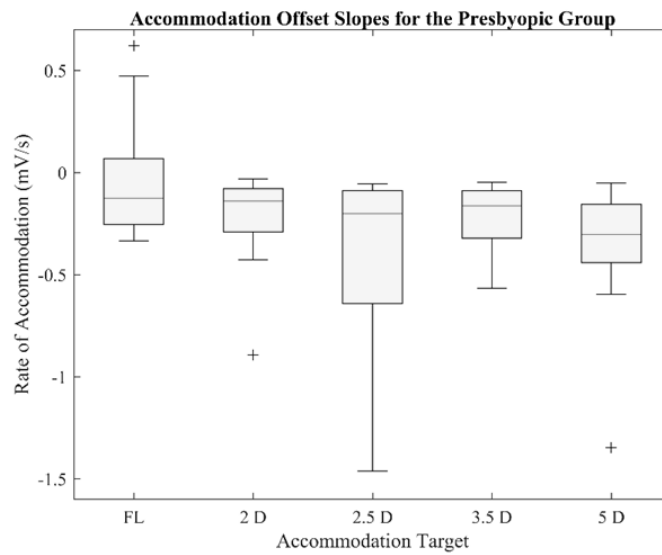
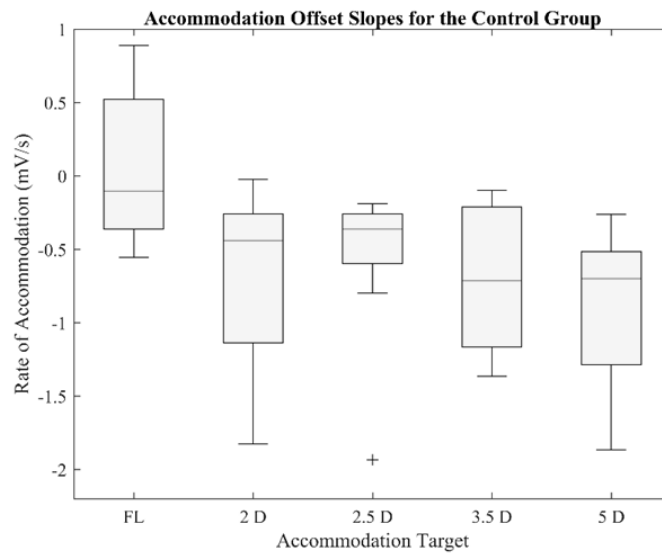


Figure 23: Top: Accommodation offset slopes at each of the accommodation targets for the control group. Though, from the graph, there appears to be a declension of the rate of accommodation with an increased target distance (i.e. the negative velocity increases), a large variation between subjects again obscures the presence of any trends. Looking at the medians of the boxes, the Flashlight protocol does seem to have the slowest response, and a slight increase in response velocity might be present from lower to higher accommodative demands. (n=8 at FL, 2 D, otherwise n=9) Middle: Accommodation offset slopes at each of the accommodation targets for the presbyopic group. No relationship can be seen between the accommodative demand, and the rate of accommodation observed. (n=9 at FL, otherwise n=10) Bottom: Accommodation offset slopes at each of the accommodation targets for the pseudophakic group. A very slight increase in speed might be seen with increasing accommodative demand, but this is not conclusive. (n=5 at 2 D) FL: Flashlight protocol; 2 D, 2.5 D, 3.5 D, 5 D: Accommodation Step protocol targets.

Figure 23 (top) shows the accommodation offset slopes observed for the control group at each of the Accommodation Step targets, and at the Flashlight test. Though there was not an overwhelmingly clear trend, a case could be made for an increase in the rate of speed (here, due to direction, apparent in an increasingly negative rate of change) from targets of lower accommodative demand to targets of higher accommodative demand.

As shown in Figure 23 (middle), no relationship could be established between the rate of accommodation offset and the accommodative target. A slight rate increase might be present at the 5 D target, but this was not significant.

In the pseudophakic group (Figure 23, bottom), too, no significant trend between accommodative demand and rate of accommodation offset could be determined. Based on the means of the data sets, there might be an increase in accommodative offset rate with an increase accommodative demand, but, again, this was not found to be significant. The values obtained for significance are shown in Table 11.

Table 11: Significance values recorded for accommodation offset slopes calculated using the two-point method. Values were calculated using a paired-samples t-test. Significance was taken as $p < 0.05$.

		Target	5 D	3.5 D	2.5 D	2 D
Group	Control (n = 9)	5D	X	0.67	0.113	0.447
		3.5D	0.67	X	0.137	0.622
		2.5D	0.113	0.137	X	0.28
		2D	0.447	0.622	0.28	X
		FL	0.372	0.451	0.884	0.583
		5D	X	0.174	0.708	0.238

Presbyopic (n = 10)	3.5D	0.174	X	0.165	0.808
	2.5D	0.708	0.165	X	0.067
	2D	0.238	0.808	0.067	X
	FL	0.66	0.848	0.585	0.915
Pseudophakic (n = 9)	5D	X	0.072	0.885	0.125
	3.5D	0.072	X	0.433	0.621
	2.5D	0.885	0.433	X	0.927
	2D	0.125	0.621	0.927	X
	FL	0.003	0.019	0.129	0.433

An analysis of the response tonicity (paired-samples t-test) determined that this parameter did not differ significantly between groups. As a general rule, it was observed that the control subjects returned more quickly to baseline after the accommodation signal ceased than did the presbyopic and pseudophakic subjects.

2.3.4 Accommodative Dynamics: Velocity, Acceleration, and Time Constant Calculations

Each data point was, as a second control, differentiated twice in MATLAB to produce velocity and accommodation profiles for each target. This allowed the change in the accommodative parameters over the course of the accommodative response to be analyzed. The responses seen in each group are shown in Figure 24, Figure 25, Figure 26, Figure 27, Figure 28, and Figure 29.

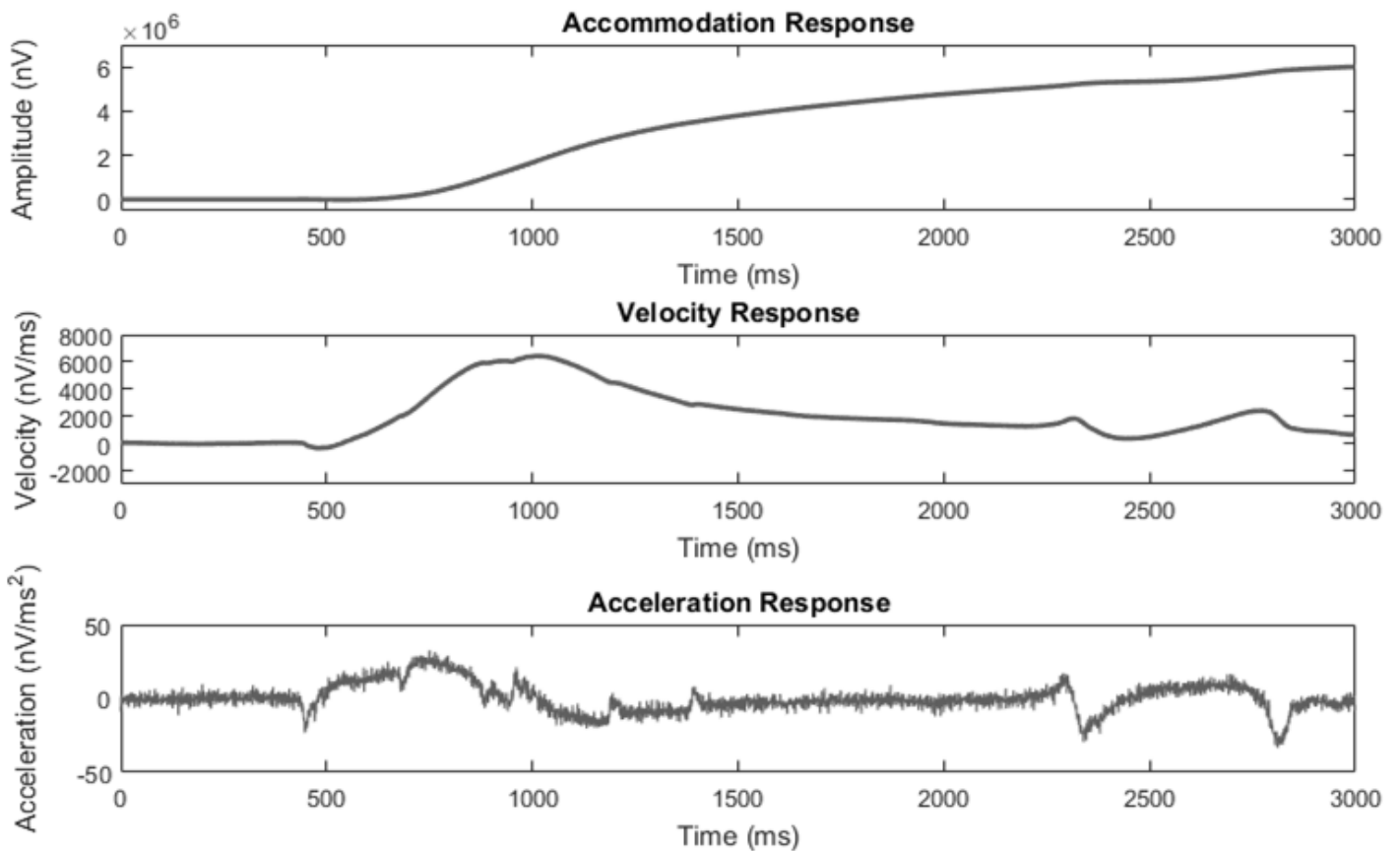


Figure 24: Accommodation onset dynamic responses for control subject SK. As can be seen from the top plot, the accommodation response occurred gradually, and did not plateau for several seconds. The velocity response was characterized by an initial rate increase at the start of accommodation (preceding the increase in accommodative amplitude), and a decrease as the response amplitude reached a plateau. In the bottom graph, the acceleration can be seen to precede both of the other measures, increase for a small period, then decrease to approximately baseline value. The noise in the acceleration plot is from the small scale, and the artifacts of two differentiations.

In Figure 24, several interesting features of the accommodative onset dynamics of a control subject are seen. The recorded accommodation signal, magnified here between 10 s and 13 s of recording time, exhibited a lag time before gradually increasing to a plateau. The velocity response occurred at a sooner time point, and increased, then decreased to approximately baseline value. Acceleration increased before the other two parameters, then decreased to its baseline value.

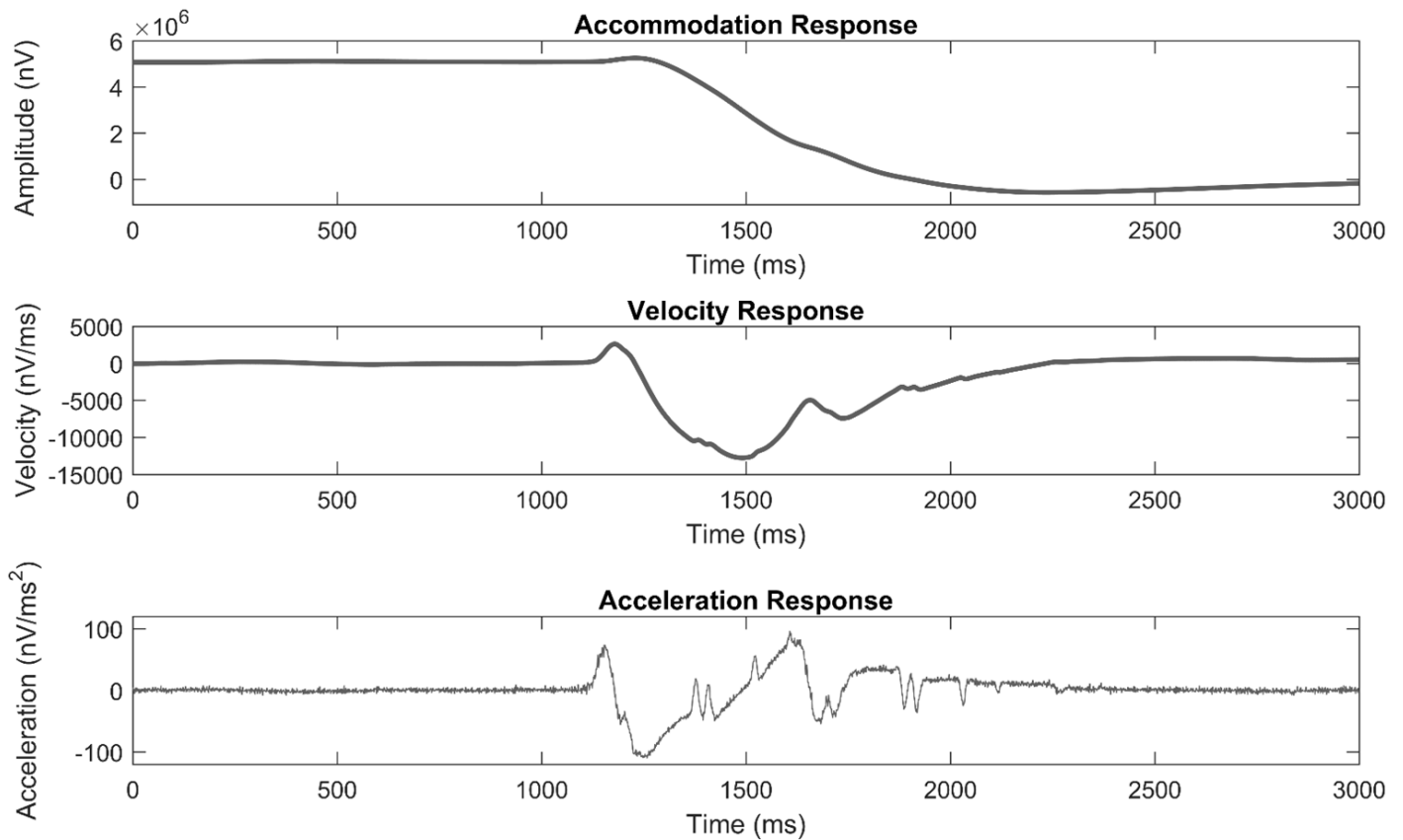


Figure 25: Accommodation offset dynamic responses for control subject SK. The signal amplitude, top, increases rather abruptly over an interval of less than 1 s. Preceding this decrease in time, the velocity response decreases sharply, then increases at a smoother, slower rate to baseline value. The acceleration signal exhibits a sharp increase, a larger, sharper decrease, and also then increases at a slower rate to its baseline value.

The decrease in accommodative offset signal amplitude occurred on a faster time scale than that of the accommodative onset signal, though it did, also, plateau at the end of accommodation offset for the control subject (Figure 25). Velocity and acceleration continued to lead the recorded signal, and both exhibited small, sharp increases, then larger, sharper decreases, before returning at a slower rate to their baseline values.

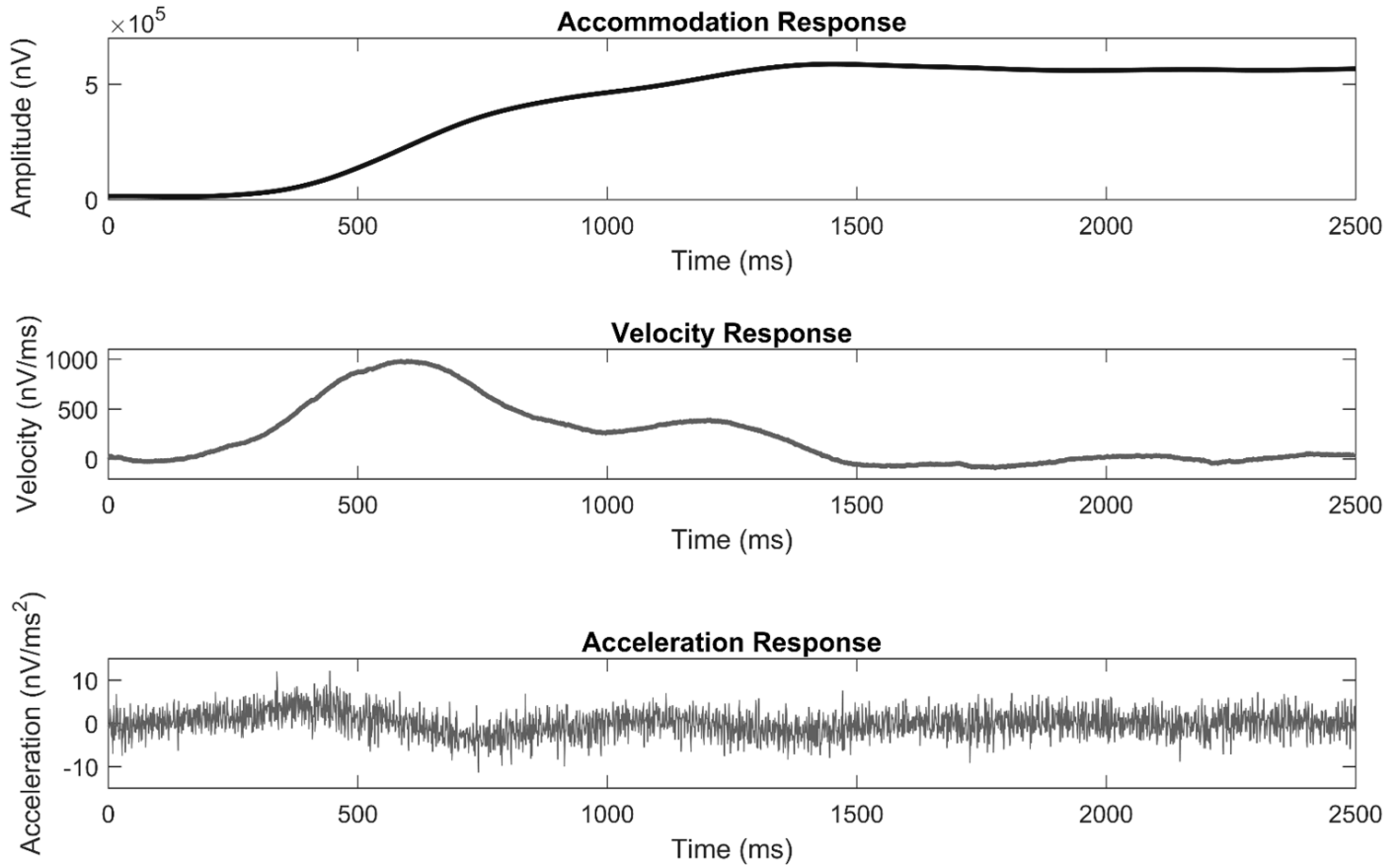


Figure 26: Accommodation onset dynamic responses for presbyopic subject TZ. The time from signal onset to plateau can here be estimated as 1.3 s (top). Velocity initially increases, then decreases at a slower rate. A very small increase, followed by a decrease, can be observed in the acceleration trace.

Unlike the signal seen from the control group subject, presbyopic subject TZ (Figure 26) exhibited a two-part velocity decrease, though, like the control group subject, the acceleration and velocity response changes occurred earlier than that of the signal amplitude. Acceleration was clearly reduced, though the velocity curve mirrored that of the control subject fairly well.

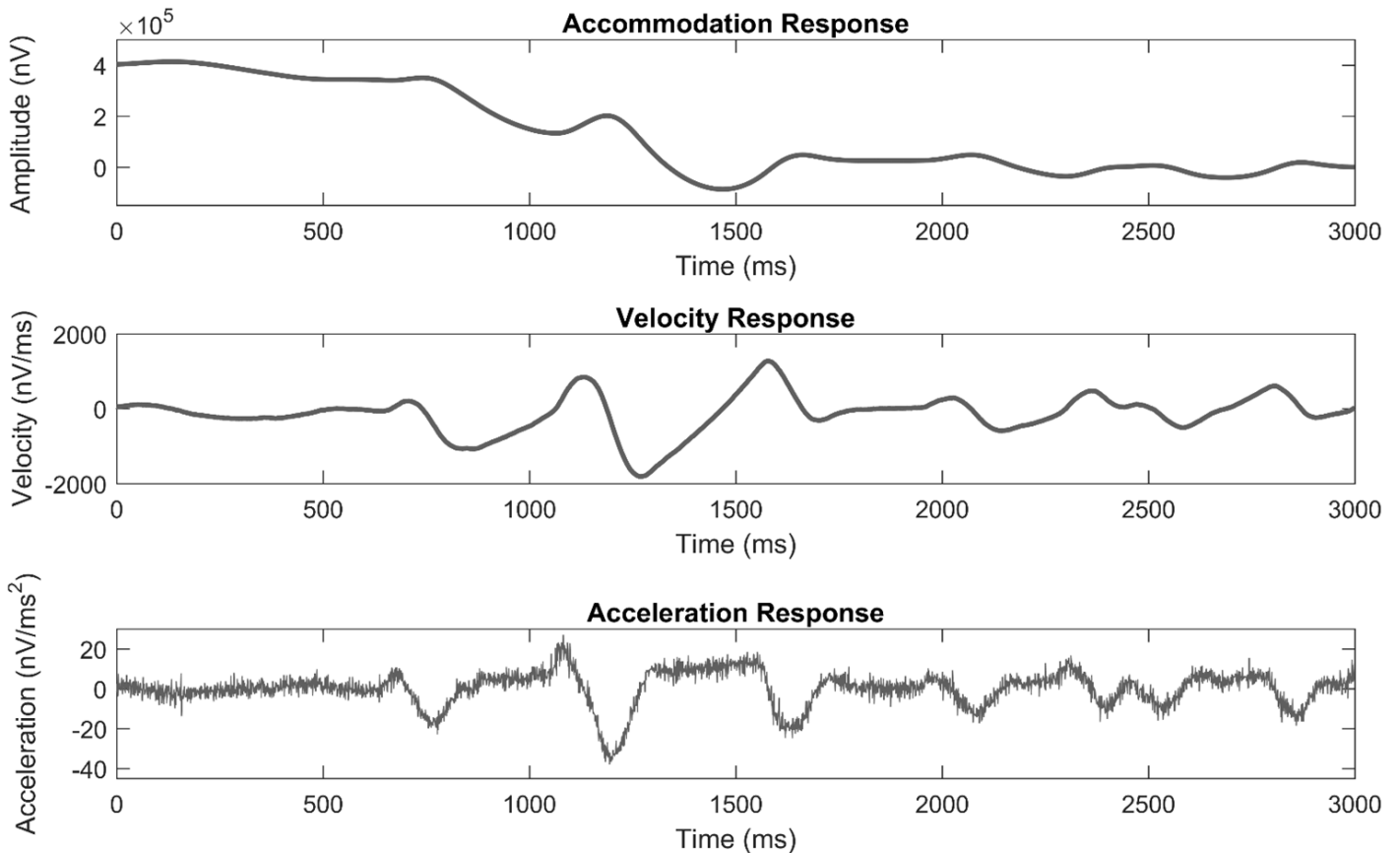


Figure 27: Accommodation offset dynamic responses of presbyopic subject TZ. Due to the vacillation of the original amplitude signal, both the velocity and acceleration profiles are rather erratic. The seemingly bi-phasic decrease in the amplitude response is an artifact caused by spikes produced by blinks; regardless, a general pattern of a fast decrease, followed by a slow increase, can be seen in each of the plots.

Figure 27 shows the dynamic response from the same presbyopic subject at accommodation offset. As with the control subject, in both the velocity and acceleration traces, a quick, steep decrease in magnitude was followed by a slower increase to the baseline value. Due to persistent blink artifacts that could not be entirely removed from the traces, the graph quantities appear multi-phasic. Though the magnitude of each quantity is much less than that observed for the control subject, similar patterns were discernible in the accommodation offset dynamic traces of both subjects.

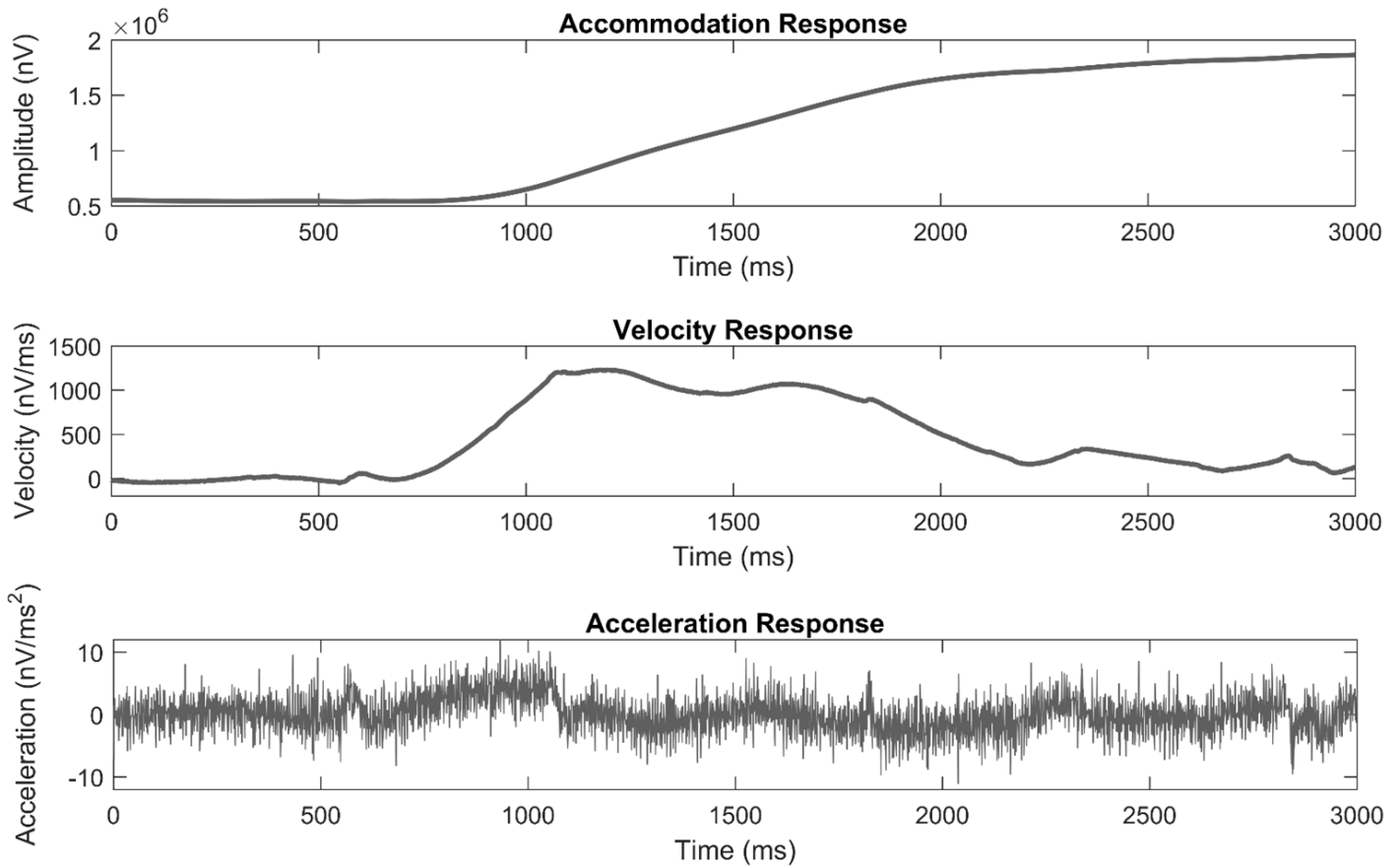


Figure 28: Accommodative onset response of pseudophakic subject HH. A characteristic accommodation response (top) shows a gradually increasing signal. Interestingly, both the acceleration and velocity responses include sharp spikes that are not present in traces from the other groups. The subject tested, HH, was implanted in the recorded eye with an AMO AR40e 3-piece IOL, and produced one of the larger response magnitudes in the pseudophakic group.

In Figure 28, the same trends as observed in both the control and presbyopic groups were evident. However, the onset responses of each of the parameters were best described as jagged, with small, sharp artifacts, as opposed to the smooth curves of the other two subjects.

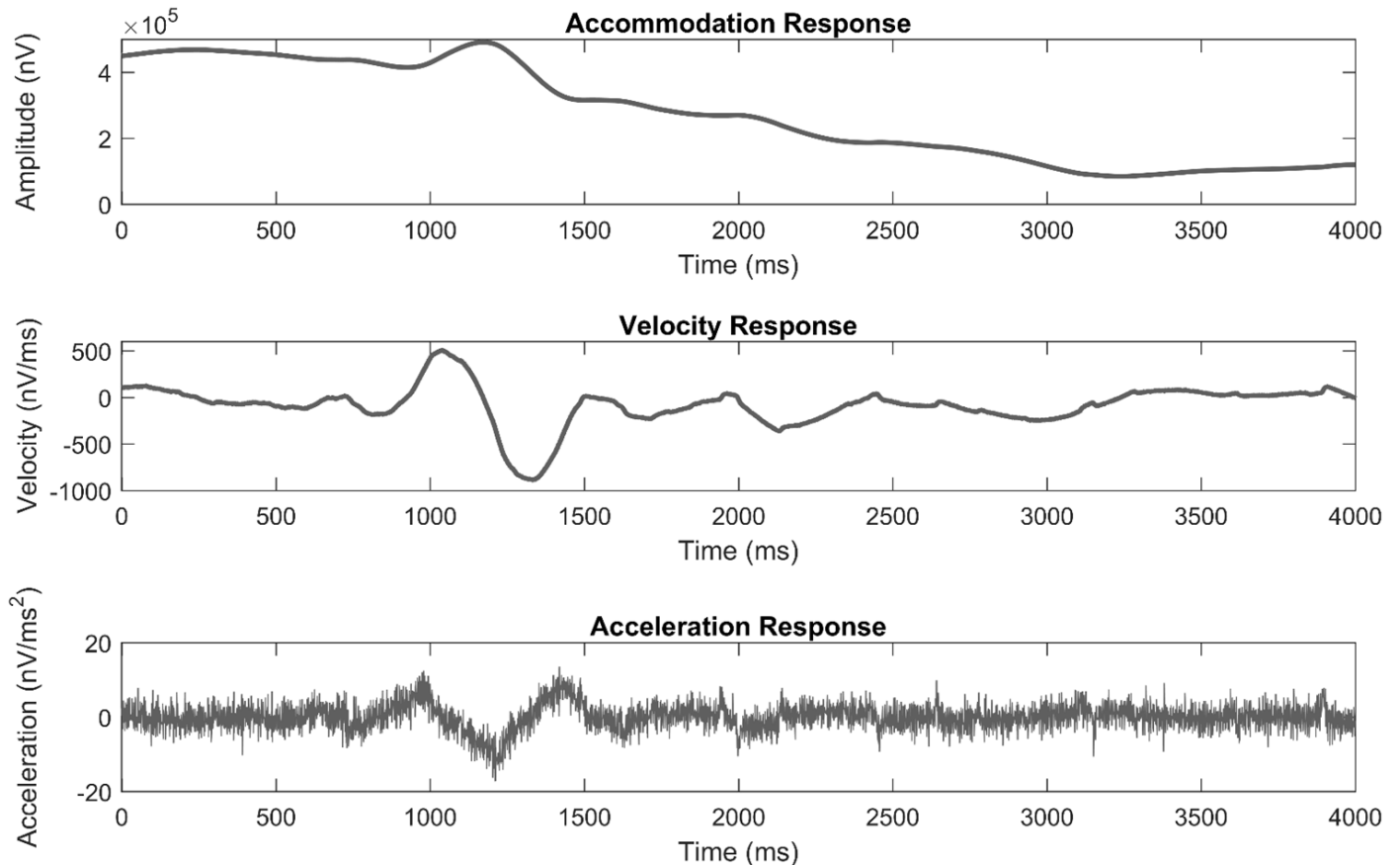


Figure 29: Accommodation offset dynamic responses of pseudophakic subject HH. As with the accommodation onset responses, the offset responses are characterized by small ridges in the velocity and acceleration traces. The velocity response and the acceleration response both exhibit similar slopes for onset and offset, in contrast to the other groups. After an initial response, both traces return to baseline value.

As with the onset response, the offset dynamic response of the pseudophakic subject (Figure 29) were characterized by small peaks, possibly the result of the IOL. A difference between the other two groups was the fact that, in the velocity and acceleration traces, the decreases and increases were approximately the same in terms of slope.

No significant differences were observed between the different target velocities for accommodation onset, though cyclopentolate did significantly lower the velocity for control subjects at the 5 D target ($p = 0.039$). Additionally, significant differences were seen between the control group and presbyopic group velocities at 3.5 D ($p = 0.014$), and

between the control group and pseudophakic group at 5 D ($p = 0.040$). At both of these targets, the control group exhibited faster velocities. Figure 30 shows the mean accommodative onset velocities for each group.

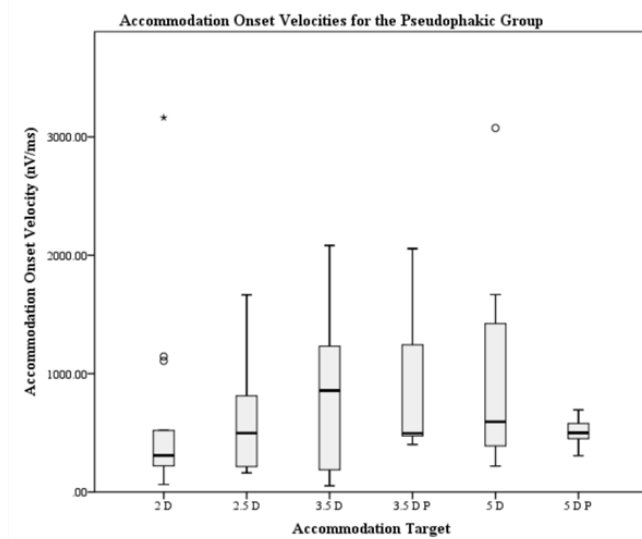
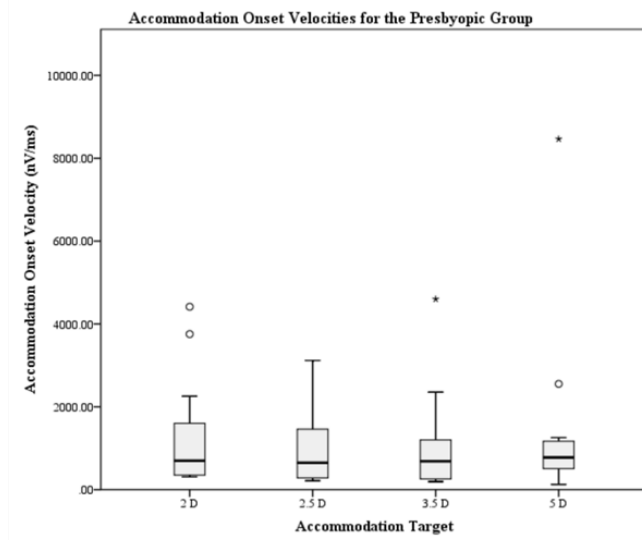
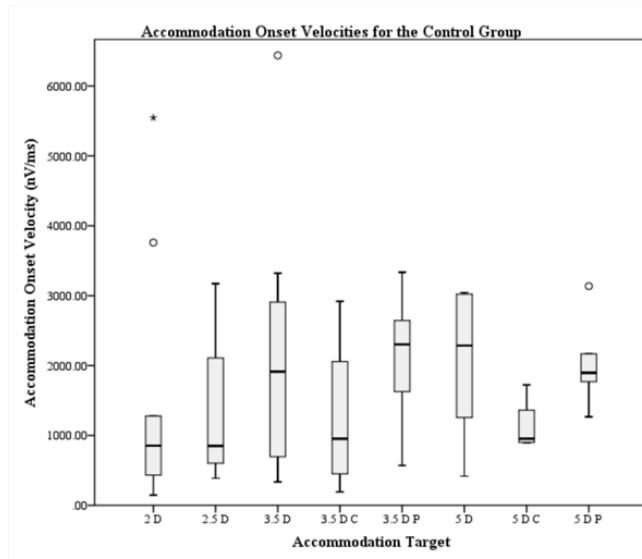


Figure 30: Accommodation onset velocity parameters calculated for each of the experimental groups. Top: Accommodation onset velocity parameters calculated for the control group at different Accommodation Step protocol targets. As can be seen from the graph, cyclopentolate resulted in a decrease in velocity, though phenylephrine had no effect. Middle: Accommodation onset velocity parameters calculated for the presbyopic group at different Accommodation Step protocol targets. A clear trend is not observable for this group, in terms of mean velocities, due to the large amount of variation between samples. Bottom: Accommodation onset velocity parameters calculated for the pseudophakic group at different Accommodation Step protocol targets. The mean accommodation onset velocities of this group show an increase in the mean velocity values between 2 D and 3.5 D, but the pattern does not continue at 5 D. Phenylephrine also appears to depress the signal observed, based on the raw values. Accommodation Step Targets: 5 D, 3.5 D, 2.5 D, 2 D. 5 D C and 3.5 D C, Accommodation Step Targets with cyclopentolate intervention. 5 D P and 3.5 D P, Accommodation Step Targets with phenylephrine intervention.

In the control group (Figure 30, top), it can be seen that the signal velocity of the accommodation onset did seem to increase with an increasing accommodative demand, though this was not, by any means, conclusive, due to the large variation observed (see the standard deviation values). As expected, cyclopentolate did seem to decrease the velocity, while phenylephrine did not seem to have an appreciable effect on the signal.

Figure 30 (middle) shows the results obtained from the presbyopic group, which was not involved in the pharmacological studies. Unlike the control group, no clear trend could be seen relating the accommodation target to the accommodation onset velocity.

In contrast to the control group, accommodative onset parameters of the pseudophakic group (Figure 30, bottom) appeared to be depressed, in terms of mean velocity, by the application of phenylephrine. Also like the control group, the mean velocity values of the pseudophakic group increased between 2 D and 3.5 D, though the pattern did not continue to 5 D. Table 12 shows the results of the paired-samples t-test for the accommodative onset parameters.

Table 12: Significance values recorded for accommodation onset slopes calculated using the differentiation method. A normal distribution was assumed based on the central limit theorem.

	Group											
	Control				Presbyopic				Pseudophakic			
Target	5D	3.5D	2.5D	2D	5D	3.5D	2.5D	2D	5D	3.5D	2.5D	2D
5 D	X	0.140	0.098	0.235	X	0.348	0.428	0.646	X	0.447	0.847	0.415
3.5 D	0.140	X	0.157	0.451	0.348	X	0.698	0.575	0.447	X	0.125	0.063
2.5 D	0.098	0.157	X	0.845	0.428	0.575	X	0.451	0.847	0.125	X	0.132

Values were calculated using a paired-samples t-test. Significance was taken as $p < 0.05$.

This pattern persisted, though with the slight difference that the 5 D control group differed significantly from the 5 D presbyopic group ($p = 0.03$), in the accommodation offset conditions. In the control group, however, there was a significant difference between the 5 D target and both the 3.5 and 2.5 D targets, with the 5 D target having a faster velocity than the other two targets. Cyclopentolate also significantly affected the control subjects at 5 D, with cyclopentolate resulting in a slower rate of change ($p = 0.05$). Though the level of significance does not reflect this, the means of each group showed a general tendency to increase with increased accommodative demand. The mean accommodative offset velocities for each group are shown in Figure 31.

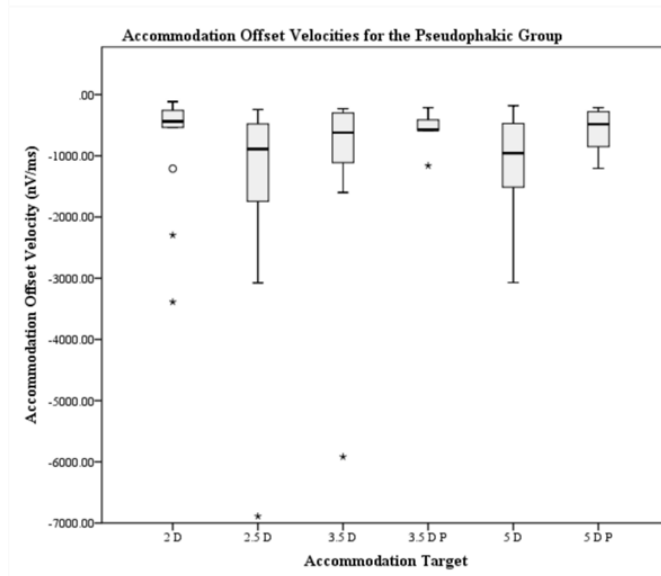
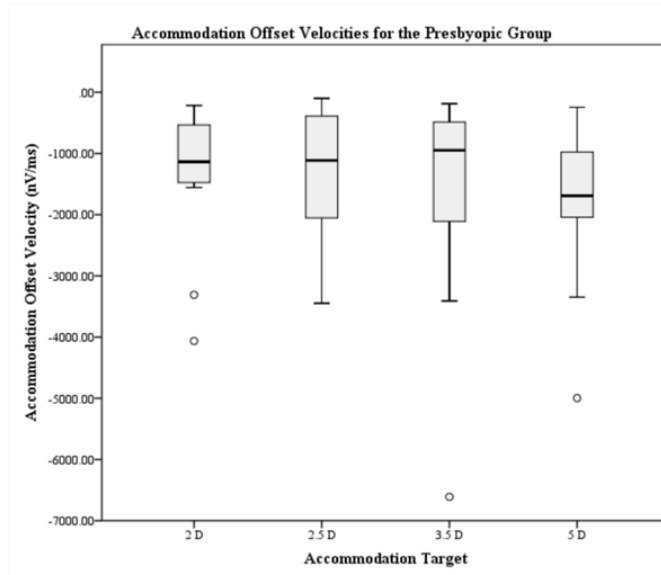
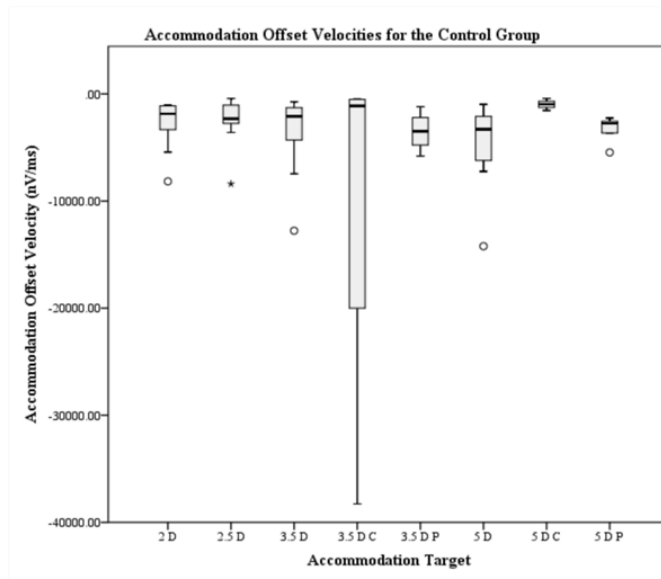


Figure 31: Accommodation offset velocity parameters calculated for each of the experimental groups. Top: Accommodation offset velocity parameters calculated for the control group at different Accommodation Step protocol targets. Generally, the mean velocity seems to increase with a concurrent increase in the accommodative demand. Cyclopentolate appears to decrease the velocity observed, while phenylephrine does not seem to have an appreciable effect. Middle: Accommodation offset velocity parameters calculated for the presbyopic group at different Accommodation Step protocol targets. The mean velocity shows an increase with an increased accommodative demand, though the standard deviations are high between the measurements. Bottom: Accommodation offset velocity parameters calculated for the pseudophakic group at different Accommodation Step protocol targets. Phenylephrine appears to cause a depression in the mean signal velocity, but no trend appears to exist between the mean velocities and the accommodative targets. Accommodation Step Targets: 5 D, 3.5 D, 2.5 D, 2 D. 5 D C and 3.5 D C, Accommodation Step Targets with cyclopentolate intervention. 5 D P and 3.5 D P, Accommodation Step Targets with phenylephrine intervention.

As in the accommodation onset velocity measurements, the accommodation offset velocities for the control group (Figure 31, top) appeared to generally increase with an increased accommodative demand. Cyclopentolate depressed the mean velocity observed in the 5 D case ($p = 0.05$), and phenylephrine, though it might have slightly depressed the signal velocity, did not show an overwhelming effect. Note the extremely high standard deviation between measurements of 3.5 D with cyclopentolate; this is most likely responsible for the high velocity observed at this target.

From Figure 31 (middle), it is apparent that, as opposed to the accommodative onset velocities, the accommodative offset velocities of the presbyopic groups increased with an increase in accommodative demand. It should, however, be noted that these are raw data values, and the standard deviation between measurements is high; therefore, these results should be viewed as a possible trend, rather than as a conclusive increase with increased accommodation.

Figure 31 (bottom) shows the accommodative offset velocities calculated for the pseudophakic group. In this group, no trend was observed between the mean velocity and the accommodative demand, and, once again, phenylephrine appeared to cause a depression in the signal. Due to the high variation between the measurements, and the relatively small size of the group tested with phenylephrine, these results are not, however, conclusive proof that phenylephrine lowers accommodation offset velocity for pseudophakes. Significance values obtained from independent samples t-testing is shown in Table 13.

Table 13: Significance values recorded for accommodation offset slopes calculated using the differentiation method.

	Group											
	Control				Presbyopic				Pseudophakic			
Target	5D	3.5D	2.5D	2D	5D	3.5D	2.5D	2D	5D	3.5D	2.5D	2D
5 D	X	0.039	0.016	0.121	X	0.251	0.041	0.153	X	0.765	0.411	0.194
3.5 D	0.039	X	0.079	0.505	0.251	X	0.411	0.549	0.765	X	0.053	0.242
2.5 D	0.016	0.079	X	0.717	0.041	0.411	X	0.907	0.411	0.053	X	0.037

Values were calculated using a paired-samples t-test. Significance was taken as $p < 0.05$.

An additional parameter analyzed was the peak acceleration seen in each group. For accommodation onset, the acceleration did not differ significantly between groups. No consistent pattern was seen in the acceleration, though, in the presbyopic group, the 5 and 2 D target accelerations were significantly different, as were the 3.5 and 2.5 D target accelerations. Figure 32 show the accommodation onset acceleration parameters for each group.

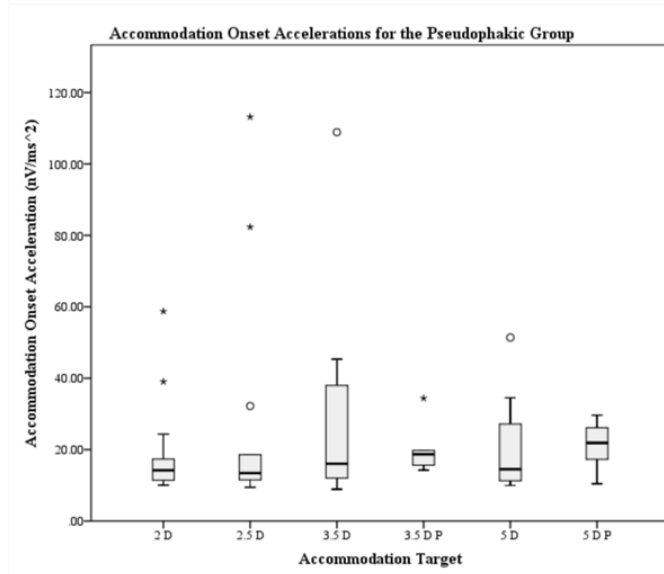
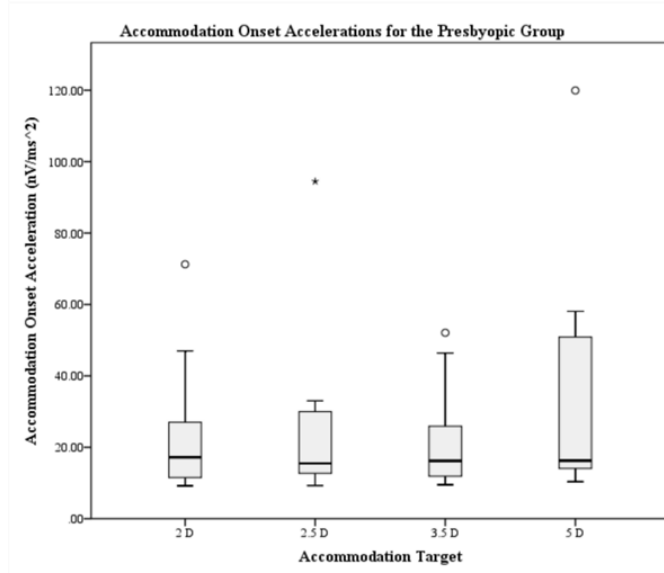
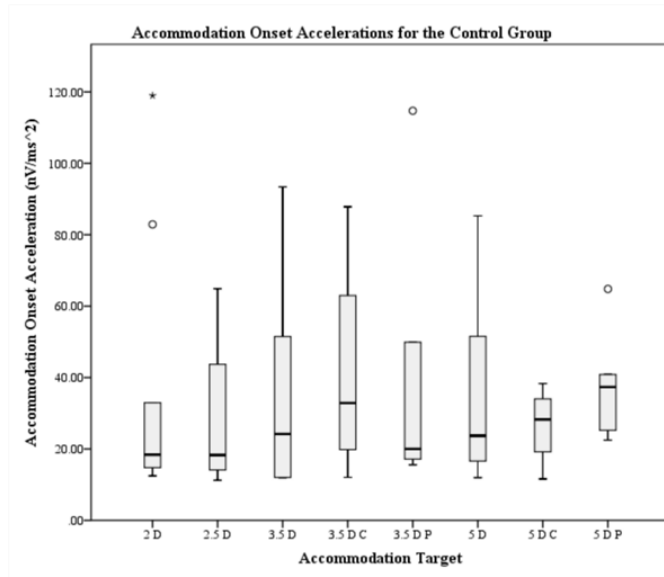


Figure 32: Accommodation onset acceleration parameters calculated for each of the experimental groups. Top: Accommodation onset acceleration parameters calculated for the control group at different Accommodation Step protocol targets. Looking only at the mean acceleration values, cyclopentolate appears to depress the signal at 5 D, while phenylephrine does not. Note the high variations between the measurements. Middle: Accommodation onset acceleration parameters calculated for the presbyopic group at different Accommodation Step protocol targets. Though there is an increase in the mean acceleration at 5 D, this is most likely due to the large value observed for the maximum acceleration and high standard deviation at this target. Bottom: Accommodation onset acceleration parameters calculated for the pseudophakic group at different Accommodation Step protocol targets. Though the mean acceleration appears to have a greater magnitude at the 2.5 D and 3.5 D targets, this can be explained by the appreciably higher maximum accelerations used in the calculation. Phenylephrine did not affect the mean acceleration to a measureable extent. Accommodation Step Targets: 5 D, 3.5 D, 2.5 D, 2 D. 5 D C and 3.5 D C, Accommodation Step Targets with cyclopentolate intervention. 5 D P and 3.5 D P, Accommodation Step Targets with phenylephrine intervention.

As can be seen in Figure 32 (top), cyclopentolate seemed to depress the 5 D mean acceleration, but not at 3.5 D ($p = 0.936$ at 5 D, $p = 0.313$ at 3.5 D). No clear increase was seen between the targets; indeed, for the accommodation onset acceleration parameters for the control group, the onset acceleration remained roughly similar for each target. It is also enlightening to look at the maximum and minimum acceleration values for the 5 D cyclopentolate measurements: the range of values seen was, here, much lower, and the maximum acceleration for this target was the lowest of all the maximum onset accelerations calculated.

In Figure 32 (middle), the accommodation onset accelerations of the presbyopic group are shown. As in the control group, no large difference was apparent between accommodation targets in terms of mean acceleration, except at 5 D. The 5 D increase most likely resulted from an artifact (such as a blink) in the original signal that could not be removed prior to differentiation.

As can be seen in Figure 32 (bottom), the mean accommodation onset accelerations of the pseudophakic group, as with the other two groups, did not differ based on target; rather, they remained constant regardless of the accommodative demand. At 2.5 D and 3.5 D, the calculated quantity was artificially raised, due to the presence of large outliers; the standard deviation reflects this. Once again, significance was tested using a paired-samples t-test; values from this test are shown in Table 14.

Table 14: Significance values recorded for accommodation onset accelerations.

	Group											
	Control				Presbyopic				Pseudophakic			
Target	5D	3.5D	2.5D	2D	5D	3.5D	2.5D	2D	5D	3.5D	2.5D	2D
5 D	X	0.992	0.332	0.944	X	0.062	0.892	0.023	X	0.245	0.381	0.876
3.5 D	0.992	X	0.440	0.968	0.062	X	0.006	0.153	0.245	X	0.944	0.220
2.5 D	0.332	0.440	X	0.319	0.892	0.006	X	0.607	0.381	0.944	X	0.280

Values were calculated using a paired-samples t-test. Significance was taken as $p < 0.05$.

The accommodation offset accelerations did not differ significantly between groups, nor did they differ for target distance or pharmacological interference for any of the groups. Values for the accommodative offset accelerations are given in Figure 33.

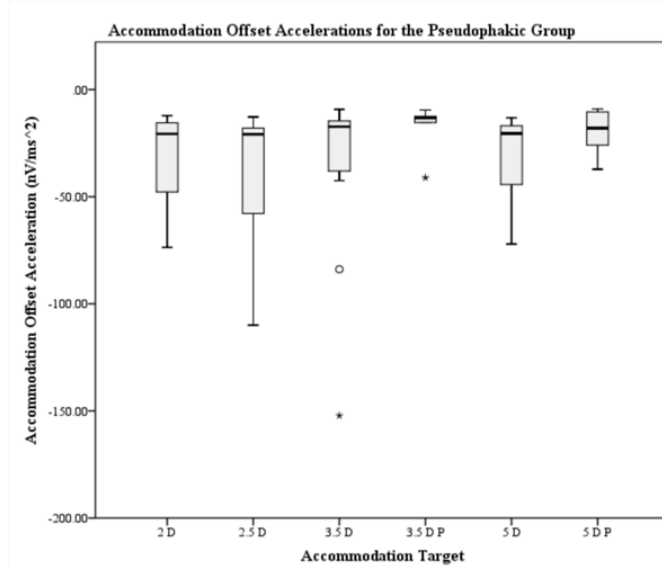
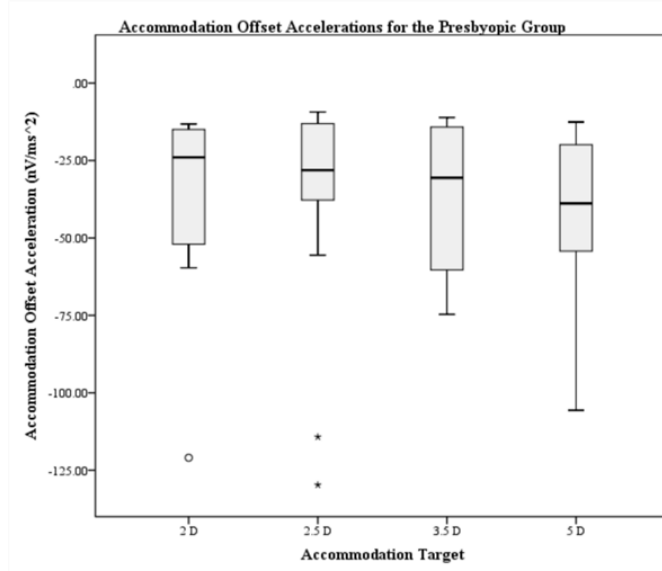
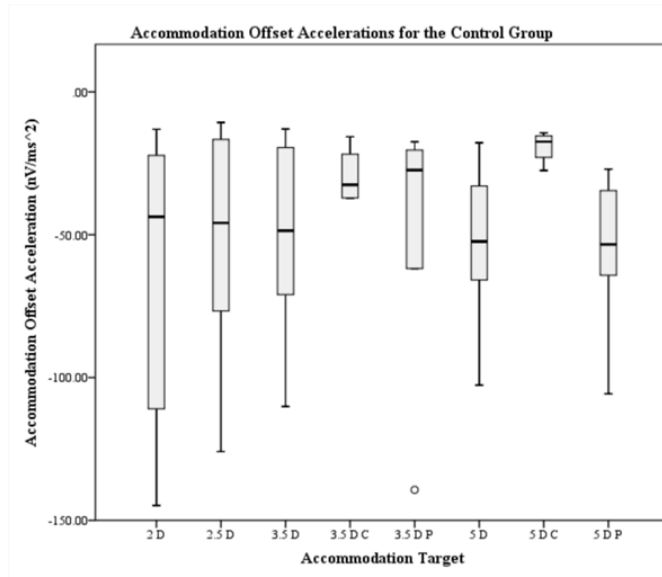


Figure 33: Accommodation offset accelerations calculated for each experimental group. Top: Accommodation offset acceleration parameters calculated for the control group at different Accommodation Step protocol targets. Note the relatively constant mean accelerations, which differ only with cyclopentolate. Middle: Accommodation offset acceleration parameters calculated for the presbyopic group. None of the targets differed significantly from other targets in terms of the accommodation offset acceleration. Bottom: Accommodation offset acceleration parameters calculated for the pseudophakic group. No significant differences can be observed between different accommodation targets, or between tests performed with or without phenylephrine. The negative value indicates acceleration in the opposite direction as that of accommodation. Accommodation Step Targets: 5 D, 3.5 D, 2.5 D, 2 D. 5 D C and 3.5 D C, Accommodation Step Targets with cyclopentolate intervention. 5 D P and 3.5 D P, Accommodation Step Targets with phenylephrine intervention.

Figure 33 (top) shows the accommodation offset acceleration values calculated for the control group. Though the differences were not significant, it is interesting to note that the mean accelerations for the tests with cyclopentolate are smaller than those of the other tests.

As with the control group, the accommodation offset accelerations of the presbyopic group did not differ significantly between targets (Figure 33, middle). Though the difference between the control group and the presbyopic group accommodation offset accelerations is not significant (paired-samples t-test, $p = 0.517$ at 5 D, $p = 0.227$ at 3.5 D, $p = 0.602$ at 2.5 D, and $p = 0.073$ at 2 D), it is interesting to note that the mean values calculated for the presbyopic group were slightly lower than those calculated for the control group.

Once again, the acceleration offset values calculated for the pseudophakic group (Figure 33, bottom) did not differ significantly between accommodation targets, or between tests performed normally versus with phenylephrine. Though the difference is not significant, it is interesting to compare the accommodation offset mean acceleration values between the three groups: slight differences can be seen between the values, with the greatest mean acceleration observed for the control group, and the smallest values in the pseudophakic group. Significance values are shown in Table 15.

Table 15: Significance values recorded for accommodation offset accelerations.

Group		
Control	Presbyopic	Pseudophakic

Target	5D	3.5D	2.5D	2D	5D	3.5D	2.5D	2D	5D	3.5D	2.5D	2D
5 D	X	0.818	0.817	0.598	X	0.305	0.692	0.206	X	0.782	0.385	0.960
3.5 D	0.818	X	0.954	0.563	0.305	X	0.706	0.983	0.782	X	0.685	0.742
2.5 D	0.817	0.954	X	0.594	0.692	0.706	X	0.557	0.385	0.685	X	0.536

Values were calculated using a paired-samples t-test. Significance was taken as $p < 0.05$.

The final accommodation dynamics parameter calculated was the time constant, τ . This constant represents the time taken for the response amplitude to reach 63% of the final amplitude value. For the accommodation onset response, no significant differences in time constants were observed between each of the three groups. The presbyopic group showed no significant differences between any of the targets, while the control group only differed significantly between the 2.5 and 2 D targets. In the pseudophakic group, however, both the 2.5 and 2 D targets were significantly different than the 5 D target. The general trend in the pseudophakic group was an increase in time constant with an increased accommodative demand. Calculated values for the accommodation onset time constant are shown in Figure 34.

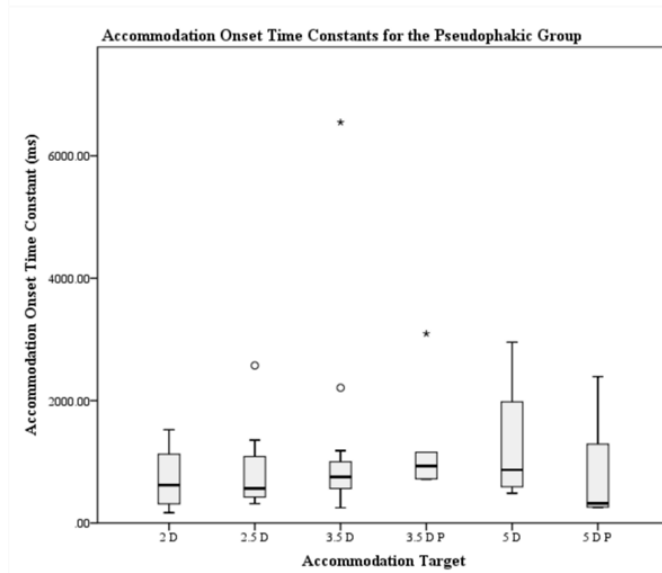
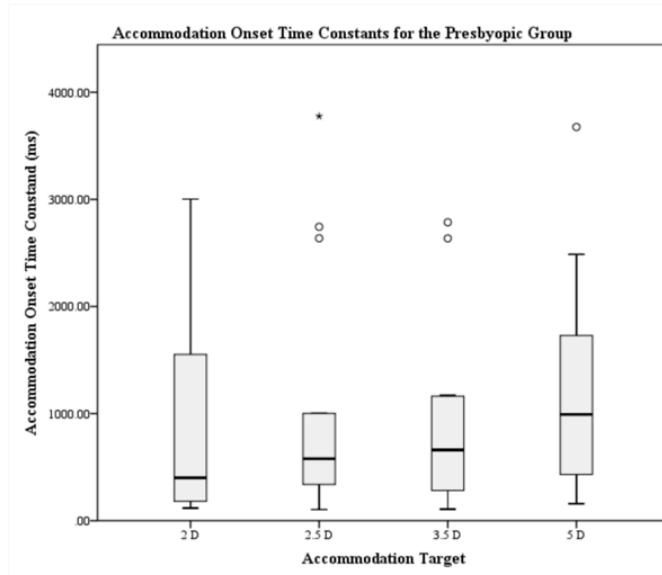
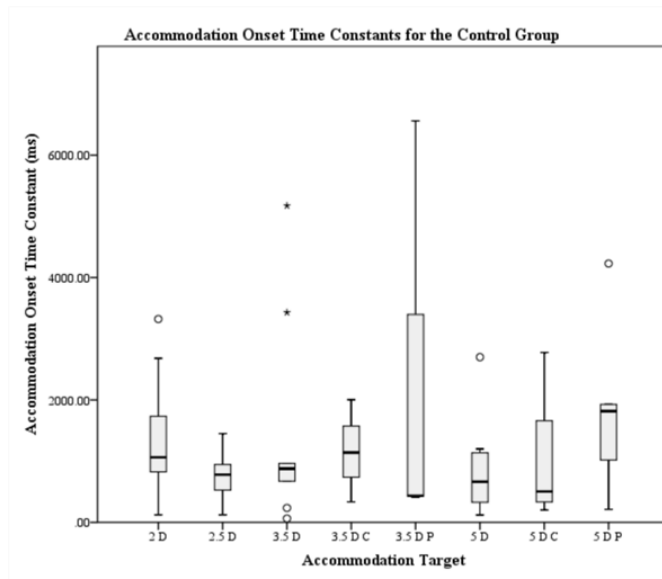


Figure 34: Accommodation onset time constants calculated for each experimental group. Top: Accommodation onset time constant calculated for the control group. A wide range of values are present, and no significant differences exist between targets. Middle: Accommodation onset time constant calculations for the presbyopic group. Bottom: Accommodation onset time constant calculations for the pseudophakic group. A significant difference exists between 2 D and 5 D, and between 2.5 D and 5 D. Accommodation Step Targets: 5 D, 3.5 D, 2.5 D, 2 D. 5 D C and 3.5 D C, Accommodation Step Targets with cyclopentolate intervention. 5 D P and 3.5 D P, Accommodation Step Targets with phenylephrine intervention.

Figure 34 (top) shows the time constants calculated for the accommodation onset of the control group. No pattern was visible between the different targets, and no targets differed significantly from each other.

In Figure 34 (middle), the time constants for the accommodation onset of the presbyopic group is shown. No significant differences existed between the accommodation targets.

The accommodation onset time constants for the pseudophakic group are shown in Figure 34 (bottom). Significant differences existed between the 2 D and 5 D targets, and between the 2.5 D and 5 D targets. In this group, a pattern could be seen of increasing time constant with an increased accommodative demand. Significance values obtained for the groups are displayed in Table 16.

Table 16: Significance values recorded for accommodation onset time constants.

	Group											
	Control				Presbyopic				Pseudophakic			
Target	5D	3.5D	2.5D	2D	5D	3.5D	2.5D	2D	5D	3.5D	2.5D	2D
5 D	X	0.186	0.517	0.122	X	0.784	0.908	0.817	X	0.953	0.012	0.022
3.5 D	0.186	X	0.499	0.293	0.784	X	0.777	0.522	0.953	X	0.961	0.320
2.5 D	0.517	0.499	X	0.031	0.908	0.777	X	0.592	0.012	0.961	X	0.536

Values were calculated using a paired-samples t-test. Significance was taken as $p < 0.05$.

For the accommodation offset time constants, there did not appear to be a pattern relating the time constants to the accommodation target, though the presbyopic and pseudophakic groups did demonstrate significant differences between the 2 and 5 D targets. The control group differed significantly from the pseudophakic group at 5 D, while the presbyopic group differed significantly from the pseudophakic group at 3.5 D.

Because of the random nature of the differences, it is not thought that a consistent pattern is present here.

Figure 35 shows the accommodation offset time constant values calculated for each group.

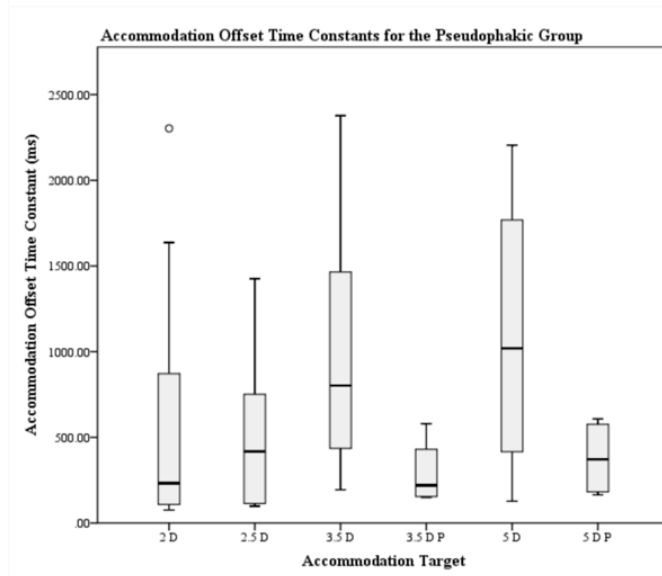
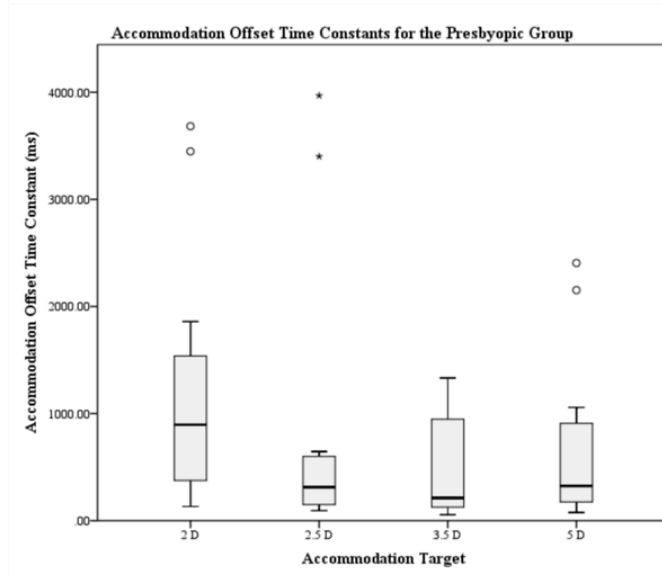
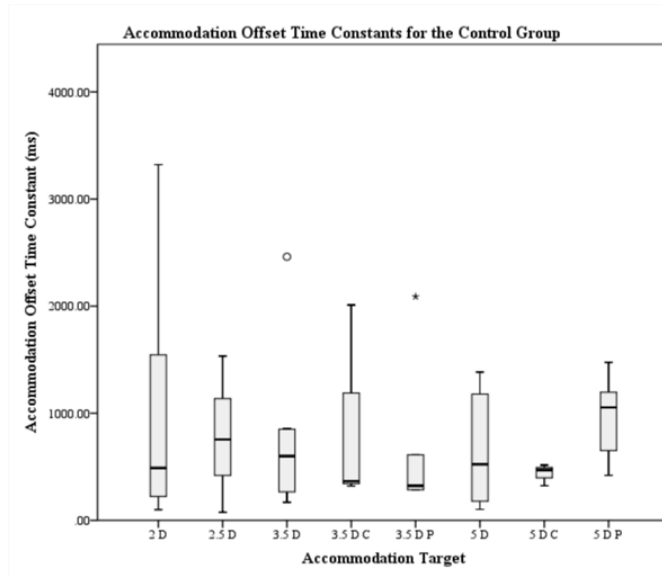


Figure 35: Accommodation offset time constants calculated for each of the experimental groups. Top: Accommodation offset time constant parameters calculated for the control group. No significant differences are present between the accommodation targets. Middle: Accommodation offset time constant parameters calculated for the presbyopic group. A significant difference is seen between the 2 D and 5 D targets. Bottom: Accommodation offset time constant parameters calculated for the pseudophakic group. A significant difference can be seen between the 2 D and 5 D targets. Accommodation Step Targets: 5 D, 3.5 D, 2.5 D, 2 D. 5 D C and 3.5 D C, Accommodation Step Targets with cyclopentolate intervention. 5 D P and 3.5 D P, Accommodation Step Targets with phenylephrine intervention.

In Figure 35 (top), the time constants of the accommodation offsets for the control group are shown. No significant differences existed between targets in this group.

Figure 35 (middle) lists the time constants of the presbyopic group's accommodation offset responses. A significant difference existed between 2 D and 5 D, but not other patterns or differences were observed.

The accommodation offset time constants for the pseudophakic group are shown in Figure 35 (bottom). The time constants at 2 D and 5 D differed significantly from each other, but no other significant differences were observed. Significance values obtained using a paired-samples t-test for the accommodation offset time constants are shown in Table 17.

Table 17: Significance values recorded for accommodation offset time constants. Values were calculated using a paired-samples t-test. Significance was taken as $p < 0.05$.

	Group											
	Control				Presbyopic				Pseudophakic			
Target	5D	3.5D	2.5D	2D	5D	3.5D	2.5D	2D	5D	3.5D	2.5D	2D
5 D	X	0.337	0.165	0.294	X	0.491	0.410	0.006	X	0.449	0.017	0.131
3.5 D	0.337	X	0.947	0.610	0.491	X	0.234	0.057	0.449	X	0.166	0.266
2.5 D	0.165	0.947	X	0.395	0.410	0.234	X	0.464	0.017	0.166	X	0.991

Values were calculated using a paired-samples t-test. Significance was taken as $p < 0.05$.

2.3.5 Pharmacological Measurements

A total of fifteen pharmacological investigations were performed with both the control and pseudophakic groups (as mentioned in 2.3.1.1, one control subject, ER, was excluded). Table 18, below, summarizes these experiments based on subject and date.

Table 18: A summary of the subjects and drug interventions used in the pharmacological trials

Subject	Group	Date	Drug
AD	Pseudophakic	6/28/2014	Phenylephrine
AR	Control	3/4/2014	Cyclopentolate
CL	Control	4/16/2014	Cyclopentolate
CL	Control	4/16/2014	Phenylephrine
EL	Pseudophakic	6/25/2014	Phenylephrine
FV	Pseudophakic	7/15/2014	Phenylephrine
KB	Control	2/19/2014	Phenylephrine
LW	Pseudophakic	5/30/2014	Phenylephrine
NG ¹	Control	5/14/2014	Cyclopentolate
NG ¹	Control	5/14/2014	Phenylephrine
SK	Control	2/26/2014	Phenylephrine
SR ¹	Pseudophakic	7/3/2014	Phenylephrine
YO ¹	Control	2/25/2014	Cyclopentolate
YO ¹	Control	7/17/2014	Phenylephrine

¹Pharmacological trials were performed on a different day than those from the final step accommodation trial measurements.

2.3.5.1 Phenylephrine Intervention

An analysis of the control group results indicated that there was no significant difference between the results obtained from the normal accommodation step trials and those obtained from the same trials after application of phenylephrine (3.5 D, $p = 0.353$; 5 D, $p = 0.186$). For several subjects, the magnitude of accommodation with phenylephrine was actually greater than that observed for the normal trials; however, as will be discussed later, this is consistent with the high variation seen between measurements performed on different days. Pharmacological tests in the control group were performed on different days due to the length of time needed for the pharmacological intervention to take effect. Figure 36 shows the Accommodation Step results from a normal condition compared with the phenylephrine condition for the control group.

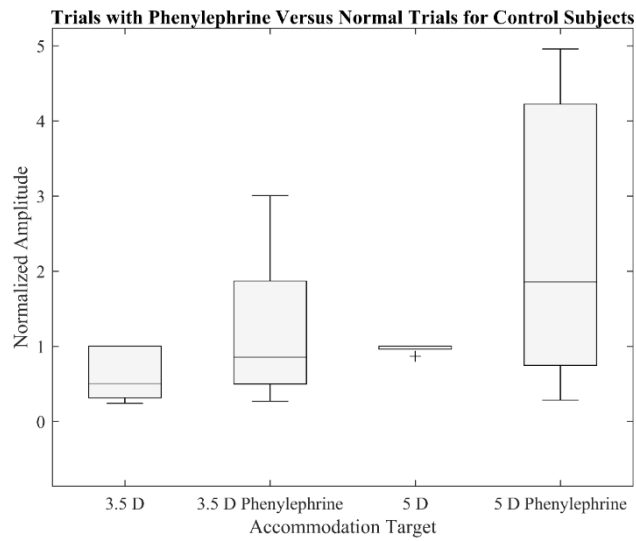


Figure 36: Normalized accommodation amplitudes seen in the regular accommodation step trials and those performed under the effects of phenylephrine for control subjects. The phenylephrine, in each case, resulted in a higher amplitude than that observed with cyclopentolate.

As in the control case, phenylephrine did not significantly affect the accommodation amplitudes seen in the pseudophakic subjects (Figure 37) (3.5 D, $p = 0.878$; 5 D, $p = 0.765$). Three subjects participated in both tests on their second visit (EL, LW, SR), while the other two (AD, FV) were tested on their first visit.

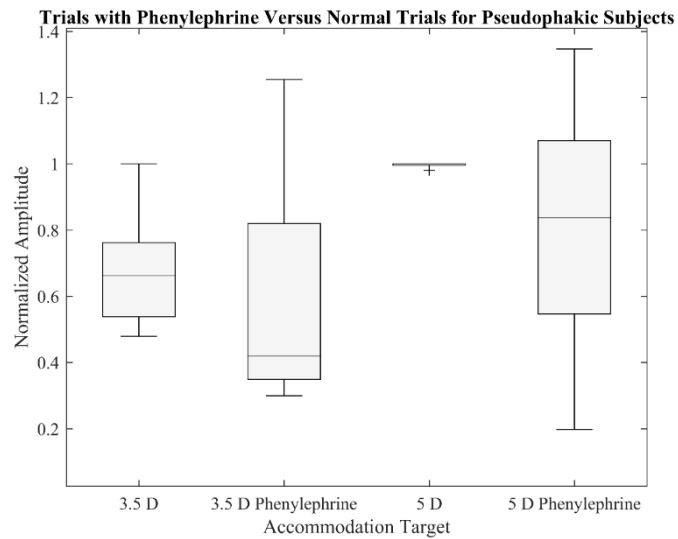


Figure 37: Normalized accommodation amplitudes seen in the regular accommodation step trials and those performed under the effects of phenylephrine for pseudophakic subjects. No significant difference exists between the two conditions.

2.3.5.2 Cyclopentolate Intervention

Five control group subjects were tested with cyclopentolate. In most subjects, these tests were performed on different days than the regular Accommodation Step experiments, due to the long amount of time needed for the cyclopentolate to induce cycloplegia. Comparing the cycloplegic responses with the normal responses, a significant difference was found between the normal and pharmacological condition at 5 D, but not at 3.5 D (Figure 38) (3.5 D, $p = 0.157$; 5 D, $p = 0.045$).

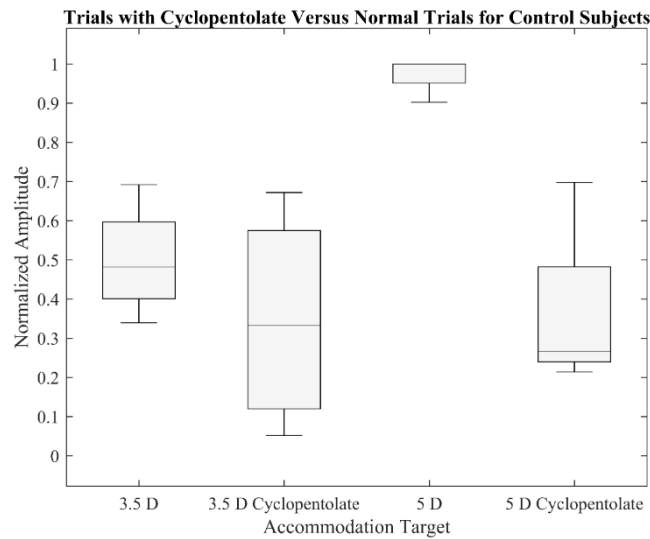


Figure 38: Normalized accommodation amplitudes seen in the regular Accommodation Step trials and those performed under the effects of cyclopentolate for control subjects. Though the effect is not apparent at the 3.5 D target, a significant difference can be observed between the normal and cyclopentolate conditions at 5 D.

At the 5 D target, where the accommodation amplitude differed significantly from the amplitude seen for the regular accommodation step tests, the change was drastic: a $63.2 \pm 22.2\%$ change between the values was seen. It should be noted that there was also a decrease between the 3.5 D cases, especially when compared to the maximum value recorded for the same testing day; however, this difference was not significant.

2.3.6 IOL Type

Though the study cohort was not large enough to comprehensively or conclusively evaluate the effect of IOL model on the performance of pseudophakic subjects, preliminary data indicate that a trend might exist between the model and the maximum accommodation amplitude achieved by the subject. These amplitudes are shown in Table 19.

Table 19: Comparison of the maximum amplitudes recorded for pseudophakic subjects and the IOL model from each subject.

Subject	IOL Model	1-Piece or 3-Piece	Manufacturer	Maximum Amplitude (mV)
AD	SN60AT AcrySof®	1-piece	Alcon®	2.59
DH	Tecnis® PCB00	1-piece	Abbott Medical Optics	0.55
EL	Tecnis® PCB00	1-piece	Abbott Medical Optics	0.52
FV	Tecnis® PCB00	1-piece	Abbott Medical Optics	0.82
HH	AMO AR40e	3-piece	Advanced Medical Optics®	1.01
LG	Tecnis® ZCB00	1-piece	Abbott Medical Optics	1.90
LK	Tecnis® ZA9003	3-piece	Abbott Medical Optics	0.98
LW	Tecnis® ZA9003	3-piece	Abbott Medical Optics	0.84
SR	Tecnis® PCB00	1-piece	Abbott Medical Optics	1.12

2.3.7 Intra-Individual Variations

As the experiments progressed, it was noted that a large variation seemed to exist between intra-subject IOL trials. In order to assess the reliability of measurements, percent differences between different trials were calculated. Six presbyopes, six pseudophakes, and one control subject were evaluated in this manner. Two subjects, RP and LG (presbyopic and pseudophakic, respectively) made repeat visits, but, due to issues of fit with the electrode used on one of the trials, only one viable measurement session was performed. The individual percent differences between trials are shown in Table 20.

Table 20: Percent differences between maximum accommodation amplitudes observed between trials for the same subject. The variation between amplitudes is high between different trials.

Subject (Group)	FL (%)	2 D (%)	2.5 D (%)	3.5 D (%)	5 D (%)	Days between Measurements
CL (Control)	42.4	95.1	48.0	93.0	24.5	30
AD (Presbyope)	50.9	59.2	62.7	0.17	108	17
AN (Presbyope)	62.1	91.3	95.2	38.3	51.6	47
EH (Presbyope)	60.5	96.9	37.5	3.53	58.0	82

ES (Presbyope)	159	22.3	5.12	88.4	0.56	64
NN (Presbyope)	34.9	117	78.0	33.6	34.9	47
TZ (Presbyope)	69.0	70.2	70.1	18.9	10.5	12
EL (Pseudophake)	52.8	38.3	32.3	105	24.6	41
FV (Pseudophake)	85.6	88.3	61.5	4.25	34.9	6
HH (Pseudophake)	73.3	16.9	48.4	103	109	82
LK (Pseudophake)	25.0	13.1	107	16.7	134	16
LW (Pseudophake)	122	50.8	128	142	60.8	44
SR (Pseudophake)	29.1	33.5	12.9	32.4	NA	27

2.4 Discussion

2.4.1 Origin of the Recorded Signal

The signal recorded during the experimental study mirrored in shape the signals recorded by other groups when plotting refraction over time for an accommodation step response [(Baumeister, et al., 2010), (Beers & van der Heijde, 1996), (Campbell & Westheimer, 1960), (Kasthurirangan & Glasser, 2006), (Shirachi, et al., 1978)]. However, though the shape is very similar, the unit being measured is an electrical signal, rather than an objective measure of subject focus. This means that the signal measured in the present study was an inherent property present in the eye, rather than a changing optical quantity measured indirectly.

Because the recording was non-invasive, it is unlikely that any cellular potentials were measured. Based on the position of the two concentric rings on the electrode, a more likely explanation is that the signal measured was a type of electromyographic recording pertaining to the action of accommodation. As the accommodative apparatus, particularly the ciliary muscle, changed position beneath the electrode rings, a difference in potential was generated, with greater movement resulting in a stronger electrical signal.

This signal can reasonably be concluded to originate from the accommodative apparatus based on the pre-experimental investigations performed. It was shown that the signal did not greatly vary with extraocular movements or pupil changes, though it was highly dependent on a correct electrode fit. As the ciliary muscle is, essentially, a circle, a misalignment of an overlying electrode would unbalance the whole measurement system, explaining the dramatically different results seen from a relatively small central displacement of the electrode (see Section 2.2.8.2.2).

The amplitude of the recorded signal varied based on the experimental group. As to be expected with a signal measuring accommodative amplitude, older test subjects displayed significantly smaller signals than their younger counterparts. Countless studies have been performed, showing that the maximum accommodative amplitude decreases with age [(Atchison, 1995), (Baumeister & Kohnen, 2008), (Charman, 2008), (Croft et al., 1998), (Duane, 1922), (Richdale et al., 2013)]; reasons for this are, however, still unknown. An illuminating question then becomes, with the current signal, what conclusions can be drawn from the decrease in amplitude seen with age, and the fact that many of the pseudophakes, a group that had a higher mean age than the presbyopes, nevertheless surpassed the presbyopic group in signal amplitude? Assuming the signal to be, as previously postulated, a measure of muscle movement, the simple answer is that an age-related decrease in amplitude is the result of less movement of the accommodative apparatus.

The reasons for this, however, require more speculation. A decrease in ciliary muscle strength with age has been conclusively disproven [(Croft et al., 2009), (Croft et al., 2008), (Lütjen-Drecoll et al., 2010), (Richdale et al., 2013), (Shao et al., 2015), (Strenk et al., 2010), (Strenk et al., 2006), (Tamm et al., 1992), (Tamm et al., 1992)]; though this decrease in strength, if translated to smaller movements, would explain the age-related increase seen in these experiments, it would not explain the difference seen between presbyopes and pseudophakes. If the ciliary muscle were truly deteriorating with age, both groups should be similar in terms of signal amplitude, or the pseudophakic

group should display even lower signal amplitudes than those seen in the presbyopic group. This is, clearly, not the case.

A better explanation for both parts of the question is a restriction in movement with increasing age, a restriction that is at least partially alleviated by IOL implantation surgery. Strenk et al. (2010) investigated the ciliary muscle position using MRI; they found that, with the implantation of an IOL, the position of the ciliary muscle was translated to one that resembled its position in a young eye. This would explain the higher signals seen with the pseudophakes than with the presbyopes, as, then, the ciliary muscle would have more space to move in the pseudophakic subject. To take a broader view of the question, the results obtained from the experiments provide evidentiary support to the geometric theory of presbyopia, which postulates a change in geometry and movement restrictions as the underlying cause of presbyopia.

2.4.2 General Experimental Group Signal Characteristics

One of the many challenges inherent in measuring accommodation is the high degree of variability observable between different individuals, and even between repeat measurements of the same individual [(Allen et al., 2010), (Baumeister et al., 2010), (Beers & van der Heijde, 1996), (Beers & van der Heijde, 1994), (Crawford et al., 1989), (Drexler et al., 1997), (Kasthurirangan & Glasser, 2006), (Schaeffel et al., 1993), (Shirachi et al., 1978), (Sun & Stark, 1986)]. The experimental study described here was no different, in terms of the great variation in accommodative measurements. However, several generalizations can be made regarding the different groups.

Prior to measurements of accommodation, subjects were measured using the method described by Duane (1922) to ascertain their maximum accommodative amplitudes. As mentioned previously, a measurement of less than 2.5 D (greater than 40 cm) was not possible, due to the length of the ruler used. The accommodative amplitudes

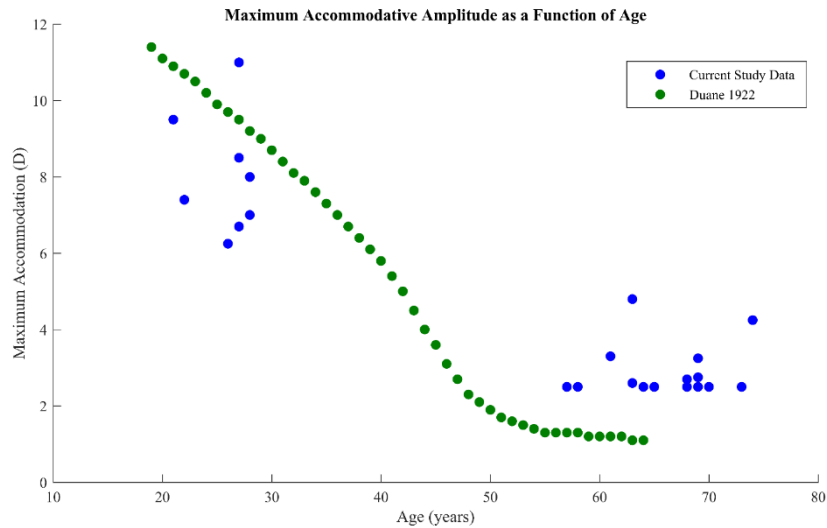


Figure 39: Maximum subjective accommodative amplitudes of the experimental groups plotted as a function of age. The minimum measurable accommodative amplitude in the current study was 2.5 D. Shown in green are the mean maximum accommodative amplitudes determined by Duane [(Duane, 1922)].

of the recorded eye for each subject corresponded well to previously-defined graphs of maximum accommodative amplitude as a function of age, and are shown in Figure 39.

2.4.2.1 Control Group

The control group, in general, produced the highest accommodative amplitude signals, as anticipated. Of these subjects, two (NG and ZL) could be considered myopic, while the rest were emmetropic. The refractive error did not seem to have any appreciable effect on the ability of these subjects to accommodate, though the small amount of subjects with refractive correction measured does not allow for this to be conclusively proven.

Clearly, certain subjects did accommodate to a much higher range, in terms of signal amplitude, than other subjects. Subject SK had, by far, the highest accommodative amplitude seen throughout the experiments, despite the fact that he was one of the older control subjects measured (27 years old). Interestingly, subject SK produced signals almost six times higher than the youngest subject measured (SD, 21 years old), though SD had a higher measured subjective maximum accommodation (SD: 9.5 D, SK: 8.5 D). This underscores the high variability that can be observed between subjects, and suggests

that an assessment of subjective maximum accommodative amplitude is not sufficient for assessing the total accommodative capability of a subject, or for estimating the potential signal strength observed with the recording method used here.

A final interesting note about the control group is that the maximum measured amplitude occurred, for two subjects (KB and SK), at 3.5 D, rather than 5 D. Clearly, each subject had the ability to focus at 5 D, so, hypothetically, this should have produced a maximum signal. Fatigue seems unlikely, since this phenomenon occurred for a minority of the control group, and since the differences between the 5 D and 3.5 D signals were not very large. This could be explained by accommodative lag, whereby the eye underaccommodates at near distances [(Charman, 2008), (Richdale et al., 2013), (Seidemann & Schaeffel, 2003)]; another possibility is a slight shift in the electrode position, or even a change in the effort exerted by the subject.

2.4.2.2 Presbyopic Group

Presbyopic subjects ranged in age from 57 to 69 years old, and presented with a variety of spherical and, in two cases, aspherical refractive errors. Two subjects, ES and TZ, required aspherical refractive correction; four subjects (AK, AN, EH, ES) were hyperopic; four subjects were myopic (AD, NS, RP, TZ); and two subjects (EK, NN) were emmetropic. Those subjects who reported higher subjective maximum accommodative amplitudes did not perform better than those with lower amplitudes, and refractive errors did not seem to affect the maximum measured accommodation voltage. Age, though clearly a factor in the development of presbyopia, also did not correlate with the maximum subjective accommodation amplitudes or measured accommodation amplitudes in this group.

Measurement of presbyopic subjects was perhaps the most difficult, because the experimental task required them to focus as much as possible without any visual feedback. Motivated subjects seemed to perform the best. Fit issues were most noticeable in this group, with a poor fit inevitably leading to poor recordings. This is probably because, with such a small signal, any change in position would reduce the magnitude to

an almost unnoticeable level. As an example of this, initial measurements of subject RP produced no useable results, due to a poor electrode fit (the electrode was too large, and fell out several times over the course of the experimental session). With a “tighter” lens, repeat measurements were successful for this subject, though the measured signal was still small (0.47 mV).

Several of the presbyopic subjects exhibited ocular anomalies. These included optic disc anomalies (NS); dermatochalasis (NN); tilted discs, dry eyes, and peripapillary atrophy (ES); and potential early-stage glaucoma (AK). None of these conditions are expected to affect accommodation, and these subjects were, therefore, included in the study. Though the pathologies are different, none seemed to cause a clear decrease in accommodative amplitude.

For many of the presbyopic subjects, the maximum accommodative amplitude measured occurred at a different target than 5 D, which usually produced a maximum response in the control group. This can be explained by a lack of visual feedback: at higher targets, despite the fact that the subject attempted to accommodate, no clear image would be visible, making it hard to gauge the amount of effort required. The majority of the subjects in this group would not have been able to focus on the two nearest targets at 3.5 and 5 D; therefore, it is not surprising that maximum values are seen for ranges at greater distances.

2.4.2.3 Pseudophakic Group

Members of the pseudophakic group ranged in age from 64 to 74 years old, making the subjects, on average, older than those in the presbyopic group. Interestingly, many of the pseudophakic subjects produced higher maximum accommodative signal amplitudes than their presbyopic counterparts. Once again, though a decline in amplitude from the control group was seen, older subjects did not necessarily generate lower maximum accommodation signals than younger presbyopic group members.

Most of the group members were implanted with an IOL a year or two prior to experimentation; only subject HH was implanted at an earlier time point (recorded eye

implantation approximately three years previously). The potential implications of IOL implantation with regards to the experiment will be discussed later; suffice it to say that the length of time of IOL implantation did not affect the magnitude of accommodation measured.

Several anomalies were also present in the eyes of the pseudophakic subjects. These included corneal scarring (EL), peripapillary atrophy (HH), amblyopia (LK), vessel narrowing (LW), and an iris defect (AD, from a glaucoma operation in 1988). In the case of the amblyopic subject, the non-affected eye was used for the contact lens recording. Otherwise, the conditions did not affect the overall signal quality and amplitude of the subjects.

2.4.3 Accommodative Signal Qualities

As mentioned in previous sections, several different parameters of the accommodative response were measured, both to ascertain the best method of predicting the accommodative target, and to compare the current measurements with those taken in previous studies. It should once again be emphasized that studies in accommodation are fraught with inconclusive and contradictory results that vary with the measurement method and experimental protocol [(Bailey, 2011)]. Additionally, though previous studies have employed imaging techniques and indirect measurements, this is the first that directly measures a signal from the accommodative process; there is, therefore, a measure of deviation expected from the results of other methods.

2.4.3.1 Maximum Accommodative Amplitude

This quantity was, by far, the most repeatable and predictable measurement. As a rule, the maximum accommodative amplitude could be described by a linear relationship, with higher accommodative amplitudes indicating a closer target. There were, of course, exceptions to this rule, but the overall pattern remained consistent.

From the results, it is clear that a highly individualistic method is needed to predict the accommodative target based on the amplitude measured, one that can be re-calibrated, so to speak, for subjects. Training could be used as a supplement, but it is clear that any method utilizing the maximum accommodative amplitude signal would need a type of calibration measurement. Because this is the direct signal used, this is also the easiest and most reliable to incorporate into an accommodative device, as long as the precautions mentioned above are taken.

2.4.3.2 Maximum Accommodative Velocity

Several methods were used to estimate the maximum accommodative velocities of the subjects, namely, a simple two-point slope-calculation algorithm, and a differentiation of the data points. In a typical accommodation step response, two maximum accommodative velocities are present: one for the onset of accommodation, and one for the offset of accommodation. Because these parameters are thought to involve different biological components, they will be treated separately.

2.4.3.2.1 Accommodative Onset Velocity

The accommodative onset velocity is the velocity of the signal (in this case, nV/ms) from the starting point of accommodation to the steady-state response, at which point the subject has stabilized his or her focus on the target. Most research papers report this in terms of D/s, or in terms of the movement of a particular component of the accommodative plant per second [(Bharadwaj & Schor, 2006), (Bharadwaj & Schor, 2005), (Campbell & Westheimer, 1960), (Croft et al., 1998), (Sun & Stark, 1986)]. As with many facets of the accommodative process, this one has still not conclusively been ascertained.

Of the methods used to determine the peak velocity, many rely on the derivatives of models describing the accommodative amplitude over time, many of which are some variant of $y=y_0(1-e^{-t/\tau})$ [(Allen et al., 2010), (Campbell & Westheimer, 1960), (Kasthurirangan & Glasser, 2006), (Kasthurirangan & Glasser, 2005), (Ostrin & Glasser,

2007), (Shao et al., 2015), (Shirachi et al., 1978)]. This would produce a good approximation of the response velocity, if the model is both an extremely good fit, and a true approximation of the response curve. Because there is still some doubt as to the best model to describe the accommodative response [(Shirachi, et al., 1978)], both methods of analysis used in this experiment were chosen based on their independence from prior assumptions relating to the accommodation/time curve. It should be pointed out, however, that differentiating the responses also increases the noise of the signal, producing the possibility of false maxima or minima from such interfering signals as blink artifacts.

The first method, a simple two-point method, did not yield any significant differences in velocity between the groups and the accommodative targets, with the exception of a difference between the 2 D and 5 D target in the control group. All groups were significantly different from the flashlight test, which, considering the difference in control mechanisms, is to be expected.

Though the accommodative onset response velocity has been widely examined, few groups have come to a consensus regarding what, if anything, affects this parameter. Age has been considered as one factor; several groups have reported a decrease in velocity with age [(Croft et al., 1998), (Kasthurirangan & Glasser, 2006)], while others maintain that age does not affect the velocity [(Baumeister et al., 2010), (Mordi & Ciuffreda, 2004)]. Another factor considered has been the starting point of accommodation, with some studies indicating an increase in velocity with a nearer starting point [(Bharadwaj & Schor, 2006), (Kasthurirangan & Glasser, 2005)], and others showing no velocity change with the starting point [(Baumeister et al., 2010)]. Finally, a dependence on the response amplitude has been studied; in those studies that have explored the changes in velocity with response amplitude, most have found that the accommodative velocity increases with the response demand [(Bharadwaj & Schor, 2005), (Schaeffel et al., 1993), (Schor & Bharadwaj, 2006), (Schor & Bharadwaj, 2005)].

The results of the current investigation indicate a lack of dependence of the accommodative onset velocity on any of the parameters mentioned. Because the signals

recorded are, presumably, a type of signal created by muscle movement, it would be expected that, if the ciliary muscle does not degenerate with age, a similar and unchanging velocity would be expected for the accommodative onset. Most of the accommodative velocity comes from the active movement of the ciliary muscle, which, in turn, releases tension on the zonules. For this part of the response, the lens would be expected to provide most of the resistance.

2.4.3.2.2 Accommodative Offset Velocity

The accommodative offset (or disaccommodation) velocity can be best described as the speed of the response when changing from an accommodated (contracted) state to an unaccommodated (relaxed) state, a process also known as disaccommodation. Though it might seem superfluous to discuss the accommodative offset velocity separately from the onset velocity, the two quantities are, in fact, different in terms of response shape. Presumably, from an anatomical standpoint, different elements are also involved in these two processes [(Beers & van der Heijde, 1996), (Beers & van der Heijde, 1994), (Fisher, 1988)].

In the initial two-point analysis of the accommodative offset velocities, most accommodation offset velocities were similar, with only the pseudophakic group showing a difference between the flashlight condition and each of the step responses. Conversely, an analysis of the accommodative offset slopes performed using the differentiated responses resulted in several significant differences for the Accommodation Step protocol conditions (control group: between 5 D and 3.5 D, 5 D and 2.5 D; presbyopic group: 5 D and 2.5 D; pseudophakic group: 2.5 D and 2 D). The accommodative offset slopes at the 5 D and 3.5 D targets differed significantly between the control group and the presbyopic group, and between the control group and the pseudophakic group.

As with the accommodative onset velocity, there is disagreement as to which parameters affect the accommodative offset velocity, and to what extent they affect it. The present study indicates that there does seem to be some dependence on the target,

though this effect is perhaps minimized by the inability of presbyopic and pseudophakic subjects to accommodate clearly to nearer targets, and by the potential prevalence of blink artifacts of higher velocities than the accommodation offset velocities. Because of the observed difference between the highest response demand in both of the older groups and the younger group, one of several conclusions can be drawn: first, that the accommodative offset velocity slows with age; secondly, that the signal begins to saturate with age; and, finally, that, due to a control system without feedback, the older patients attempt to accommodate to a certain level, but are not able to reach it at the higher targets. Each of these explanations is plausible; however, due to the fact that presbyopes and pseudophakes clearly produce different signals at different targets, though with different amplitudes than the control subjects, the answer is probably a combination of age-related restraint of muscle movement coupled with an inability to accurately gauge the accuracy of accommodation at closer targets.

2.4.3.2.3 Differences between Accommodative Onset and Offset Velocities

A further topic of dissension in the field of accommodative dynamics is whether a difference exists between the accommodative onset and offset velocities. Anatomically, two different processes are involved: in accommodative onset, a process of contraction involving the active ciliary muscle, and, in accommodative offset, the relaxation of the ciliary muscle and the passive lens elements [(Beers & van der Heijde, 1996), (Beers & van der Heijde, 1994), (Fisher, 1988)]. Assuming that active elements are involved in the onset, while offset happens passively, differences between the two measurements would be expected.

For control subjects in the current study, such a difference appears to exist, or at least there is a trend towards a difference between accommodation onset and offset velocities. Significant differences were found between 5 D and 2 D targets; while the other targets were not significantly different, they were different enough to indicate a trend towards a difference between the measurements (3.5 D: $p=0.084$, 2.5 D: $p=0.065$).

Accommodative offset occurs at a faster rate than accommodative onset, which is consistent with the results of several studies [(Beers & van der Heijde, 1994), (Croft et al., 1998), (Kasthurirangan & Glasser, 2006)]. In the young human eye, assuming that the accommodative offset consists mainly of elements returning to their pre-accommodative state, i.e. the zonules elastically stretching the lens into an unaccommodated position, this result makes sense.

Interestingly, in the presbyopic group, a significant difference between onset and offset velocities was found at only one target (3.5 D), and no significant differences at all in the pseudophakic group. Croft et al. [(Croft et al., 1998)] suggest that the difference between accommodative onset and offset velocities occurs only until around the age of twenty, at which time the two parameters become essentially equal. Another study [(Heron & Charman, 2004)], using human subjects between the ages of 18 and 49, also did not find a significant difference between accommodative velocity onset and offset. This change in dynamics is likely the result of aging effects. Assuming the ciliary muscle is operating at its full potential throughout life, the changes in accommodative offset velocity must stem from other elements in the system. As the lens becomes less deformable with age, it would logically follow that the response, hampered by this element, would experience a decrease in speed.

2.4.3.3 Maximum Accommodative Acceleration

The maximum amplitude of both the onset and offset accelerations were assessed by taking the derivatives of the previously-derived velocity amplitudes. By taking the second derivative, there is a further increase in the amount of noise seen in the signal; this should be kept in mind when analyzing the results. However, it is believed that the acceleration amplitudes reported here are a true reflection of the dynamics of the recorded signal.

2.4.3.3.1 Accommodative Onset Acceleration

Accommodative onset acceleration was taken to be the first derivative of the velocity, or the second derivative of the signal, observed at the start of the response trigger. This parameter closely followed the time course of the velocity and movement parameters for the current experiment, as expected. However, determining the role that acceleration of the signal plays in the accommodative process is difficult to quantify.

Few studies have dealt directly with the acceleration properties of the accommodative signal. Baumeister, Wendt, and Glasser (2010) found that the acceleration of the response was independent of the starting point of accommodation, but increased with the response magnitude. Bharadwaj and Schor (2005) found exactly the opposite, with the peak acceleration remaining independent of the response magnitude, but dependent on the starting point. This latter conclusion generally reflects the results of the present experiment, though, within the presbyopic group, significant differences were found between different targets that would tend to contradict this conclusion. It is doubtful that these significant values in the presbyopic group represent a true pattern; more likely, they are the result of blink artifacts recorded during the time period in question. Due to the nature of the responses, it was almost impossible to separate blinks from velocity and accommodation traces, especially in presbyopic subjects with a small accommodative signal.

Interestingly, no significant difference between the three different groups for accommodative onset acceleration was observed. This indicates that the acceleration dynamics of accommodation are unaffected by age, which is an intriguing possibility in terms of finding a suitable control signal for an external device. For the current study, however, the accommodative onset signal is not a suitable candidate; it does not change between target distances, and, so, would not provide the essential element of distance dependence for a predictive system.

2.4.3.3.2 Accommodation Offset Acceleration

As with the accommodation onset response acceleration, Baumeister et al. (2010) assert that the acceleration offset response is invariant of the response amplitude, and

independent of the starting point. Conversely, Bharadwaj and Schor (2006) argue that, though the peak acceleration during accommodation offset observed is not dependent on the response magnitude, it is dependent of the starting position. The results observed in the present study are consistent with those of the former; no significant differences were seen between any targets, or between the three groups, for the accommodation offset acceleration.

As with the accommodation onset acceleration, it appears that the accommodation offset acceleration is invariant with age. Because each accommodation offset target started at one of the target focusing distances, and ended consistently at 0.5 D, it can also be conclusively stated that, in the present experiment, the starting point of the accommodation offset response does not appear to affect the overall peak acceleration amplitude. Thus, once again, though this is a quantity that does not degrade or change with age, it does not provide cues as to distance of focus, rendering it unsuitable as a control signal.

2.4.3.3.3 Differences between Accommodative Onset and Offset Accelerations

In keeping with the results of Baumeister et al. (2010), both the accommodative onset and offset accelerations appear to be invariant of starting position and target distance. Future analyses could reveal a dependence of the acceleration temporal properties on some distance-related parameter. The results of the current analysis indicate that both the accommodative onset and offset accelerations are similar in quantity, and do not differ with target distance. This conclusion implies that the accelerations are not affected by age, or by the response amplitude demanded.

2.4.3.4 Time Constant and Calculated Fit of the Accommodative Response

2.4.3.4.1 Calculated Fits of the Accommodative Response

The time constant of the accommodation curve is generally described as the amount of time needed for the signal to reach 63% of its final value [(Anderson et al., 2010), (Mordi & Ciuffreda, 2004), (Shirachi et al., 1978)]. Here, the parameter was calculated using a curved fit to the response in question; given either the equation

$$y = A(1 - e^{-t/\tau})$$

for accommodation, or

$$y = A(e^{-t/\tau})$$

for disaccommodation, the curve was fit to the response to solve for the maximum value (A) and the time constant (τ). Several examples are shown in Figure 40, Figure 41, Figure 42, and Figure 43.

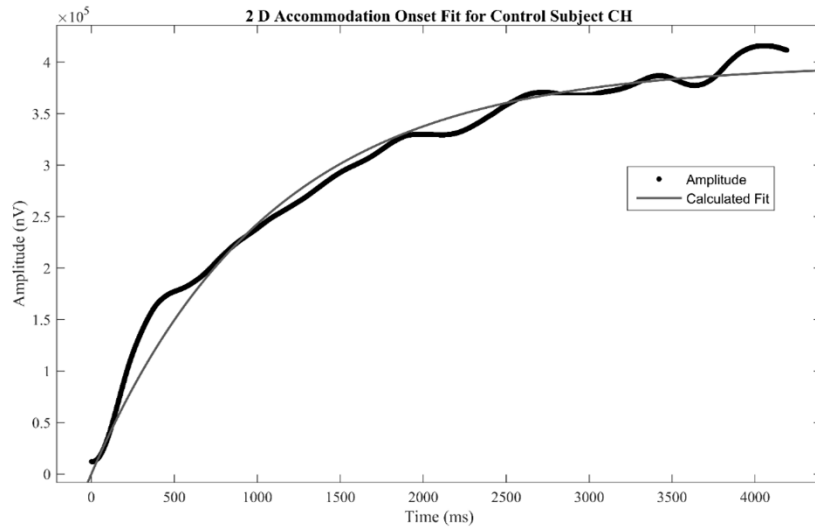


Figure 40: Example of a good fit calculation, shown here for the 2 D signal for control subject CH. In this graph, the calculated fit curve (shown in blue) closely follows the general trend of the recorded amplitude for the accommodation onset.

As can be seen in Figure 40, several good fits were made, though most of these were achieved for the less noisy signals of the control group. With fits such as these, an accurate estimation of the time constant could be performed with a degree of certainty.

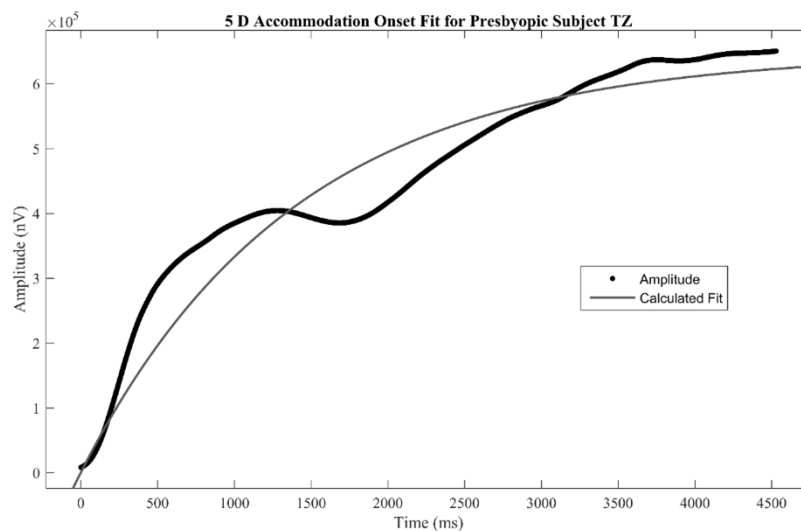


Figure 41: Example of a fit that does not accurately estimate the parameters of the accommodative curve. Because of the seeming two stages of increase, the final maximum accommodative amplitude is underestimated. Shown: Presbyopic subject TZ, 5 D target.

More difficult were cases such as those shown in Figure 41. This accommodation curve was made difficult, in terms of fitting, by the two phases of increase, both of which with a different curve. These phases could be the result of a redoubled effort on the part of the subject to accommodate beyond his normal effort; for this reason, both phases were included in the curve fit analysis, as the exclusion of either stage would mean losing relevant information about the accommodative process. Values calculated for fits such as this were less conclusive, and were seen more as estimates than concrete values.

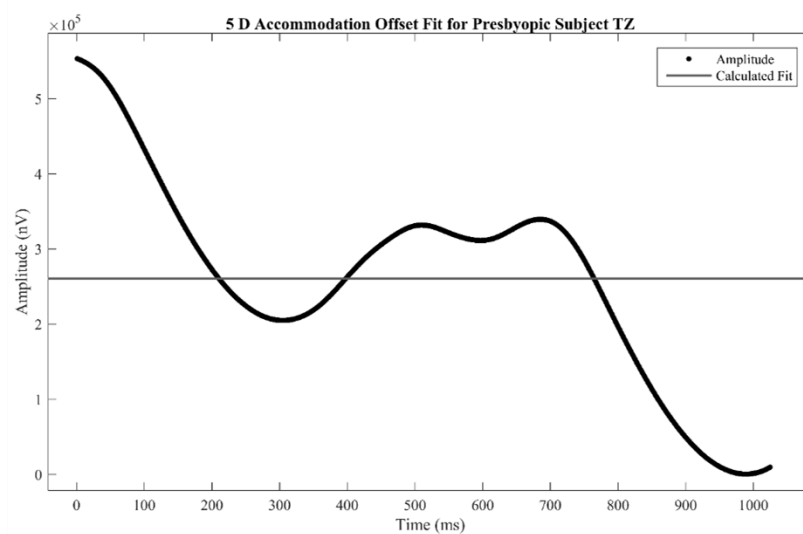


Figure 42: Example of a fit where two different curves are present, but are separated by a time interval. As can be shown above, this led to an inability to estimate a combined curve; in these cases, one of the two curves was chosen for analysis. Shown: 5 D target signal from presbyopic subject TZ.

The fit problem occurred more frequently, and with more problematic results, in the accommodative offset cases, as shown in Figure 42. In cases where this type of signal occurred, it was impossible to fit a curve to the offset response, due to the presence of a time interval between the two different curves. Because the curves were relatively similar, and because disaccommodation, unlike accommodation, is a passive process, in cases such as these, only one of the curves was chosen for fitting. Once again, results obtained from such an analysis should be viewed as estimates, as it is possible that some information was lost with the exclusion of one of the curves.

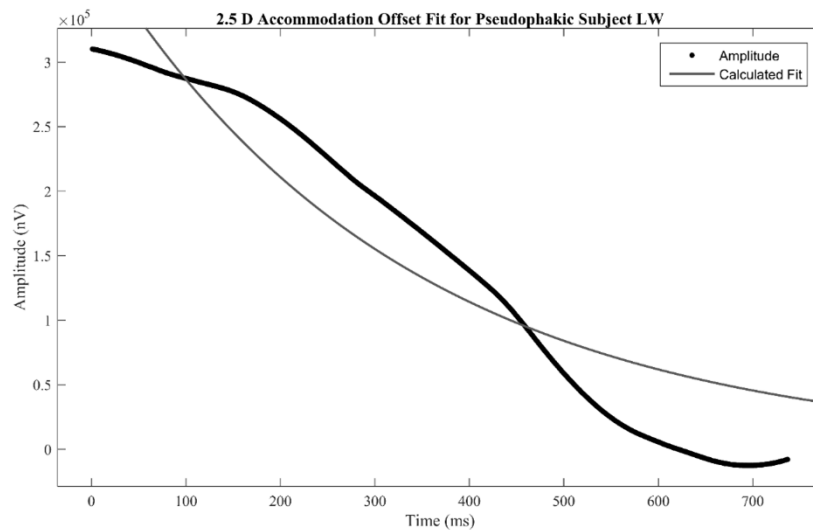


Figure 43: Example of an accommodative response where the curved fit equation describes only a small portion of the overall response. As can be seen, this led to an erroneous calculation of the accommodative response, and was, in most cases, subsequently restricted to a small portion of the entire response. Shown: 2.5 D accommodation response from pseudophakic subject LW.

In Figure 43, the recorded amplitude was of an abnormal shape at the top portion, achieving the expected shape only towards the end of the response. A good fit was not possible when the entire curve was measured, and, so was limited to the portion of the response which exhibited the expected disaccommodation response. This analysis could not be relied upon to produce a reliable value for starting accommodation (in the previous formulas, A), as the asymptote was never approached.

As can be seen from these examples, there were obstacles (sometimes significant) involved in the fitting of curves to the response values. In cases such as those shown in Figure 42 and Figure 43, the only option to achieve some level of fit was to choose a small portion of the total response for measurement. This usually led to an artificially small time constant. A similar problem is present in Figure 41; though the curve does provide an acceptable approximation of the combined stages seen in the signal, the maximum accommodative amplitude is underestimated, and the time constant is artificially lengthened.

This was not an insurmountable problem in the case of the maximum accommodative amplitude, as this parameter was calculated independently. However,

the calculation of the time constant does suffer from the problems with fit described above. To combat this problem in the best way possible, each curve was manually fit to the accommodative response, with window size and amplitudes zeroed at onset. Though this helps to better describe the fit, the reader should keep in mind that, in many cases, the time constant is overestimated in the accommodation onset response, and underestimated in the accommodation offset response.

Though the problems with fit do not lead to a conclusive time constant analysis, they do pose an intriguing question: is the basic model to describe accommodative dynamics truly a reflection of the behavior of the signal? Many groups [(Allen et al., 2010), (Beers & van der Heijde, 1994), (Campbell & Westheimer, 1960), (Kasthurirangan & Glasser, 2006), (Kasthurirangan & Glasser, 2005), (Ostrin & Glasser, 2007), (Shao et al., 2015), (Shirachi et al., 1978)] have used the exponential equations, or a variant thereof, to describe a recorded accommodation signal, but the equation might not describe the behavior of the system as a whole. Consider the example of a presbyope, similar to that shown in Figure 43, where there are clearly two distinct responses. This particular subject, in addition to being one of the developers of the experiment, remarked that he benefited from verbal encouragement throughout the experimental procedure: it allowed him to redouble his efforts to focus on a target, though he received no visual feedback as to the efficacy of those efforts. The accommodation signal does not decrease, but, rather, pauses briefly at one amplitude, then shoots to another amplitude. This would indicate that, though the accommodative response is itself a process controlled by the parasympathetic nervous system and, thus, involuntary, voluntary control can be exerted to produce a greater response than would normally be observed.

The existence of several phases in the accommodation response, ostensibly produced by a voluntary effort, would indicate a need for a modified curve fit for presbyopic and pseudophakic subjects. Though it is beyond the scope of this work to ascertain the characteristics of this new curve, a general suggestion to include a voluntary component in future accommodation models can be made. Because, in many cases, the signal does not return to its original resting accommodation state after the accommodation

response [(Ostrin & Glasser, 2005)], a better measure of maximum accommodative amplitude is also needed. In the current study, accommodation onset was used for the calculation of the peak signal amplitude; however, a method incorporating both accommodative onset and offset would provide a greater degree of accuracy.

2.4.3.4.2 Time Constants

2.4.3.4.2.1 Accommodative Onset Time Constants

The accommodative onset time constants calculated in this study are much greater than those reported in previous studies, with values variously calculated to be: 100 ms in young subjects to 200 ms in subjects in the fourth decade of life [(Sun & Stark, 1986)]; 255 ms for far targets, and 440 ms for near targets [(Shirachi, et al., 1978)]; and 120 – 360 ms [(Mordi & Ciuffreda, 2004)]. In the present study, the values did not differ significantly between experimental groups, but ranged from 104.1 ms to 6560 ms. Though some values fell within the range of those expected, many that ranged to several seconds were also present.

Because of the difficulty in fitting some of the data sets to curves (discussed in the previous pages), the values seen are necessarily exaggerated for the accommodative onset. Additionally, no trend exists regarding the distance/time constant relationship. This is consistent with the results from several studies [(Mordi & Ciuffreda, 2004), (Schor & Bharadwaj, 2005)], though there are, also, contradictory study results. Some groups have found a dependence of the time constant on the response amplitude, or on age [(Beers & van der Heijde, 1994), (Kasthurirangan & Glasser, 2005), (Shirachi et al., 1978), (Sun & Stark, 1986)]. Of these, most find an increase in the time constant with an increase in age and/or response amplitude.

An increase in time constant during the accommodative onset phase would suggest a longer time to reach the peak accommodative amplitude. A lack of changes in these parameters indicate the ability of the accommodative system to reach any target in approximately the same amount of time, regardless of the distance. If the velocity of the

signal increased for increased target distances, it would be expected that the time constant would not need to change reach the desired amplitude; however, our results do not indicate a significant increase in velocity with an increased response distance. Mathematically, this produces a problem, as some parameter must increase to deal with the increased load to the system. A clear increase in amplitude is seen with an increased response amplitude, but none of the parameters measured appear to significantly change with the response amplitude. It should be remembered that all of the parameters calculated are calculated from subject *averages*, rather than each individual subject trace. A future study involving the analysis of each subject, separate from his or her group, would shed more light on the role each parameter plays in accommodation.

2.4.3.4.2.2 Accommodative Offset Time Constant

As for the accommodative onset time constant, no real pattern in terms of significance between targets or experimental groups was found in the accommodative offset time constants. The literature is, once again, divided on this issue: some have found that the time constant does not change with age or response target [(Beers & van der Heijde, 1994), (Kasthurirangan & Glasser, 2005)], while others have found changes with one or both of the aforementioned parameters [(Shirachi et al., 1978), (Sun & Stark, 1986)].

Values for the accommodative offset time constant reported in the literature are fairly similar to those reported for the accommodative onset time constant. The values calculated in the present investigation are generally greater than those reported in the literature, with a range of 470.18 ms to 1270.56 ms. Because the offset of the accommodation response involves mostly passive processes, it follows logically that a similar value would be observed for each target, as was the case here.

2.4.3.4.2.3 Differences between Accommodative Onset and Offset Time Constants

In the present study, no significant difference was found between accommodative onset and offset time constant values. Based on the present study results, the accommodative onset and offset responses have approximately the same temporal response to an accommodative trigger.

This finding is interesting in several respects. If a similar response from both accommodative onset and offset is seen in control subjects, why does the pattern continue into the presbyopic condition, where the accommodative plant has been compromised? Once again, the geometric theory of presbyopia development offers a plausible explanation. If the accommodative onset movements are restricted, the accommodative offset movements must also be necessarily restricted, each movement being the product of elements in the same system. This observation is further confirmed by the continuation of the trend in pseudophakes, where, though there is increased movement, the time constant of both the onset and offset remain similar.

A second question is the lack of increase in the time constants for both onset and offset with age. Though they respond similarly, why are the time constant values between pseudophakes, presbyopes, and control subjects nonetheless similar? This could also be described as an effect of presbyopia development. With the development of presbyopia, the accommodative plant, receiving no visual feedback, could simply respond as it always did, with the same temporal signal characteristics. When presbyopic subjects exert an extraordinary voluntary effort, it appears that, rather than one magnified signal, the accommodative plant performs another iteration of the action just performed. The time constant of each separate effort is similar; if both were combined this would, of course, indicate a greater value, but fail to describe the dynamic characteristics of the process.

2.4.4 Pharmacological Measurements

The pharmacological measurements performed in this investigation provide an invaluable source of information with regard to the control signals generated during

accommodation. Both drugs used (cyclopentolate and phenylephrine) have been postulated to have an effect on the accommodative process. Each pharmacological intervention will be discussed separately.

2.4.4.1 Phenylephrine Intervention

Phenylephrine is routinely used in accommodation studies to dilate the pupil, allowing for easier measurement of the accommodative system [(Bharadwaj et al., 2009), (Bharadwaj & Schor, 2006), (Bharadwaj & Schor, 2005), (Crawford et al., 1989), (Drexler et al., 1997), (Dubbelman et al., 2005), (Heron & Charman, 2004), (O'Neil & Brodkey, 1970), (Stark & Atchison, 1997)]. The drug itself is used in concentrations of 2.5% and 10% for eye drops, and functions as a stimulant for the sympathetic nervous system. Assuming total parasympathetic innervation of the ciliary muscle, no effect should be seen on the resulting accommodation parameters; however, if the sympathetic nervous system plays a role, increased activity, caused by the application of phenylephrine, would lead to a decrease in accommodative activity.

Side-stepping the rather heated debate of the role of the sympathetic nervous system in accommodation, results from previous studies can be analyzed. Several studies [(Culhane et al., 1999), (Dubbelman et al., 2005), (Garner et al., 1983), (Rosenfield et al., 1990), (Zetterström, 1984)] have found that accommodative amplitude does decrease with the application of phenylephrine at varying concentrations, while others [(Crawford et al., 1989), (Gilmartin et al., 1992), (O'Neil & Brodkey, 1970), (Ostrin & Glasser, 2004), (Sarkar et al., 2012), (Richdale et al., 2012)] assert that the effect of phenylephrine is mild or non-existent on the accommodation process. The current experimental results indicate that phenylephrine, applied in a 2.5% concentration, has no effect on the resulting accommodative signal.

These results suggest that the sympathetic nervous system does not largely contribute to the recorded signal. In terms of accommodative amplitude changes, objective and subjective accommodation measurements were not performed after the instillation of phenylephrine drops; therefore, the signal measured is one purely

dependent on the actual movements occurring during accommodation. No dynamic parameters, either for accommodation onset or offset, were affected by the drug.

2.4.4.2 Cyclopentolate Intervention

Cyclopentolate is commonly used in clinical investigations to dilate the pupil and prevent accommodation. The expected effect of this drug is to completely inhibit accommodative activity, preventing the subject from focusing at near targets. An attenuation, or a complete cessation, of signal activity was expected from this investigation.

Only control subjects underwent the cyclopentolate examinations, but the effects of the drug are well-established, and can be generalized to include the expected behavior of the population as a whole. Indeed, significant differences, in addition to being present in the accommodative amplitudes, also presented themselves between the 5 D normal step target and cycloplegia condition for the velocity of both the accommodative onset and offset. The velocities were found to be greatly reduced as compared to the normal condition when the 5 D test with cyclopentolate was performed. Interestingly, the other accommodative dynamic parameters were unaffected by the application of the drug.

It is expected that the 3.5 D target would behave similarly, though this was not reflected in the recorded results. This can be attributed to the fact that the cyclopentolate had probably not fully taken effect at the 3.5 D target (this target was always performed before the 5 D target test), and, therefore, does not reflect a true state of cycloplegia. There is also the possibility that, being a farther target, the 3.5 D target does induce some level of accommodative signal, simply because the patient is better able to estimate the distance.

2.4.5 Variations of the Signal with IOL Type

Due to the small number of subjects in the present experiment, and the variety of IOLs encountered, the results cannot be used to draw statistically-relevant conclusions.

However, due to the process of IOL implantation, and the fact that different signal characteristics were seen in subjects with different IOLs, it is interesting to discuss the results in more detail. Ten pseudophakes were measured over the course of the experiment; of these, nine were used for final analysis, and are discussed below.

Of the subjects tested, eight were implanted with an IOL manufactured by Abbott Medical Optics, while one had an IOL from Alcon. The highest amplitude seen was from the subject with the Alcon implant. There was no trend between the maximum amplitude, and the number of pieces the IOL contained, consistent with the results of Nemeth et al. [(Nemeth, et al., 2008)]. Most subjects were implanted within a year of the experiment; several subjects were implanted several years prior to the experiment, but did not seem to suffer from a reduced signal magnitude compared to the other subjects.

Among subjects with the same IOL, the results were variable. Two subjects with ZA9003 lenses produced signals of similar magnitude, at 0.98 and 0.84 mV. Though these results were fairly close, tests between subjects with the PCB00 IOL yielded amplitudes of 0.55, 0.52, 0.82, and 1.12 mV. No clear distinction can, therefore, be made, regarding the merits of one lens over another for accommodation.

It is suggested that future studies seek to expand upon these findings by recruiting subjects with the same IOL model, implanted within a similar time frame, and of a similar age. A larger cohort would allow for conclusions to be drawn, regarding the efficacy of particular IOLs in allowing for greater accommodation in pseudophakes.

2.4.6 Case Study: Intra-Individual Comparison

One subject, AD, was measured in both her phakic and pseudophakic eyes. Subject AD was a sixty-four year old woman, slightly myopic (-0.75 D) in the pseudophakic (right) eye, and hyperopic in the presbyopic (left) eye (+2.0 D, though a +4.0 D lens was needed during the experiment). AD was implanted with an Alcon IOL (SN60AT Acrysof) less than one year before the start of the study. Initially, she was rejected as a candidate for the present study, due to the presence of a large iris (and

possibly ciliary structure) defect sustained from a glaucoma operation twenty-six years previously. As she performed very well in the pseudophakic group, however, she was also asked to participate in the presbyopic measurements. Different electrodes were used in the different trial measurements, but it is believed that the results are, nonetheless, comparable.

The maximum signal amplitude measured in AD's pseudophakic eye (2.59 mV) was much higher than that measured in her presbyopic eye (1.35 mV), though she was the highest responder in both groups. This would seem to indicate that, assuming that the signal for accommodation is equal between both eyes, some factor allowed for a higher response in the eye with the IOL. Such a phenomenon could be explained by the geometry theory of accommodation: because the IOL eye had less restriction of movement than its presbyopic counterpart, it was able to move more, and, thus, produce a higher signal than that seen in the companion presbyopic eye.

The subject did report some difference of accommodation between the two eyes during monocular testing, stating that she could clearly see the target in her right (pseudophakic) eye at 2.5 D, but could not with the left (presbyopic) eye. Because 2.5 D was the lowest possible accommodation measured by the test, it is difficult to say whether there was a true difference between the accommodative abilities in each eye, or whether the better accommodation in the pseudophakic eye was due to the differences in visual acuity. The subject's pseudophakic eye was myopic, allowing her to "see" at closer distances due to the natural shape of the eye; the presbyopic eye was highly hyperopic, which would have the opposite effect, and further curtail accommodative efforts by the subject.

Overall, though a single case cannot, of course, be taken as a conclusion of an entire population, the between-eye comparison of subject AD supports the geometric theory of presbyopia development. A greater accommodative amplitude was measured in the pseudophakic eye than in the presbyopic eye, though both eyes could not, ostensibly, provide feedback at the distances measured. Clearly, the implantation of the

IOL affects the amplitude of the accommodative signal, if not the overall amplitude of accommodation of the subject.

2.5 Conclusions

The present study has provided invaluable information, in terms of a novel and effective way of measuring the accommodative signal of a human subject, and also in better describing the principles and mechanisms of accommodation. From the repeatability of the trial measurements, it is plain that the contact lens electrode developed is an accurate way to measure a signal that, previously, could not be quantified non-invasively. It is hoped that, with the adoption of this electrode as a measurement tool, groups studying the accommodative mechanism will finally have a standard method of measurement with which to produce comparable and meaningful results.

As to the signal being measured, it is likely a measurement of the movement of the accommodative apparatus. Though this is not, in itself, a direct measure of the ciliary muscle's electrical activity, it is an indicator of the amount of movement of the ciliary body. Therefore, a decrease in measured signal amplitude is closely correlated with a decline in the movement of the ciliary body. As it has been conclusively established that the ciliary muscle's properties do not decline with age, the logical interpretation of the results seen in the present study is that the muscle movement is being somehow restricted. This conforms to the geometric theories of accommodation, which state that the ciliary muscle movement is restricted with age, and, therefore, not able to actuate the necessary level of accommodative activity.

After analyzing the results of the study, the best signal parameter to act as a control for a neuroprosthetic device is the maximum accommodation amplitude measured. The amplitudes of accommodation for each group could be described by a straight line, one which increased in amplitude for each accommodative demand increase. Therefore, for the second part of this work, the control signal used will be the maximum accommodative amplitude signal.

Though the present studies provide a good groundwork for the use of a contact lens electrode in the measurement of accommodation, future work should be performed to better characterize certain aspects of the accommodative signal. Because the end goal of this part of the experiment was to find a suitable control signal for a prosthetic device, several parameters, mostly temporal measurements of the accommodative signal (latency, time to peak magnitude/velocity/acceleration, etc.) were not explored. It is beyond the scope of this project to individually explore each parameter of accommodative dynamics; suffice it to say that further parameters of the signal could be calculated, such as response duration and the time at which the acceleration signal reaches its peak. For such a study, more rigorous controls in terms of timing would need to be implemented, and a robust method for pinpointing the exact initiation of the signal would need to be developed. Future studies should focus on establishing the normal temporal characteristics of the accommodative signal, as well as on the establishment of the repeatability of such parameter measures as velocity, acceleration, and time constant.

3. DEVICE DEVELOPMENT

3.1 Introduction

Based on the results of the ciliary muscle study, namely, that the maximum accommodation amplitude is a factor that can be used to accurately predict accommodation in a subject, a device could be created to use this signal in effecting accommodation. By using the ciliary muscle signal to control this device, a better clinical intervention for presbyopia could be developed, one that uses the control signals from the patient to provide a natural accommodative response. The following sections detail the development of this device.

3.2 Device Requirements

3.2.1 Target User

The user for this device will be either presbyopic or pseudophakic, with the inability to accommodate to 2.5 D or less. Necessarily, this means that the user will be at least fifty years old [(Atchison, 1995), (Charman, 2008)]. It is expected that the user will be under the supervision of an ophthalmologist (i.e. routine check-ups). Other aging factors will also, most likely, be present in the user (medications, ocular conditions associated with aging, reduced mobility).

3.2.2 Feasibility Criteria

In order for the design to be a viable solution, several criteria must be met. Safety is, of course, a high priority; because the measuring electrode is in direct contact with the sclera, current from the device would cause pain (worst case), or, in smaller levels, a tingling sensation and phosphenes [(Naycheva et al., 2012)]. Though the latter two are harmless to the user, both are disconcerting, and should be avoided.

Mobility is also a prime concern. The user should be able to utilize the device while performing his or her daily routines, which could include shopping, driving, etc. This necessarily implies that the device cannot be too heavy or bulky, and cannot require a constant power supply from an electrical outlet.

Ease of use and low maintenance are other key features that the device should possess. Different users will have different educational backgrounds, and different levels of comfort with technology. The device should be easy to use, and require the least possible amount of user effort for operation.

Durability is a major point, simply because of the age of the user. The device should be able to withstand wear and tear within the range of daily possibilities, i.e. dropping, rain, and normal medical procedures. As an intervention, the device will not be effective unless it can withstand the rigors of daily life.

3.2.3 Merit Criteria

Several criteria are described here that, while not necessary for the final design of the device, would make the device more desirable for the user. Adjustability is a feature that would increase the utility of the device; it was seen previously that accommodative amplitudes fluctuate widely for the same subject (see Section 2.3.7), which would indicate the need for comparable adjustability in the device. This could be in terms of signal magnification, or in terms of the final accommodative output.

Refractive correction would also make the device more desirable for a user. If the device could correct spherical refraction, or piggyback onto an existing corrective system, the utility for the user would be increased. An additional aspect to this, in the case of completely replacing an existing refractive correction, would be to produce the correction while factoring in the effects of accommodation.

Appearance and inconspicuousness of the device are another factor to consider. This includes the final appearance of the system, as well as the level of potential

irritability that could be caused to the user. Such an irritation could be in the form of, for example, noise produced by the device.

A large range of refraction would be an asset in the final design. This would include the level of gradation of the steps; for example, step sizes of about 0.25 D would be optimal. It would be desirable for the device to be able to accommodate from 0 to +5 D, at the very least; this would allow for most levels of near work.

Finally, though not of paramount importance at this stage of development, cost is a factor to consider. Depending on the level of insurance coverage, the customer base will be reduced by a prohibitively-costly product. For the prototype, this cost will necessarily be much higher, but the design should allow for low-cost modifications.

The merit criteria for rating the design ideas, together with scaling and weighting factors, are presented in Table 21.

Table 21: The merit criteria used in the design selection, shown with weighting and scaling values. Each merit criterion is evaluated separately. Weighting indicates the relative importance of the criterion, and is the factor by which the scaling number chosen is multiplied. The number for scaling is chosen based on its relation to the scaling descriptions listed.

Merit Criterion	Weighting	Scaling		
		Good (100)	Acceptable (50)	Poor (25)
Appearance	40%	Does not cause the user to feel self-conscious;	Appears slightly bulky and/or out of place;	Is very obtrusive;
		Does not bother the user at all during normal wear time	Irritates the user slightly, but not enough to cause physical or mental distress	Irritates the user greatly
Adjustability	25%	Can be adjusted to measure all possible voltage values from presbyopic and pseudophakic users	Can be adjusted to measure 75% - 99% of the range of presbyopic and pseudophakic voltages	Can measure less than 75% of the expected voltage range for presbyopes and pseudophakes
Range of Refraction	20%	Allows for refractive	Allows for refractive	Allows for refractive

		adjustment greater than 5 D;	adjustment up to 5 D;	adjustment less than 5 D;
		Is adjustable in steps smaller than 0.5 D	Is adjustable in steps of 0.5-0.75 D	Is adjustable in steps of 0.75 D or greater
Refractive Correction	10%	Corrects greater than or equal to +5 D/-5 D, in addition to accommodative correction	Corrects greater than or equal to +3 D/- 3 D, in addition to accommodative correction	Cannot correct for refractive error in addition to accommodative correction
Cost	5%	Costs less than \$100 to manufacture	Costs between \$100 and \$500 to manufacture	Costs over \$500 to manufacture

3.2.4 Design Selection

The main component in the final design is the variably refractive lens. Two possible configurations are the use of a liquid crystal lens, and the use of a lens that uses a mechanical medium to actuate a change in refraction. For each model, a preliminary design was developed.

Liquid crystal lenses are used in a plethora of devices, including webcams [(Castellano, 1972), (Tomita & Nabeshima, 1997)]. The devices are operated by passing an electrical signal through the medium; this causes the crystals to change orientation, and, therefore, index of refraction. Many advantages are realized with this type of lens: because the lenses are controlled electrically, they are easy to integrate in an electrical system. There are no moving parts, eliminating the long-term effects that would be seen with manual fatigue, and preventing any irritating noises caused by moving parts. These lenses are not as bulky as their mechanically-actuated counterparts, and have a much wider range of refraction that does, additionally, allow for myopic correction. There are, however, several drawbacks to this approach: these lenses are much more costly than a

mechanical model, sensitive to temperature, and require a high voltage (over 20 V) delivered in a waveform.

Mechanically-actuated lenses work by a change in a mechanical parameter which causes a corresponding change in refraction. Several designs achieve this by dials which fill a deformable bag with more or less of a specific liquid, or, as in the case of the commercially-available Adlens[®] Adjustables[™], a dial which moves one lens in front of another to achieve a specific refraction [(Nisper & Stevens, 2014), (Nisper & Stevens, 2016)]. These devices are very affordable (around €30), and are already made to be adjustable. However, the range of refraction offered by these lenses is low (for Adjustables[™], -6 D to +3 D) and, due to their self-contained nature, it is more difficult to integrate them into a control system. This could be done with the use of a motor mounted to the glasses, but at the cost of adding weight to the glasses frame, and the noise produced by the motor. The integration of a motor would require a separate power source, and could potentially introduce problems with interfering magnetic fields (i.e. in the case of a pacemaker or ambient electromagnetic signals).

Because both design approaches meet the feasibility criteria described in Section 3.2.2, the final design selection was performed using a decision matrix evaluating the merit criteria scores of each design. Table 22 shows the matrix used to choose the final design.

Table 22: Comparison of the merit criteria scores for each design. Each design is given a rating, based on how well the design meets the criteria presented previously. This value is multiplied by the weighting to give the final score. The design with the highest score is the liquid crystal lens.

Merit Criterion	Weighting	Liquid Crystal Lens		Mechanical Lens	
		Rating	Score	Rating	Score
Appearance	0.40	90	56	40	16
Adjustability	0.25	100	25	100	25
Range of Refraction	0.20	100	20	50	10
Refractive Correction	0.10	100	10	25	2.5
Cost	0.05	50	2.5	100	5
Total	1		113.5		58.5

3.2.5 Explanation of Design Selection

Though the mechanical lens model is the clear winner in terms of cost, there are several problems to consider in terms of incorporating such a lens into a design. Though the frames are very attractive in terms of design, appearing like a set of regular glasses, the clarity and size of the field of view can be greatly restricted.

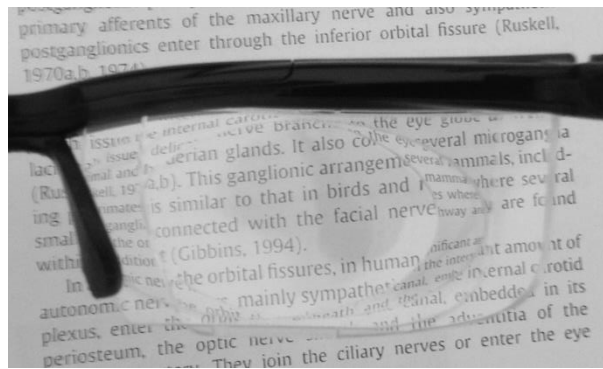


Figure 44 shows an example of this.

shows an example

Figure 44: Peripheral distortion observed with Adlens Adjustables™, a mechanical model of variably-refractive lens.

To actuate the dial at the side of the glasses, the use of a motor would be almost mandatory. Though there are several motors that are small enough to fit on the glasses frame, these motors would add weight to the frame, and necessitate the use of a second power supply (additional batteries).

Additionally, a mechanical lens does not possess the wide range of refractive powers that a liquid crystal lens can achieve, nor are the gradations between the different

refractive powers as fine. Because a significant portion of the population requires corrective lenses for visual tasks, it is almost certain that some level of refractive correction would be necessary for a percentage of the patients, in addition to the requisite refractive corrections during accommodation. The mechanical lens design is therefore not suitable for such a large patient group as the liquid crystal lens design.

3.3 Device Specifications

A liquid crystal lens was chosen for the final design. This design, as a preliminary sketch, can be seen in Figure 45.

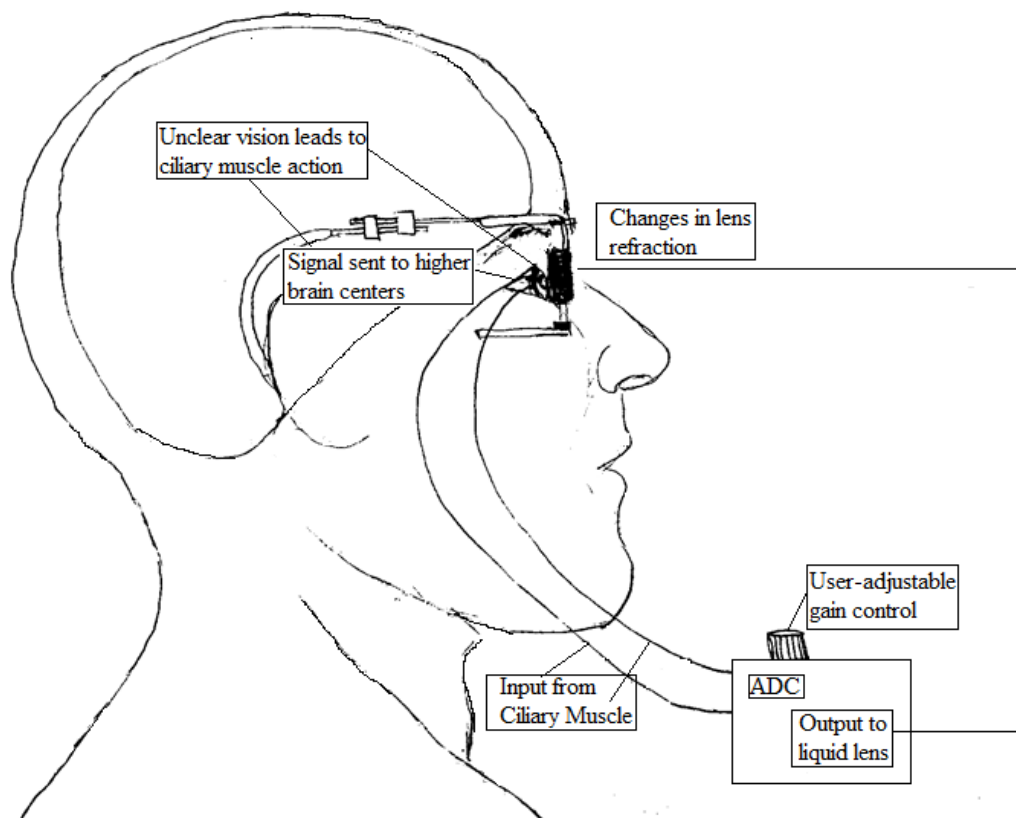


Figure 45: Conceptual sketch of the final device design. A recording from the ciliary muscle is processed by the device, which sends a signal to adjust the lens in the glasses.

This design is intended to allow users to correct their vision outside of a clinical setting, making it imperative for the final device to be user-friendly and durable. The overall device will consist of the liquid lens, mounted on a glasses frame, as well as an external control unit. As described in Section 2.2.1, a contact lens electrode will be the means of recording signals from the user. Because a wide range of signals was seen in experimental measurements, several different parameters will be alterable by the user to best suit his or her specific needs. Because the device is meant to be portable, batteries will provide power. Figure 46 shows a flow diagram of the final design.

Subsystems were divided into several groups, based on functionality and location. These subsystems were termed signal conditioning, user interface, housing, signal

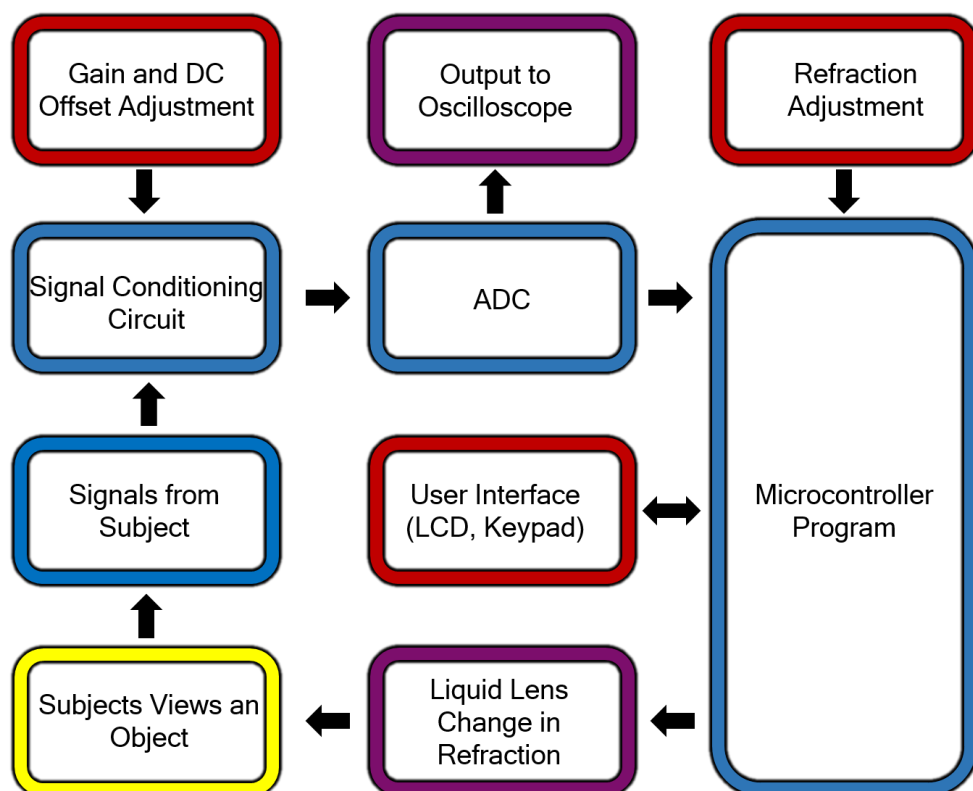


Figure 46: Flow diagram of the final device design. Purple boxes indicate device outputs, blue indicate signal processing elements, and red indicate user inputs.

processing and communication, liquid crystal lens, and power subsystems

3.3.1 Liquid Crystal Lens Subsystem

3.3.1.1 Liquid Crystal Lens Selection

Of paramount importance to the final design was the selection of a suitable liquid crystal lens, with the necessary components for integration into a finished system. This included the need for some common mode of communication with an external circuit, i.e. I²C functionality.

Initially, a mechanically-tunable liquid crystal lens (model ML-55-106-NOC-LD, Optotune Switzerland AG, Dietikon, Switzerland) was considered, mainly for its large aperture (55 mm) and refractive power range (0-133 D). However, after consultation with the company, the model was rejected due to its inability to be integrated without actuation into an electrically-controlled system, and its pending unavailability (the company was switching production to electrically-controlled tunable lenses).

A second lens from Optotune was also considered, the EL-10-30 electrically-tunable lens. This model could be actuated by the application of a specific current level across the lens, resulting in refractions of between 8.3 and 20 D. Though such a lens is, hypothetically, able to be integrated into an electrical system, its integration into a microcontroller-driven system, which outputs only high or low voltages, would considerably complicate the design. Additionally, the lens could not be used to correct negative refractions, or to provide the range of refractive powers needed. Therefore, this lens was also rejected.

The Arctic 39N0 (Varioptic, Lyons, France) was the next lens consideration. This lens can be integrated into an electrical system via a driver board which contains three different lens driver ICs, each of which is able to communicate with a microcontroller via an I²C protocol, an industry standard serial bus. The refractive power ranges from -15 D to +15 D, meaning that, in addition to accommodative refraction, the lens is capable of correcting spherical refractive errors. This was the lens chosen for the final design.

3.3.1.2 Liquid Lens Housing

The Arctic 39N0 development kit contained flex cables and a case for the lens; in order to lessen development time, and to simplify construction, these cables and case were chosen for use in the final design. This is shown in Figure 47.



Figure 47: The Arctic 39N0 lens shown alone (left) and assembled with the components provided by the manufacturer (right).

In order to use the lens as a visual aid, a frame was required to hold the lens in place. A sunglasses frame with the lenses removed was initially conceptualized, but this entailed problems in terms of fixating the lens, and in terms of adjusting the lens for different face shapes. To solve this problem, shooting glasses (Model 300 Schiessbrillen, Gehmann GmbH & Co. KG, Karlsruhe, Germany) were modified to hold the lens in place. These glasses are adjustable at several different points, allowing users to modify the position based on face shape.

An additional component requiring consideration in terms of housing was the driver board. The board attaches to the lens via flex cables; these flex cables are, however, short in length, and fragile. To combat this problem, the board was also mounted on the glasses frame. It should be noted that only one out of the three available ICs was used for the final design; however, it was impossible to physically separate the different ICs

from one another without destroying the circuit. Therefore, the entire board was mounted, as shown in Figure 48.

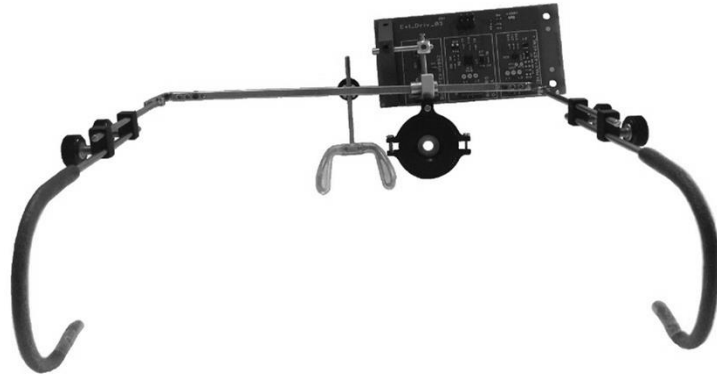


Figure 48: Completed glasses mount, constructed from a modified shooting glasses frame. The driver board is anchored above the lens. The knobs shown allow for adjustment of the ear and nose pieces.

The system received input from six different pins, delivered from a ribbon cable plugged in to the driver board. Because the ribbon cable included in the kit was too short to allow for much movement, a longer cable was constructed in-house. The communication between the microcontroller and the liquid crystal lens subsystem is described in greater detail in Section 3.3.2.

3.3.1.3 Liquid Lens Driver Selection

As mentioned previously, three different liquid lens drivers were fabricated onto the driver board: Maxim 14574 (Maxim Integrated, San Jose, CA, USA), Rogers D388A (Rogers Corporation, Chandler, AZ, USA), and Supertex HV892 (Microchip Technology Inc., Chandler, AZ, USA). Each of these driver ICs were powered by 3.3 V inputs, and controlled by two pins (SDA and SCL) of the I²C bus.

The HV892 was chosen for several reasons. A main factor selection was the circuit construction; the other IC circuits required inductors for operation, whereas the HV892 did not. In future iterations, this would reduce the complexity of the circuit if it were later built in-house to reduce the overall size of the design. Additionally, the circuit itself was much simpler in construction than those required for operation by the other ICs.

Finally, the HV892 contained a simple write-only protocol, allowing data to be written to the IC without the need for the performance of other operations.

3.3.2 Signal Processing and Communication Subsystem

This subsystem involves the integration of all signals received from the user and external components, such as the liquid crystal lens (user interface components are addressed separately in Section 3.3.4). For the main processing component, a PIC18F4520 microcontroller was used (Microchip Technology Inc.). This microcontroller was chosen due to its large amount of input/output pins (36) and features, including the ability to communicate with the liquid lens driver IC chosen (Supertex HV892) using I²C protocol.

3.3.2.1 Analog to Digital Conversion

In order to allow the signal to be interpreted as a meaningful value by the microcontroller, the analog signal recorded from the patient, once it is processed by the signal conditioning circuit (Section 3.3.3), must be converted from an analog to a digital value. This is done through the use of an analog-to-digital converter (ADC).

The PIC18F4520 contains a built-in 10-bit ADC, which was originally used for the design. Using reference values of 0 V and 5 V, a 10-bit ADC would yield 1023 different steps with values of:

$$V_{\text{step}} = \frac{V_{\text{max}}}{2^n - 1} = \frac{5 \text{ V}}{2^{10} - 1} = \frac{5 \text{ V}}{1023} = 0.00489 \text{ V} = 4.9 \text{ mV}$$

However, it was thought that a higher resolution was needed for the conversion. Therefore, an Adafruit ADS1015 12-bit ADC module (Adafruit Industries, New York, NY, USA) was substituted. Repeating the previous calculation, a 12-bit ADC with reference values of 0 V and 5 V would have 4095 different steps, with values of:

$$V_{\text{step}} = \frac{V_{\text{max}}}{2^n - 1} = \frac{5 \text{ V}}{2^{12} - 1} = \frac{5 \text{ V}}{4095} = 0.00122 \text{ V} = 1.2 \text{ mV}$$

This module communicates on the I²C bus, so it is easily integrated into the design.

Briefly, the device runs in continuous conversion mode, constantly converting the analog signal it receives into the corresponding digital signal, in this case in millivolts. Pins A0 and A1, input and output pins, are connected to the outputs of the signal conditioning circuit (signal and virtual ground, respectively). The final circuit configuration is shown in Figure 49. Outputs are provided at the points shown in the figure to allow for direct measurement of the analog signal by an oscilloscope.

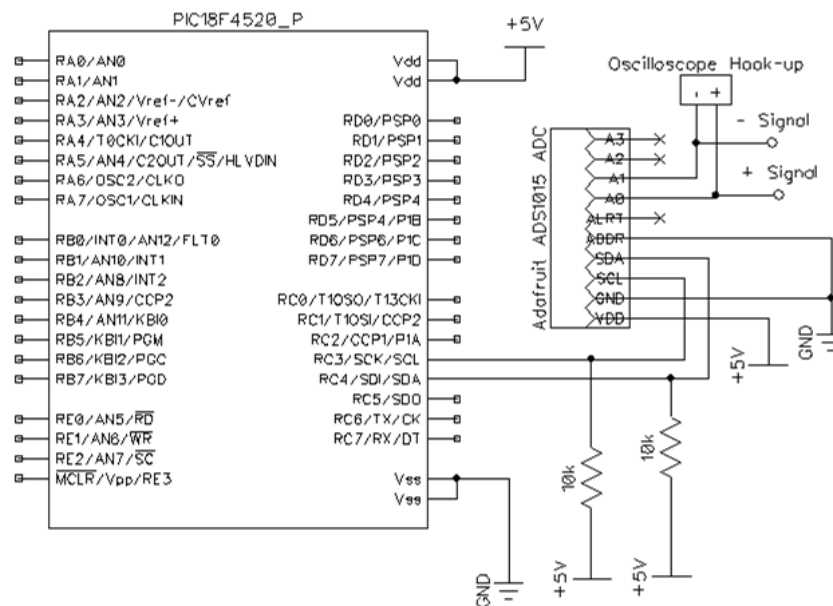


Figure 49: Diagram of the final ADC circuit used in the design. The microcontroller is connected to the Adafruit ADS1015 ADC module through the SDA and SCL pins (both pulled up with 10 k Ω resistors). For testing purposes, an oscilloscope hook-up was added to allow the values seen by the ADC to be displayed externally.

3.3.2.2 Voltage Level Conversion

Unlike the PIC18F4520 microcontroller, which requires a 5 V power supply for operation, the HV892, which controls the lens, runs on only 3.3 V. Therefore, the power and I²C bus source must be reduced from 5 V to 3.3 V.

The first problem is easily fixed. Using a voltage regulator (LM317, Texas Instruments Inc., Dallas, TX, USA), the 5 V power supply can be reduced to 3.3 V, thereby reducing the need for a separate battery. Figure 50 shows the voltage regulator circuit used to achieve this power reduction.

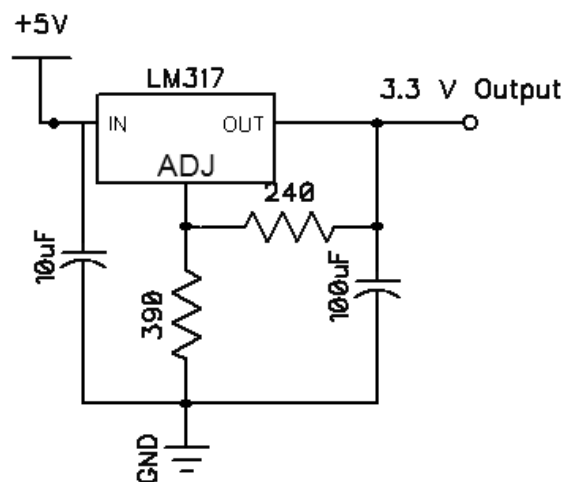


Figure 50: Circuit used to reduce the 5 V power supply to 3.3 V. 5 V is input from the battery, while the 390 Ω and 240 Ω resistors adjust the voltage based on the equation $V_o = V_{REF} [1 + (R_2 / R_1)] = 1.25 \text{ V} [1 + (390 \Omega / 240 \Omega)] = 1.25 \text{ V} (2.625) = 3.28 \text{ V}$. Capacitors are added to further stabilize the voltage.

The second issue is the reduction of power on the I²C bus. Unlike a power supply, the I²C communication protocol requires precise timing, and is therefore not reducible with a simple voltage regulator or a voltage divider. Special ICs do exist for this purpose, and one (Sparkfun Logic Level Converter - Bi-directional, Sparkfun Electronics, Niwot, CO, USA) was chosen to preserve the I²C timing, while allowing for the 3.3 V power supply switch. The circuit configuration using the Logic Level Converter is shown in Figure 51.

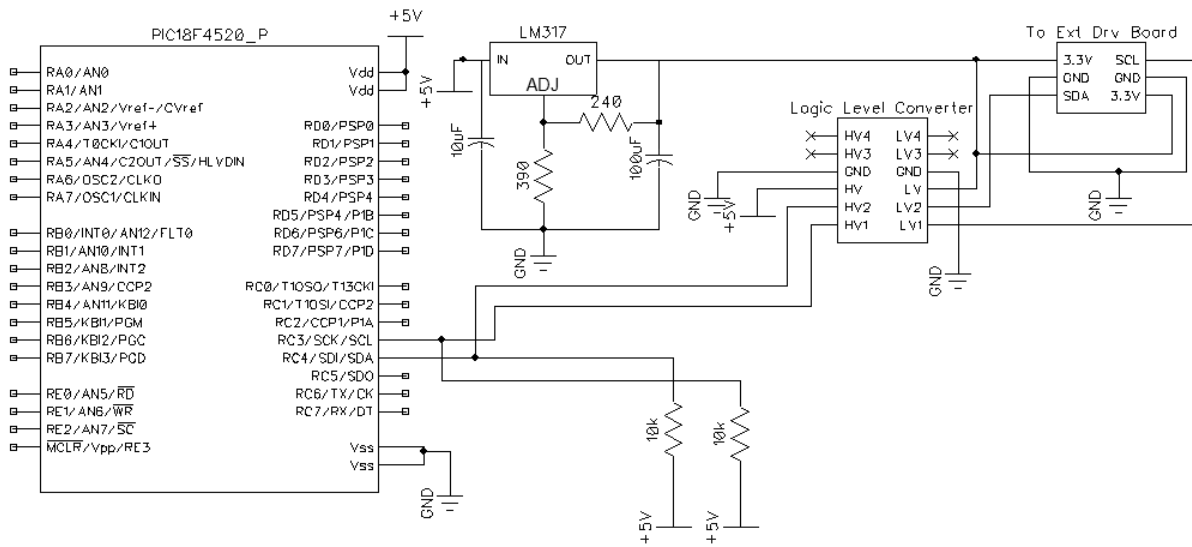


Figure 51: Circuit used to reduce the voltage of the I²C bus from 5 V to 3.3 V. The Logic Level Converter provides an input to the external driver board, specifically the liquid lens driver IC HV892. The lower voltage is produced by the LM317 voltage regulator circuit.

3.3.2.3 Signal Processing

The goal of the signal processing circuit was to accurately read the value from the signal conditioning circuit, calculate the corresponding refraction, and send a signal to the liquid crystal lens to change the refractive power to the calculated value. The signal processing flow can then, in essence, be divided into three separate parts: value acquisition, refractive calculation, and lens actuation. These separate parts are discussed in detail in the following sections.

3.3.2.3.1 Value Acquisition

The ADS1015 ADC continually converts the signal received from the signal conditioning circuit; therefore, the microcontroller must read this signal at certain specific times, and convert the value into a usable quantity. As mentioned previously, the PIC18F4520 can work with values up to 5 V. Therefore, a good quantity for calculation would be the analog voltage input into the ADC.

To perform this calculation, the PIC18F4520 reads a 16-bit value from the ADC in two steps: first, the high byte is read, followed by the low byte. The read value is

converted according to the data sheet, by being multiplied by 0.188 to give the value in millivolts.

3.3.2.3.2 Refractive Calculation

In order to calculate the desired refraction, a strategy for accommodative measurements must first be obtained. As discussed in previous sections, measurements of accommodation are notoriously variable between both individuals and between measurement sessions. This means that a strategy based on the use of look-up tables or specific values will not be as effective as one that assumes completely new values for each measurement.

Normalized accommodative values could generally be described by a linear regression model in most subjects (see Section 2.3.1). It seems appropriate, then, to include the accommodative amplitude in any measurement strategy, especially since time-dependent values (velocity, time constant, etc.) require a uniformity of timing values that would be very difficult to replicate outside a clinical setting. An additional constraint was the timing; if a calibration phase were to be included in the final design, it would need to be as short as possible. Because the accommodative amplitude could be directly calculated from the ADC input, the length of time of such a calibration cycle would take would be minimized.

In order to provide a predictive linear model for refraction versus accommodative effort, a calibration sequence was included at each start-up. Two values were measured: accommodative effort at 0 D (distance viewing), and accommodative effort at 5 D. The following equation was used to find the slope of the linear model:

$$\text{Slope (mV/D)} = \frac{(5 \text{ D Signal mV} - 0 \text{ D Signal mV})}{(5 \text{ D} - 0 \text{ D})} = \frac{(5 \text{ D Signal mV} - 0 \text{ D Signal mV})}{5 \text{ D}}$$

This equation yields a slope with units of mV/D; once the slope is calculated, the following equation can be used to calculate the target refraction from the measured electrical potential:

$$\text{Target Refraction (D)} = \frac{(\text{Measured Signal mV} - 0 \text{ D Signal mV})}{\text{Slope mV/D}}$$

The initial signal at 0 D is initially subtracted to remove the baseline measured electrical activity from the subsequent refraction calculations.

3.3.2.3.3 Lens Actuation

Once the target refraction is calculated, this value is converted into a hexadecimal value for communication to the HV892 and the liquid crystal lens. In the Arctic 39N0 data sheet, a formula is provided for diopter/code conversion [(Parrot SA Confidential, n.d.)]. A table of these conversions was made, and values between -3 D and 5 D with steps of 0.5 D were pre-calculated. The program chooses the step best corresponding to the calculated target refraction, then stores the value for communication over the I²C bus.

3.3.3 Signal Conditioning Subsystem

Perhaps the most important part of the device is the signal conditioning subsystem. The voltage input from the subject's accommodative effort is in the range of millivolts (see Section 2.3.2); the ADC and microcontroller are not equipped to handle such a low voltage signal, with such relatively small changes, meaning that the signal must be amplified. Because it is in direct contact with the user, it is imperative that the signal conditioning circuit prevent unwanted electrical discharges [(The Council of the

European Communities, 1993)]. Finally, the circuit must provide an accurate representation of the initial voltage recorded from the user.

3.3.3.1 Stage 1: Amplification, Feedback, and Protection

An instrumentation amplifier is traditionally used in biomedical measurement systems. These are operational amplifiers with very high input impedance, common mode rejection ratio (CMRR), low drift, and low noise. The INA128 (Texas Instruments Inc., Dallas, TX, USA) was chosen as the instrumentation amplifier in this application.

One goal of the design was to maximize the CMRR, or the degree to which signals common to both inputs is rejected by the amplifier [(Horowitz & Hill, 2015)]. For a gain of 100, the CMRR is 125; gain is set on the INA128 by the following equation:

$$\text{Gain}=1+ \frac{50 \text{ k}\Omega}{R_G}$$

Choosing an R_G value of 400Ω , the gain is found to be 126. Adding two decoupling capacitors between the positive and negative DC power supplies and ground to decrease noise, the following circuit, shown in Figure 52, is obtained:

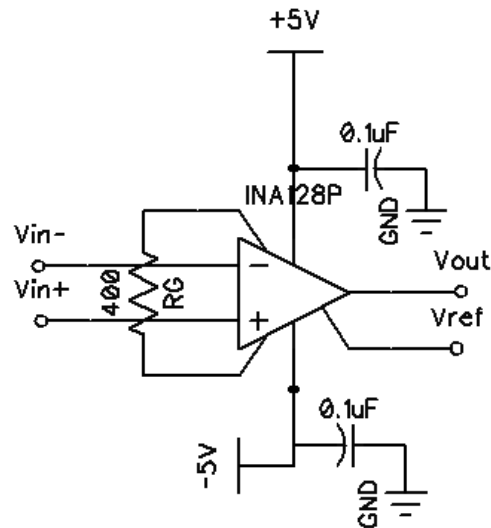


Figure 52: Circuit diagram of the initial INA128 circuit, shown with a gain of 126 and decoupling capacitors on the power supplies. The resistor labeled R_G is used to set the gain, while the capacitors tying the power supply to ground stabilize the power buses.

An additional consideration is the necessity of adding an input bias current return path, which prevents saturation of the amplifier and the flow of current into the subject. Resistors with values of $47\text{ k}\Omega$ were added between each input and ground, following the suggestion of the data sheet [(Texas Instruments Inc., 2005)]. With this addition, the circuit of Figure 53 is created.

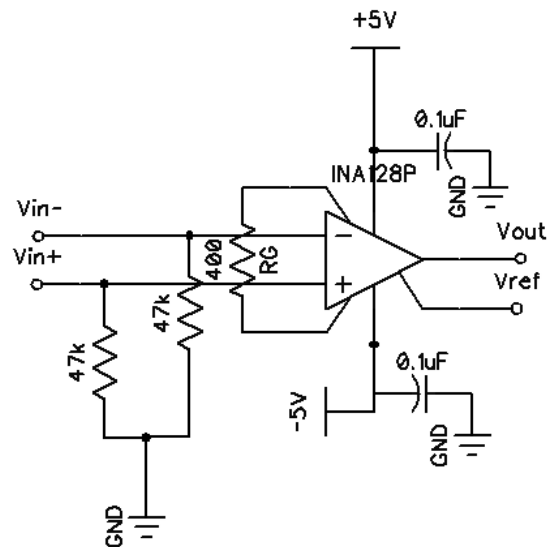


Figure 53: INA128 circuit shown with input bias current return paths at the inputs (in each case, a 47 k Ω resistor connected to ground). This circuit addition provides protection for the user against electric shock.

In order to provide protection to both the user and the device in case of a large electric signal at the inputs, diode clamping was implemented to keep the voltage experienced by the device between -5 V and 5 V. Commonly-used 1N4148 diodes were used in this circuit, shown in Figure 54.

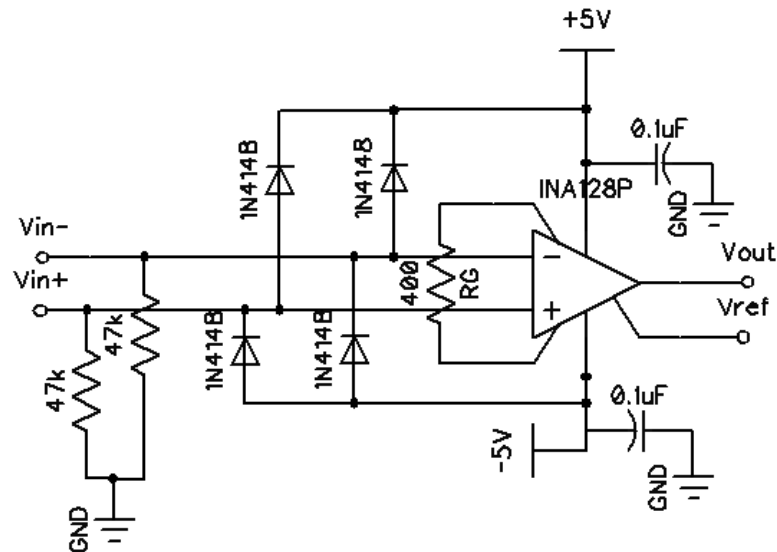


Figure 54: INA128 circuit shown with diode clamping (here, four 1N4148 diodes connected to the power supplies). The addition of diode clamps locks the signal voltage seen by the instrumentation amplifier between -5 V and 5 V, preventing damage to the chip from higher voltages.

A driven right leg circuit can cancel out additional noise by feeding the signal recorded from a reference electrode back into the instrumentation amplifier [(Texas Instruments Inc., 2005)]. A precision op-amp with two different amplifying components, the OPA2131 (Texas Instruments Inc., Dallas, TX, USA) was chosen for the active element in this circuit, mainly for its small size, similar power needs (i.e. it can share power supplies with the INA128), and recommendation for this application by the manufacturer. Following the example of the INA128 data sheet [(Texas Instruments Inc., 2005)], the driven right leg circuit added is shown in Figure 55.

The output of this portion of the circuit is a low-noise signal with a gain of 126. To give a practical example, taking a typical presbyopic response amplitude of 0.6 mV, the output from the circuit would be:

$$V_{\text{out}} = 0.6 \text{ mV} \times 126 = 75.6 \text{ mV} = 0.0756 \text{ V}$$

Given that the ADC has been configured for signal amplitudes between 0 V and 5 V, with levels of 1.2 mV per step, this signal is large enough to be measured. However,

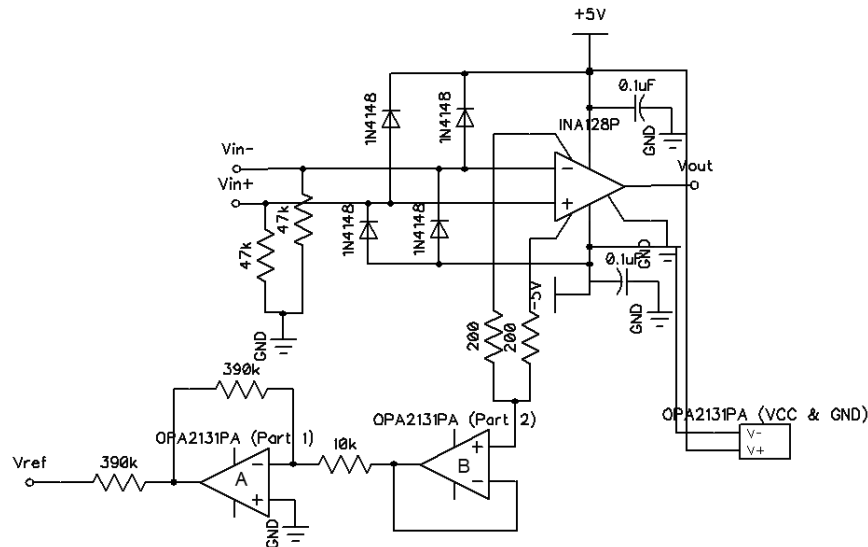


Figure 55: Completed INA128 circuit, showing including the driven right leg circuit (OPA2131 components, bottom left). The complete first stage includes diode clamping to prevent high voltage fluctuations, an input bias current return path to protect the user, and a driven right leg circuit to cancel out noise.

magnifying the signal further would allow for the full range to be used, meaning more values could be calculated when the signal changed.

3.3.3.2 Stage 2: Gain Amplification

In order to take full advantage of the range of the ADC, a 5 D signal should, after signal conditioning, be as close to 5 V as possible, reflecting its status as the maximum possible accommodative amplitude. For calculation purposes, a buffer of 1 V was added to prevent device saturation; therefore, the target voltage was set to 4 V. This can be easily achieved using a non-inverting op-amp circuit as the second stage in the signal conditioning circuit [(Horowitz & Hill, 2015)]. For a presbyopic user with a maximum amplitude of 4.755 mV, in the middle range of the values used, the gain needed can be calculated using:

$$V_{\max} = G_1 \times G_2 \times V_{\text{in}}$$

Plugging the chosen value into the equation, G_2 , the gain needed in the second stage, is obtained.

$$4 \text{ V} = 126 \times G_2 \times 0.004755 \text{ V} \rightarrow G_2 = 66.76$$

A typical non-inverting op-amp circuit is shown in Figure 56.

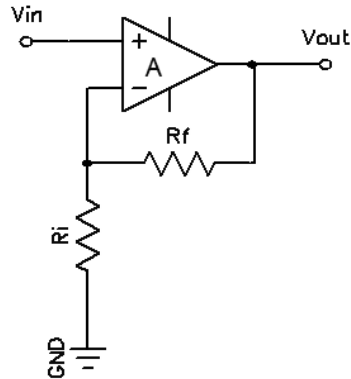


Figure 56: Typical non-inverting op-amp circuit. The signal, V_{in} , is multiplied by the gain (controlled by R_i and R_f resistors) to give the output, V_{out} .

The gain for this circuit is given by:

$$G=1+\frac{R_f}{R_i}$$

Choosing an arbitrary value of $10\ \Omega$ for R_i , R_f is found to be approximately $667\ \Omega$. A resistor value of $680\ \Omega$ is a close match, yielding a final second-stage gain of 69. For this circuit, a general-purpose op-amp, the uA741 (STMicroelectronics N.V., Geneva, Switzerland), was chosen, due to its robust nature and ubiquity. Figure 57 shows the non-inverting op-amp circuit with the appropriate resistor values.

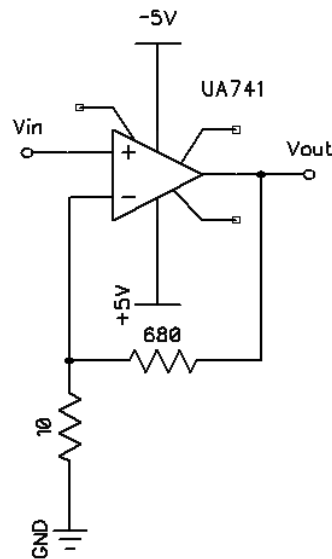


Figure 57: Non-inverting op-amp circuit configuration for a presbyopic user with 4.8 mV signal at maximum amplitude. This circuit provides a gain of 69 to the incoming signal.

Though this circuit is suitable for a presbyope with middle-range maximum accommodative signal, it is not suitable for a presbyope able to achieve a higher signal, i.e. 1 mV. Therefore, a variable gain element was added to the circuit, allowing the user to change the amount of gain based on his or her recorded ciliary muscle signal. Based on an analysis of the experimental data, the presbyopic and pseudophakic subjects were divisible into six different groups. Table 23 shows these different groups, together with the appropriate gain element as calculated using the gain equation.

Table 23: Groups chosen for gain calculations, the average maximum accommodative signal seen in each group, and the calculated required gain in stage 2 for each group. Gains were calculated to achieve a maximum processed signal of 4 V.

Group	Maximum Accommodative Signal (mV)	Calculated G_2
1	0.414	76.68
2	0.476	66.76
3	0.910	34.89
4	0.735	43.19
5	1.918	16.56
6	2.857	11.11

To allow for the gain adjustment between the groups, a rotary switch with six different positions was installed as shown in Figure 58.

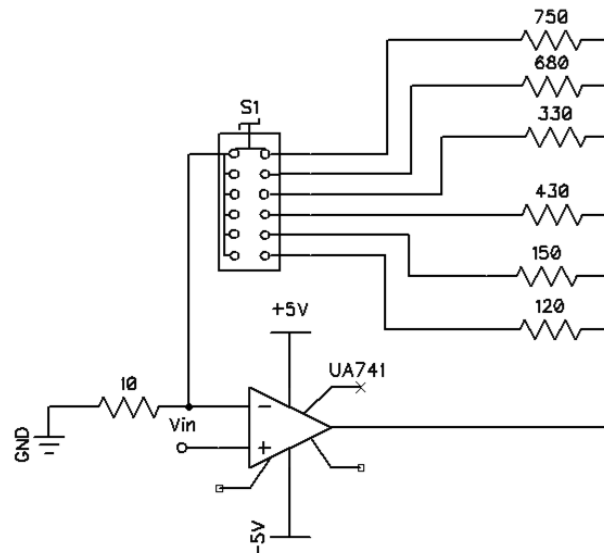


Figure 58: Stage 2 circuit with user-adjustable variable gain. For each group, a different gain was calculated, and this gain was achieved with the resistors shown in the figure.

An additional consideration during signal acquisition is the removal of DC signals from the actual recorded signal. These signals can potentially cause problems during signal acquisition by saturating the amplifier, as well as by distorting the value of the measured signal. The uA741 has offset voltage capabilities, when wired with a potentiometer whose wiper is connected to the negative power bus. A final Stage 2 circuit, with adjustable gain and voltage offset, was then constructed as shown in Figure 59.

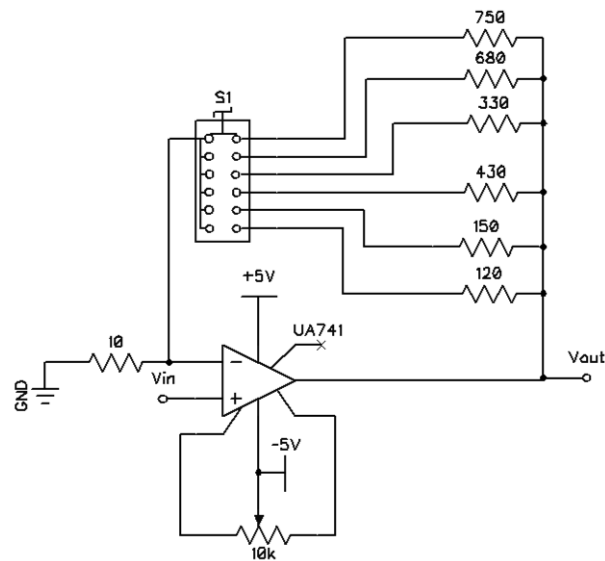


Figure 59: Completed Stage 2 circuit with adjustable gain and adjustable DC offset elements. The DC offset is connected to pins 1 and 5 of the op-amp, with the wiper at -5 V.

3.3.4 User Interface Subsystem

The user interface subsystem is defined as the portions of the device with which the user interacts on a regular basis. This includes LCD screens, keypads, dials, switches, and buttons. Because the user does regularly interact with this subsystem, it is crucial that elements involved in this subsystem be easy to use and easy to understand.

In order for the system to communicate with the user, it is necessary for some sort of visual element to be present. Because the information transmitted and received is neither graphic nor extensive, a simple two-line LCD screen was chosen as the display module. Though many modules contain the option for backlighting, this option was not used to reduce the design needs. The module chosen for the final design was an HDM20216H-3 20-character, 2-line LCD module (Hantronix, Inc., Cupertino, CA, USA). A schematic for the circuit connecting the module to the microcontroller is shown in Figure 60.

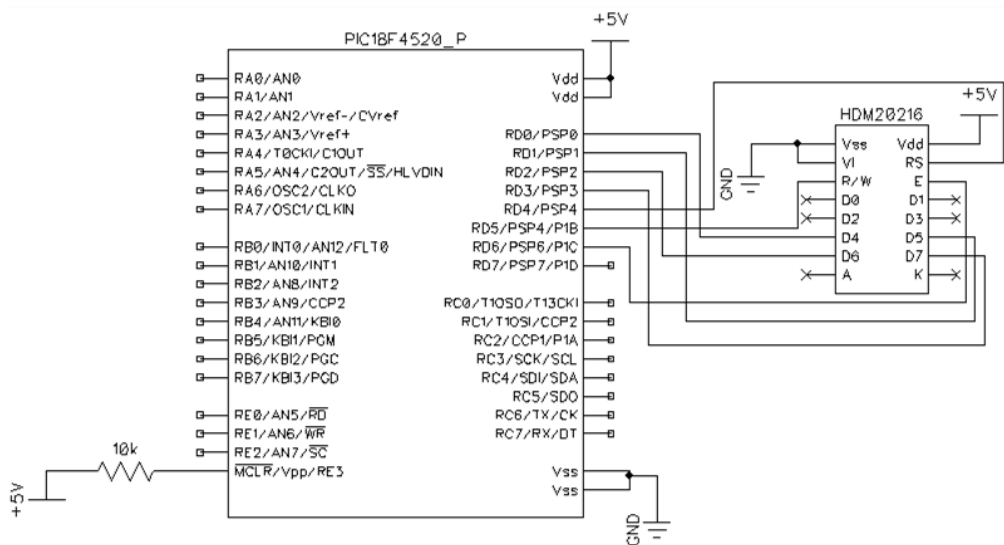


Figure 60: Schematic of the HDM20216 LCD screen connected to the PIC18F4520. The 10 k Ω resistor tied to the 5 V power supply ensures proper operation of the LCD screen when the circuit is turned on and off.

Another important element for communication is a general-purpose input device. Two input devices specific to the signal conditioning subsystem have already been discussed; however, these are subsystem-specific, and do not communicate directly with the microcontroller. They therefore do not directly alter the refractive power calculations from the microcontroller.

For general program interaction, such as instructing the microcontroller when to start and end a calibration sequence, a keypad was chosen as the best option. Because the target user is of a mature age [(Hoogendam et al., 2014)], and, therefore, has reduced fine motor movement, the best option for a keypad is one with relatively large buttons. To simplify construction and programming, a keypad with a matrix configuration, where the circuit required to interface the keypad to the microcontroller is built-in to the keypad itself, was desirable. The Parallax 4x4 Matrix Membrane Keypad (#27899) (Parallax, Inc., Rocklin, CA, USA) was chosen, due to its large keys and flat construction, and wired as shown in Figure 61.

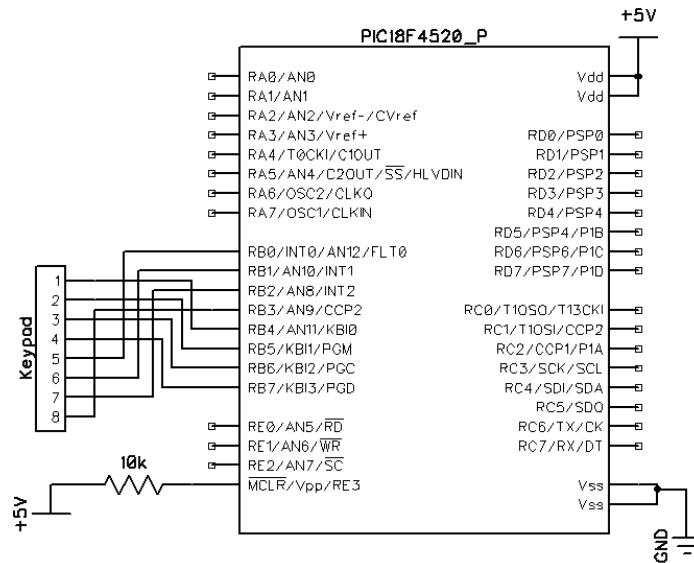


Figure 61: Schematic of the Parallax Matrix Membrane Keypad connected with the PIC18F4520. The pins are wired to the B ports of the microcontroller, which are configured as inputs.

Because the user must make adjustments in the initial refractive correction, an element to control this was needed. Though a keypad would also serve this purpose, the operation of the device would be complicated by the need to either read in a target, or by the repetitive typing of one key for increase or decrease in refraction. A more intuitive method was to use a dial, which the user rotates to the desired position. This was achieved by the addition of a 2.2 k Ω potentiometer, with the wiper at the microcontroller output, and the inputs at 0 V and 5 V.

A method was also needed to integrate the user adjustments described in Section 3.3.3, namely, the switch controlling the Stage 2 gain and the potentiometer controlling the offset. Both modalities would benefit from the addition of a knob unit, allowing the user to control the parameters more easily. These knobs, as mentioned earlier, would need to be large and easy to grasp. Such knobs were used in the final construction of the device.

3.3.5 Power Subsystem

The most problematic aspect of devising a power supply for the device is the requirement for a negative power supply for correct op-amp operation. This almost arbitrarily requires the integration of two batteries into the design. An additional consideration is the need to create identical power supplies, as inequalities could affect the signal measurements and calculations.

A traditional approach is the use of two 9 V batteries in series, with a voltage regulator at each battery. This would produce two constant values of -5 and +5 V, relative to the virtual ground. However, there are several downsides to this approach. First, depending on the battery location in the device, the user might have to take apart the entire device to replace the batteries, potentially damaging circuit elements and compromising device functionality. An additional consideration is the large size of two 9 V batteries, which would reduce the available space in the housing for other circuit elements. Finally, voltage regulators heat up with prolonged operation, requiring the need for bulky heat sinks.

A different approach is to use rechargeable batteries. In addition to reducing the overall cost of batteries during the lifetime of the device, rechargeable batteries, if equipped with the proper circuitry, can be charged using a computer and a connector. Because this connector could be placed as a socket, externally to the circuitry, the user would not have to disassemble the device in order to recharge or replace the batteries. Though the circuitry described would add to the space used by the power subsystem, many rechargeable batteries are actually fairly thin. Overall, the rechargeable batteries would reduce the amount of housing real estate used, as compared to a traditional 9 V battery approach. These were used in the final design construction.

4. DEVICE CONSTRUCTION

4.1 Introduction

Details of the development of the device were explored in the previous section. This section will discuss the construction of the device, including modifications performed in each of the subsystems. Tests to ascertain the functionality of the device will also be described here. Finally, future design suggestions and modifications will be explored.

4.2 Design Construction Details

4.2.1 Liquid Crystal Lens Subsystem

As discussed previously, the lens was housed in the casing provided by the manufacturer, and the assembly was mounted onto a shooting glasses frame. During construction, the issue of a plug for the ribbon cable attached to the driver board was raised. Initially, the plug was contained in a small plastic housing connected to the main device housing by insulated wires. However, this construction was not very robust, and rendered unnecessary by the utilization of a longer ribbon cable.

The final plug assembly is shown in Figure 62. First, the plug was wired to a protoboard (SparkFun Snappable Protoboard, SparkFun Electronics, Boulder, CO, USA), and, subsequently, attached, such that the pins were exposed for attachment, but the metal components did not touch the aluminum housing. The plug was labeled at the first pin to prevent user confusion. On the ribbon cable, this was indicated at both ends with an

arrow; on the driver board, the first position was denoted by a square, rather than a round, solder point.



Figure 62: Final construction of the ribbon cable plug. A label is visible over the pin position where pin number 1 of the ribbon cable should be attached.

4.2.2 Signal Processing and Communication Subsystem

The signal processing and communication subsystem probably underwent the least amount of modification during the construction process. At the core of the construction, the microcontroller holder was soldered to a SparkFun Snappable Protoboard (SparkFun Electronics, Boulder, CO, USA), the whole length of which was used for the circuit. Metal wires were used to construct the circuit, based on the schematics already presented.

In order to allow for the microcontroller to be taken out of the assembly for programming modifications, a pin holder was used. Initially, in an attempt to isolate the user from the power supply, the circuitry of this subsystem was powered by a separate battery; however, due to the low power used in the design, the fact that the device was not connected to a power line, and the protective circuitry in the signal conditioning subsystem, this idea was discarded. The microcontroller was powered by the same

positive voltage and virtual ground as used by the signal conditioning circuit. The completed circuit is shown in Figure 63.

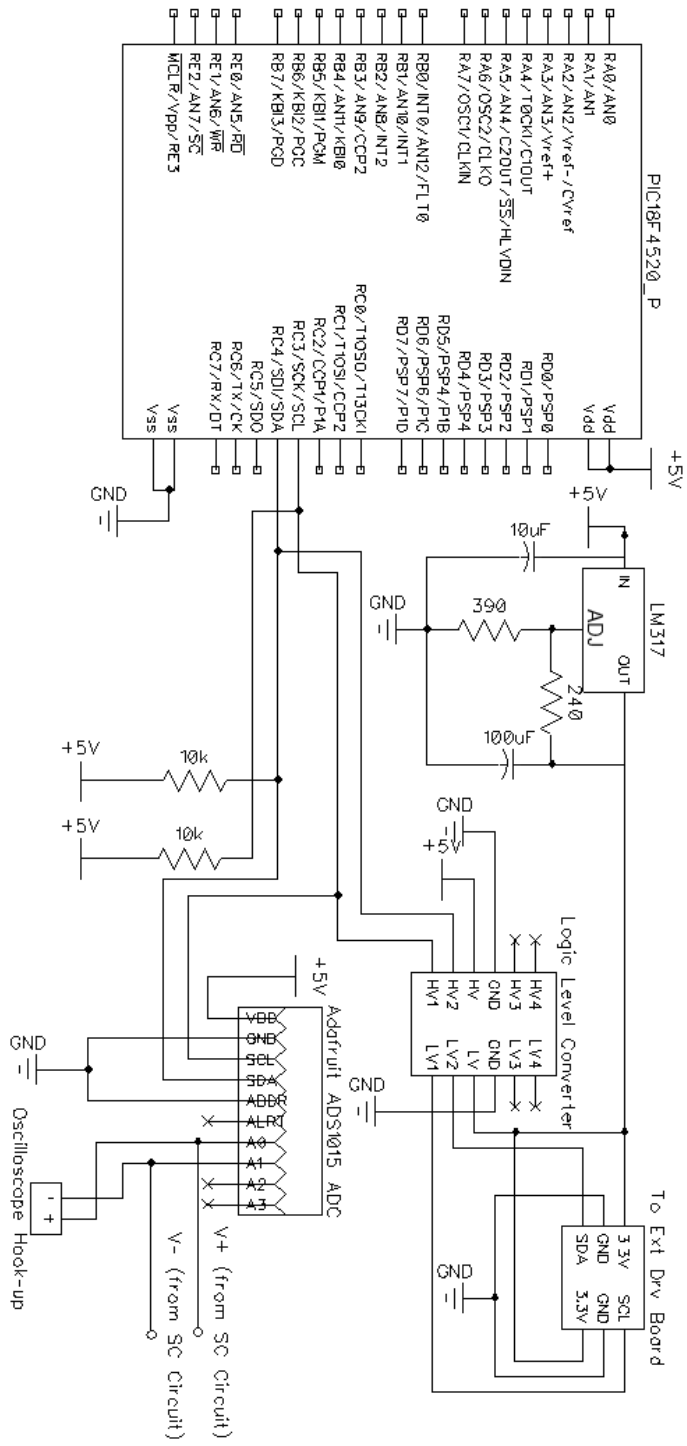


Figure 63: Completed signal processing and communication subsystem circuit.

4.2.3 Signal Conditioning Subsystem

This subsystem underwent the greatest amount of changes during the construction process. The addition of an optoisolator was also considered to provide maximum protection to the user. Because the device is not running on a high-power supply, or capable of experiencing surges from power lines, the addition of such a component would have been superfluous.

During the first design iteration, an LM324 (Texas Instruments Inc.) differential amplifier was used as the initial signal conditioning stage. An LM324 does not require a balanced dual power supply, and therefore would reduce the number of batteries used, as well as the overall size of the device. However, this IC has a much lower CMRR than an instrumentation amplifier, and less gain control; it was rejected in favor of the INA128.

The signal conditioning subsystem was also constructed on its own protoboard, though only a portion of the entire board was used. Both the INA128 and uA741 were placed in holders soldered to the board, though the OPA2131, due its configuration (soldered into a breakout board from SparkFun Electronics), was soldered directly to the board. Connections were made using thin insulated wire, and between boards by jumper wires. Inputs to the system from the user were constructed using plugs and a plastic outer casing, in order to prevent interference from the aluminum housing or cross-signal interference. The completed circuit schematic is shown in Figure 64.

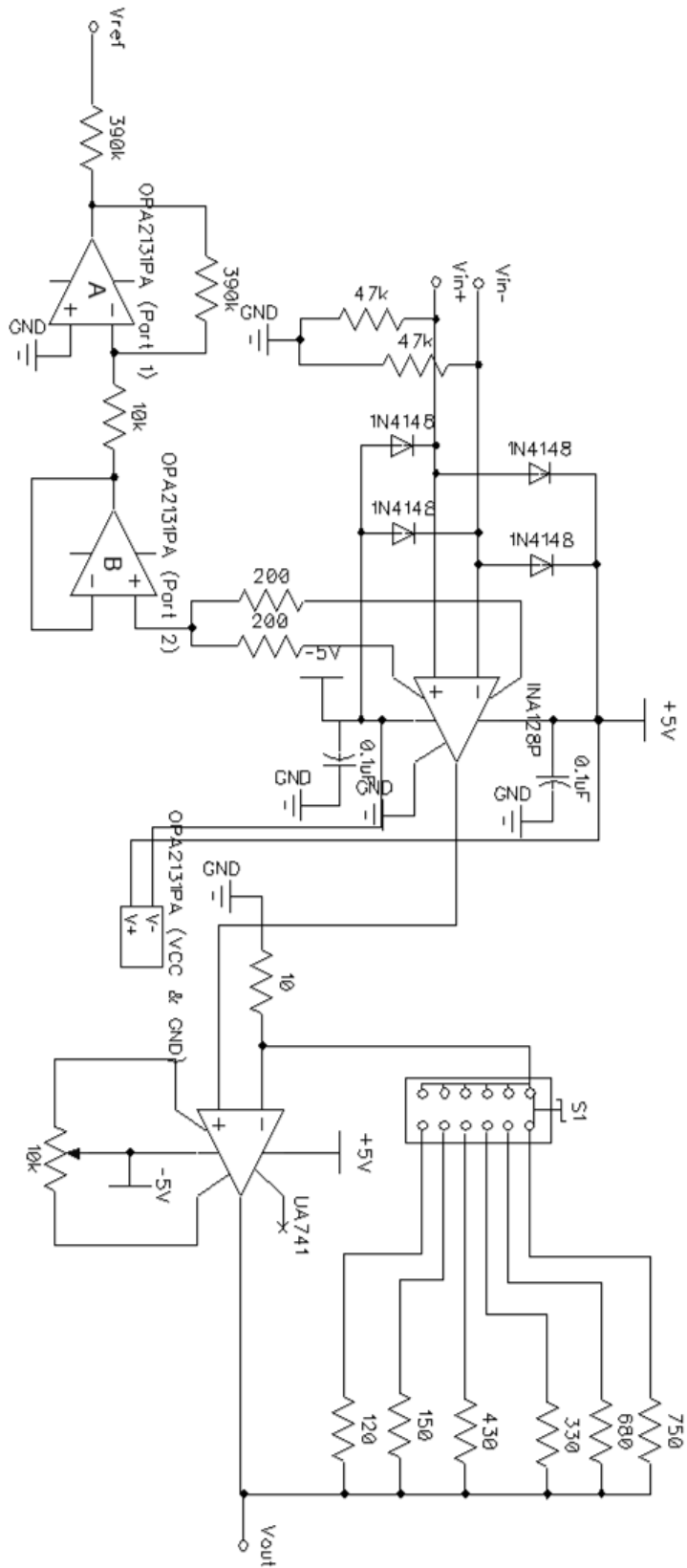


Figure 64: Completed signal conditioning circuit schematic.

4.2.4 User Interface Subsystem

The user interface subsystem circuitry was constructed on the same board as the signal processing and communication subsystem circuitry. Each component was externally fixed to the housing, then wired to an appropriate location on the board. The LCD module was attached to the front; in order to allow for better component modification during and after assembly, a plug was used to connect the module to the board. Using the adhesive back of the keypad, the keypad was affixed to the left side of the housing, and plugged in to pins on the board. The completed circuitry is shown in Figure 65.

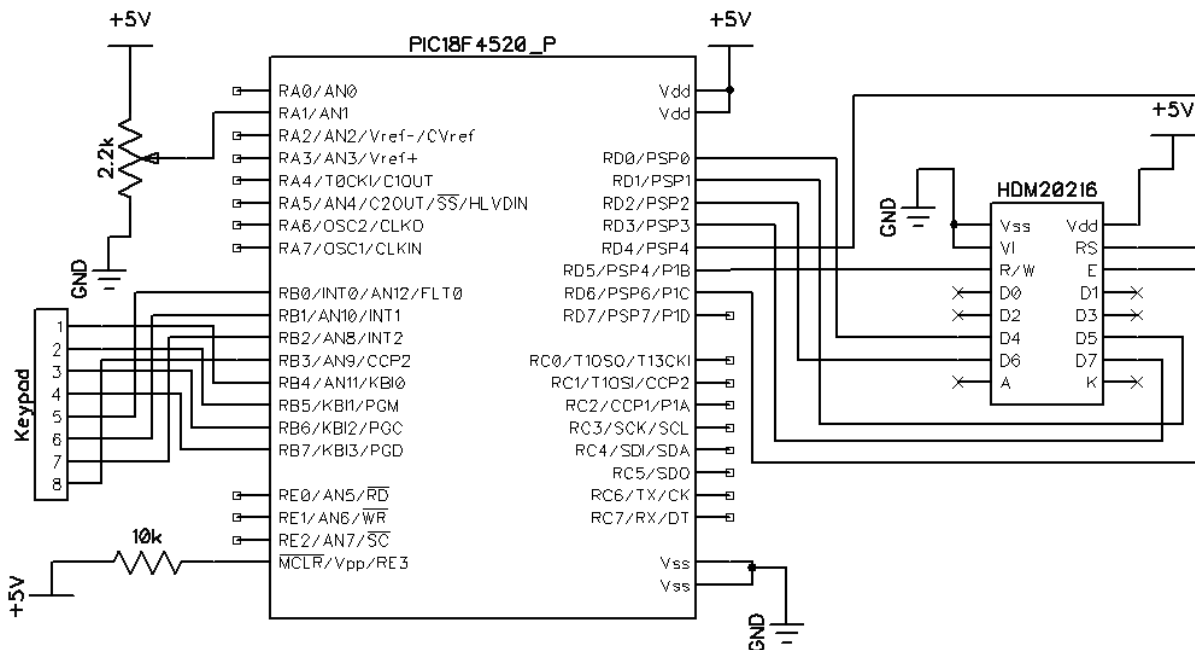


Figure 65: Schematic of the completed user interface subsystem circuitry. This subsystem includes a keypad, potentiometer, and LCD screen.

The keypad, LCD screen and front potentiometer, and Stage 2 adjustment knobs are shown in Figure 66, Figure 67, and Figure 68.



Figure 66: Constructed keypad element of the user interface subsystem.



Figure 67: View of the constructed LCD module, time, and/refraction adjustment knob.



Figure 68: Constructed gain adjustment switch and DC offset knob for Stage 2 adjustment. The gain adjustment switch is a rotary switch, whereas the DC offset knob is a potentiometer.

The refractive control was initially set in steps of 0.5 D, from -3.5 to 4 D, based on the position of the potentiometer wiper. This was changed to -5 D to 5 D in steps of 0.25 D in order to provide more accurate refractive correction.

Another feature added during construction was time adjustment, used for the time interval between lens actuations. It was suggested by Dr. Zrenner that users might want a faster or slower lag time between corrections, allowing for better customization of the device to the user's specific requirements. The lag time was originally set to be 1 s; using the same potentiometer as that used for the refractive adjustment, the capability was added to change this from 120 ms to approximately 1.5 s, in intervals of approximately 0.1 s. To control these time changes, a built-in delay function was used.

A final change in this subsystem was the addition of a UART interface, to allow for the different key parameters (measured signal voltage, target refraction, and code sent to the HV892) to be recorded and analyzed on a computer. For this addition, a variable was calculated to allow for accurate communication timing, based on the following formula (8-bit, asynchronous mode, low speed, 4 MHz clock frequency, 4800 baud rate):

$$BR = \frac{F_{osc}}{(64 \times (spbrg + 1))} \rightarrow spbrg = \frac{4 \times 10^6 \text{ Hz}}{4800 \times 64} - 1 \approx 12$$

The final circuit was modified to allow outputs at pins 25 and 26 of the microcontroller, which were connected to a USB to UART cable (FTDI Chip TTL-232R-Rpi, Future Technology Devices International Ltd., Glasgow, United Kingdom). Data transmitted over the UART bus was read using PuTTY software (PuTTY, Release 0.67, Simon Tatham).

4.2.5 Power Subsystem

The power system, also, underwent many changes over the course of device construction. Originally, two 9 V batteries were used to power the system (discussed in Section 3.3.5). This circuit schematic is shown in Figure 69. The 9 V battery system was abandoned due to the bulkiness of the batteries, and the difficulty in changing the batteries.

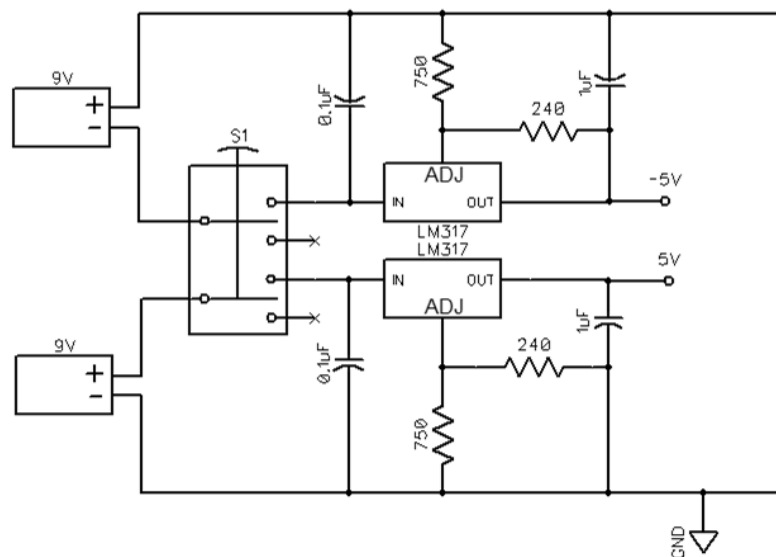


Figure 69: Original power supply circuit construction with two 9 V batteries. The use of two batteries in series provides two power supplies of -5 V and +5 V.

Commercially-available power banks (Votcraft 2600 mAh PB-14 Power Bank, Conrad Electronic International GmbH & Co. KG, Wels, Austria) were then used as a second attempt. The power banks were disassembled, and jumper wires soldered directly to the output pins. Unfortunately, most commercially-available power banks run at a lower voltage than 5 V; the voltage generated from the battery, due to the circuit wiring, was not enough to power the device.

Finally, a rechargeable Li-Po battery (Sonstige LiPo Akku 1000 mAh, EXP GmbH, Saarbrücken, Germany) was purchased for use with an Adafruit PowerBoost 500 Charger (Adafruit Industries). The Adafruit PowerBoost module outputs a steady 5.2 V, and contains a micro USB plug for charging the battery. To create a dual voltage supply, the voltage outputs from the PowerBoost module were wired in series, with a positive and negative output wired together to create a virtual ground. The modules are also wired with an LED indicator light which glows blue when the batteries are fully-powered, and yellow when the battery charge is running low.

4.2.6 Housing Subsystem

As mentioned previously, an aluminum housing was chosen to contain the circuitry. The structure was modified in-house by the University of Tübingen Eye Hospital workshop.

For the internal protoboards, pieces of plastic were glued to the walls of the housing to create slots into which the protoboards could slide, fixing them in place. To control the power supply, a rocker switch was fitted into a hole on the back of the device. Two holes were made for the charger sockets, which were attached to a piece of plastic screwed in to the wall of the housing. The two potentiometers and the rotary switch were fitted with external knobs, then attached to the housing through holes drilled into the respective positions. For the keypad, a small square hole was created in the left side of the housing, allowing the cable attached to the microcontroller to pass through. The

batteries were held in place by a plastic connector, which could be tightened or loosened by external screws. These elements are shown in Figure 70.

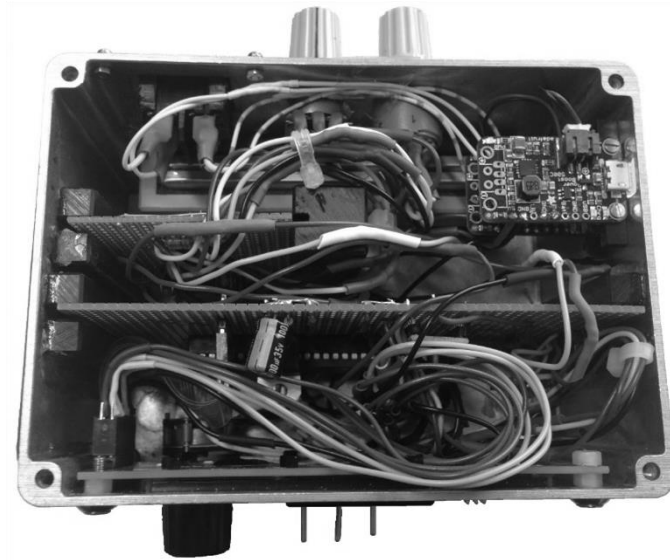


Figure 70: Inside view of the constructed device housing.

4.3 Final Device Construction

The final device as constructed is shown in Figure 72 (front view), Figure 71 (right side view), Figure 74 (left side view), and Figure 73 (back view).



Figure 72: Front view of the final constructed device. REF indicates the knob used to adjust refraction and timing. P, N, and G are the plugs for the positive, negative, and ground electrodes, respectively. S and G are the sockets for the oscilloscope signal and ground. Finally, at the right hand side, the ribbon cable plug is shown, with the first pin labelled.



Figure 71: Right side view of the constructed device. The two holes, labeled CHARGERS, indicate the sockets for the micro USB cables for charging.



Figure 74: Left side view of the constructed device. The keypad is attached via its adhesive backing to the side of the device, while a slot (not visible) allows for egress of the cable.



Figure 73: Back view of the constructed device. The on/off switch is shown to the right, while GAIN and DC OFF are the rotary switch and potentiometer that control the Stage 2 signal conditioning gain and DC offset, respectively. The screws at the bottom are used to loosen or tighten the internal battery holder.

5. TESTING THE FINISHED DEVICE

5.1 Pre-Clinical Tests

Before performing any tests with human subjects, a method was developed to assess the performance and efficacy of the device using the signals previously recorded from actual experimental subjects. To do this, a Keysight function generator (33522B Waveform Generator, 30 MHz, 2-Channel with Arb, Keysight Technologies, Santa Rosa, CA, USA) and associated software (33503A BenchLink Waveform Builder Pro Software, Keysight Technologies, Santa Rosa, CA, USA) was used. Variable intervals, each including one complete accommodation signal, were loaded into the BenchLink software, and sent to the generator with the experimental parameters (1000 samples/s). To record the signals after processing by the signal conditioning circuit, an oscilloscope (TDS 2014C, Tektronix, Inc., Beaverton, OR, USA) was attached to the signal/ground sockets at the front of the device. To observe the refractive changes caused in the liquid crystal lens by the generated signals, a webcam was set up at the liquid lens, and the output was displayed and recorded on a laptop (HP EliteBook Folio 9470m, HP Inc., Palo Alto, CA, USA) using AMCAP software (Version 8.12, Microsoft Corp., Redmond, WA, USA).

In order to produce a calibration signal for a maximum amplitude, a steady 0.6 mV DC signal, reflecting the maximum of the subject in question, TZ, was generated using the circuit by using a voltage divider circuit. A typical example of such a circuit is shown in Figure 75.

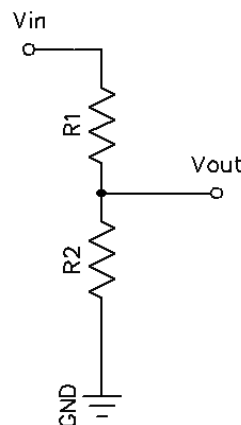


Figure 75: Schematic of a voltage divider circuit. The voltage, V_{out} , is given by V_{in} multiplied by a quantity determined by the resistors ($R_2 / (R_2 + R_1)$).

The equation describing V_{out} is:

$$V_{out} = V_{in} \left(\frac{R_2}{R_1 + R_2} \right)$$

Using an arbitrary value for R_2 of 100Ω , a target V_{out} of 0.6 mV , and a V_{in} of 5 V , the above equation can be solved for R_1 :

$$R_1 = \left(R_2 \times \frac{V_{in}}{V_{out}} \right) - R_2 = \left(100 \Omega \times \frac{5 \text{ V}}{0.0006 \text{ V}} \right) - 100 \Omega = 833.233 \Omega$$

Choosing a close resistor value of $760 \text{ k}\Omega$, the output should be close to the desired maximum voltage ($\sim 0.658 \text{ mV}$). The schematic of the circuit used for testing is shown in Figure 76.

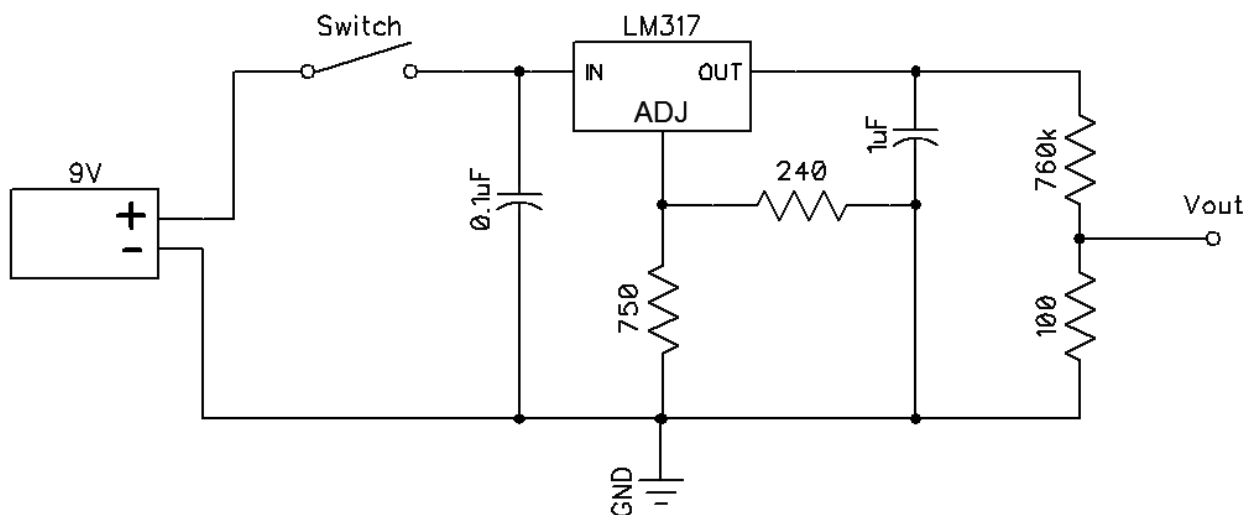


Figure 76: Voltage divider circuit used to provide the simulated maximum accommodative amplitude during testing. The circuit generated a voltage of approximately 0.66 mV , a value corresponding to a typical maximum presbyopic accommodation signal amplitude.

Thus, the final test set-up contained an oscilloscope, waveform generator, webcam, maximum amplitude output circuit, and a recording laptop. The entire set-up is shown in Figure 77.

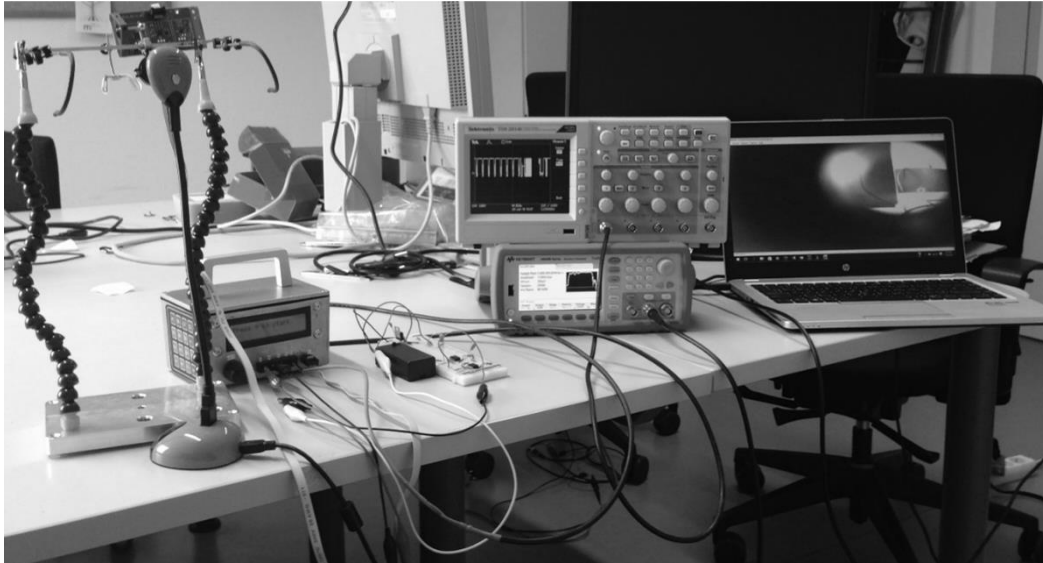


Figure 77: Set-up used for testing the device. On the left, a webcam is set up to capture the view through the lens. The device is shown plugged in to the function generator, above which is an oscilloscope for measuring the voltage output. The webcam output is recorded on the laptop at the left. For calibration, the maximum amplitude generator circuit is used (shown beside the device).

Tests were performed with two different sample signals, as described in the following sections.

5.1.1 Test of Signals from Presbyopic Subject TZ

Because the main aim of the project was to provide an assistive device for presbyopes and pseudophakes, the 5 D signal from presbyopic subject TZ was first tested. Before importation, the baseline of the signal was adjusted to begin at 0 V, though the latter part of the signal still contained a negative component. A 20 s window, encompassing the entire accommodation and disaccommodation signal, as well as 5 s of total baseline activity, was imported into the BenchLink Waveform Builder software, a screen shot of which is shown in Figure 78.

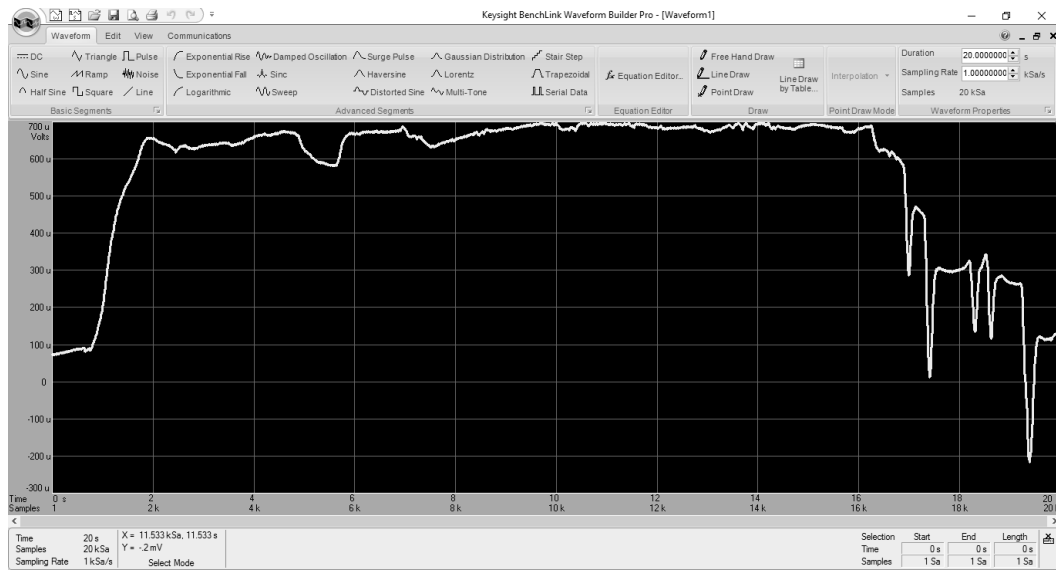


Figure 78: Screen shot of the accommodative signal (TZ, 5 D) imported into the BenchLink Waveform Builder Software. The x-axis is time, the y-axis is amplitude (shown in μV).

The signal was then sent to the Keysight Waveform Generator using the following parameters: 1 kSa/s (1000 samples per second), high level 0.70 mV, low level -0.20 mV.

Once the Waveform Generator had received the signal, the signal was first directly tested with the oscilloscope; unfortunately, due to the very low signal amplitude, the oscilloscope used was not able to perform an accurate measurement. To ensure that the correct signal was being produced, two further checks were performed. First, to check the amplitude, the Waveform Generator was connected to a digital multimeter (UNI-T® UT803 True RMS Multimeter, Uni-Trend Technology Limited, Dong Guan, China) configured to measure a DC voltage. This showed that the device was, indeed, producing a signal in the desired amplitude range. Secondly, the input signal values were scaled to bring the value to the range of hundreds of millivolts, and the signal was recorded using the oscilloscope. The results are shown below in Figure 79.

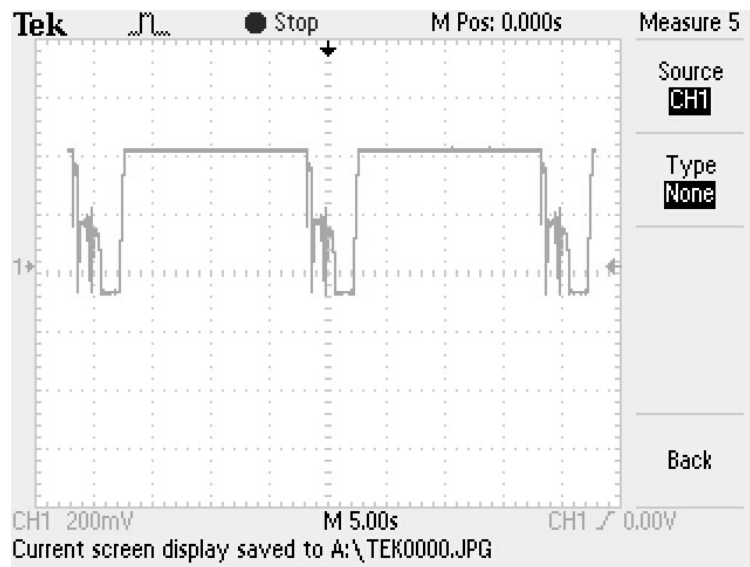


Figure 79: Screen shot of test signal delivered directly to the oscilloscope. The signal shown has been scaled to be in the range of hundreds of millivolts to allow detection by the oscilloscope. As can be seen from the figure, this waveform, generated by the waveform generator, matches, in shape, the signal measured for subject TZ.

Once it was ascertained that the correct signal was being output from the waveform generator, the entire assembly was reconstructed, and the test was performed. For the calibration sequence, the positive and negative pins were connected to the signal and ground, respectively, of the test circuit shown in Figure 76. During the 0 D calibration, the power was turned off; for the 5 D calibration, the power was turned on.

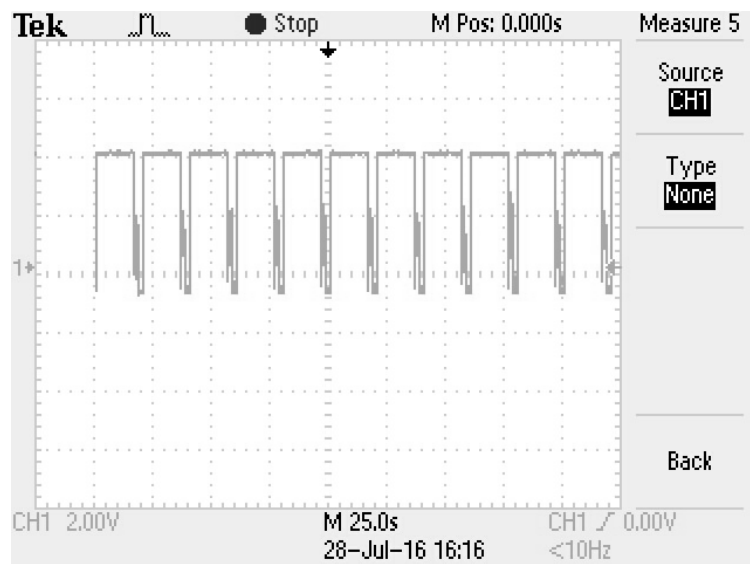


Figure 80: Screen shot of the oscilloscope recording captured from the device signal conditioning circuit using signals from subject TZ.

Subsequently, the device was connected to the waveform generator, and the waveform generation was triggered. The oscilloscope signal recorded can be seen in Figure 80.

From the webcam, the following images, shown in Figure 81, were obtained.

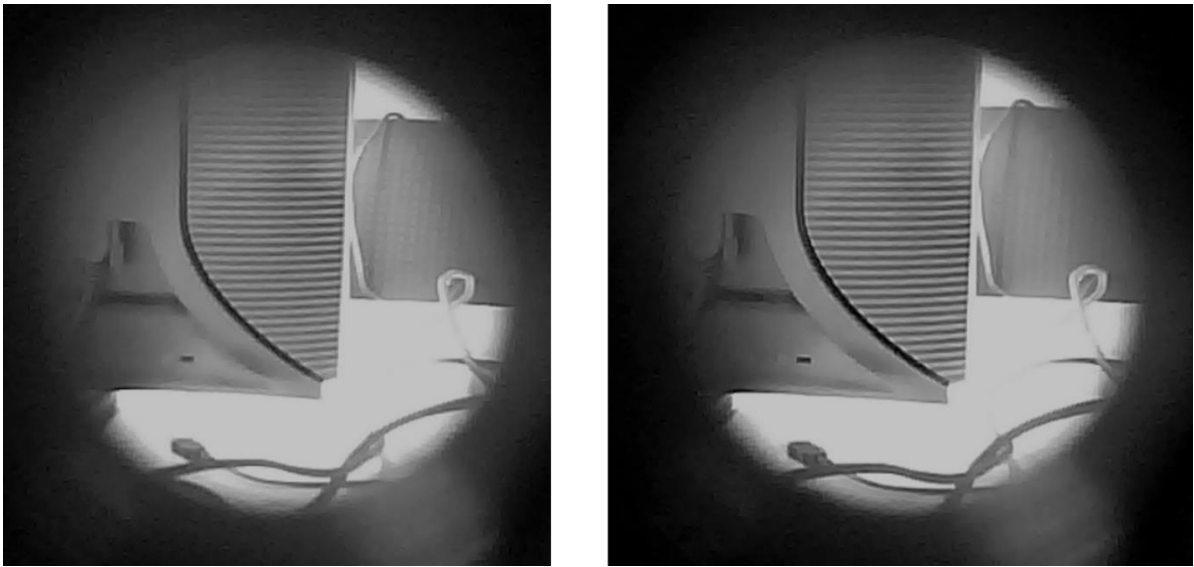


Figure 81: Images obtained at defocus (left) and focus (right) signal points from the 5 D signal of subject TZ.

5.1.2 Test of Staircase Signal from Control Subject CH

In order to evaluate the ability of the device to provide different levels of accommodative correction, the staircase signal from subject CH was used. The reader will recall that this signal tested four different accommodation targets, starting at 5 D and ending at 2 D. Because this signal was much larger than the presbyopic and pseudophakic signals generally used, it was scaled down to the general presbyopic range, i.e. tenths of a millivolt. The same calibration circuitry as was used for the previous test was used in this test, and the test procedure was preserved.

Figure 82 shows the oscilloscope output recorded using this protocol. As can be seen from the figure, the voltage levels are distinctly different with the different accommodation targets.

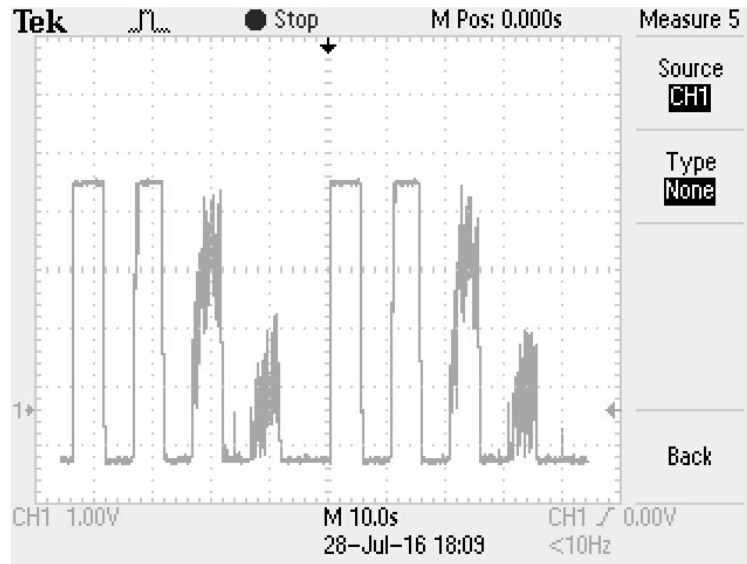


Figure 82: Oscilloscope screen shot of the signal conditioning circuit output using an input signal from subject CH.

5.2 Clinical Investigations

In addition to trials using signals from the original experiment, several of the original participants were invited to test the new device and provide feedback. Several qualitative trials, as well as one quantitative psychophysical trial, were performed.

5.2.1 Qualitative Trials

5.2.1.1 Initial Usability Assessment

For the first clinical investigations, two subjects from the first experiment, HH (pseudophake) and EH (presbyope), were invited to offer their opinions on the functionality of the device. Both were fitted with an electrode used in the original

experimental trials. Calibration of the device was performed by having each subject look at the 0.5 D target, then the 5 D target, of the original experimental apparatus. This provided each subject with a slope, as discussed in the previous sections.

Both subjects then read a lighted ETDRS chart placed at a distance (used for visual acuity tests), and, in the near range, a flip book used to test near vision. As an additional measure, a magazine was used to further measure near vision. Near vision targets were presented at a distance of approximately 20 cm, while the far target was placed at a distance of approximately 2 m away from the subject.

Compared with the normal condition, both subjects were able to better read with the device. EH could not read as much as HH, but she was still able to read most of the lighted chart, and many of the phrases appearing on the card. HH could read a great amount of small text at a near condition with the device, and could also read from the magazine. HH reported no problems with switching his gaze from a near to far target, though both complained that the refraction of the lenses jumped frequently.

Though no measurable values were obtained from this test, the initial question of functionality was, with these results, favorably answered. With the success of this test, further investigations were planned to more concretely evaluate the functioning of the device.

5.2.1.2 Initial Psychophysical Tests

For the initial psychophysical tests, a new electrode was constructed after the old one was broken during cleaning. A complete discussion of the new electrode is outside the scope of this work, but, as a quick note, a new type of connection was used at the electrode/wire interface, and the gap between the bands was increased. Initial measurements of the lens indicated a resistance of greater than 1 k Ω between the two leads, showing that the electrode was functional and not short-circuited.

Prior to testing, the Accommodation Step tests (see Section 2.2) were repeated for subject AN. Signals recorded from this electrode were in the range of microvolts, much smaller than those of the first experiment. Regardless, it was decided to continue with the experiments for device testing.

Two screens were placed in front of the subject, one at 2 m and one at approximately 40 cm. A custom program created using PsychoPy [(Peirce, 2009), (Peirce, 2007)] was used to generate words of varying sizes (degree visual angle) on each of the computer screens, each using a list of German words. This program recorded the psychophysical responses of the subject, both with and without the assistive device.

An analysis of the data results indicated no significant difference existed between the normal condition and with the assistive device. However, it should be noted that the subject greatly preferred the assistive device, stating that her vision in this condition was clearer than when she was only able to use her normal refractive correction. The device measured a maximum at 5 D of $-68.92 \mu\text{V}$, and a minimum at 0.5 D of $-114.87 \mu\text{V}$, both of which were consistent with the signals recorded to characterize the electrode.

5.3 Proof of Concept

5.3.1 Methods

Prior to the arrival of the subject, the contact lens electrode was cleaned with Ecco Compact Pure Clean non-abrasive cleaner (MPG&E). Subsequently, the electrode was rinsed with Perfect Gentle Saline Solution (MPG&E). The electrode is shown in Figure 83.



Figure 83: A view of the modified electrode, worn by subject NN. New, thin wires attached at the center of the lens provided a more comfortable fit for the subject, while a sturdier connecting cable ensured the stability of the system.

The general set-up for each of the four tests composing the proof of concept experiment was the same. One computer screen was placed at a distance of 4 m from the subject, while another computer screen was positioned on a table in front of the subject. The subject was positioned on a stool that allowed for lateral rotation, so that the subject could turn to see the correct screen. A chin rest was positioned in front of this second screen, such that the distance from the subject's eye to the screen was 20 cm. These positions were measured prior to the commencement of recording. The left (non-fixating) eye was occluded with an eye patch taped to the chin rest.

For the psychophysical investigations, a program, PsychoPy [(Peirce, 2007)], was used. This program displayed random German words at different sizes (degree visual angle), allowing for the subject's thresholds for near and far targets to be determined using two interleaved Kaernbachs staircase methods. Words were displayed in a random order on either the far or near computer screens, with the subject asked to read the word displayed. After a visual verification by the test giver, the answer, as yes or no, was recorded by the program, and used in the determination of the next appropriate target size.

5.3.1.1 Experimental Tests

In order to conclusively determine the efficacy of the device, several different tests were performed, both with and without the device and electrode. These tests are described below.

1. Near/Far Vision Ratio Control Test

A word with a letter size of 1.80 mm was displayed on the screen nearest to the subject. Different lenses were placed in front of the subject's focusing eye, and the subject was asked whether these lenses improved his vision to the point where the word was visible.

2. PsychoPy Control Test

After the first test, a second test was performed to measure the subject's visual acuity at different points. Different words were displayed in different font sizes, alternating back and forth between the screens. At the end, two curves were generated which described the near and far visual acuities, respectively.

3. Espion Signal Test

Prior to this test, the electrode was applied to the left (non-fixating) eye of the subject (see Section 2.2.7). The leads from the contact lens and ground electrode were plugged into the Espion module, and the signal was checked for magnitude. In this test phase, the subject was instructed to look at the far computer screen (far signal), or at the instructions printed on a tube of Vidisec gel held approximately 20 cm from the subject's eye.

4. PsychoPy Device Test

The electrode leads and subject ground were removed from the espion system, and plugged into the device. After a brief calibration period (used for the device), the subject was instructed to perform the test in the same way as in the PsychoPy Control Test. This test was performed twice; in the second run of the test, the output from the

device was measured via the serial cable from the device to a laptop. The serial output from the device was recorded by PuTTY software, then copied and saved to a text file.

5.3.1.2 Analysis

Using the visual angle parameters from the program, the LogMAR (Logarithm of the Minimum Angle of Resolution) [(Bailey & Lovie, 1976)] value for each recorded point was estimated using the following formula:

$$\text{LogMAR} = \log_{10}[(\text{Visual Angle} \div 5) \times 60]$$

Results were divided into results from the near target and results from the far target, then graphed. In order to determine the threshold of vision, the last three correct values recorded before wrong answers were averaged for each test condition, with near target analysis performed separately from far target analysis. An independent samples t-test was performed using IBM SPSS (IBM Corporation) to test the differences between the means of each condition, with a significance level of $p < .05$.

The device serial output contained several pieces of information, importantly, the voltage measured by the device at specific time points, and the corresponding code sent to the HV892 driver board. During calibration of the device, the time between the sending of codes to the HV892 was always set at 700 ms. The recorded signal was aligned with the appropriate target based on time. It was impossible to obtain an absolutely accurate time reference, as the different tests were performed on different computers; however, start and end times were recorded for each part of the test. Alignment of the signal was performed by fitting the first target to the best result in this time range. Once the fit was performed, the serial data set absolute time was adjusted accordingly. These results were then graphed.

5.3.2 Results

In total, three different sets of psychophysical curves were generated over the course of the experiment. Figure 84 shows the test performed by the subject without visual correction.

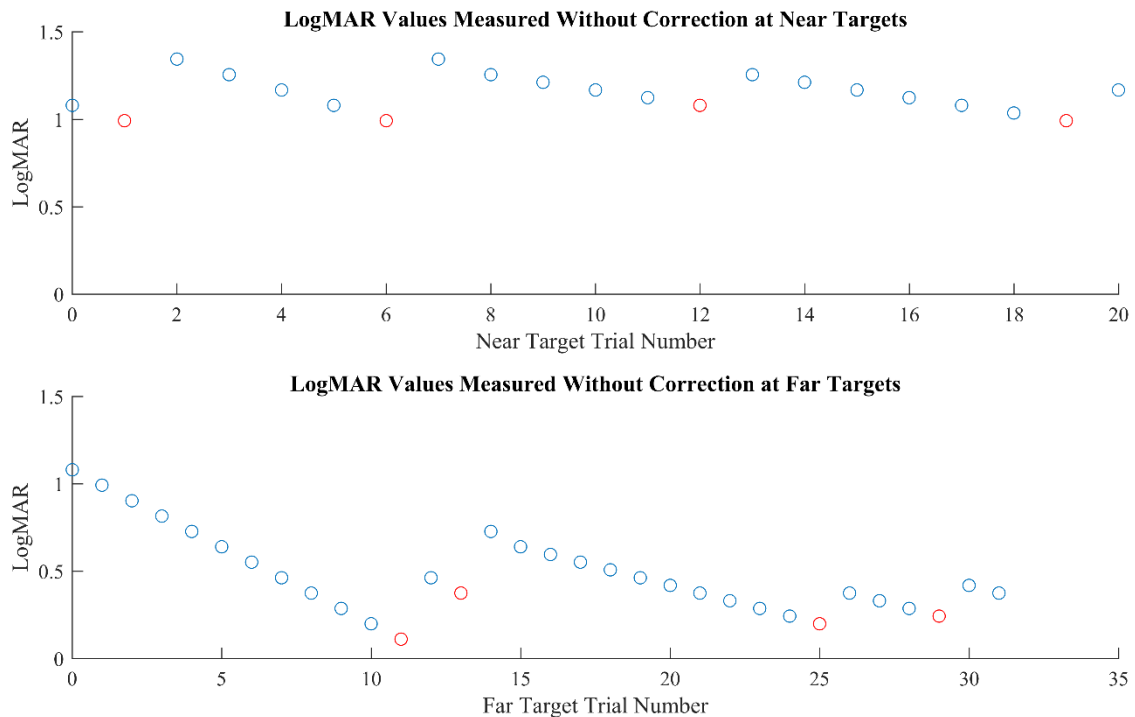


Figure 84: Psychophysical experiment curves recorded during a test without visual correction. The near target results are shown in the top graph, and the far target results in the bottom graph. Incorrect answers are represented by red circles. Note the higher LogMAR values recorded for the near targets than for the far targets, indicating that the visual acuity of the subject was much better at far distances. This is a result to be expected of a presbyopic subject.

As is evident in the figure, the subject scored lower at far targets than at near targets. This indicates that the visual acuity of the subject was better at distant targets, and corresponds with the expected results of a presbyope. For both near and far targets, the subject consistently erred at letters of a similar size.

Two tests were performed with the device, differing in terms of device calibration and the use of the serial output from the device. The first test is shown in Figure 85.

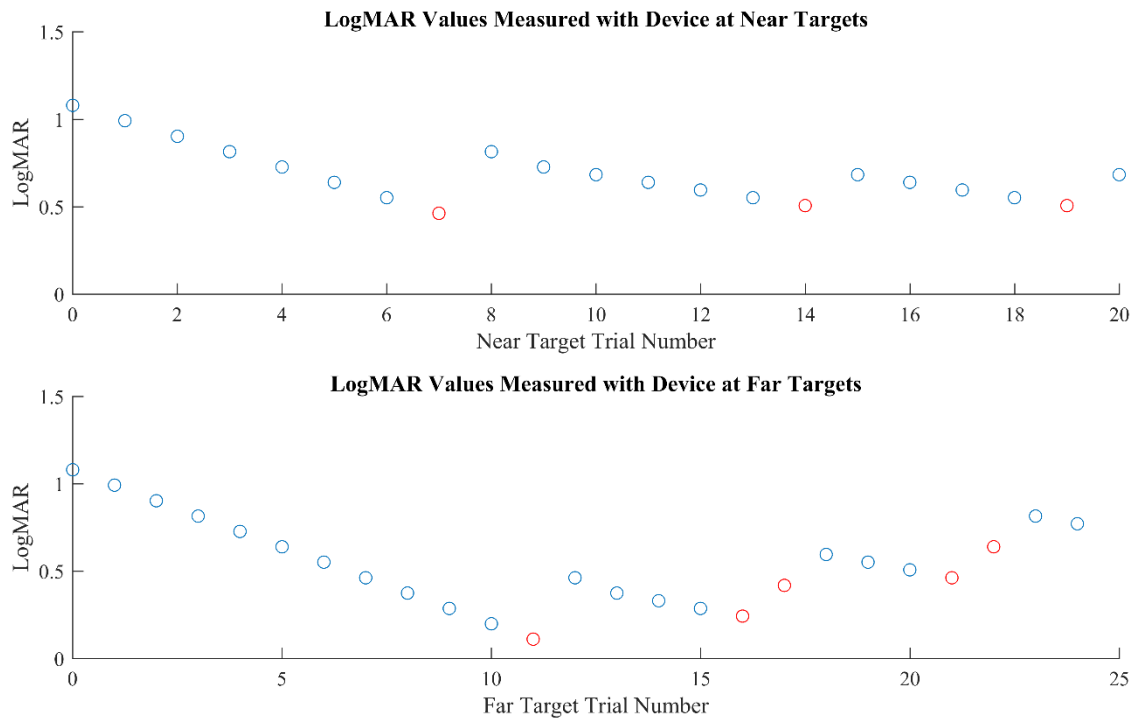


Figure 85: Psychophysical experiment curves recorded during a test with the corrective device. The near target results are shown in the top graph, and the far target results in the bottom graph. Incorrect answers are represented by red circles. A marked improvement is observed in terms of visual acuity between this results, and the results obtained without visual correction.

It is immediately apparent that the LogMAR values at near targets appear lower than those observed in the no correction condition. The far target appears unchanged between this experiment and the no correction condition; this result is also expected, as the improvement of accommodation, necessarily a process occurring at near targets, would not affect the ability of the subject to see at far distances.

Figure 86 shows the results obtained from the repetition of this test.

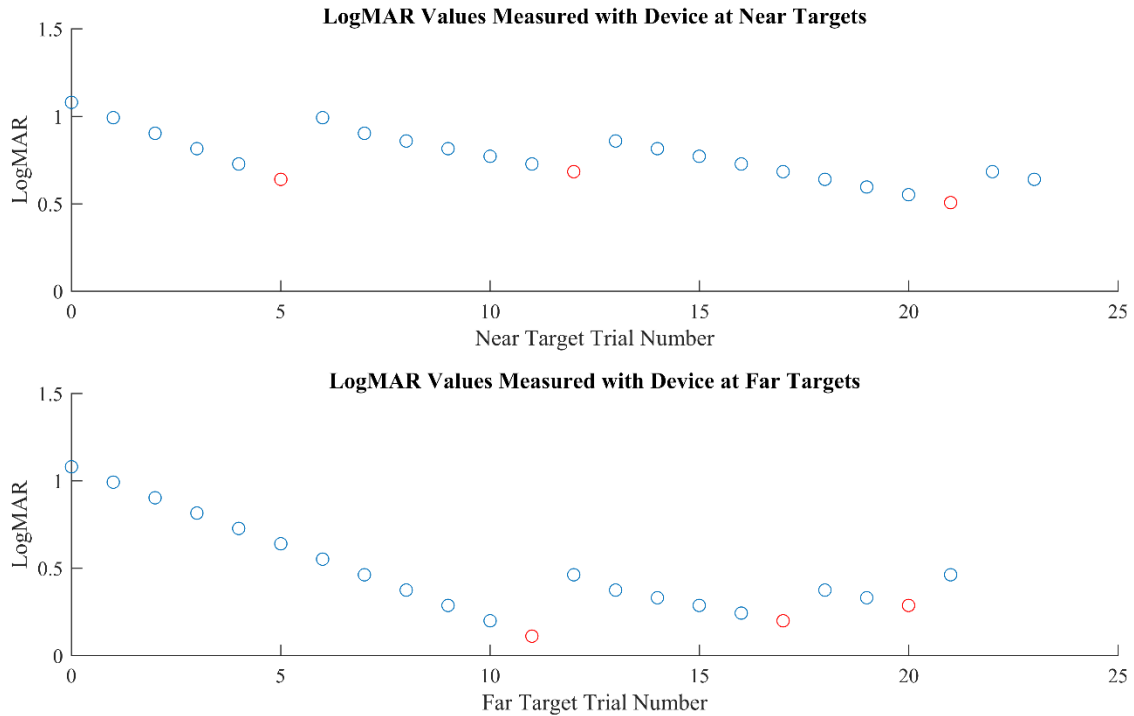


Figure 86: Psychophysical experiment curves recorded during the second test with the corrective device. The near target results are shown in the top graph, and the far target results in the bottom graph. Incorrect answers are represented by red circles. The results, as in the first device test, indicate a better visual acuity at near targets than the test performed without the device.

Results from this test, as in the first test with the device, indicate an increase in near target visual acuity, with no apparent change in far target visual acuity.

In order to quantify these results, the thresholds of both the near and far targets were determined in each condition. Figure 87 shows the LogMAR values of the last correct right answer before a wrong answer for the near target conditions.

Comparison of LogMAR Values Scored by Subject in Trials With and Without Device at Near Distances

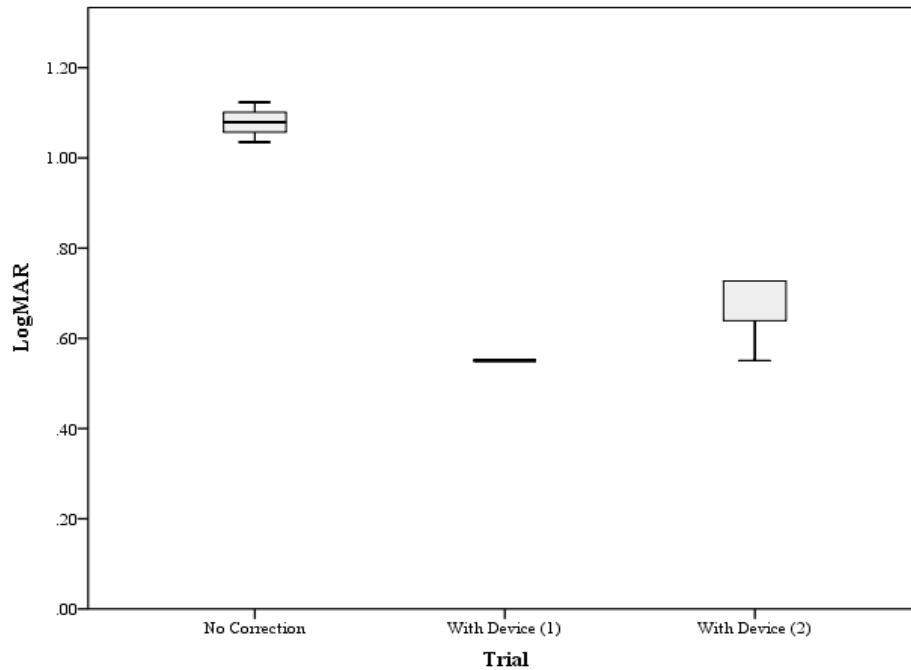


Figure 87: Threshold LogMAR values for near targets both with and without the device. The values were obtained by taking the last correct answer before the subject answered incorrectly. Using the device, the LogMAR value was significantly lower, indicating a higher visual acuity, than the values obtained without correction.

Using a paired-samples t-test, the differences between the conditions with and without the device were found to be significant (control and trial 1, $n = 7$, $p = 0.001$; control and trial 2, $n = 7$, $p = 0.028$). However, between the device trials, no significant differences were found ($n = 6$, $p = 0.184$). This shows that the use of the device significantly increased the visual acuity of the subject at near targets, and that the results are repeatable between sessions.

In Figure 88, the same results, but for the far target conditions, are shown.

Comparison of LogMAR Values Scored by Subject in Trials With and Without Device at Far Distances

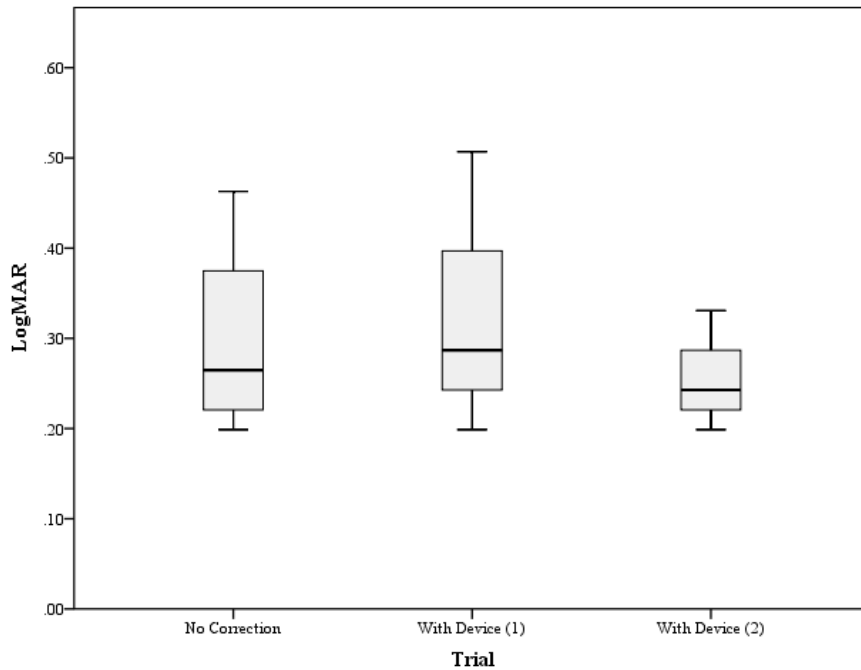


Figure 88: Threshold LogMAR values for far targets both with and without the device. The values were obtained by taking the last correct answer before the subject answered incorrectly. Using the device, the LogMAR value was not significantly different than that recorded without the device.

No significant differences in LogMAR values were observed for the far targets between the two conditions (paired-samples t-test: control and trial 1, $n = 7$, $p = 0.840$; control and trial 2, $n = 7$, $p = 0.678$). Similarly, no significant difference was observed between the LogMAR values of the two device trials ($n = 6$, $p = 0.300$). This result indicates that the device did not affect the subject's visual acuity at far targets, and the results were repeatable between device trials.

To better analyze the signal properties, the amplified signal from the device was recorded via a serial port. After adjusting to the best estimation of time, the amplified accommodation signal, together with the attempted target, were aligned. This is shown in Figure 89.

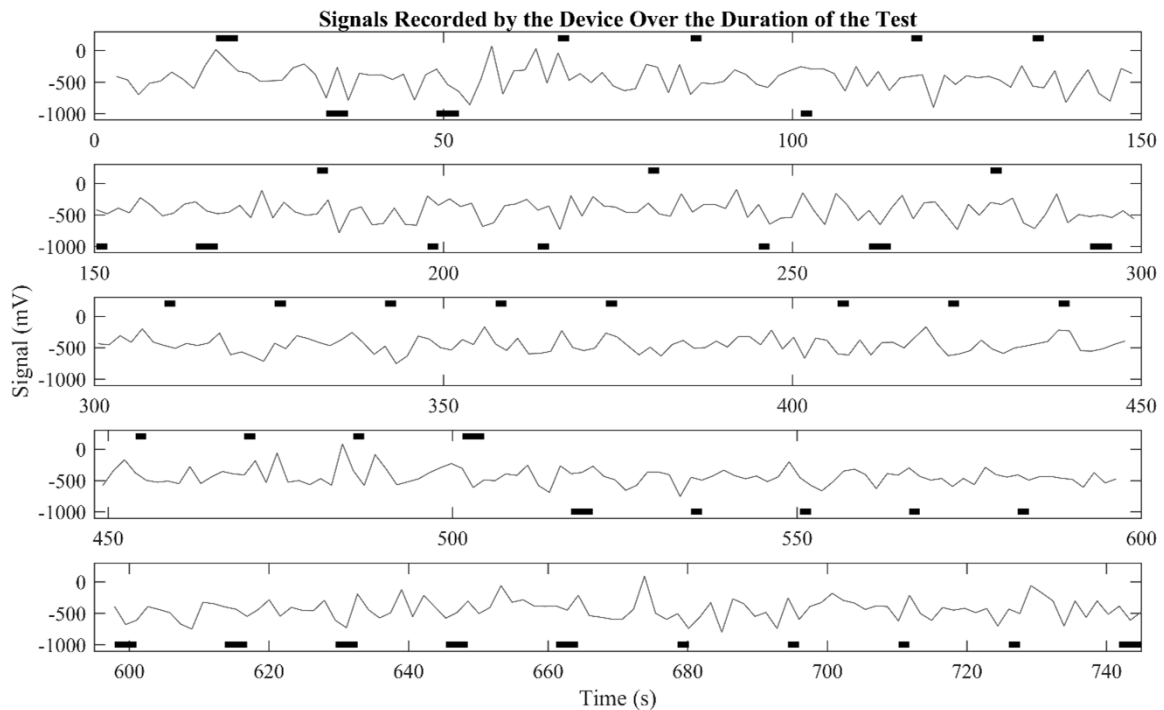


Figure 89: The amplified signal generated by the device, shown with the targets displayed at each time point, graphed for the entire duration of the test. Black bars indicate points at which a target was presented; to reflect the relative amplitude required for distance, bars at the bottoms of the graphs represent near targets, and bars at the tops of the graphs represent the far targets. As can be seen from this figure, the subject's signal amplitude was reversed, with more negative accommodation signals corresponding to nearer targets.

The black bars in the figure represent the time points at which a specific target was presented, with near targets appearing at the bottom, and far targets appearing at the top, of the graphs. Signal amplitudes recorded during the presentation of the targets were noted for both near and far distances, but a paired-samples t-test did not find a significant difference between the target amplitudes ($p = 0.604$) with respect to target distance.

5.4 Discussion

In order to provide a definitive proof of concept, a multi-part experiment was designed to ensure that any beneficial results obtained were the product of the device,

rather than any intervening factors. To this end, several investigations were performed without the electrode and without the device, allowing the subject's baseline level to be accurately measured. This provided a useful comparison point for the results.

Several design changes were made to the electrode prior to the experiment. These changes were thought to be beneficial for the magnification of the signal, and for subject comfort. Though the subject did report that the electrode sat comfortably over the duration of the experiment (approximately 1.5 hours with the electrode), the signals measured were much smaller than those measured with the previous electrode design iteration, with amplitudes of around 10 μV , rather than several tenths of a millivolt. The device was designed for signals in the mV range, but it is able to also work with smaller signals. With the change in signal amplitude, the signal, even after amplification, was approximately 10 mV to several hundred millivolts. This could, potentially, reduce the sensitivity of the device to changes in measured signal amplitudes; however, even with this potential reduction, the device was clearly an effective means of improving accommodation.

The fact that two repeated trials both yielded an improvement in near visual acuity demonstrates that the device developed is an effective means of restoring accommodation non-invasively. It is also important to note that the visual acuity of the subject with respect to far targets was not significantly affected by the device; this shows conclusively that the device affected only the portions of vision compromised by the inability to accommodate. Clearly, these results are very exciting, as this device is the first to control an accommodative lens using the natural accommodation pathway of a presbyope.

An analysis of the signal amplitudes did not yield significant differences between the means of the signals for far and near target distances. On the surface, this would imply that the device changed randomly, without direction, and, by chance, allowed the subject to read the presented word. However, it should be noted that several assumptions were made in analyzing the data: first, that there was an equal amount of time between data points in both the serial and computer outputs; second, that the timing was correctly matched between each measured element; and, third, that the device serial output matched

the current state of the device. It is very difficult to state that each of these assumptions is true, and, indeed, the lack of significance between measurements is almost certainly due to the fact that at least one of these assumptions was false. The signal recorded is, certainly, very noisy, due to the much-reduced magnitude of the accommodation signal (~ 0.4 mV design value versus $10 \mu\text{V}$ experimental value). However, clear changes could be observed between the different target distances, and the subject was able to sustain the same refractive state over several data points. Improvements in experimental methodology will provide a better evaluation of the control signal in future applications.

As a final note, it should be repeated that, in psychophysical investigations, there is a clear improvement in near visual acuity with the use of the device. Though the measurement of the signal is, certainly, a parameter to be considered for future trials, it has not been characterized sufficiently to allow conclusions to be drawn. The meaningful results presented here were those verified psychophysically through the use of several experimental tests, and these prove that, with the aid of the constructed device, a presbyopic subject is able to accommodate to a greater extent than could be expected from a natural situation.

5.5 Future Design Suggestions

Though the device described in this dissertation is fully functional, and performs the desired tasks, several modifications are suggested to improve the device. First, the device should be made smaller. This could easily be done by having the circuits fabricated on printed circuit boards (PCBs), which would reduce the size of the internal components. For the prototype described, the programming was changed several times, requiring the removal and replacement of the microcontroller; for this purpose, a fixed microcontroller would not have answered. Because the program has now been finalized, this would be a desirable feature for future device iterations.

Along with this change would be a smaller housing. A reduction in the final mass of the device would be desirable, as would a sleeker, less noticeable housing design. It is suggested that a plastic casing be used in future iterations to reduce both the cost and the weight of the device, as well as to allow for easier device manufacturing.

Though this was not done due to time constraints, an HV892 driver circuit made either in-house or on a PCB would reduce the price of the device, as well as the weight and bulk of the glasses holder. In a similar vein, rather than using flex cables to control the lens, a board could be manufactured with regular jumper wires connecting the lens to the HV892. A less conspicuous casing for the lens could then be used, which would reduce both the costs and the overall weight of the device.

Finally, at a later time, it would be a decided advantage to make the device wireless. There are two points which require long cables in the current prototype: the attachment to the contact lens electrode, and the ribbon cable attachment to the driver board. This would increase the user comfort, though it would most likely lead to increases in costs and a much more complex design.

In order to allow for more accurate testing and evaluation of future design iterations, it is imperative that the experimental procedure be adjusted to prevent inconclusive results. The times between each measurement device should be synchronized, allowing for the results to be more easily coordinated. A second desired change would be a shorter presentation time for each word; this would prevent random guesses which could lead to false positive results.

5.6 Conclusions

A novel device to actuate a liquid crystal lens in response to a recorded accommodative signal has been constructed. After testing with the actual signals recorded during testing, and after preliminary clinical investigations, it has been found that the device functions as desired, and is able to provide an accommodative response

based on an input signal. Additionally, the device offers features such as initial refractive correction, time adjustment, DC offset adjustment, and gain adjustment.

The goal of this project was to create a device that could replace current clinical interventions for presbyopia, such as IOLs. The developed device is much less invasive than an IOL, and carries none of the associated surgical risks. Additionally, this device boasts a much smaller cost. In terms of smaller interventions, such as reading glasses, the device provides a much larger range of refractive correction, in addition to correcting pre-existing spherical refractive errors.

In conclusion, the device developed over the course of this project is a viable alternative to the current options for presbyopia correction. There are several small adjustments that should be made before production for a wider clinical population, but the overall design is sufficient to ensure refractive correction for presbyopic and pseudophakic individuals. It is expected that this device will be a valuable addition in both future studies pertaining to the ciliary muscle and accommodation, and also to the improvement of quality of life for persons suffering from presbyopia.

SUMMARY

Several goals were pursued in the development of this work, including the development of a novel *in vivo* method to measure the ciliary muscle of a human subject non-invasively during accommodation, the characterization of the recorded muscle signals based on the accommodative abilities of the subject (control, presbyopic, or pseudophakic), and the development of a device that would utilize the recorded muscle signals to mimic the appropriate level of accommodation for the user, actuated through the use of a variable refractive lens. The different elements of the thesis are explored in different sections of this dissertation.

Prior to the development of an assistive device that compensates for missing accommodative ability, trials to record the accommodative signals of the ciliary muscle during accommodation were performed, using a custom contact lens electrode. Three groups, each composed of ten subjects, were examined: control subjects, presbyopic subjects, and pseudophakic subjects. The effects of different pharmacological agents were additionally examined. From these trials, it was discovered that the novel recording method used produced results that were both useable and repeatable.

An analysis of the recorded signals revealed that the parameter most sensitive to changes in accommodative effort was the maximum signal amplitude elicited by focusing on pre-defined targets set at different distances. This parameter differed between groups, with presbyopes showing the lowest signal amplitudes, and control subjects exhibiting the highest amplitudes. Interestingly, the pseudophakic group was able to produce stronger accommodative signals than the presbyopic group. Though cyclopentolate depressed the accommodative amplitudes recorded, phenylephrine did not have an effect.

Using the results from the ciliary muscle studies, an assistive device was developed. Signals recorded from the contact lens electrode were amplified, then, using a linear relationship of distance versus accommodative signal, the device predicted the target refraction. To achieve this refraction, a liquid crystal lens was used, the refractive

power of which could be controlled by the processed ciliary muscle signal. In preliminary proof-of-concept trials, the visual acuity of presbyopic subjects at near targets was found to significantly increase when using the device, while the far visual acuity remained unaffected. This proves that the device is able to use the neural signals produced by the ciliary muscle in order to simulate accommodation through the use of a liquid crystal lens, the refractive power of which is controlled by electrical ciliary muscle response.

ZUSAMMENFASSUNG

In dieser Arbeit wurden mehrere Ziele verfolgt: Die Entwicklung einer neuartigen *in vivo*-Methode zur nicht-invasiven Messung der elektrischen Potentiale des Ziliarmuskels des Menschen während der Akkommodation; die Charakterisierung der aufgezeichneten Muskelsignale auf der Grundlage der Fähigkeit zur Akkommodation des Patienten (gesunde Probanden, Presbyope oder Pseudophake) und die Entwicklung einer Vorrichtung, die die aufgezeichneten Muskelsignale nutzen für eine „künstliche Akkommodation“ durch eine von Muskelaktivität modulierte externe Refraktionsanpassung. Die verschiedenen Elemente der Arbeit werden in den verschiedenen Abschnitten dieser Dissertation beschrieben.

Zunächst wurden Versuche zur Aufzeichnung der elektrischen Signale des Ziliarmuskels während Akkommodation unter Verwendung einer Kontaktlinselektrode durchgeführt. Drei Gruppen, mit jeweils zehn Probanden, wurden untersucht: Kontrollpersonen, Presbyope und Pseudophake. Zusätzlich wurden die Wirkungen verschiedener pharmakologischer Wirkstoffe untersucht. Durch diese Versuche konnte nachgewiesen werden, dass das neuartige Aufzeichnungsverfahren Ergebnisse lieferte, die sowohl nutzbar als auch wiederholbar waren.

Eine Analyse der aufgezeichneten Signale zeigte, dass der empfindlichste Parameter für eine Änderung bei der Akkommodationsanstrengung das maximale Signal einer vordefinierten Amplitude war. Dieses Signal unterschied sich zwischen den Probandengruppen; die Presbyopen zeigten den schwächsten, die gesunden Probanden den stärksten Signalausschlag. Interessanterweise konnte bei den Pseudophaken ein stärkeres Signal als bei den Presbyopen registriert werden. Bei den untersuchten Medikamenten konnte Cyclopentolat die Signale der Akkommodation unterdrücken, bei Phenylephrin konnte dieser Effekt nicht beobachtet werden.

Nach Auswertung der Ergebnisse der Messungen am Ziliarmuskel konnte ein Steuergerät gebaut werden, das die mit einer Kontaktlinse aufgenommene Signale nutzt.

Zunächst mußten die Signale verstärkt werden. Über eine lineare Beziehung zwischen Entfernung und Akkommodationssignal konnte die notwendige refraktive Anpassung vorhergesagt werden. Für die Einstellung der gewünschten Refraktion wurde eine elektronisch ansteuerbare Linse aus Flüssigkristallen benutzt. In ersten Versuchen konnte gezeigt werden, dass das Gerät bei einem Presbyopen das Nah-Sehen deutlich verbesserte, während es keinen negativen Einfluss auf das Sehen in der Ferne hatte. Dies beweist, dass das gebaute Gerät in der Lage ist, über die noninvasive Ableitung neuromuskulärer elektrischer Signals des Ziliarmuskels die Akkommodation mit Hilfe einer ansteuerbaren Flüssigkristalllinse an die Akkommodationsnotwendigkeit anzupassen.

REFERENCES

- Adler-Grinberg, D., 1986. Questioning our classical understanding of accommodation and presbyopia. *Am J Optom & Physiol Optics*, July, 63(7), pp. 571-580.
- Allen, P., Charman, W. & Radhakrishnan, H., 2010. Changes in dynamics of accommodation after accommodative facility training in myopes and emmetropes. *Vision Res*, May, 50(10), pp. 947-955.
- Anderson, H. A., Glasser, A., Manny, R. E. & Stuebing, K. K., 2010. Age-related changes in accommodative dynamics from preschool to adulthood. *Invest Ophthalmol Vis Sci*, January, 51(1), pp. 614-622.
- Armaly, M., 1968. Degeneration of the ciliary muscle and iris sphincter following resection of the ciliary ganglion. *Trans Am Ophthalmol Soc*, Volume 66, pp. 475-502.
- Atchison, D. A., 1995. Accommodation and presbyopia. *Ophthal Physiol Opt*, July, 15(4), pp. 255-272.
- Bailey, I. & Lovie, J., 1976. New design principles for visual acuity letter charts. *Am J Optom Physiol Opt*, 53(11), pp. 740-745.
- Bailey, M. D., 2011. How should we measure the ciliary muscle?. *Invest Ophthalmol Vis Sci*, March, Volume 52, pp. 1817-1818.
- Baumeister, M. & Kohnen, T., 2008. Akkommodation und Presbyopie. Teil 1: Physiologie der Akkommodation und Entwicklung der Presbyopie. *Der Ophthalmologe*, June, 105(6), pp. 597-610.
- Baumeister, M., Wendt, M. & Glasser, A., 2010. Influence of amplitude, starting point, and age on first- and second-order dynamics of Edinger-Westphal-stimulated accommodation in rhesus monkeys. *Invest Ophthalmol Vis Sci*, October, 51(10), pp. 5378-5390.
- Bausch & Lomb, 2015. *Boston XO2: Bausch & Lomb*. [Online]
Available at: <http://www.bausch.com/ecp/our-products/contact-lenses/gp-lens-materials/boston-xo2>

- Beers, A. P. A. & van der Heijde, G. L., 1994. In vivo determination of the biomechanical properties of the component elements of the accommodation mechanism. *Vision Res*, November, 34(21), pp. 2897-2905.
- Beers, A. P. A. & van der Heijde, G. L., 1996. Age-related changes in the accommodation mechanism. *Optom Vis Sci*, April, 73(4), pp. 235-242.
- Beers, A. P. A. & van der Heijde, G. L., 1996. Analysis of accommodation function with ultrasonography. *Doc Ophthalmol*, March, Volume 92, pp. 1-10.
- Bharadwaj, S. R. & Schor, C. M., 2006. Dynamic control of ocular disaccommodation: first and second-order dynamics. *Vision Res*, March, 46(6-7), pp. 1019-1037.
- Bharadwaj, S. R. & Schor, C. M., 2006. Initial destination of the disaccommodation step response. *Vision Res*, June, 46(12), pp. 1959-1972.
- Bharadwaj, S. R., Vedamurthy, I. & Schor, C. M., 2009. Short-term adaptive modification of dynamic ocular accommodation. *Invest Ophthalmol Vis Sci*, July, 50(7), pp. 3520-3528.
- Bharadwaj, S. & Schor, C., 2005. Acceleration characteristics of human ocular accommodation. *Vision Res*, January, 45(1), pp. 17-28.
- Bito, L. Z., Kaufman, P. L., DeRousseau, C. J. & Koretz, J., 1987. Presbyopia: an animal model and experimental approaches for the study of the mechanism of accommodation and ocular ageing. *Eye*, March, 1(2), pp. 222-230.
- Burd, H. J., Judge, S. J. & Cross, J. A., 2002. Numerical modelling of the accommodating lens. *Vision Res*, August, 42(18), pp. 2235-2251.
- Burd, H. J., Judge, S. J. & Flavell, M. J., 1999. Mechanics of accommodation of the human eye. *Vision Res*, May, 39(9), pp. 1591-1595.
- Campbell, F. W. & Westheimer, G., 1960. Dynamics of accommodation responses of the human eye. *J Physiol*, May, 151(2), pp. 285-295.
- Castellano, J. A., 1972. *Liquid crystal color display*. United States of America, Patent No. US3703329A.
- Charman, W. N., 2008. The eye in focus: accommodation and presbyopia. *Clin Exp Optom*, May, 91(3), pp. 207-225.

- Crawford, K., Terasawa, E. & Kaufman, P. L., 1989. Reproducible stimulation of ciliary muscle contraction in the cynomolgus monkey via a permanent indwelling midbrain electrode. *Brain Res*, December, 503(2), pp. 265-272.
- Croft, M. A. et al., 1998. Accommodation dynamics in aging rhesus monkeys. *Am. J. Physiol.*, Volume 275, pp. R1885-R1897.
- Croft, M. A. et al., 2013. Extralenticular and lenticular aspects of accommodation and presbyopia in human versus monkey eyes. *Invest Ophthalmol Vis Sci*, Volume 54, pp. 5035-5048.
- Croft, M. et al., 2006. Accommodative ciliary body and lens function in rhesus monkeys, I: normal lens, zonule and ciliary process configuration in the iridectomized eye. *Invest Ophthalmol Vis Sci*, March, 47(3), pp. 1076-1086.
- Croft, M. et al., 2016. Accommodative movements of the lens/capsule and the strand that extends between the posterior vitreous zonule insertion zone & the lens equator, in relation to the vitreous face and aging. *Ophthalmic Physiol Opt*, January, 36(1), pp. 21-32.
- Croft, M. et al., 2008. Surgical intervention and accommodative responses I: centripetal ciliary capsule and lens movements in rhesus monkeys of various ages. *Invest Ophthalmol Vis Sci*, December, 49(12), pp. 5484-5494.
- Croft, M. et al., 2009. Age-related changes in centripetal ciliary body movement relative to centripetal lens movement in monkeys. *Exp Eye Res*, December, 89(6), pp. 824-832.
- Croft, M. et al., 2013. Accommodative movements of the vitreous membrane, choroid, and sclera in young and presbyopic human and nonhuman primate eyes. *Invest Ophthalmol Vis Sci*, 54(7), pp. 5049-5058.
- Culhane, H., Winn, B. & Gilmartin, B., 1999. Human dynamic closed-loop accommodation augmented by sympathetic inhibition. *Invest Ophthalmol Vis Sci*, 40(6), pp. 1137-1143.
- Drexler, W. et al., 1997. Biometric investigation of changes in the anterior eye segment during accommodation. *Vision Res*, 37(19), pp. 2789-2800.

- Duane, A., 1922. Studies in monocular and binocular accommodation, with their clinical application. *Trans Am Ophthalmol Soc*, Volume 20, pp. 132-157.
- Dubbelman, M., van der Heijde, G. & Weeber, H., 2005. Change in shape of the aging human crystalline lens with accommodation. *Vision Res*, Volume 45, pp. 117-132.
- Du, C. et al., 2012. Anterior segment biometry during accommodation imaged with ultralong scan depth optical coherence tomography. *Ophthalmology*, 119(12), pp. 2479-2485.
- Fisher, R., 1969. The significance of the shape of the lens and capsular energy changes in accommodation. *J Physiol*, Volume 201, pp. 21-47.
- Fisher, R., 1988. The mechanics of accommodation in relation to presbyopia. *Eye*, Volume 2, pp. 646-649.
- Fisher, R. F., 1971. The elastic constants of the human lens. *J Physiol*, Volume 212, pp. 147-180.
- Fisher, R. F., 1977. The force of contraction of the human ciliary muscle during accommodation. *J Physiol*, Volume 270, pp. 51-74.
- Flügel, C., Bárány, E. & Lütjen-Drecoll, E., 1990. Histochemical differences within the ciliary muscle and its function in accommodation. *Exp Eye Res*, Volume 50, pp. 219-226.
- Flügel-Koch, C., Croft, M., Kaufman, P. & Lütjen-Drecoll, E., 2016. Anteriorly located zonular fibres as a tool for fine regulation in accommodation. *Ophthalmic Physiol Opt*, Volume 36, pp. 13-20.
- Garner, L., Brown, B., Baker, R. & Colgan, M., 1983. The effect of phenylephrine hydrochloride on the resting point of accommodation. *Invest Ophthalmol Vis Sci*, 24(4), pp. 393-395.
- Gilmartin, B., Bullimore, M. A., Winn, B. & Owens, H., 1992. Pharmacological effects on accommodative adaptation. *Optometry and Vision Science*, 69(4), pp. 276-282.
- Gilmartin, B., Mallen, E. & Wolffsohn, J., 2002. Sympathetic control of accommodation: evidence for inter-subject variation. *Ophthalm Physiol Opt*, Volume 22, pp. 366-371.

- Goldberg, D., 2011. Computer-animated model of accommodation and theory of reciprocal zonular action. *Clin Ophthalmol*, Volume 5, pp. 1559-1566.
- Goldberg, D., 2015. Computer-animated model of accommodation and presbyopia. *J Cataract Refract Surg*, 41(2), pp. 437-445.
- Harper, D. G., 2014. Bringing accommodation into focus: the several discoveries of the ciliary muscle. *JAMA Ophthalmology*, May, 132(5), pp. 645-648.
- Hermans, E. A., Dubbelman, M., van der Heijde, G. L. & Heethaar, R. M., 2006. Estimating the external force acting on the human eye lens during accommodation by finite element modelling. *Vision Res*, Volume 46, pp. 3642-3650.
- Heron, G. & Charman, W. N., 2004. Accommodation as a function of age and the linearity of the response dynamics. *Vis Res*, Volume 44, pp. 3119-3130.
- Hoogendam, Y. et al., 2014. Older age relates to worsening of fine motor skills: a population-based study of middle-aged and elderly persons. *Front Aging Neurosci*, 6(259), pp. 1-7.
- Horowitz, P. & Hill, W., 2015. *The Art of Electronics*. 3rd ed. New York: Cambridge University Press.
- Izci, Y. & Gonul, E., 2006. The microsurgical anatomy of the ciliary ganglion and its clinical importance in orbital traumas: an anatomic study. *Minim Invas Neurosurg*, Volume 49, pp. 156-160.
- Judge, S. & Cumming, B., 1986. Neurons in the monkey midbrain with activity related to vergence eye movement and accommodation. *J Neurophysiol*, 55(5), pp. 915-930.
- Kasthurirangan, S. & Glasser, A., 2005. Influence of amplitude and starting point on accommodative dynamics in humans. *Invest Ophthalmol Vis Sci*, 46(9), pp. 3463-3472.
- Kasthurirangan, S. & Glasser, A., 2006. Age related changes in accommodative dynamics in humans. *Vis Res*, Volume 46, pp. 1507-1519.
- Kaufman, P. et al., 1991. Parasympathetic denervation of the ciliary muscle following panretinal photocoagulation. *Curr Eye Res*, 10(5), pp. 437-455.

- Klaproth, O., Titke, C., Baumeister, M. & Kohnen, T., 2011. Akkommodative Introkularlinsen - Grundlagen der klinischen Evaluation und aktuelle Ergebnisse. *Klin Monatsbl Augenheilkd*, Volume 228, pp. 666-675.
- Korbmacher, C. et al., 1990. Membrane voltage recordings in a cell line derived from human ciliary muscle. *Invest Ophthalmol Vis Sci*, 31(11), pp. 2420-2430.
- Koretz, J. F. & Handelman, G. H., 1982. Model of the accommodative mechanism in the human eye. *Vision Res*, Volume 22, pp. 917-927.
- Koretz, J. & Handelman, G., 1983. A model for accommodation in the young human eye: the effects of lens elastic anisotropy on the mechanism. *Vision Res*, 23(12), pp. 1679-1686.
- Koretz, J. & Handelman, G., 1986. Modeling age-related accommodative loss in the human eye. *Mathematical Modelling*, Volume 7, pp. 1003-1014.
- Kotulak, J. & Schor, C., 1986. A computational model of the error detector of human visual accommodation. *Biol Cybern*, Volume 54, pp. 189-194.
- Krishnan, V. & Stark, L., 1975. Integral control in accommodation. *Comput Programs Biomed*, Volume 4, pp. 237-245.
- Lichtinger, A. & Rootman, D. S., 2012. Intraocular lenses for presbyopia correction: past, present, and future. *Curr Opin Ophthalmol*, 23(1), pp. 40-46.
- Lütjen-Drecoll, E. et al., 2010. Morphology and accommodative function of the vitreous zonule in human and monkey eyes. *Invest Ophthalmol Vis Sci*, 51(3), pp. 1554-1564.
- Lütjen-Drecoll, E., Shimizu, T., Rohrbach, M. & Rohen, J., 1986. Quantitative analysis of 'plaque material' between ciliary muscle tips in normal- and glaucomatous eyes. *Exp Eye Res*, Volume 42, pp. 457-465.
- Lütjen-Drecoll, E., Tamm, E. & Kaufman, P., 1988. Age changes in rhesus monkey ciliary muscle: light and electron microscopy. *Exp Eye Res*, Volume 47, pp. 885-899.
- Lütjen-Drecoll, E., Tamm, E. & Kaufman, P., 1988. Age-related loss of morphologic responses to pilocarpine in rhesus monkey ciliary muscle. *Arch Ophthalmol*, Volume 106, pp. 1591-1598.

- Markwardt, K., Magnino, P. & Houppang, I., 1997. Histamine induced contraction of human ciliary muscle cells. *Exp Eye Res*, Volume 64, pp. 713-717.
- Masuda, H. et al., 1998. M3-type muscarinic receptors predominantly mediate neurogenic quick contraction of the bovine ciliary muscle. *Gen Pharmac*, 30(4), pp. 579-584.
- Masuda, H. et al., 1997. Nitric oxide-induced ciliary muscle relaxation during contraction with endothelin-1 is mediated through elevation of cyclic GMP. *Curr Eye Res*, Volume 16, pp. 1245-1251.
- May, P. & Warren, S., 1993. Ultrastructure of the macaque ciliary ganglion. *J Neurocytology*, Volume 22, pp. 1073-1095.
- Mays, L. & Gamlin, P., 1995. Neuronal circuitry controlling the near response. *Curr Opin Neurobiol*, Volume 5, pp. 763-768.
- Mordi, J. A. & Ciuffreda, K. J., 2004. Dynamic aspects of accommodation: age and presbyopia. *Vis Res*, Volume 44, pp. 591-601.
- Nankivil, D. et al., 2015. The zonules selectively alter the shape of the lens during accommodation based on the location of their anchorage points. *Invest Ophthalmol Vis Sci*, 56(3), pp. 1751-1760.
- Nankivil, D. et al., 2009. Effect of anterior zonule transection on the change in lens diameter and power in cynomolgus monkeys during accommodation. *Invest Ophthalmol Vis Sci*, 50(8), pp. 4017-4021.
- Naycheva, L. et al., 2012. Phosphene thresholds elicited by transcorneal electrical stimulation in healthy subjects and patients with retinal diseases. *Invest Ophthalmol Vis Sci*, November, 53(12), pp. 7440-7448.
- Nemeth, G. et al., 2008. A comparison of accommodation amplitudes in pseudophakic eyes measured with three different methods. *Eye*, Volume 22, pp. 65-69.
- Nisper, J. & Stevens, R., 2014. *Variable-power lens*. Europe, Patent No. WO2014124707A1.
- Nisper, J. & Stevens, R., 2016. *Adjustable Lens and Article of Eyewear*. United States of America, Patent No. US20160004102A1.

- Ober, M. & Rohen, J., 1979. Regional differences in the fine structure of the ciliary epithelium related to accommodation. *Invest Ophthalmol Vis Sci*, 18(7), pp. 655-664.
- O'Neil, W. D. & Brodkey, J., 1970. A nonlinear analysis of the mechanics of accommodation. *Vision Res*, Volume 10, pp. 375-391.
- Ostrin, L. & Glasser, A., 2004. The effects of phenylephrine on pupil diameter and accommodation in rhesus monkeys. *Invest Ophthalmol Vis Sci*, January, 45(1), pp. 215-221.
- Ostrin, L. & Glasser, A., 2005. Comparisons between pharmacologically and Edinger-Westphal-stimulated accommodation in rhesus monkeys. *Invest Ophthalmol Vis Sci*, 46(2), pp. 609-617.
- Ostrin, L. & Glasser, A., 2007. Edinger-Westphal and pharmacologically stimulated accommodative refractive changes and lens and ciliary process movements in rhesus monkeys. *Exp Eye Res*, 84(2), pp. 302-313.
- Ostrin, L. & Glasser, A., 2007. Effects of pharmacologically manipulated amplitude and starting point on Edinger-Westphal-stimulated accommodative dynamics in rhesus monkeys. *Invest Ophthalmol Vis Sci*, 48(1), pp. 313-320.
- Pang, I., Matsumoto, S., Tamm, E. & DeSantis, L., 1994. Characterization of muscarinic receptor involvement in human ciliary muscle cell function. *J Ocul Pharmacol*, 10(1), pp. 125-136.
- Park, C. et al., 2016. Revisiting ciliary muscle tendons and their connections with the trabecular meshwork by two photon excitation microscopic imaging. *Invest Ophthalmol Vis Sci*, 57(3), pp. 1096-1105.
- Parrot SA Confidential, n.d. *TEDS for Arctic 39N0, Document 140901*. s.l.:s.n.
- Peirce, J., 2007. PsychoPy - Psychophysics software in Python. *J Neurosci Methods*, 162(1-2), pp. 8-13.
- Peirce, J., 2007. PsychoPy - Psychophysics software in Python. *J Neurosci Methods*, 162(1-2), pp. 8-13.
- Peirce, J., 2009. Generating stimuli for neuroscience using PsychoPy. *Front Neuroinform*, 2(10), pp. 1-8.

- Pepose, J. S., 2008. Maximizing satisfaction with presbyopia-correcting intraocular lenses: the missing links. *Am J Ophthalmol*, 146(5), pp. 641-648.
- Petrash, J. M., 2013. Aging and age-related diseases of the ocular lens and vitreous body. *Invest Ophthalmol Vis Sci*, Volume 54, pp. ORSF54-ORSF59.
- Popiolek-Masajada, A. & Kasprzak, H., 2002. Model of the optical system of the human eye during accommodation. *Ophthal Physiol Opt*, Volume 22, pp. 201-208.
- Richdale, K. et al., 2012. The effect of phenylephrine on the ciliary muscle and accommodation. *Optom Vis Sci*, October, 89(10), pp. 1507-1511.
- Richdale, K., Bullimore, M., Sinnott, L. & Zadnik, K., 2016. The effect of age, accommodation, and refractive error on the adult human eye. *Optom Vis Sci*, 93(1), pp. 3-11.
- Richdale, K. et al., 2013. Quantification of age-related and per diopter accommodative changes of the lens and ciliary muscle in the emmetropic human eye. *Inves Ophthalmol Vis Sci*, 54(2), pp. 1095-1105.
- Rohen, J., Eichhorn, M., Kaufman, P. & Erickson-Lamy, K., 1990. Ciliary neuromuscular morphology in cynomolgus monkeys after ciliary ganglionectomy. *Graefe's Arch Clin Exp Ophthalmol*, Volume 228, pp. 49-54.
- Rohen, J. & Rentsch, F., 1969. Der konstruktive Bau des Zonulaapparates beim Menschen und dessen funktionelle Bedeutung. Morphologische Grundlagen für eine neue Akkommodationstheorie. *Graefe's Arch Klin Exp Ophthalmol*, Volume 178, pp. 1-19.
- Rohen, J. W., 1979. Scanning electron microscopic studies of the zonular apparatus in human and monkey eyes. *Invest Ophthalmol Vis Sci*, 18(2), pp. 133-144.
- Rosenfield, M., Gilmartin, B., Cunningham, E. & Dattani, N., 1990. The influence of alpha-adrenergic agents on tonic accommodation. *Curr Eye Res*, 9(3), pp. 267-272.
- Samuel, U., Lütjen-Drecoll, E. & Tamm, E., 1996. Gap junctions are found between iris sphincter smooth muscle cells but not in the ciliary muscle of human and monkey eyes. *Exp Eye Res*, Volume 63, pp. 187-192.

- Sarkar, S., Hasnat, A. & Bharadwaj, S., 2012. Revisiting the impact of phenylephrine hydrochloride on static and dynamic accommodation. *Indian J Ophthalmol*, 60(6), pp. 503-509.
- Schachar, R. A., 2012. *The Mechanism of Accommodation and Presbyopia*. Amsterdam: Kugler Publications.
- Schaeffel, F., Wilhelm, H. & Zrenner, E., 1993. Inter-individual variability in the dynamics of natural accommodation in humans: relation to age and refractive errors. *J Physiol*, Volume 461, pp. 301-320.
- Schor, C. & Bharadwaj, S., 2005. A pulse-step model of accommodation dynamics in the aging eye. *Vision Res*, May, 45(10), pp. 1237-1254.
- Schor, C. & Bharadwaj, S., 2006. Pulse-step models of control strategies for dynamic ocular accommodation and disaccommodation. *Vision Res*, January, 46(1-2), pp. 242-258.
- Seidemann, A. & Schaeffel, F., 2003. An evaluation of the lag of accommodation using photorefractometry. *Vision Res*, February, 43(4), pp. 419-430.
- Shao, Y. et al., 2015. Age-related changes in the anterior segment biometry during accommodation. *Invest Ophthalmol Vis Sci*, 56(6), pp. 3522-3530.
- Sheppard, A. & Davies, L., 2010. In vivo analysis of ciliary muscle morphologic changes with accommodation and axial ametropia. *Invest Ophthalmol Vis Sci*, 51(12), pp. 6882-6889.
- Sheppard, A. & Davies, L., 2011. The effect of ageing on in vivo human ciliary muscle morphology and contractility. *Invest Ophthalmol Vis Sci*, 52(3), pp. 1809-1816.
- Shirachi, D. et al., 1978. Accommodation dynamics I. Range nonlinearity. *Am J Opt & Physiol Optics*, 55(9), pp. 631-641.
- Stark, L., 1988. Presbyopia in light of accommodation. *Am J Optom & Physiol Optics*, 65(5), pp. 407-416.
- Stark, L. & Atchison, D., 1997. Pupil size, mean accommodation response and the fluctuations of accommodation. *Ophthalmic Physiol Opt*, July, 17(4), pp. 316-323.

- Strenk, S. et al., 1999. Age-related changes in human ciliary muscle and lens: a magnetic resonance imaging study. *Invest Ophthalmol Vis Sci*, 40(6), pp. 1162-1169.
- Strenk, S., Strenk, L. & Guo, S., 2006. Magnetic resonance imaging of aging, accommodating, phakic, and pseudophakic ciliary muscle diameters. *J Cataract Refract Surg*, 32(11), pp. 1792-1798.
- Strenk, S., Strenk, L. & Guo, S., 2010. Magnetic resonance imaging of the anteroposterior position and thickness of the aging, accommodating, phakic, and pseudophakic ciliary muscle. *J Cataract Refract Surg*, 36(2), pp. 235-241.
- Sugawara, R. et al., 2006. Agonist and antagonist sensitivity of non-selective cation channel currents evoked by muscarinic receptor stimulation in bovine ciliary muscle cells. *Auton Autacoid Pharmacol*, Volume 26, pp. 285-292.
- Sun, F. & Stark, L., 1986. Dynamics of accommodation: measurements for clinical application. *Exp Neurol*, 91(1), pp. 71-79.
- Suzuki, R., 1983. Neuronal influence on the mechanical activity of the ciliary muscle. *Br J Pharmacol*, Volume 78, pp. 591-597.
- Tamm, E., Baur, A. & Lütjen-Drecoll, E., 1992. Synthesis of extracellular matrix components by human ciliary muscle cells in culture. *Curr Eye Res*, 11(4), pp. 333-341.
- Tamm, E. et al., 1992. Age-related loss of ciliary muscle mobility in the rhesus monkey: role of the choroid. *Arch Ophthalmol*, Volume 110, pp. 871-876.
- Tamm, E., Flügel, C., Baur, A. & Lütjen-Drecoll, E., 1991. Cell cultures of human ciliary muscle: growth, ultrastructural and immunocytochemical characteristics. *Exp Eye Res*, Volume 53, pp. 375-387.
- Tamm, E., Flügel, C., Stefani, F. & Lütjen-Drecoll, E., 1994. Nerve endings with structural characteristics of mechanoreceptors in the human scleral spur. *Invest Ophthalmol Vis Sci*, 35(3), pp. 1157-1166.
- Tamm, E., Flügel-Koch, C., Mayer, B. & Lütjen-Drecoll, E., 1995. Nerve cells in the human ciliary muscle: ultrastructural and immunocytochemical characteristics. *Invest Ophthalmol Vis Sci*, 36(2), pp. 414-426.

Tamm, E. et al., 1995. Innervation of myofibroblast-like scleral spur cells in human and monkey eyes. *Invest Ophthalmol Vis Sci*, 36(8), pp. 1633-1644.

Tamm, E. & Lütjen-Drecoll, E., 1996. Ciliary Body. *Microsc Res Tech*, 1 April, Volume 33, pp. 390-439.

Tamm, E., Lütjen-Drecoll, E., Jungkunz, W. & Rohen, J., 1991. Posterior attachment of ciliary muscle in young accommodating old, presbyopic monkeys. *Invest Ophthalmol Vis Sci*, 32(5), pp. 1678-1692.

Tamm, E., Lütjen-Drecoll, E. & Rohen, J., 1990. Age-related changes of the ciliary muscle in comparison with changes induced by treatment with prostaglandin F_{2α}. An ultrastructural study in rhesus and cynomolgus monkeys. *Mech Aging Develop*, Volume 51, pp. 101-120.

Tamm, S., Tamm, E. & Rohen, J., 1992. Age-related changes of the human ciliary muscle. A quantitative morphometric study. *Mech Ageing Dev*, Volume 62, pp. 209-221.

Texas Instruments Inc., 2005. *INA128/INA129*. s.l.:s.n.

Texas Instruments Inc., 2013. *LM317 3-Terminal Adjustable Regulator*. s.l.:s.n.

The Council of the European Communities, 1993. *Council Directive 93/42/EEC of 14 June 1993 concerning medical devices*, s.l.: s.n.

Thieme, H., Nass, J., Nuskovski, M. & Wiederholt, M., 1999. The effects of the carbonic anhydrase inhibitors methazolamide, diclofenamide and dorzolamide on trabecular meshwork and ciliary muscle contractility. *Exp Eye Res*, Volume 69, pp. 455-458.

Toates, F. M., 1970. A model of accommodation. *Vision Res*, Volume 10, pp. 1069-1076.

Tomita, S. & Nabeshima, T., 1997. *Liquid crystal shutter control circuit for a video camera having a synchronized strobe flash*. United States of America, Patent No. US5619266A.

Tscherning, M., 1920. *Dioptrics of the Eye, Functions of the Retina Ocular Movements and Binocular Vision*. Philadelphia: The Keystone Publishing Company.

Van Cauwenberge, F. & Rakic, J.-M., 2014. Les nouvelles possibilités de traitement de la presbytie. *Rev Med Liège*, 69(5-6), pp. 361-365.

Van de Sompel, D., Kunkel, G. J., Hersh, P. S. & Smits, A. J., 2010. Model of accommodation: contributions of lens geometry and mechanical properties to the development of presbyopia. *J Cataract Refract Surg*, Volume 36, pp. 1960-1971.

von Helmholtz, H., 1867. *Handbuch der physiologischen Optik*. s.l.:Voss.

Vrabec, F., 1974. Age changes of the inner surface of the trabecular meshwork shown by the replica technique. *Invest Ophthalmol*, 13(12), pp. 950-953.

Weale, R. A., 1962. Presbyopia. *Brit J Ophthalmol*, Volume 46, pp. 660-668.

Weeber, H. A. & van der Heijde, G. L., 2007. On the relationship between lens stiffness and accommodative amplitude. *Exp Eye Res*, Volume 85, pp. 602-607.

Wiederholt, M., Thieme, H. & Stumpff, F., 2000. The regulation of trabecular meshwork and ciliary muscle contractility. *Prog Ret Eye Res*, 19(3), pp. 271-295.

Zetterström, C., 1984. The effect of phenylephrine on the accommodative process in man. *Acta Ophthalmol*, 62(6), pp. 872-878.

Zimmermann, A. & Rohen, J., 1970. Histometrische Untersuchungen über das Ciliarepithel von Primaten bei verschiedenen Kontraktionszuständen der Ciliarmuskels. *Graefes Arch Klin Exp Ophthalmol*, Volume 179, pp. 294-301.

ERKLÄRUNG ZUM EIGENANTEIL DER DISSERTATIONSSCHRIFT

Die Arbeit wurde in der Universitäts Tübingen Augenklinik unter Betreuung von Prof. Dr. med. Dr. hc. mult. Eberhart Zrenner durchgeführt.

Die Konzeption der Studie erfolgte in Zusammenarbeit mit Torsten Straßer, Ditta Zobor, und Eberhart Zrenner.

Die Versuche wurden von mir in Zusammenarbeit mit Dominic Hillerkuss, Frank Schaeffel, Torsten Straßer, Ditta Zobor, und Eberhart Zrenner durchgeführt.

Die statistische Auswertung erfolgte eigenständig durch mich.

Ich versichere, das Manuskript selbständig verfasst zu haben und keine weiteren als die von mir angegebenen Quellen verwendet zu haben.

Leverkusen, den

APPENDIX A: CODE

```

/* File: FinalwUARTftp.c
* Other files needed: LCDModule2.c, LCDModule2.h
* Author: Maggie Clouse. LCD module files, see files for author information.
Thanks to DarioG and Ren from Microchip forums for sample code (floating
variables).
* Pin connections: 1 - with 10k to 5V
3 - input from 2.5k pot
11 - 5V, 2.5k pot
12 - GND, 2.5k pot
18 - to ADS1015 (pin 3), Logic Level

Converter, pulled up w/10k
19 - Pin 11, HDM20216-3
20 - Pin 12, HDM20216-3
21 - Pin 13, HDM20216-3
22 - Pin 14, HDM20216-3
23 - to ADS1015 (pin 4), Logic Level

Converter, pulled up w/10k
25 - TX, yellow wire, to RX
26 - RX, red wire, to TX
27 - Pin 4, HDM20216-3
28 - Pin 5, HDM20216-3
29 - Pin 6, HDM20216-3
31 - GND
32 - 5V
33 - Pin 5, Parallax keypad
34 - Pin 6, Parallax keypad
35 - Pin 7, Parallax keypad
36 - Pin 8, Parallax keypad
37 - Pin 1, Parallax keypad
38 - Pin 2, Parallax keypad
39 - Pin 3, Parallax keypad
40 - Pin 4, Parallax keypad

*
* Created on March 1, 2016
*Version Oct. 10, 2016
*/

// Header Files
#include <p18f4520.h>

```

```

#include <delays.h>
#include <stdio.h>
#include "i2c.h"
#include <adc.h>
#include <math.h>
#include <stdlib.h>
#include <string.h>
#include "LCDModule2.h"
#include <usart.h>

// Configuration Bits
#pragma config OSC = INTIO67 // Internal osc
#pragma config WDT = OFF
#pragma config LVP = OFF
#pragma config BOREN = OFF
#pragma config PWRT = OFF

// Define Constants
#define DELAY_TIME 10
#define SWITCH_DELAY 10
#define SWITCH_TIME 10
#define LCD_DELAY 10

// Local Function Prototypes
unsigned char findSwitch(void);
void CalibrationSequence(void);
void CalibrationSequence2(void);
void FindKey(void);
void EquationCalculation(void);
void ShutOff(void);
void AdjustRefraction(void);
void AdjustTiming(void);

// Global Variables
int temp;
int pin;
int mySum;
int mySum1;
unsigned char keyPattern[]={0b01110111, 0b10110111, 0b11010111,
0b11100111,
0b11011011, 0b11101011,
0b01111011, 0b10111011,

```

```

0b11011101, 0b11101101,
0b11011110, 0b11101110};
    unsigned char keySymbol[]={ '1','2','3','A',
                                '4','5','6','B',
                                '7','8','9','C',
                                '*','0','#','D'};

    unsigned char i, currentKey;
    char line1[20];
    char line2[80];
    int mySlope;
    int myIntercept;
    float myRatio;
    float myTarget;
    int myCode;
    int Lbyte, Hbyte;
    int value;
    int myNew;
    int myRefraction;
    int myInitial;
    float myIR;
    int myTime;
    int TimeVal;
    int TimeDisp;
    char buf[20];
    int med1;

#pragma code

void main(void)
{
    Delay10KTCYx(10); //Used to allow everything 1 s for start-up
    /*****
    *****
    This section initializes I2C, ADC, keypad, Timer0 functions.
    *****/
    /*****/

    //I2C Initialization
    OpenI2C(MASTER,SLEW_OFF); //Opens Master mode for I2C

```

```

SSPADD=9; //Sets 400 kHz I2C clock
OSCCONbits.IRCF2=1; //Sets internal oscillation at 4 MHz
OSCCONbits.IRCF1=1;
OSCCONbits.IRCF0=0;
IdleI2C();

//USART Initialization
OpenUSART(USART_TX_INT_OFF & USART_RX_INT_OFF &
USART_ASYNCH_MODE & USART_EIGHT_BIT & USART_BRGH_LOW &
USART_CONT_RX, 12); //Sets asynchronous, 8-bit mode, 4800 Baud, low speed

//ADC Initialization
TRISAbits.TRISA1=1; //Sets RA0 as input for analog (patient signal,
from INA128 circuit)
ADCON1=0x0E; //Settings for the ADC; references are at 0 and 5 V

OpenADC(ADC_FOSC_8&ADC_RIGHT_JUST&ADC_2_TAD,
ADC_CH1&ADC_INT_OFF&ADC_REF_VDD_VSS,14);
SetChanADC(ADC_CH1); //Input to pin 3

//For keypad
TRISB=0x0F;
PORTB=0x0F;

//Set lens to 0D (HV892 board)
StartI2C();
IdleI2C();
WriteI2C(0x46); //Address, write to lens
IdleI2C();
WriteI2C(0xAD); //0.5D correction
IdleI2C();
StopI2C();
IdleI2C();

//Configure ADS1015
StartI2C(); //Initializes I2C transfers
IdleI2C();
WriteI2C(0b10010000); //This is the address of the ADS1015 module
(Starting write mode)
IdleI2C();
WriteI2C(0b00000001); //Pointer to Config register of the ADS1015
IdleI2C();
WriteI2C(0b00000000); //MSB of config

```



```

IdleI2C();
WriteI2C(0b10000011); //LSB of config
IdleI2C();
StopI2C();

//Pointer for ADS1015 (read conversion)
IdleI2C();
StartI2C();
IdleI2C();
WriteI2C(0b10010000); //Address of ADS1015, writing
IdleI2C();
WriteI2C(0b00000000); //Pointer to conversion register (which needs to
be read)
IdleI2C();
StopI2C();

//Start sequence
XLCDInit();
XLCDClear();
XLCDL1home();
XLCDDisplayOnCursorOff();
EnablePullups();

//Wait until 9 is pressed before starting
do
{
    XLCDClear();
    XLCDL1home();
    XLCDDisplayOnCursorOff();
    EnablePullups();
    XLCDPutRomString("Press 9 to start");
    FindKey();
}
while(pin!='9');

//Refraction adjustment
do
{
    FindKey();
    AdjustRefraction(); //Adjusts the refraction based on
voltage through potentiometer
    XLCDClear();

```

```

        XLCDL1home();
        XLCDDisplayOnCursorOff();
        EnablePullups();
        XLCDPutRomString("Refraction: Press 4");
        XLCDL2home();
        sprintf(line2,"%d.%1u D", (int) myIR, (int) fabs(((myIR -
(int) myIR ) * 10)));
        XLCDPutRamString(line2); //Display initial refraction
value

    }
    while(pin!='4'); //Stop operation when 4 is pressed
    myCode=myInitial; //This stores the final adjustment code
    StopI2C();

//Display the results of the initial adjustment

    XLCDClear();
    XLCDL1home();
    XLCDDisplayOnCursorOff();
    EnablePullups();
    XLCDPutRomString("Refraction");
    XLCDL2home();
    sprintf(line2,"%d.%1u D", (int) myIR, (int) fabs(((myIR - (int)
myIR ) * 10))); //Displays refraction value
    XLCDPutRamString(line2);
    Delay10KTCYx(10);

//Timing Adjustment Sequence

do
    {
        FindKey();
        AdjustTiming(); //Adjusts the timing based on voltage
through potentiometer
    }
    while(pin!='5'); //Stop operation when 5 pressed

//0D Calibration Sequence
    XLCDClear();
    XLCDL1home();
    XLCDDisplayOnCursorOff();

```

```

    EnablePullups();
    XLCDPutRomString("Calibration 0D:");
    XLCDL2home();
    XLCDPutRomString("Press 2 to start");
    CalibrationSequence();

//5D Calibration Sequence
    XLCDInit();
    XLCDClear();
    XLCDL1home();
    XLCDDisplayOnCursorOff();
    EnablePullups();
    XLCDPutRomString("Calibration 5D:");
    XLCDL2home();
    XLCDPutRomString("Press 1 to start");
    CalibrationSequence2();
    EquationCalculation();

//Main Program
    while (1)
    {
        do
        {
            FindKey(); //Look for a key press
            //Read ADC
            IdleI2C();
            StartI2C();
            IdleI2C();
            WriteI2C(0b10010001); //ADS1015 address, read
mode
            Hbyte=ReadI2C(); //Reads upper values of ADC
            AckI2C();
            Lbyte=ReadI2C(); //Reads lower values of ADC
            AckI2C();
            value = ((unsigned int) Hbyte) << 8 | Lbyte;
            myNew=(float)value*6144.0/32767.0; //This gives
the mV value of the voltage measured
            Delay10KTCYx(TimeVal);
            XLCDClear();
            XLCDL1home();
            sprintf(line1, "Measured=%d mV", myNew);
            XLCDPutRamString(line1);
            sprintf(buf, "\r\n%d mV", myNew);

```

```

        putsUSART(buf); //Send mV to UART bus
        Delay10KTCYx(TimeVal);
        StopI2C();
//Write to HV892
        IdleI2C();
        StartI2C();
        WriteI2C(0x46); //Start writing to HV892
        IdleI2C();
        myRatio=(myNew-(float)mySum)/(float)mySlope;
//Calculates the target refraction
        myTarget=(float)myRatio + (float)myIR; //Adds
the initial refraction to the target refraction
        sprintf(buf,"\t%d D", myTarget);
        putsUSART(buf); //Send target refraction to
UART bus
        if (myTarget< -3.0)
            {
                myCode=0x9B;
            }
        else if (myTarget>=-3.0 && myTarget<-2.5)
            {
                myCode=0x9D;
            }
        else if (myTarget>=-2.5 && myTarget<-2.0)
            {
                myCode=0x9F;
            }
        else if (myTarget>=-2.0 && myTarget<-1.5)
            {
                myCode=0xA2;
            }
        else if (myTarget>=-1.5 && myTarget<-1.0)
            {
                myCode=0xA4;
            }
        else if (myTarget>=-1.0 && myTarget<-0.5)
            {
                myCode=0xA6;
            }
        else if (myTarget>=-0.5 && myTarget<0.0)
            {
                myCode=0xA9;
            }

```

```
else if (myTarget>=0.0 && myTarget<0.5)
    {
        myCode=0xAC;
    }
else if (myTarget>=0.5 && myTarget<1.0)
    {
        myCode=0xAE;
    }
else if (myTarget>=1.0 && myTarget<1.5)
    {
        myCode=0xB1;
    }
else if (myTarget>=1.5 && myTarget<2.0)
    {
        myCode=0xB3;
    }
else if (myTarget>=2.0 && myTarget<2.5)
    {
        myCode=0xB6;
    }
else if (myTarget>=2.5 && myTarget<3.0)
    {
        myCode=0xB8;
    }
else if (myTarget>=3.0 && myTarget<3.5)
    {
        myCode=0xBB;
    }
else if (myTarget>=3.5 && myTarget<4.0)
    {
        myCode=0xBD;
    }
else if (myTarget>=4.0 && myTarget<4.5)
    {
        myCode=0xC0;
    }
else if (myTarget>=4.5 && myTarget<5.0)
    {
        myCode=0xC2;
    }
else if (myTarget>5.0)
    {
        myCode=0xC7;
```

```

    }

    WriteI2C(myCode);
    sprintf(buf, "\t%d", myCode);
    putsUSART(buf); //Send HV892 code to UART

bus

    IdleI2C();
    XLCDClear();
    XLCDL1home();
    XLCDDisplayOnCursorOff();
    EnablePullups();
    sprintf(line1, "Code sent: %d", myCode);
    XLCDPutRamString(line1);
    XLCDL2home();
    sprintf(line2,"%d.%1u D", (int) myTarget, (int)
fabs(((myTarget - (int) myTarget ) * 10)));
    XLCDPutRamString(line2);
}
while(pin!='0'); //If pin = 0, continue; else, loop
    XLCDClear();
    XLCDL1home();
    XLCDDisplayOnCursorOff();
    EnablePullups();
    XLCDPutRomString("Quit?");
    XLCDL2home();
    XLCDPutRomString("Y=7, N=8");
    Delay10KTCYx(25);
    FindKey();
    ShutOff();

}
}
/*****
***
unsigned char findSwitch(void)
* Input Variables:    none
* Output Return:     currentKey
* Overview:          Keypad scanner
*****
*****/
unsigned char findSwitch(void)
{

```

```

    PORTB = 0xEF;    // col#4 low
    for (i = 0; i < 16; i++)
        if (PORTB == keyPattern[i]) currentKey = keySymbol[i];
    PORTB = 0xDF;    // col#3 low
    for (i = 0; i < 16; i++)
        if (PORTB == keyPattern[i]) currentKey = keySymbol[i];
    PORTB = 0xBF;    // col#2 low
    for (i = 0; i < 16; i++)
        if (PORTB == keyPattern[i]) currentKey = keySymbol[i];
    PORTB = 0x7F;    // col#1 low
    for (i = 0; i < 16; i++)
        if (PORTB == keyPattern[i]) currentKey = keySymbol[i];

    return currentKey;
}

/*****
***
void FindKey(void)
* Input Variables:    none
* Output Return:     none
* Overview:          Keypad scanner
*****/
void FindKey(void)
{
    while (PORTB==0x0F);
        Delay10KTCYx(SWITCH_DELAY);
        pin=findSwitch();
        temp=PORTB & 0x0F;
        while (temp != 0x0F)
            temp= (PORTB & 0x0F);
        Delay10KTCYx(SWITCH_DELAY);
}
/*****
***
void CalibrationSequence(void)
* Input Variables:    none; takes input from ADS1015
* Output Return:     mySum
* Overview:          When 2 is pressed, reads the value from the
ADS1015,
converts the value, and returns it to
mySum. The

```

```

                                                                    voltage read is displayed on the LCD. 0D
Calibration
*****
****/
void CalibrationSequence(void)
{
    pin=='0';

    //Wait for user to press 2
    do
    {
        FindKey();
    }
    while (pin!='2');

    //Read the voltage when 2 is pressed
    if (pin=='2')
    {
        IdleI2C();
        StartI2C();
        IdleI2C();
        WriteI2C(0b10010001); //ADS1015 address, read mode
        Hbyte=ReadI2C(); //Read the high register
        AckI2C();
        Lbyte=ReadI2C(); //Read the low register
        AckI2C();
        value = ((unsigned int) Hbyte) << 8 | Lbyte;
        mySum=(float)value*6144.0/32767.0; //Convert to a
number
        XLCDClear();
        XLCDL1home();
        XLCDPutRomString("Voltage at 0D:");
        XLCDL2home();
        sprintf(line2,"%d", mySum); //Display the number
calculated
        XLCDPutRamString(line2);
        Delay10KTCYx(100); //1 s delay
        StopI2C();
    }
}
/*****
***
void CalibrationSequence2(void)

```



```

* Input Variables:    none; takes input from ADS1015
* Output Return:     mySum1
* Overview:          When 1 is pressed, reads the value from the
ADS1015,
                                converts the value, and returns it to
mySum1. The
                                voltage read is displayed on the LCD. 5D
Calibration
*****
****/
void CalibrationSequence2(void)
{
    pin=='0';

    //Wait for user to press 1
    do
        {
            FindKey();
        }
    while (pin!='1');

    //Read the voltage when 1 is pressed
    if (pin=='1')
        {
            IdleI2C();
            StartI2C();
            IdleI2C();
            WriteI2C(0b10010001); //ADS1015 address, read
mode
            Hbyte=ReadI2C(); //Read high register
            AckI2C();
            Lbyte=ReadI2C(); //Read low register
            AckI2C();
            value = ((unsigned int) Hbyte) << 8 | Lbyte;
            mySum1=(float)value*6144.0/32767.0; //Convert
to a number

            XLCDClear();
            XLCDL1home();
            XLCDPutRomString("Voltage at 5D:");
            XLCDL2home();
            sprintf(line2,"%d", mySum1);
            XLCDPutRamString(line2); //Display the number
calculated

```

```

        Delay10KTCYx(100); //1 s delay
        StopI2C();
    }
}

/*****
***
void EquationCalculation(void)
* Input Variables:    none; uses mySum1, mySum
* Output Return:     mySlope
* Overview:          Calculates the linear slope from the calibration
                    sequences
*****
*****/
void EquationCalculation(void)
{
//Calculations
    mySlope=(mySum1-mySum)/5; //(y2-y1)/(x2-x1) --> (5Dval-
0Dval)/(5D-0D)=x val/D
    myIntercept=myInitial; //Value at 0D is the intercept (x=0)

//LCD Display of the slope
    XLCDClear();
    XLCDL1home();
    XLCDDisplayOnCursorOff();
    EnablePullups();
    XLCDPutRomString("Calculated slope:");
    XLCDL2home();
    sprintf(line1,"%d", mySlope);
    XLCDPutRamString(line1);
    Delay10KTCYx(TimeVal);
}

/*****
***
void ShutOff(void)
* Input Variables:    pin press
* Output Return:     none
* Overview:          If 7 is pressed, shut down; if not, go back to loop
*****
*****/
void ShutOff(void)
{

```

```

    if (pin=='7')
    {
        StopI2C();
        IdleI2C();
        CloseI2C();
        XLCDClear();
        XLCDL1home();
        XLCDPutRomString("Turn off device.");
        Delay10KTCYx(25); //Delay 1s
        XLCDDisplayOff();
    }
    else
        return;
}
/*****
***
void AdjustRefraction(void)
* Input Variables:    none
* Output Return:     none
* Overview:          Reads pot input, compares voltage to list to find
                    correct refraction
*****
*****/
void AdjustRefraction(void)
{
    IdleI2C();
    StartI2C();
    WriteI2C(0x46);
    IdleI2C();
    ConvertADC();
    while (BusyADC());
    myRefraction=ReadADC();
    if (myRefraction< 18)
        {
            myCode=0x93; // -5.0 D
            myIR=-5.0;
        }
    else if (myRefraction>=18 && myRefraction<39)
        {
            myCode=0x94; //-4.75D
            myIR=-4.75;
        }
}

```

```
else if (myRefraction>=39 && myRefraction<61)
{
    myCode=0x96; //-4.5D
    myIR=-4.5;
}
else if (myRefraction>=61 && myRefraction<83)
{
    myCode=0x97; //-4.25
    myIR=-4.75;
}
else if (myRefraction>=83 && myRefraction<105)
{
    myCode=0x98; //-4.0D
    myIR=-4.0;
}
else if (myRefraction>=105 && myRefraction<126)
{
    myCode=0x99; //-3.75D
    myIR=-3.75;
}
else if (myRefraction>=126 && myRefraction<148)
{
    myCode=0x9B; //-3.5D
    myIR=-3.5;
}
else if (myRefraction>=148 && myRefraction<170)
{
    myCode=0x9C; //-3.25D
    myIR=-3.25;
}
else if (myRefraction>=170 && myRefraction<191)
{
    myCode=0x9D; //-3.0D
    myIR=-3.0;
}
else if (myRefraction>=191 && myRefraction<213)
{
    myCode=0x9E; //-2.75D
    myIR=-2.75;
}
else if (myRefraction>=213 && myRefraction<235)
{
    myCode=0xA0; //-2.5D
```

```
        myIR=-2.5;
    }
else if (myRefraction>=235 && myRefraction<257)
    {
        myCode=0xA1; //-2.25D
        myIR=-2.25;
    }
else if (myRefraction>=257 && myRefraction<278)
    {
        myCode=0xA2; //-2.0D
        myIR=-2.0;
    }
else if (myRefraction>=278 && myRefraction<300)
    {
        myCode=0xA3; //-1.75D
        myIR=-1.75;
    }
else if (myRefraction>=300 && myRefraction<322)
    {
        myCode=0xA4; //-1.5D
        myIR=-1.5;
    }
else if (myRefraction>=322 && myRefraction<344)
    {
        myCode=0xA5; //-1.25D
        myIR=-1.25;
    }
else if (myRefraction>=344 && myRefraction<365)
    {
        myCode=0xA7; //-1.0D
        myIR=-1.0;
    }
else if (myRefraction>=365 && myRefraction<387)
    {
        myCode=0xA8; //-0.75D
        myIR=-0.75;
    }
else if (myRefraction>=387 && myRefraction<409)
    {
        myCode=0xA9; //-0.5D
        myIR=-0.5;
    }
else if (myRefraction>=409 && myRefraction<430)
```

```
{
    myCode=0xAA; //-0.25D
    myIR=-0.25;
}
else if (myRefraction>=430 && myRefraction<452)
{
    myCode=0xAC; //0.0D
    myIR=0.0;
}
else if (myRefraction>=452 && myRefraction<474)
{
    myCode=0xAD; //0.25D
    myIR=0.25;
}
else if (myRefraction>=474 && myRefraction<496)
{
    myCode=0xAE; //0.5D
    myIR=0.5;
}
else if (myRefraction>=496 && myRefraction<517)
{
    myCode=0xB0; //0.75D
    myIR=0.75;
}
else if (myRefraction>=517 && myRefraction<539)
{
    myCode=0xB1; //1.0D
    myIR=1.0;
}
else if (myRefraction>=539 && myRefraction<561)
{
    myCode=0xB2; //1.25D
    myIR=1.25;
}
else if (myRefraction>=561 && myRefraction<583)
{
    myCode=0xB3; //1.5D
    myIR=1.5;
}
else if (myRefraction>=583 && myRefraction<604)
{
    myCode=0xB4; //1.75D
    myIR=1.75;
}
```

```
    }
else if (myRefraction>=604 && myRefraction<626)
    {
        myCode=0xB5; //2.0D
        myIR=2.0;
    }
else if (myRefraction>=626 && myRefraction<648)
    {
        myCode=0xB7; //2.25D
        myIR=2.25;
    }
else if (myRefraction>=648 && myRefraction<669)
    {
        myCode=0xB8; //2.5D
        myIR=2.5;
    }
else if (myRefraction>=669 && myRefraction<691)
    {
        myCode=0xB9; //2.75D
        myIR=2.75;
    }
else if (myRefraction>=691 && myRefraction<713)
    {
        myCode=0xBB; //3.0D
        myIR=3.0;
    }
else if (myRefraction>=713 && myRefraction<735)
    {
        myCode=0xBC; //3.25D
        myIR=3.25;
    }
else if (myRefraction>=735 && myRefraction<756)
    {
        myCode=0xBD; //3.5D
        myIR=3.5;
    }
else if (myRefraction>=756 && myRefraction<778)
    {
        myCode=0xBE; //3.75
        myIR=3.75;
    }
else if (myRefraction>=778 && myRefraction<800)
    {
```

```
        myCode=0xBF; //4.0D
        myIR=4.0;
    }
else if (myRefraction>=800 && myRefraction<822)
    {
        myCode=0xC1; //4.25
        myIR=4.25;
    }
else if (myRefraction>=822 && myRefraction<843)
    {
        myCode=0xC2; //4.5D
        myIR=4.5;
    }
else if (myRefraction>=843 && myRefraction<865)
    {
        myCode=0xC3; //4.75D
        myIR=4.75;
    }
else if (myRefraction>=865 && myRefraction<887)
    {
        myCode=0xC4; //5.0D
        myIR=5.0;
    }
else if (myRefraction>=887 && myRefraction<908)
    {
        myCode=0xC6; //5.25D
        myIR=5.25;
    }
else if (myRefraction>=908 && myRefraction<930)
    {
        myCode=0xC7; //5.5D
        myIR=5.5;
    }
else if (myRefraction>=930 && myRefraction<952)
    {
        myCode=0xC8; //5.75D
        myIR=5.75;
    }
else if (myRefraction>=952)
    {
        myCode=0xC9; //6.0D
        myIR=6.0;
    }
}
```



```

        WriteI2C(myCode);
        Delay10KTCYx(10);
        IdleI2C();
    }
    /*****
***
void AdjustTiming(void)
* Input Variables:    none
* Output Return:     none
* Overview:          Reads pot input, compares voltage to list to find
                    correct time
*****
*****/
void AdjustTiming(void)
{
    ConvertADC();
    while (BusyADC());
    myTime=ReadADC();
    if (myTime< 68)
    {
        TimeVal=10;
        TimeDisp=100;
    }
    else if (myTime>=68 && myTime<136)
    {
        TimeVal=20;
        TimeDisp=200;
    }
    else if (myTime>=136 && myTime<204)
    {
        TimeVal=30;
        TimeDisp=300;
    }
    else if (myTime>=204 && myTime<272)
    {
        TimeVal=40;
        TimeDisp=400;
    }
    else if (myTime>=272 && myTime<340)
    {
        TimeVal=50;
        TimeDisp=500;
    }
}

```

```
    }  
else if (myTime>=340 && myTime<408)  
{  
    TimeVal=60;  
    TimeDisp=600;  
}  
else if (myTime>=408 && myTime<476)  
{  
    TimeVal=70;  
    TimeDisp=700;  
}  
else if (myTime>=476 && myTime<544)  
{  
    TimeVal=80;  
    TimeDisp=800;  
}  
else if (myTime>=544 && myTime<612)  
{  
    TimeVal=90;  
    TimeDisp=900;  
}  
else if (myTime>=612 && myTime<680)  
{  
    TimeVal=100;  
    TimeDisp=1000;  
}  
else if (myTime>=680 && myTime<748)  
{  
    TimeVal=110;  
    TimeDisp=1100;  
}  
else if (myTime>=748 && myTime<816)  
{  
    TimeVal=120;  
    TimeDisp=1200;  
}  
else if (myTime>=816 && myTime<884)  
{  
    TimeVal=130;  
    TimeDisp=1300;  
}  
else if (myTime>=884 && myTime<952)  
{
```

```
        TimeVal=140;
        TimeDisp=1400;
    }

    else if (myTime>952)
    {
        TimeVal=150;
        TimeDisp=1500;
    }
    XLCDClear();
    XLCDL1home();
    XLCDDisplayOnCursorOff();
    EnablePullups();
    XLCDPutRomString("Press 5 when done");
    XLCDL2home();
    sprintf(line1,"Time = %d ms", TimeDisp);
    XLCDPutRamString(line1);
    Delay10KTCYx(10);

}
```


Trial InformationDate of Electrophysiological Investigation: / /2014Investigator(s): _____

Room light luminance at paper behind distant target: _____

Filename	Type of Test	Comments*

* please provide information: miosis or cycloplegia

Final Comments: _____

SIGNATURE: _____

APPENDIX C: USER'S GUIDE



Margaret M. Clouse

Table of Contents

Introduction	225
General Features	225
General Safety Information	225
Included Components	226
System Description.....	226
Control Console.....	226
Spectacle System	229
Operating Instructions	230
Materials Needed.....	230
Before Turning on the Device	230
Turning on the Device	231
Using the Device	232
Adjusting the Refraction During Operation	234
Adjusting the DC Offset	234
Adjusting the Gain.....	235
Turning Off the Device.....	235
Charging the Device	236
Troubleshooting.....	236
Problems with the Lens	236
Problems with the Power Supply.....	237
Blue Light Turns On.....	237
Blue Light Doesn't Turn On (One or Both Boards).....	237








Introduction

The Refractor! is a refractive assistance device for those suffering from presbyopia. It senses the accommodative signal present in the ciliary muscle of the eye, and uses that signal to allow the user to focus on near objects. This manual instructs the user in the operation of The Refractor!.

General Features

- Manual DC offset adjustment allows users to adjust the baseline voltage without interfering with operation
- Manual signal magnification (gain) allows the user to select one of six gain settings, based on the user's individual signal magnitude
- Refraction adjustment knob allows the user to pre-set the lens at a specific refraction, based on his or her visual needs
- Rechargeable batteries prevent the need for constant device maintenance
- User interface (LCD and keypad) guides the user through the device workings, and allows for easy refraction adjustment during operation
- Optional oscilloscope output allows clinicians to view the magnified signal on an oscilloscope before the device processes it
- Handle for easy transport
- Easy charging with micro-USB ports
- Adjustable spectacle system fits a wide variety of faces

General Safety Information

-  Do not expose The Refractor! to water or open flames.
-  Do not use The Refractor! before consulting your physician.
-  Do not use The Refractor! for purposes other than those indicated.
-  Do not charge the batteries while the device is in use.
-  Do not expose The Refractor! to excessive heat.
-  Turn off The Refractor! after each use.
-  Do not remove the batteries.



Only use with the Tübingen-Boston XO₂ electrode and a ground electrode.



Make sure the electrodes are correctly placed.



Do not touch the Micro-USB sockets while the device is in use.

Included Components

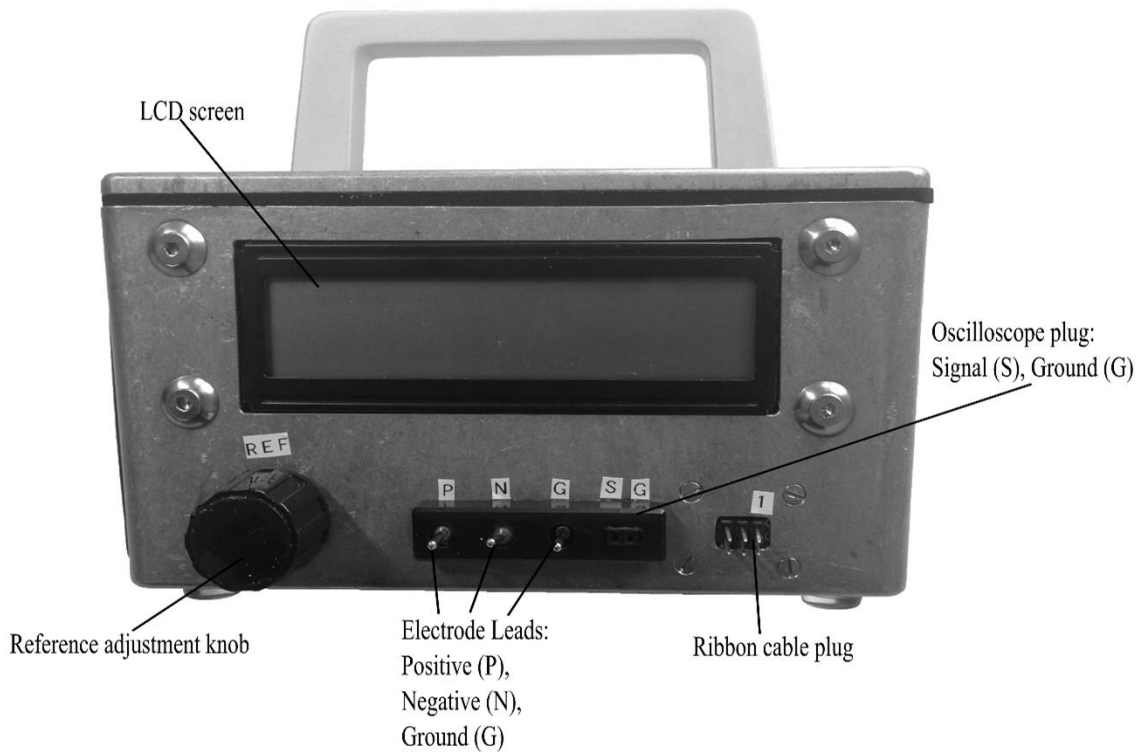
Please make sure the following components are available before operating The Refractinator!:

- 1 Tübingen-Boston XO₂ contact lens electrode
- 1 ground electrode (with necessary abrasive gels, electrode gel, etc.)
- 2 USB to Micro-USB cables
- 1 pin-to-BNC cable (optional)
- 1 battery-powered oscilloscope (optional)
- 1 Spectacle System
- 1 2x3 ribbon cable
- 1 control console

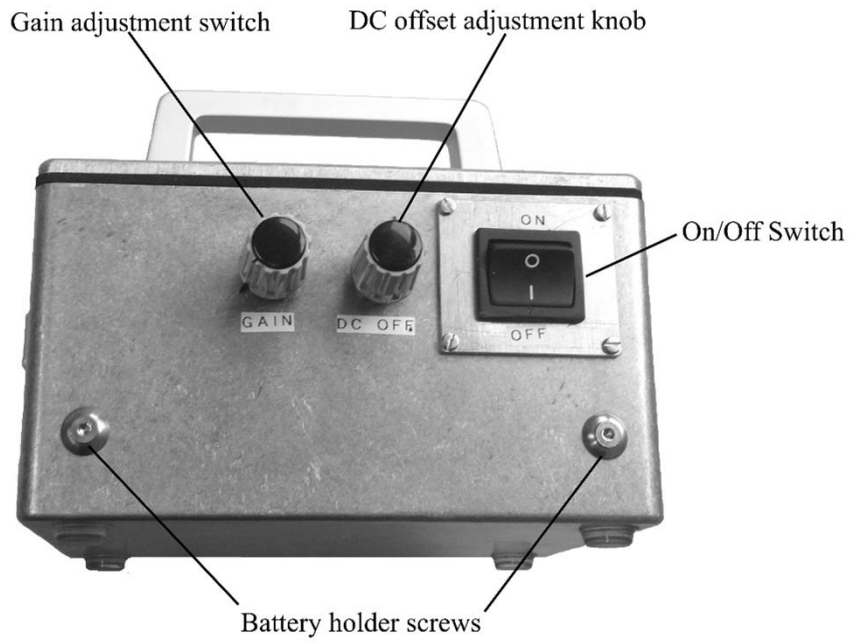
System Description

Control Console

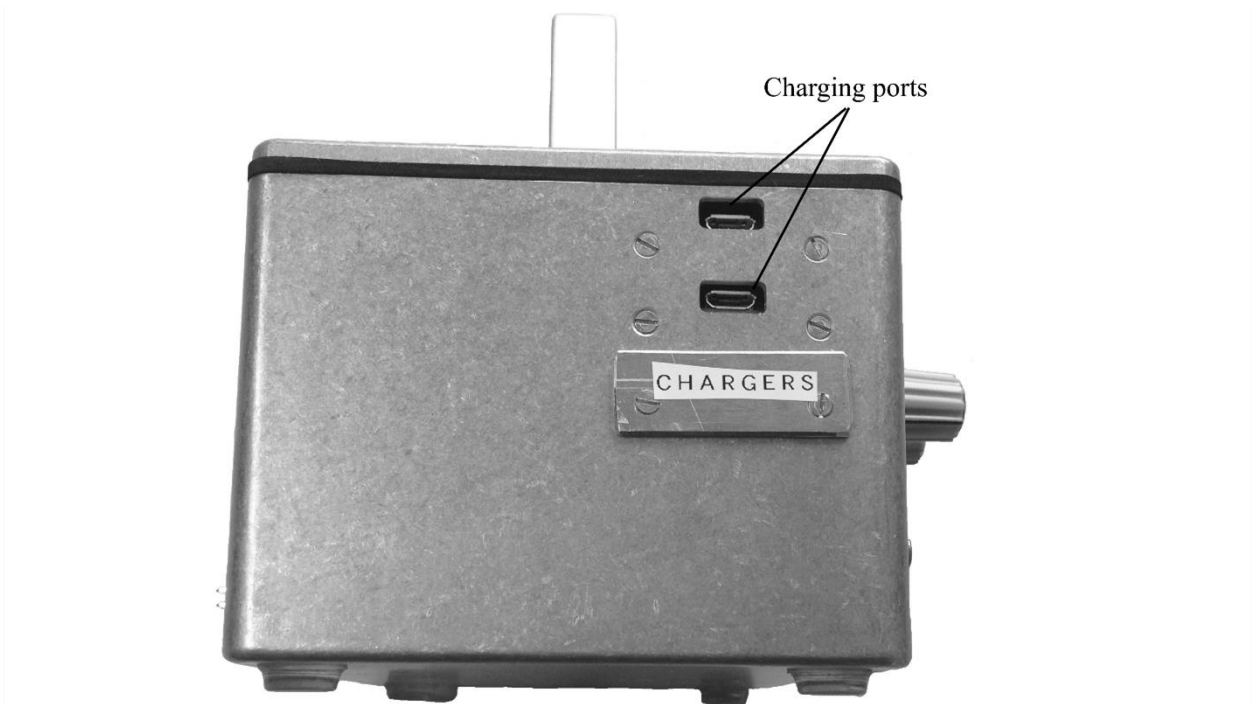
Front View



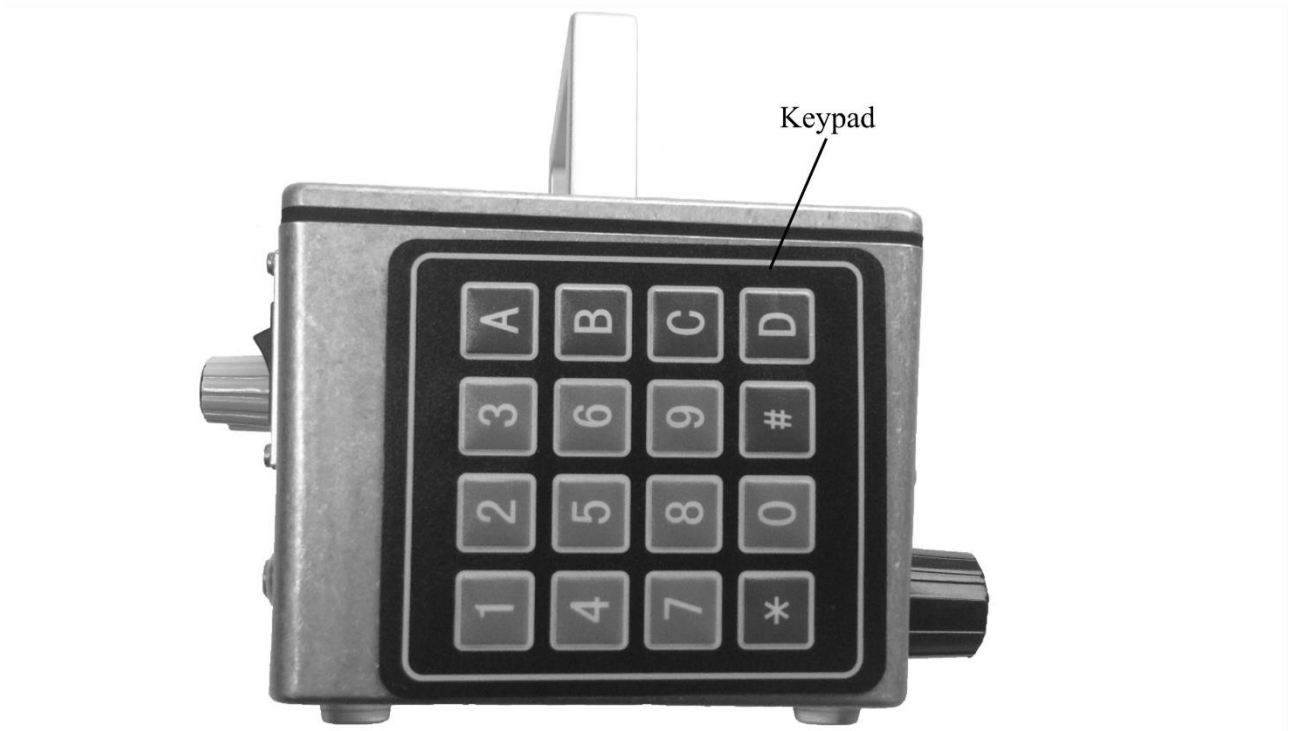
Back View



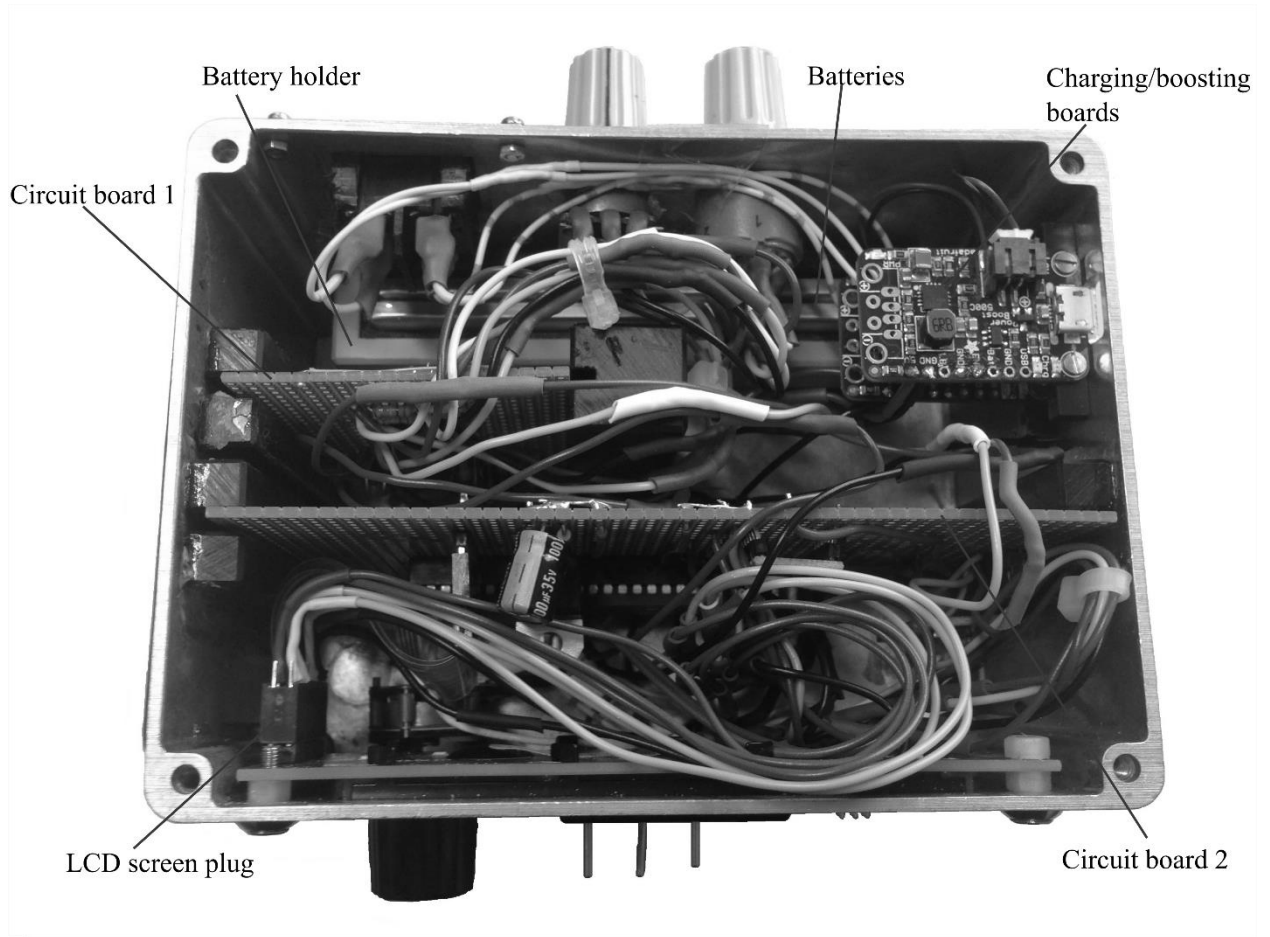
Right View



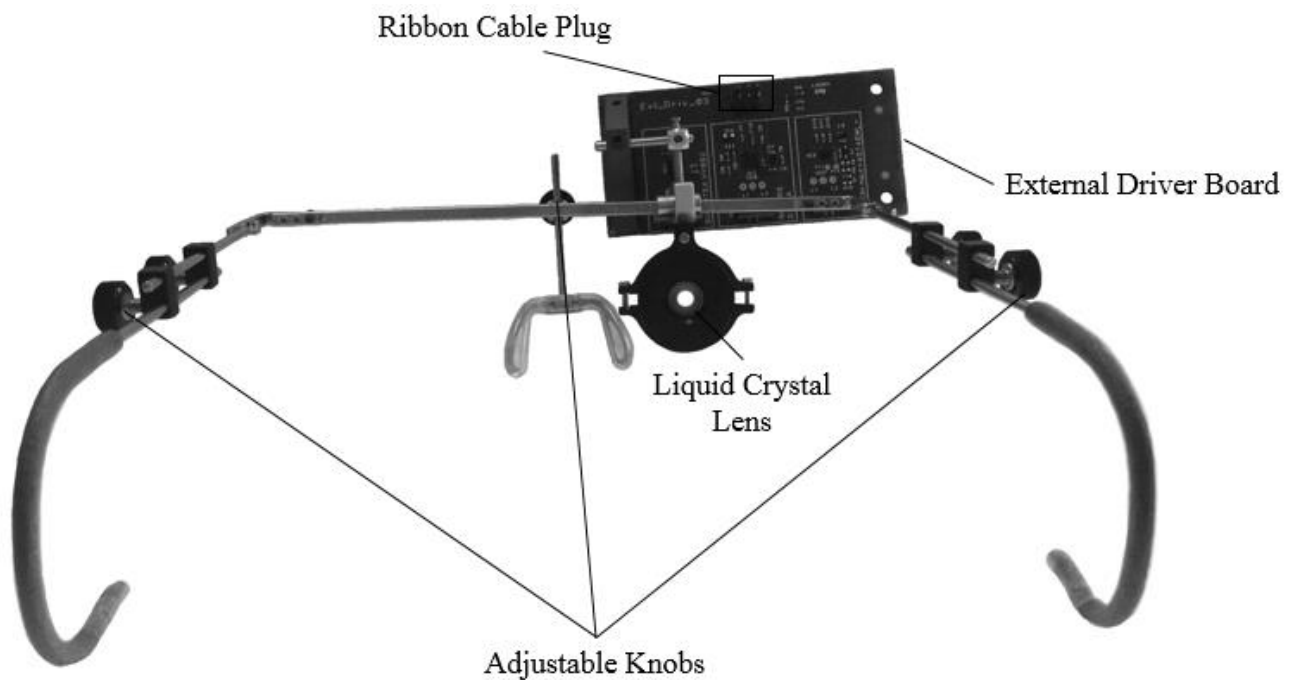
Left View



Inside View



Spectacle System



Operating Instructions

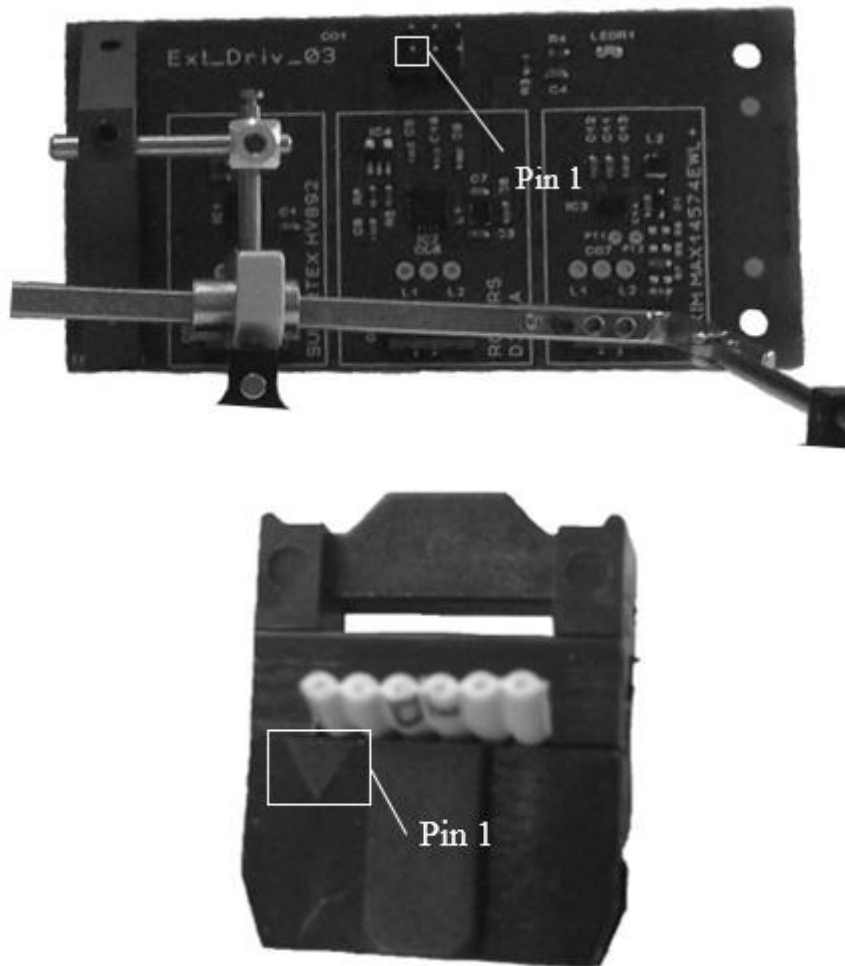
Materials Needed

- 1 Tübingen-Boston XO₂ contact lens electrode
- 1 Ground electrode (with necessary abrasive gels, electrode gel, etc.)
- 3 USB to Micro-USB cables
- 1 Spectacle System
- 1 2x3 ribbon cable
- 1 control console

Before Turning on the Device

1. **ADJUST** the spectacle system to fit comfortably
2. **STERILIZE** the Tübingen-Boston XO₂ electrode
3. **APPLY** the ground electrode
4. **PLUG IN** the Tübingen-Boston XO₂ electrode, taking care that the leads are plugged in to the correct sockets (labeled)
5. **PLUG IN** the ground electrode into its labeled socket

6. **PLUG IN** the ribbon cable. The small arrow on the ribbon cable socket goes to Pin 1 (see diagram below)



7. **APPLY** the Tübingen-Boston XO_2 electrode
 8. **PUT ON** the spectacle system

Turning on the Device

1. **FLIP** the rocker switch at the back of the device to “ON”.
2. **WATCH** the screen. It should display the following message:

Press 9 to start

Using the Device

1. **PRESS** 9 on the keypad. The following message should appear:



Refraction: Press 4

2. **ADJUST** the knob labeled “REF” until vision is clear
3. **PRESS** 4 on the keypad. Two screens will be displayed. The first displays the calculated refraction:



Refraction

The second screen will say this:



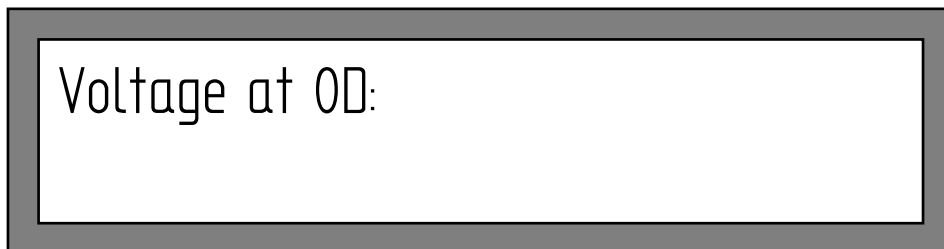
Press 5 when done

4. **ADJUST** the knob labeled “REF” until the correct time between measurements is shown.

5. **PRESS 5** on the keypad. The following screen will be displayed:



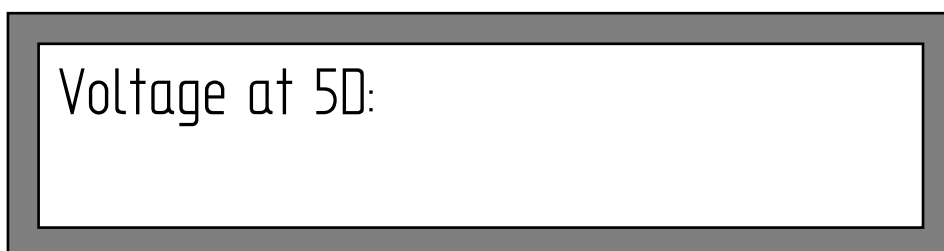
6. **FIXATE** on a marked point two meters away. Continue fixating.
7. **PRESS 2**
8. **WAIT** for 1 second. Two screens will appear:



The second screen will read:



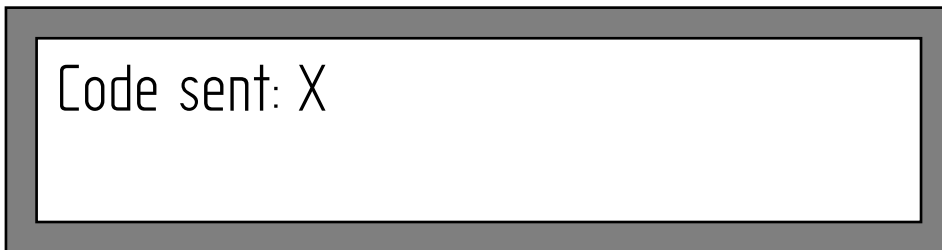
9. **FOCUS** on a marked point 20 cm away. Continue focusing.
10. **PRESS 1**
11. **WAIT** for 1 second. The following screens will appear:



The second screen will read:

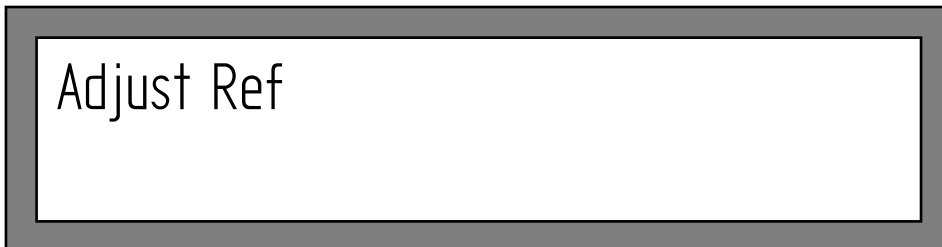


12. The device is ready to use. While the device is running, the following screen will be displayed, showing the code sent to the board and the lens refraction:



Adjusting the Refraction During Operation

1. **PRESS** 5 until the following message appears:



2. **TURN** the knob labeled “REF” until vision is clear when viewing objects at a 2 meter distance.
3. **PRESS** 4 when finished with the adjustment.
4. **CONTINUE** using the device as before.

Adjusting the DC Offset

1. **TURN** the knob labeled “DC OFF” on the back of the device until the desired voltage is reached.

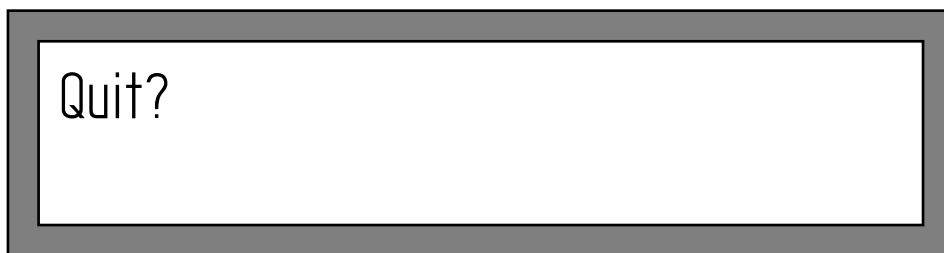
Adjusting the Gain

1. **TURN** the rotary switch labeled “GAIN” on the back of the device to one of the six positions. The table below shows the different gains at different positions:

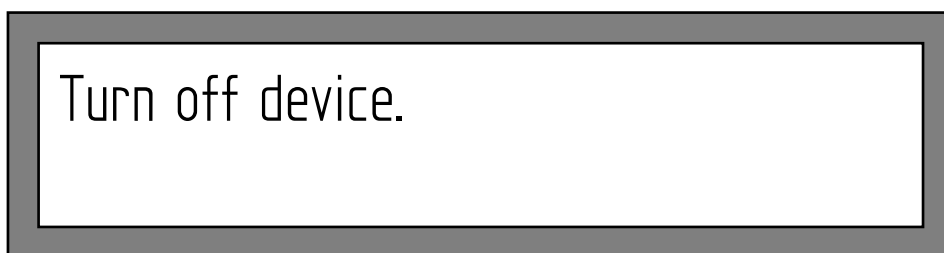
Switch Position	Gain Factor	Suggested User
1	9720	Presbyope, low signal
2	7992	Presbyope, medium signal
3	4212	Presbyope, high signal
4	6048	Pseudophake, low signal
5	1944	Pseudophake, medium signal
6	1296	Pseudophake, high signal

Turning Off the Device

1. **PRESS** 0 until the following message appears:



2. **PRESS** 8 to cancel, or to quit **PRESS** 7 until the following message appears:



3. **FLIP** the rocker switch to “OFF” to turn off the device.

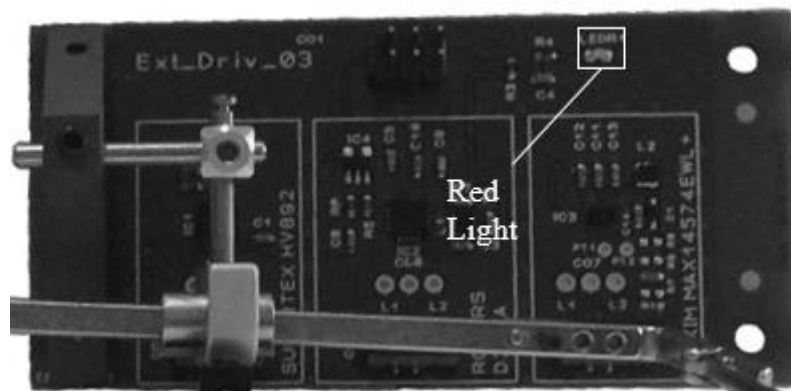
Charging the Device

1. **PLUG** two Micro-USB to USB cables into the two Micro-USB ports on the device.
2. **CONNECT** the USB parts of each cable to a computer USB port. A yellow light will appear at the Micro-USB plugs.
3. **UNPLUG** the cables when a green light appears at the Micro-USB ports. For a completely empty battery, the charging time is approximately seven hours.

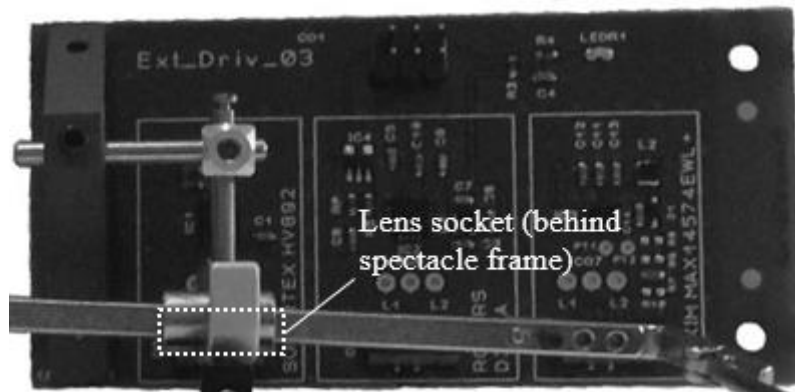
Troubleshooting

Problems with the Lens

1. **CHECK** the board on the spectacle system. A red light should appear when the device is on:



2. If the red light is not illuminated, **CHECK** both ends of the ribbon cable to make sure they are plugged in.
3. **ENSURE** that the ribbon cable is oriented correctly (black arrow to Pin 1 on both devices).
4. **ENSURE** that the yellow cable connecting the lens to the board is firmly plugged in to the Supertex HV892 socket on the board:



5. **TURN** the device off for 30 seconds, then switch it back on.

Problems with the Power Supply

1. **ENSURE** the device is turned off.
2. **UNSCREW** the lid of the device.
3. **LOCATE** the two charger/booster boards.
4. Without touching the inside of the device, **TURN** the device on.
5. **CHECK** both of the boards.

Blue Light Turns On

1. **TURN OFF** the device.
2. **CHARGE** the batteries.

Blue Light Doesn't Turn On (One or Both Boards)

1. **TURN OFF** the device.
2. **UNPLUG** the batteries from the sockets on the board(s), using pliers.
3. **PLUG** the batteries back in.
4. **ENSURE** that no part of the boards are touching metal surfaces.
5. **REPLACE** battery.

AUTHOR'S CONTRIBUTIONS

The experimental set-up for the Ciliary Muscle Measurements experiments was designed by Prof. Eberhart Zrenner and Ditta Zobor, and created by Torsten Straßer and Dominic Hillerkuss. Contact lens electrode development was led by Prof. Zrenner, Ditta Zobor, Torsten Straßer, and Ralf Rudolf. Software for the photorefractor was created by Frank Schaeffel, and modified, as needed, by the author and Torsten Straßer. The study concept originated with Eberhart Zrenner and Ditta Zobor. Experimental investigations were performed by the author, Torsten Straßer, and Ditta Zobor. All data analyses described here were performed by the author.

The created device was developed by the author. Circuitry was constructed by the author, while housing elements were machined by the University of Tübingen Eye Hospital Workshop. Code was developed by the author, with help from Torsten Straßer. Code for the ADS1015 ADC conversion was, in part, from the work of Microchip forum user DarioG. LCD code was originally created by Naveen Raj and David Fisher; modifications were performed by the author. Proof-of-concept experiments were developed by the author, Torsten Straßer, and Eberhart Zrenner.

ACKNOWLEDGEMENTS

I would like to thank Prof. Eberhart Zrenner for his wonderful mentoring and supervision, as well as Dr. Torsten Straßer for being a great councilor and advisor. Thanks to all of my colleagues, as well as all of the faculty of the University of Tübingen Eye Hospital, for support in research and experimentation.

For giving me the opportunity to pursue this amazing research opportunity, I would like to thank the Hector Fellow Academy for providing funding for the project.